COUPLING BETWEEN FLUID FLOW AND DEFORMATION IN POROUS CRUSTAL ROCKS

A DISSERTATION

SUBMITTED TO THE DEPARTMENT OF GEOPHYSICS

AND THE COMMITTEE ON GRADUATE STUDIES

OF STANFORD UNIVERSITY

IN PARTIAL FULFILLMENT OF THE REQUIREMENTS

FOR THE DEGREE OF

DOCTOR OF PHILOSOPHY

By

Joseph Scott Walder

February 1984

TABLE OF CONTENTS

LIST OF ILLUSTRATIONS

Figure

INTRODUCTION

Many geological and geophysical phenomena and processes in the Earth's crust are profoundly influenced by interaction between the porous rocks that constitute the crust and the pore fluid contained within those rocks. This interaction may be chemical, manifesting itself through processes such as diagenesis (e.g., Berner, 1980) or redistribution of isotopes (e.g., Taylor, 1977; O'Neill and Hanks, 1980); mechanical, with pore fluids affecting the mechanisms by which rocks deform (e.g., Carter, 1976; Brace and Kohlstedt, 1980) or transmit stress waves (e.g., Nur and Simmons, 1969); or a complicated mix of chemical and mechanical processes, such as during the dewatering of a sediment pile (e.g., Weaver and Beck, 1971; Cathles and Smith, 1983).

A clear understanding of fluid-rock interaction in the Earth's crust is also of significant practical interest. One outstanding problem centers around the long-term (10^6 a) isolation of 'high-level', extremely toxic radioactive wastes generated both by commercial nuclear reactors and by military weapons-building programs. The waste-isolation scheme most favored—and already being pursued in some countries—involves burial of encapsulated waste products in what are hoped to be 'stable', 'impermeable' rocks. Despite serious efforts to understand the potential hydrologic interaction between these radioactive wastes and the biosphere, it is not obvious to many people that a 'safe' waste repository has been (or can be) found. Earth science (and earth scientists), public policy, and political forces affect each other in this controversy.

For both theoretical and practical reasons, therefore, the many earth scientists interested in crustal processes should routinely consider the hydrologic characteristics of crustal rocks as potentially important parameters.

The overall goal in this dissertation is to provide answers to several important, related questions in regards to the distribution of water in the Earth's crust:

i) At what depths is free water present?

ii) What are the porosity and permeability of crustal rocks?

iii) What is the pore pressure at depth, particularly in comparison to hydrostatic pressure?

iv) How do pore fluids interact mechanically with crustal rocks?

v) How do any or all of the hydrological parameters of the crust change in time and space?

Considerable data to help answer these questions has been gathered as a result of petroleum exploration and engineering studies (Brace, 1980), but are essentially restricted to the upper 2-3 km of the crust. Hence, answers must necessarily be based largely upon indirect evidence and model studies.

The work presented in this dissertation comprises an effort to develop simple theoretical models of some key aspects of crustal hydrology, to apply these models to understand the mechanical interaction between porous crustal rocks and the pore fluids contained therein, and to help answer the questions posed above. Throughout this dissertation, attempts are made to relate and compare our theoretical models to geological and geophysical observations from the laboratory, the field, and the subsurface.

In chapter 1, the way in which porosity-reduction processes affect permeability and pore pressure at upper- and mid-crustal depths is examined. A great deal of indirect evidence exists suggesting that pore pressure in excess of hydrostatic may be quite common. At the same time, other inferences suggest that typical crustal permeabilities are such as to preclude the maintenance of excess pore pressure for geologically significant periods of time. One way to reconcile this apparent contradiction is to consider porosity, permeability and pore pressure all to be time-dependent, rather than static. Simple mathematical models show that slow porosity/permeability reduction could profoundly affect pore pressure. Indirect evidence from thermodynamical arguments and from experimental work suggests that localized mass transfer--perhaps akin to 'pressure solution'--may be very common under crustal conditions and lead to such slow porosity/permeability changes. Such time-dependent variability of crustal hydrologic characteristics cannot be a 'one-way' phenomenon, however; regions in which pore pressure is high are likely to alternate both spatially and temporally with regions where elevated pore pressure is relieved by fracturing and the concomitant creation of relatively permeable conduits permitting egress of overpressured fluids. This notion of pore pressure variable in both time and space is considered again, in different contexts, in later chapters.

The work presented in chapters 2, 3, and 4, dealing with physical processes in accumulating sediments, grew out of an interest in the mechanisms by which excess pressures are generated in sedimentary basins. Overpressuring presents significant practical problems in petroleum exploration (e.g., Dickinson, 1953; Fertl and Timko, 1970); hence, a great deal of effort has been made not only to develop well-logging techniques to

anticipate the presence of overpressured zones, but also to understand the physical processes that cause such zones to develop.

Previous models of pore-pressure development in accumulating sediments involve a variety of assumptions about the sediments' rheological behavior. In chapter 2, such assumptions are critically examined in view of experimental data on time-dependent deformation of clays and shales, in order to construct a plausible rheological model for compaction of clay-rich sediments. It is shown that for time scales and loading rates typical of sedimentary basins, mechanical porosity change during compaction is essentially a unique function of effective pressure. This verifies assumptions made in previous models. It also facilitates the development in chapter 3, where the relative efficacy of various processes that may cause overpressuring in compacting clay-rich sediments is examined.

Pressure-enhancing phenomena--mechanical compaction, thermal expansion of pore fluid, and bound-water release during montmorillonite dehydration--all 'compete' with pore-pressure diffusion, which acts to dissipate excess pore pressure. A particularly new feature of the analysis is an explicit mathematical description of the 'source strength' of the clay-dehydration mechanism. Very rapid pore-pressure increase may result from montmorillonite dehydration, possibly leading to episodic buildup and release of overpressure. This may be related to the origin of Mississippi Valley-type Pb-Zn deposits (Cathles and Smith, 1983). The clay-dehydration mechanism may also help to explain commonly observed subsurface features, such as porosity inversions (i.e., porosity locally increasing with depth).

The work on accumulating sediments concludes in chapter 4 with an explicit accounting for one of the ubiquitous feature in sedimentary basins:

sand-shale interlayering. The analysis demonstrates clearly that sand-shale interlayering in a predominantly shale section will profoundly affect fluid-flow direction, pore-pressure development, and the dewatering history of the sediment pile.

Pore pressure must necessarily be linked to the overall stress state in a rock mass. In chapter 5, a mathematical formalism is developed showing how pore pressure, stress, strain, and temperature are coupled, and used to examine the pore-pressure history of a rock mass for two common situations: when uplifted, and when subjected to lateral tectonic compression. During uplift, pore pressure in a rock mass of low permeability (or surrounded by rocks with this property) may deviate markedly from hydrostatic. The sign of this deviation depends strongly on another phenomena associated with uplift (Bruner, in press): the probable growth of microcracks due to grain-scale stress inhomogeneities. In the likely case that microcracking is important, the compliance of the rock mass will increase, and pore pressure may climb above hydrostatic. This phenomenon could be related, in some cases, to joint formation.

During lateral compression at geologically plausible strain rates, pore pressure in low permeability rocks may climb to lithostatic on a time scale of only thousands or tens of thousands of years. This would have a major influence on the mechanical properties of the rock mass, greatly facilitating brittle deformation. This phenomenon may be of particular importance for rocks caught in zones between converging tectonic plates.

In chapter 6, the transient pulse, or pulse-decay method of permeability measurement is investigated. Coupling between pore pressure and stress may be important in the laboratory as well as for larger scale phenomena; theory

indicates that such coupling should cause an inherent sample-size dependence in the transient pulse technique. A simple experiment intended to test this prediction is described. Sample-size dependence is observed, but may be masked by effects of slight material inhomogeneity. Also examined are limitations on the pulse-decay technique that may arise as a result of nonlinear pore-pressure diffusion, with presentation of the theoretical rationale and results of another simple experiment that support the theory. The overall results are used to suggest guidelines for experimentalists intending to use the transient pulse method in the future, such that possible misinterpretation of data can be avoided.

REFERENCES

Berner, R.A., *Early diagenesis: a theoretical approach*. Princeton, New Jersey, Princeton University Press, 241 pp., 1980.

Brace, W.F., Permeability of crystalline and argillaceous rocks. *International Journal of Rock Mechanics and Mining Sciences & Geomechanics Abstracts*, *17*, 241-51, 1980.

Brace, W.F., and D.L. Kohlstedt, Limits on lithospheric stress imposed by laboratory experiments. *Journal of Geophysical Research*, *85*, 6248-52, 1980.

Bruner, W.M., Crack growth during unroofing of crustal rocks: effects on thermoelastic behavior and near-surface stresses, *Journal of Geophysical Research*, in press.

Carter, N.J., Steady state flow of rocks. *Reviews of Geophysics and Space Physics*, *14*, 301-60, 1976.

Cathles, L.M., and A.T. Smith, Thermal constraints on the formation of Mississippi Valley-type lead-zinc deposits and their implications for episodic dewatering and deposit genesis. *Economic Geology*, *78*, 983-1002, 1983.

Dickinson, G., Geological aspects of abnormal reservoir pressures in Gulf Coast Louisiana. *American Association of Petroleum Geologists Bulletin*, *37*, 410-32, 1953.

Fertl, W.H., and D.J. Timko, Occurrence and significance of abnormal-pressure formations. *Oil and Gas Journal*, *68*, No. 1, 97-108, 1970.

Nur, A., and G. Simmons, The effect of saturation on velocity in low porosity rocks. *Earth and Planetary Science Letters*, *7*, 183-93, 1969.

O'Neil, J.R., and T.C. Hanks, Geochemical evidence for water-rock interaction along the San Andreas and Garlock fault zones of California. *Journal of Geophysical Research*, *85*, 6286-92, 1980.

Taylor, H.P., Jr., Water/rock interaction and the origin of H O in granitic batholiths. *Geological Society of London Journal*, *133*, 509-58, 1977.

Weaver, C.E., and K.C. Beck, Clay-water diagenesis during burial: how mud becomes gneiss. *Geological Society of America Special Paper*, *134*, 96 pp., 1971.

CHAPTER 1
POROSITY REDUCTION AND CRUSTAL PORE-PRESSURE DEVELOPMENT

ABSTRACT

The influence of porosity-reduction processes on the hydrologic characteristics of the Earth's crust is examined. We present a simple mathematical model that shows the effect of porosity reduction on fluid-pressure development in the crust. Fluid pressure in excess of hydrostatic can be generated if porosity-reduction rates are sufficiently high. Elevated fluid pressure could in turn affect properties such as strength and seismic reflectivity. Our review of indirect evidence from laboratory, theoretical, and field studies indicates that porosity-reduction processes are active--or are very likely to be so--in large parts of the crust, crystalline as well as sedimentary. We conclude that, in general, the hydrologic properties of the Earth's crust should be time-dependent, even in regions not undergoing significant tectonic activity.

1. INTRODUCTION

The hydrologic character of the Earth's crust plays a very important role in a number of geological and geophysical phenomena. Certainly the mechanisms by which crustal rocks deform during tectonic activity are strongly influenced by the presence or absence of water, as well as by the fluid pressure, with brittle behavior favored under some conditions, ductile behavior under others [e.g., Carter, 1976; Brace and Kohlstedt, 1980]. Circulation of

crustal water has important effects on heat flow [e.g., Sleep and Wolery, 1978; Lachenbruch and Sass, 1980; Smith and Chapman, 1983], on the distribution of oxygen and hydrogen isotopes [e.g., Taylor, 1977; O'Neil and Hanks, 1980], and on ore deposit formation [e.g., Norton and Knight, 1977]. An understanding of crustal hydrologic properties is critical in evaluating the safety of nuclear waste burial schemes [e.g., Trimmer et al., 1980] and the efficiency of hot dry rock geothermal energy extraction [e.g., Morrow et al., 1981].

Several important, related questions can be posed in regards to the distribution of water in the crust:

(i) At what depths is free water present?

(ii) What is the value of aqueous fluid pressure P_f at these depths?

(iii) What is the permeability at these depths?

Answers to these questions are of necessity based largely upon indirect evidence, because published *in situ* measurements of crustal hydrologic properties reach to depths of only *ca.* 2-3 km [Brace, 1980].

The presence of free water to at least moderate depths in the crust is strongly suggested by several lines of research. Isotopic studies of batholithic rocks [e.g., Taylor, 1977; Norton and Taylor, 1979] indicate that meteoric water can circulate to depths of *ca.* 10-20 km. Some deep-crustal electromagnetic soundings have been interpreted as indicating the presence of zones of relatively low electrical resistivity, with the presence of a continuous water phase a probable cause [e.g., Nekut et al., 1977; Thompson et al., 1983]. Some laboratory studies of the electrical properties of rocks support this interpretation [Olhoeft, 1981; Shankland and Ander, 1983]. Seismology has also contributed to ideas about the hydrologic character of the crust. For example, Berry and Mair [1977] have argued that crustal low velocity zones could be due

to P_f locally in excess of hydrostatic. This argument is based upon experimental results such as those of Nur and Simmons [1969], who showed that even in very low porosity saturated rocks, compressional velocity drops markedly as P_f approaches the confining pressure P_c. Using a similar line of reasoning, Jones and Nur [1982] suggested that some reflections from deep crustal fault zones may be associated with elevated P_f within or below these zones. The hypothesis of elevated P_f has also been suggested by Raleigh and Evernden [1982] to explain the low deviatoric stresses thought to exist along plate boundaries such as the San Andreas fault.

Other inferences about crustal hydrology are based upon observations of a more geological character. For example, Fyfe et al. [1978] and Etheridge et al. [in press] have reviewed geological evidence indicating that free water, with P_f often exceeding hydrostatic, is widespread during low- to medium grade regional metamorphism. Two principal lines of evidence are:

(i) The ubiquity of mineralized fractures whose microstructure and orientation indicate that they formed in extension (see also Ramsay [1980]). On the basis of commonly accepted criteria for brittle failure, this requires that P_f exceeded the minimum principal confining stress at the time of fracture formation.

(ii) The consistency of experimentally determined phase equilibria (with P_f equal to confining pressure P_c) with natural distributions of metamorphic mineral assemblages. (The lack of independent P_f control in most metamorphic petrology experiments makes this argument difficult to assess critically, however, as emphasized by Thompson [1983].)

The above arguments clearly support the idea that free water is common, at least episodically, at upper- and mid-crustal levels. Furthermore,

the hypothesis that elevated P_f can be maintained in the crust for geologically significant periods of time is quite attractive as a basis for explaining a number of phenomena. This hypothesis carries with itself implications for the permissible values of permeability of crustal rocks. Bredehoeft and Hanshaw [1968] and Hanshaw and Bredehoeft [1968] studied simple models of crustal P_f development; they concluded that, in general, maintenance of elevated P_f for geologically significant periods of time requires horizons of very low permeability, perhaps as low as 1 ndarcy ($10^{-21}m^2$). Brace [1980], after reviewing direct and indirect estimates of crustal permeability, argued that zones with permeability of ca. 1 millidarcy ($10^{-15}m^2$) must exist down to at least 10 km depth. He therefore concluded that P_f is very unlikely to exceed hydrostatic pressure "in regions where crystalline rocks extend to the surface," and that P_f above hydrostatic in crystalline rocks could be maintained only if a cover of very low permeability (e.g., argillaceous) rocks were present [cf. Hanshaw and Bredehoeft, 1968]. Recently, Jones [1983] has examined the hypothesized relationship between seismically reflective zones and elevated P_f by combining simple models of P_f development with synthetic seismograms. He concluded that although elevated pore pressure can significantly affect the existence and amplitudes of reflected waves, such effects persist for geologically significant periods of time "only for a permeability lower than that generally observed in laboratory measurements on crustal rocks."

The apparent contradiction between the indirect evidence for widespread elevated crustal P_f, on the one hand, and the inferred relatively high permeability throughout the crust, on the other hand, may be reconciled by considering porosity, permeability, and consequently fluid pressure to be

time-dependent, rather than static. What then might be the conditions or situations for which these quantities could develop through time in such a way as to maintain P_f in excess of hydrostatic? The most obvious mechanisms potentially responsible are time-dependent changes in porosity and pore-space configuration due to (i) inelastic deformation, leading to pore closure; (ii) dissolution, including pressure solution, and redeposition of solutes; and (iii) the creation of fractures, with their subsequent healing and sealing. As porosity changes due to these processes, so will permeability.

In the next section, we present a simple mathematical model for P_f development, taking into account the role of porosity and permeability reduction. Scaling arguments lead to a criterion for assessing whether porosity reduction will be effective in producing elevated P_f. This criterion indicates approximately the porosity-reduction rate necessary to produce and maintain elevated P_f. This is illustrated by calculations of P_f development in layered crustal models. In section 3, we discuss possible mechanisms of porosity reduction and review thermodynamic arguments that porosity reduction is generally favored when P_f is less than overburden pressure. We will argue that local mass transfer is likely to be very important in effecting porosity reduction. Discussion in section 4 centers on implications of our model for interpreting tectonic processes, in particular, brittle fracture in the crust. We also examine the possible role of elevated fluid pressure in crustal low velocity zones.

2. EFFECT OF POROSITY REDUCTION ON FLUID PRESSURE

The fundamental relationships that we use in deriving a mathematical model for crustal pore-pressure development are mass conservation and

Darcy's law. Mass conservation for a fluid in a porous material is given by

$$\frac{\partial}{\partial t}(\rho_f \varphi) = -\nabla \cdot (\rho_f \vec{u}) \tag{1}$$

where

ρ_f = fluid density

φ = porosity

$\vec{u}$ = volumetric flow rate per unit area

t = time

The volumetric flow rate per unit area is related to fluid pressure by the phenomenological relationship known as Darcy's law:

$$\vec{u} = -\frac{k}{\mu}(\nabla P_f - \rho_f \vec{g}) \tag{2}$$

where

k = permeability

μ = viscosity

P_f = fluid pressure

$\vec{g}$ = acceleration due to gravity

Eqn. (2) indicates that there will be no flow when the fluid-pressure gradient is hydrostatic, i.e., when $\nabla P_f = \rho_f \vec{g}$.

Combining Eqns. (1) and (2) and expanding, we obtain

$$\rho_f \frac{\partial \varphi}{\partial t} + \varphi \frac{\partial \rho_f}{\partial t} = \frac{\rho_f k}{\mu}\nabla^2 P_f + \frac{\rho_f}{\mu}\nabla k \cdot \nabla P_f + \frac{k}{\mu}\nabla \rho_f \cdot \nabla P_f - \frac{\rho_f k}{\mu^2}\nabla \mu \cdot \nabla P_f \tag{3}$$

In the usual derivation of the diffusion equation for fluid pressure [e.g., Brace et al., 1968], permeability and viscosity are taken as constants. *Reversible*

changes in porosity and fluid density due to changes in fluid pressure are also included. In the present analysis, we want to consider in addition possible *irreversible* changes in both porosity and permeability, as they may strongly affect pore pressure development. Accordingly, we decompose the rate of change of porosity into reversible and irreversible parts:

$$\frac{\partial \varphi}{\partial t} = \left(\frac{\partial \varphi}{\partial t}\right)_{rev} + \left(\frac{\partial \varphi}{\partial t}\right)_{irrev} \tag{4}$$

(The physical nature of $(\partial \varphi / \partial t)_{irrev}$ will be discussed in section 3.) Similarly, the gradient in permeability may be written as

$$\nabla k = (\nabla k)_{rev} + (\nabla k)_{irrev} \tag{5}$$

Using Eqns. (4) and (5), we show in the appendix that the equation for fluid pressure diffusion can generally be written to a close approximation as

$$\frac{1}{c}\frac{\partial P_f}{\partial t} = \nabla^2 P_f + \frac{1}{k}(\nabla k)_{irrev} \cdot \nabla P_f + \frac{\mu \dot{\Phi}}{k} \tag{6}$$

where c is the hydraulic diffusivity, defined in the appendix, and $\dot{\Phi} = -(\partial \varphi / \partial t)_{irrev}$ is a porosity-reduction rate factor, defined so as to be positive when porosity is decreasing. The hydraulic diffusivity depends upon both permeability and porosity.

It is clear from Eqn. (6) that porosity reduction may have a significant effect on fluid-pressure development. In particular, porosity reduction ($\dot{\Phi} > 0$) will generally tend to increase fluid pressure, a point also raised by Angevine and Turcotte (1983). Gradients in permeability that arise as a result of porosity reduction will also influence fluid-pressure development.

In this chapter, we consider the special case in which porosity and porosity reduction are uniform throughout crustal layers. If we assume further that permeability is uniquely related to porosity, the changes in k due

to porosity changes will also be uniform throughout the rock mass, i.e., $(\nabla k)_{grav}$ will vanish. Fluid-pressure development will then be described by the equation

$$\frac{1}{c}\frac{\partial P_f}{\partial t} = \nabla^2 P_f + \frac{\mu \dot{\Phi}}{k} \tag{7}$$

which differs from the common P_f diffusion equation by the porosity rate-of-change term. The importance of porosity change relative to diffusive relaxation $\nabla^2 P_f$ can be highlighted by recasting Eqn. (7) into nondimensional form. For simplicity, we consider flow in only the vertical, or z, direction, where z increases with depth. We then adopt the following scalings:

$$\begin{aligned} P_f &= P_s \cdot \bar{P} \\ t &= t_s \cdot \bar{t} \\ z &= H \cdot \bar{z} \end{aligned} \tag{8}$$

where P_s, t_s, and H are characteristic scalings for fluid pressure, time, and length, respectively. Dimensionless variables are denoted by bars. For the characteristic time, t_s, we take the diffusion time scale in the absence of porosity reduction, viz.:

$$t_s = \frac{H^2}{c} \tag{9}$$

For P_s, we choose the maximum allowable excess fluid pressure, which is simply the difference between lithostatic and hydrostatic pressures at depth H, viz.:

$$P_s = \Delta\rho\, g\, H \tag{10}$$

where $\Delta\rho = \rho_r - \rho_f$, with ρ_r = rock density; g is the magnitude of $\vec{g}$. Using Eqns. (8)-(10) in Eqn. (7), we find

$$\frac{\partial \bar{P}}{\partial \bar{t}} = \frac{\partial^2 \bar{P}}{\partial \bar{z}^2} + \left(\frac{\mu \dot{\Phi} H}{\Delta \rho g k}\right) \tag{11}$$

The importance of porosity reduction in fluid-pressure development is given by the magnitude of the dimensionless grouping $(\mu \dot{\Phi} H / \Delta \rho g k) = \dot{F}$. When $\dot{F}$ is much less than 1, fluid-pressure development is essentially governed by the usual diffusion relationship. As $\dot{F}$ increases, porosity reduction plays an increasingly important role in modifying the diffusive response. For $\dot{F} > 1$, the diffusive term becomes of secondary importance and fluid pressure is primarily affected by porosity reduction. We see that the importance of porosity reduction increases as the characteristic length scale, H--that is, the depth to which porosity reduction occurs--increases, and as permeability decreases.

It is of interest to determine whether porosity-reduction processes can lead to excess fluid pressures in crystalline rocks that make up most of the Earth's crust. Consider, for example, a 10 km thick section of granitic rock undergoing porosity reduction. We assume that the rock is at pressures and temperatures typical of upper- to mid-crustal depths and has no megascopic fractures; hence, the permeability may be rather low, perhaps *ca.* 50 ndarcy, throughout much of the section [cf. Brace et al., 1968]. Ignoring effects of solutes, water viscosity should show a general decrease with depth [cf. Bolz and Tuve, 1970], from about 1 cp at the surface to *ca.* 0.1 cp at 10 km depth. For simplicity, we take $\mu = 0.2$ cp (2×10^{-4} Pa s) throughout the section. Using $\Delta \rho = 1.7$ g cm^{-3} (1.7×10^3 kg m^{-3}) and $g = 9.8$ m s^{-2}, we find that $\dot{F} = 1$ when $\dot{\Phi} = 4.2 \times 10^{-16}$ s^{-1}. In other words, if porosity reduction were to proceed throughout the 10 km thick section at a rate of *ca.* 4.2×10^{-16} s^{-1}, fluid-pressure development would deviate significantly from the purely diffusive case; excess fluid pressure would be generated and maintained. To illustrate

this process, we have computed fluid-pressure development in a layer undergoing uniform porosity reduction. Calculations have utilized a finite-difference approximation of Eqn. (7). The initial and boundary conditions are

i) $\hat{P}(t = 0) = 0$

ii) $\hat{P}(z = 0) = 0$

iii) $\frac{\partial \hat{P}}{\partial z}(z = L) = 0$

where L is the layer thickness and $\hat{P} = P_f - \rho_f g z$ is the 'excess' fluid pressure, i.e., the fluid pressure relative to hydrostatic at any depth z. The initial condition is therefore a hydrostatic fluid-pressure distribution. The last boundary condition corresponds to the case of a lower crust that is hydraulically unconnected to the upper section of thickness L. (This does not necessarily mean that the lower crust is assumed to be dry, only that it is hydraulically isolated from the upper crust.)

It seems reasonable that permeability should decrease as φ decreases. As a simple model, we have assumed a unique relationship between k and φ, motivated by recent work on hot-pressing of calcite [Bernabe et al., 1982]. This work indicates that *connected* porosity, hence permeability, may vanish at very low values of porosity. Although porosity reduction in the crust may not necessarily occur by plastic deformation, as during hot-pressing, it seems plausible that a similar phenomenon--vanishing permeability at a non-zero value of porosity--may occur nonetheless. Based on these considerations, we have assumed the following relationship:

$$k = k_0 \left(\frac{\varphi^n - \varphi_c^n}{\varphi_0^n - \varphi_c^n} \right) \qquad (12)$$

where

k_0 = initial value of permeability

φ_0 = initial value of porosity

φ_c = 'critical' porosity for through-flow

n = exponent

Hence, $k = k_0$ for $\varphi = \varphi_0$, $k = 0$ for $\varphi = \varphi_c$. With $n = 3$, Eqn. (12) is similar to the 'Kozeny' equation [cf. Brace, 1977, p. 3343, Eqn. 3], which describes the relationship between k and φ for some rocks. We have taken $n = 2$ and $\varphi_c = 0.0002$, the latter being much less than porosities typically measured for crystalline rocks ($\varphi \geq 0.001$). These values of n and φ_c should lead to a relatively conservative estimate of the effect of porosity reduction on permeability. This $k - \varphi$ relationship is illustrated in Fig. 1-1.

In Fig. 1-2 we have plotted, for several values of $\dot{\Phi}$, the dimensionless fluid pressure $\tilde{P}_f$, defined as $\tilde{P}_f = P_f / \rho_r g z$, as a function of depth for a section undergoing uniform porosity- and, hence, permeability reduction, with the relevant parameters as given above. It is clear from Fig. 1-2 that both the rate and magnitude of excess-pressure buildup would be sensitively dependent upon the rate of porosity reduction, with little excess pressure generated for $\dot{\Phi}$ much less than the 'critical' value.

Although the results presented above indicate the potential importance of porosity reduction in influencing P_f development, they do not allow us to examine the way in which *nonuniform* porosity reduction within a crystalline section would affect fluid pressure. Such nonuniform $\dot{\Phi}$ might be expected, for example, if porosity-reduction processes are dependent on temperature and

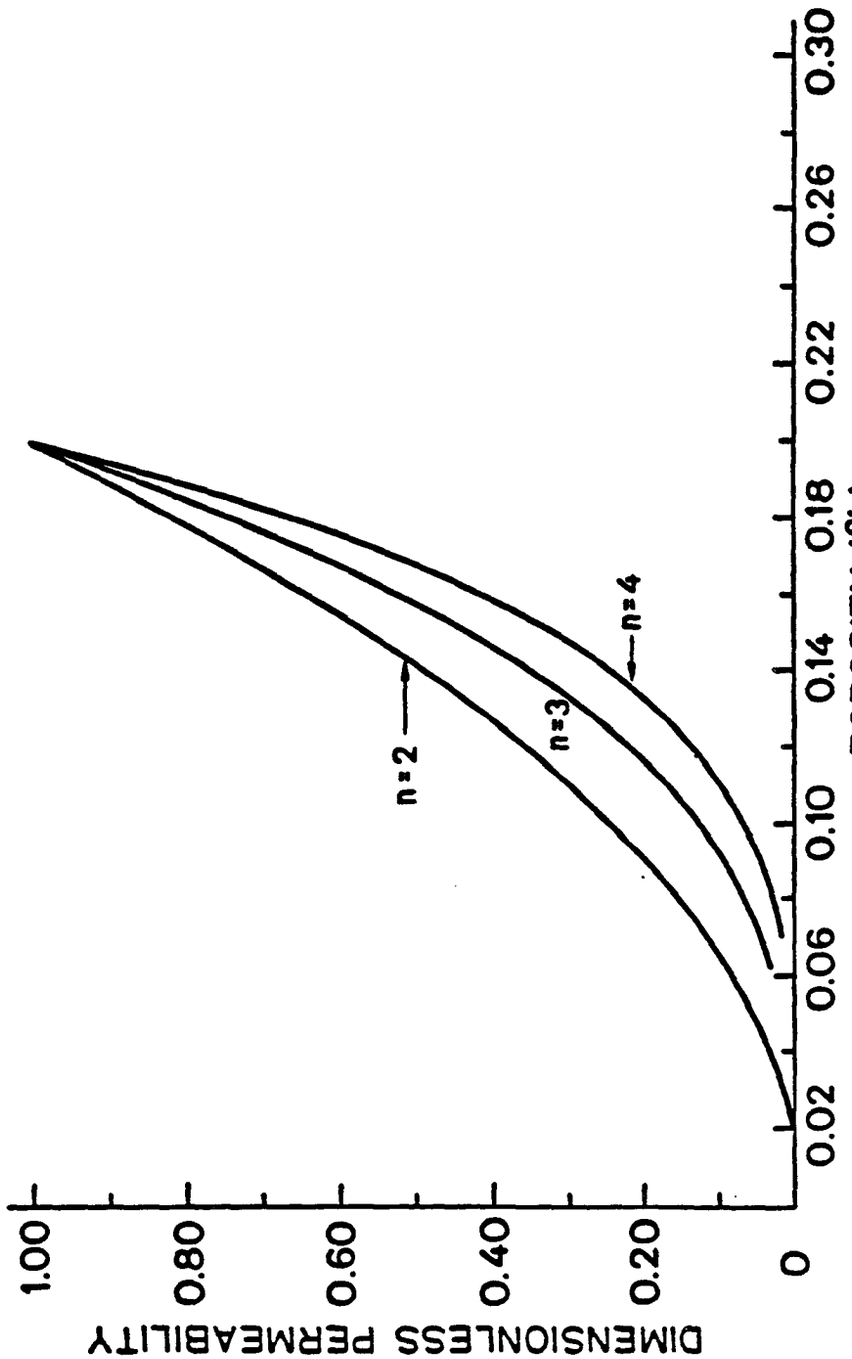

Figure 1-1: Dimensionless permeability $\frac{k}{k_0}$ as a function of porosity for the permeability-porosity relationship given by Eqn. (12). Curves have been calculated for $\varphi_0 = 0.002$, $\varphi_c = 0.0002$.

Figure 1-2: Fluid pressure as a function of depth for a 10 km thick section undergoing uniform porosity reduction, for several values of porosity-reduction rate $\dot{\Phi}$(in s^{-1}). Initial permeability is 50 ndarcy. Solid lines show hydrostatic and lithostatic pressure gradients. Dashed curves show fluid-pressure profiles that would develop after porosity reduction for 2500 a at indicated rates. Note that fluid pressure would exceed lithostatic for the largest $\dot{\Phi}$ value, which slightly exceeds the 'critical' value for this geometry and permeability.

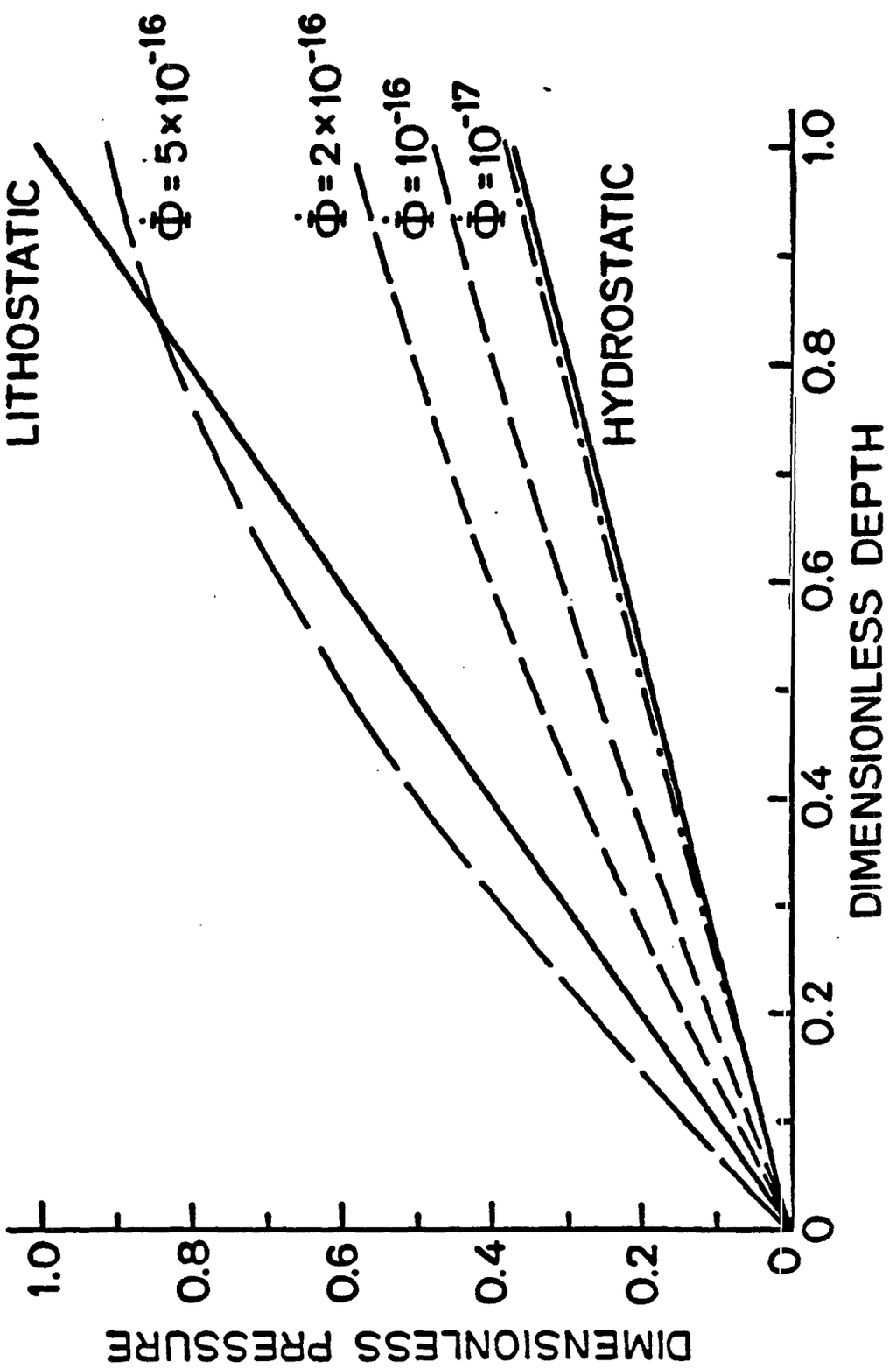
LITHOSTATIC
$\dot{\Phi}=5\times10^{-16}$
$\dot{\Phi}=2\times10^{-16}$
$\dot{\Phi}=10^{-16}$
$\dot{\Phi}=10^{-17}$
HYDROSTATIC
DIMENSIONLESS PRESSURE
DIMENSIONLESS DEPTH
0
0.2
0.4
0.6
0.8
1.0

pressure. In order to examine this situation, we have considered the plausible case of depth-dependent $\dot{\Phi}$. We have calculated P_f development in a three-layer crustal section, again using finite-difference techniques applied to Eqn. (7). Boundary and initial conditions are the same as in the previous calculations, with the added constraints that pressure and fluid flux must be continuous at interfaces between layers. These can be expressed as

$$(P_f)^u = (P_f)^l \quad at \ z = z_i \tag{13a}$$

and

$$k^u\left(\frac{\partial P_f}{\partial z}\right)^u = k^l\left(\frac{\partial P_f}{\partial z}\right)^l \quad at \ z = z_i \tag{13b}$$

where the superscripts u and l refer to the 'upper' and 'lower' layers corresponding to the interface at $z = z_i$. In these calculations, the initial values of permeability and porosity generally differ from layer to layer, as do values of $\dot{\Phi}$. Results of some calculations are shown in Figs. 1-3a-f. Although the number of parameters involved here--k, φ, $\dot{\Phi}$, and thickness for each layer--makes it very difficult to come up with a simple criterion for conditions favoring excess-pressure buildup, certain generalizations can be made. First, it appears that we can characterize fluid-pressure development during a specified time period by the excess pressure developed at the boundary between the center and lower layers. We will denote this pressure as P_E. Furthermore, the scaling arguments developed for the single-layer case suggest that excess pressure cannot arise unless permeability over at least some depth interval is quite low. Such low-permeability zones (*ca.* 50 ndarcy) probably will not occur very near the surface. We also expect the porosity distribution with depth in crystalline rocks not to vary dramatically. Accordingly, the most significant parameters (for a specified set of layer thicknesses) would appear to be k_u, the permeability of the upper layer, and

Figure 1-3: Fluid pressure as a function of depth for three-layer model, for elapsed time of 2500 a. For all plots, total thickness is 20 km; porosities are 0.3, 0.2, and 0.2 in upper, center, and lower layers, respectively; permeabilities are 50 ndarcy and 25 ndarcy in center and lower layers, respectively; porosity-reduction rates are $10^{-20}\,s^{-1}$ and $5\times10^{-18}\,s^{-1}$ in upper and lower layers, respectively.

Figure 1-3a: Upper, center and lower layer thicknesses are 8, 2, and 10 km, respectively; $\dot{\Phi}_C = 10^{-17}\,s^{-1}$; $k_y = 1\,\mu$darcy. Pressure profile is for elapsed time of 2500 a.

Figure 1-3b: Same as Figure 1-3a except $k_y = 10\,\mu$darcy.

Figure 1-3c: Same as Figure 1-3a except $\dot{\Phi}_C = 5\times10^{-18}\,s^{-1}$.

Figure 1-3d: Same as Figure 1-3b except $\dot{\Phi}_C = 5\times10^{-18}\,s^{-1}$.

Figure 1-3e: Upper, center, and lower layer thicknesses are 5, 2, and 13 km, respectively; $\dot{\Phi}_C = 10^{-17}\,s^{-1}$; $k_y = 10\,\mu$darcy.

Figure 1-3f: Same as Figure 1-3e except $\dot{\Phi}_C = 5\times10^{-18}\,s^{-1}$.

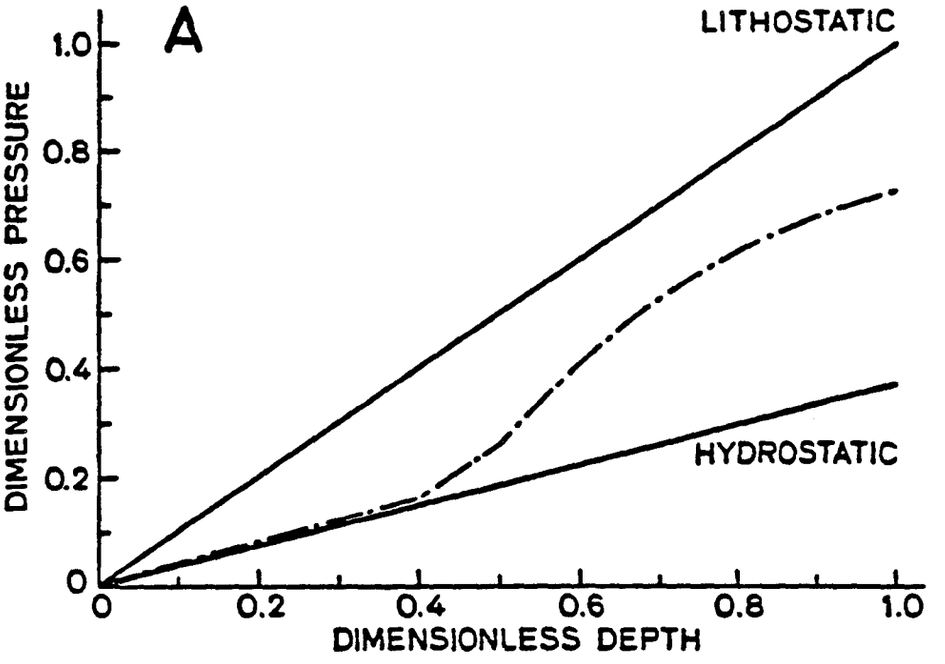
A
LITHOSTATIC
HYDROSTATIC
DIMENSIONLESS PRESSURE
DIMENSIONLESS DEPTH
0
0.2
0.4
0.6
0.8
1.0

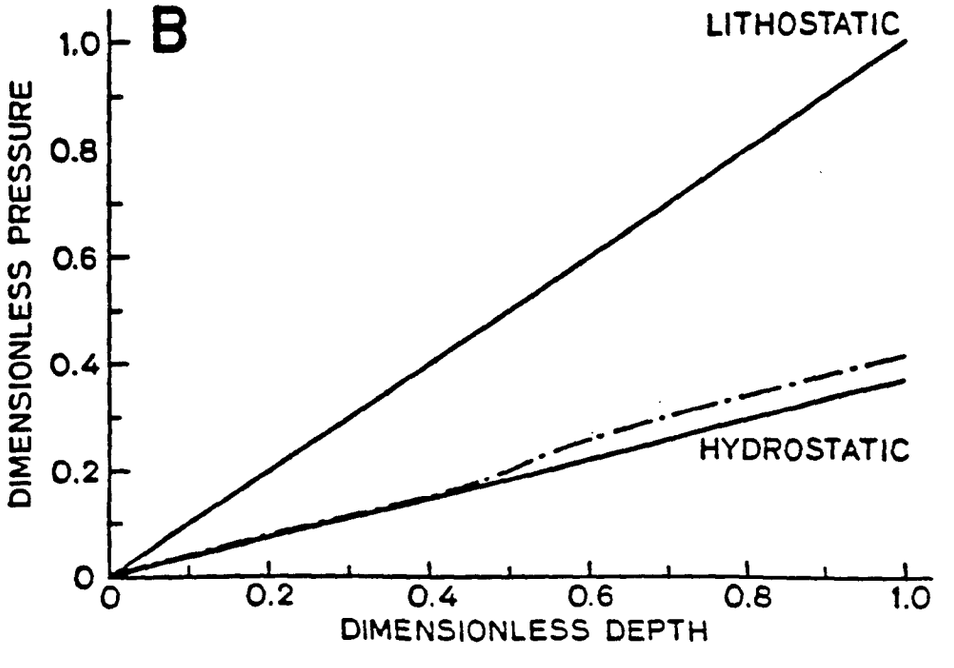
B
LITHOSTATIC
HYDROSTATIC
DIMENSIONLESS PRESSURE
DIMENSIONLESS DEPTH
0
0.2
0.4
0.6
0.8
1.0

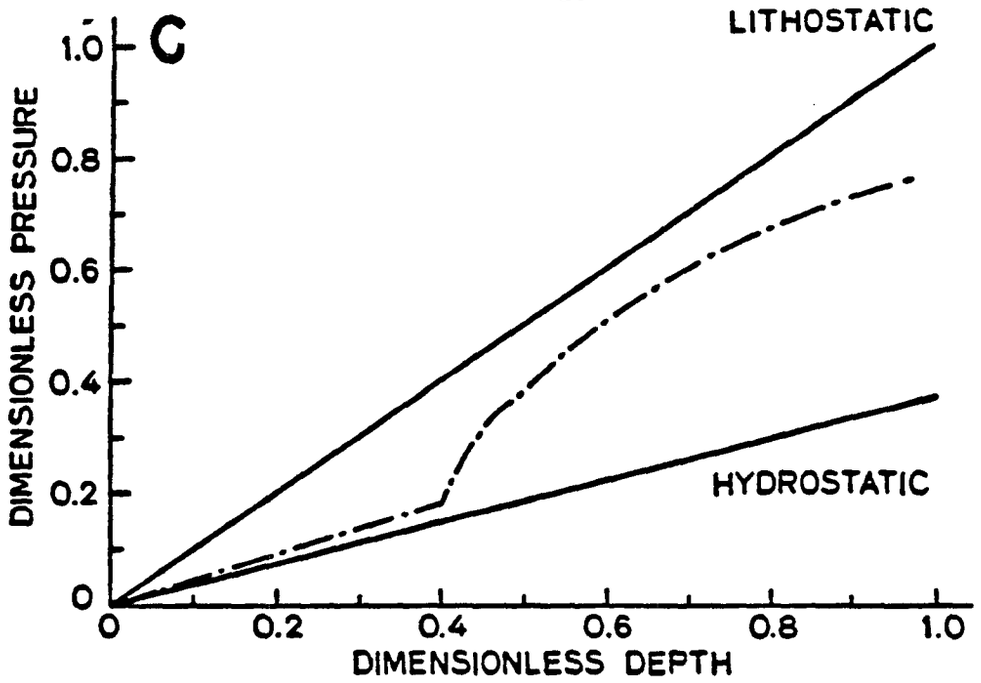
C
LITHOSTATIC
HYDROSTATIC
DIMENSIONLESS PRESSURE
DIMENSIONLESS DEPTH
0
0.2
0.4
0.6
0.8
1.0

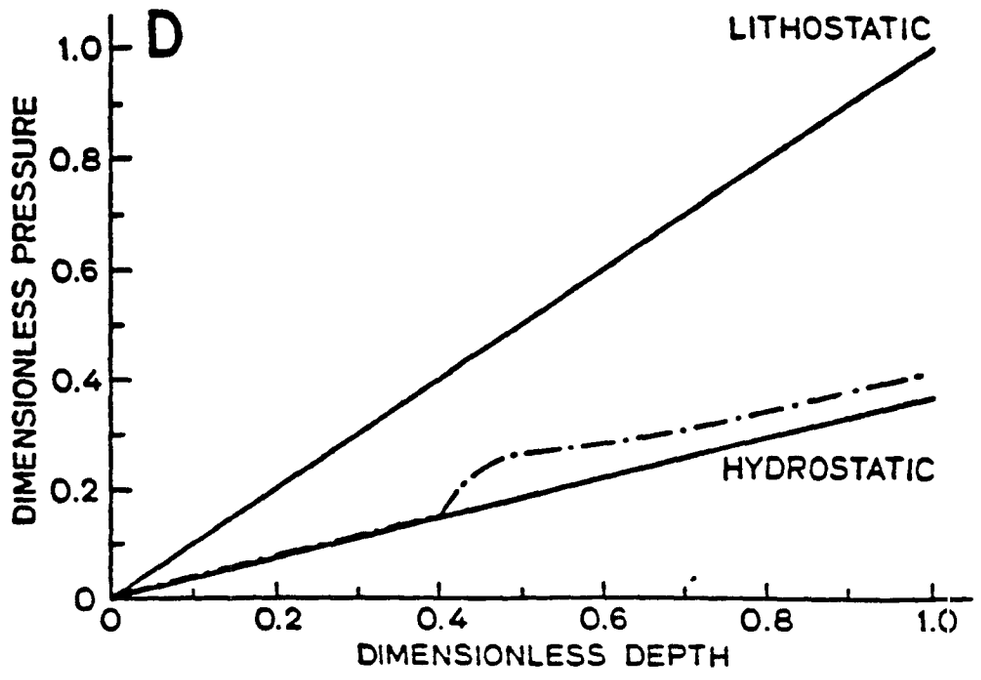
D
LITHOSTATIC
HYDROSTATIC
DIMENSIONLESS PRESSURE
DIMENSIONLESS DEPTH
0
0.2
0.4
0.6
0.8
1.0

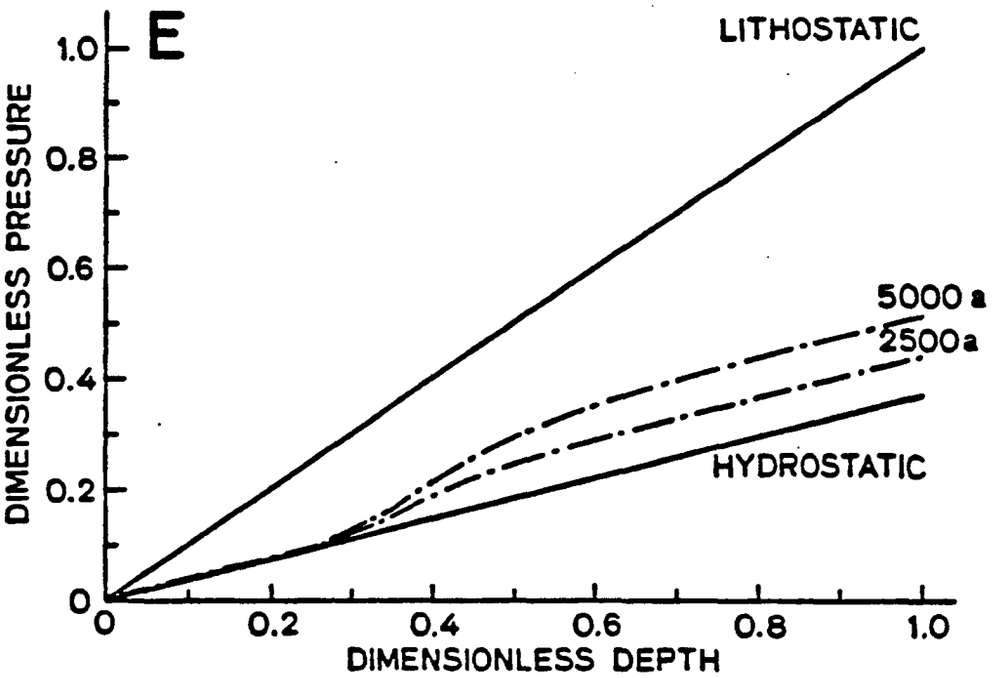
E
LITHOSTATIC
5000 a
2500 a
HYDROSTATIC
DIMENSIONLESS PRESSURE
DIMENSIONLESS DEPTH
0
0.2
0.4
0.6
0.8
1.0

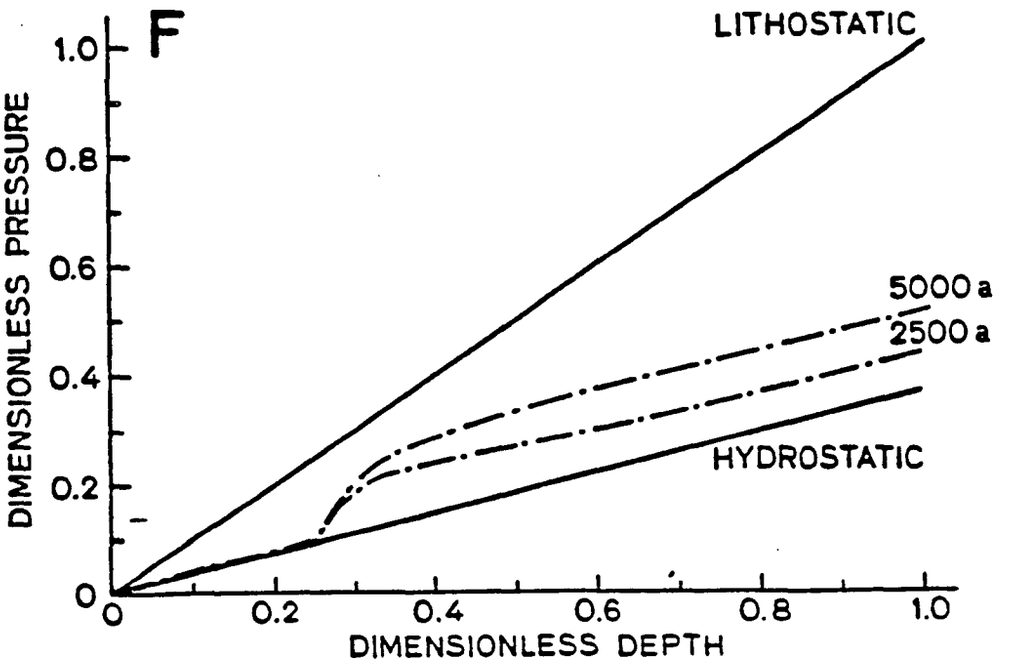
F
LITHOSTATIC
5000 a
2500 a
HYDROSTATIC
DIMENSIONLESS PRESSURE
DIMENSIONLESS DEPTH
0
0.2
0.4
0.6
0.8
1.0

$\dot{\Phi}_U$, $\dot{\Phi}_C$, and $\dot{\Phi}_L$, the porosity-reduction rates in the upper, center, and lower layers, respectively.

In Figs. 1-4a-c, we have plotted P_E as a function of k_U for upper, center, and lower layer thicknesses of 8, 2, and 10 km, respectively. In each of these figures, we treat as fixed two of the three porosity-reduction rates and vary the third as a parameter. From Fig. 1-4a ($\dot{\Phi}_U$ variable), we see that as long as porosity reduction at depth is relatively rapid ($\dot{\Phi}_C = 5\times10^{-15}\,s^{-1}$, $\dot{\Phi}_L = 5\times10^{-16}\,s^{-1}$), the effect of $\dot{\Phi}_U$ on P_E will be negligible. (As expected, P_E decreases as k_U increases.) Variations in $\dot{\Phi}_C$ and $\dot{\Phi}_L$ may be significant, however. In Fig. 1-4b, we show P_E *vs.* k_U for the case of slow, near-surface porosity reduction ($\dot{\Phi}_U = 10^{-20}\,s^{-1}$), but relatively rapid porosity reduction in the lowest part of the section ($\dot{\Phi}_L = 5\times10^{-16}\,s^{-1}$). We see that some excess pressure will be generated, even for low values ($10^{-20}\,s^{-1}$) of $\dot{\Phi}_C$; this excess pressure is a result of porosity reduction in the lowest part of the section. In fact, the magnitude of the excess pressure will show little variation for $10^{-20}\,s^{-1} < \dot{\Phi}_C < 5\times10^{-16}\,s^{-1}$; however, if $\dot{\Phi}_C > ca.\ 10^{-15}\,s^{-1}$, P_E will increase considerably. Finally, Fig. 1-4c shows P_E *vs.* k_U for $\dot{\Phi}_U = 10^{-20}\,s^{-1}$, $\dot{\Phi}_C = 5\times10^{-15}\,s^{-1}$, and $\dot{\Phi}_L$ variable. We see that with such a rapid rate of porosity reduction in the center layer, there will always be a noticeable excess-pressure development, even though the center layer is relatively thin. $\dot{\Phi}_L$ will have little effect on P_E in this case unless it exceeds $ca.\ 10^{-16}\,s^{-1}$.

It should be emphasized that in all of our P_f models, we have taken $\dot{\Phi}$ to be constant. Obviously, this would eventually lead to a state in which permeability would vanish. Continued porosity reduction in the zone of highest $\dot{\Phi}$ would then lead to rapid buildup of P_f to lithostatic. As we discuss later, this

Figure 1-4: Dimensionless excess pressure P_E (see text for definition) developed after 2500 a, as a function of k_y, the permeability of the upper layer, for three-layer model.

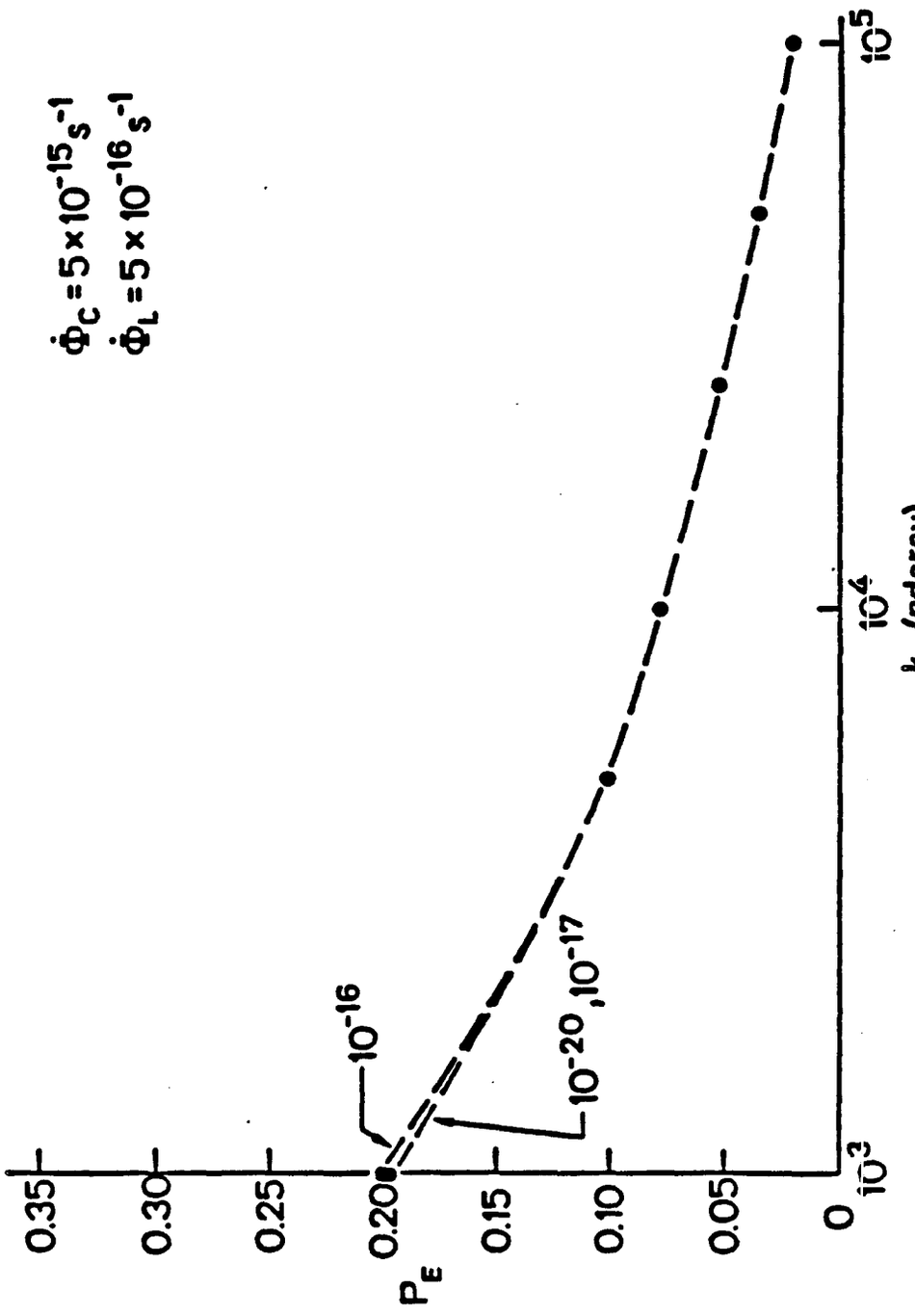

Figure 1-4a: Parameter is $\dot{\Phi}_y$ in s^{-1}.

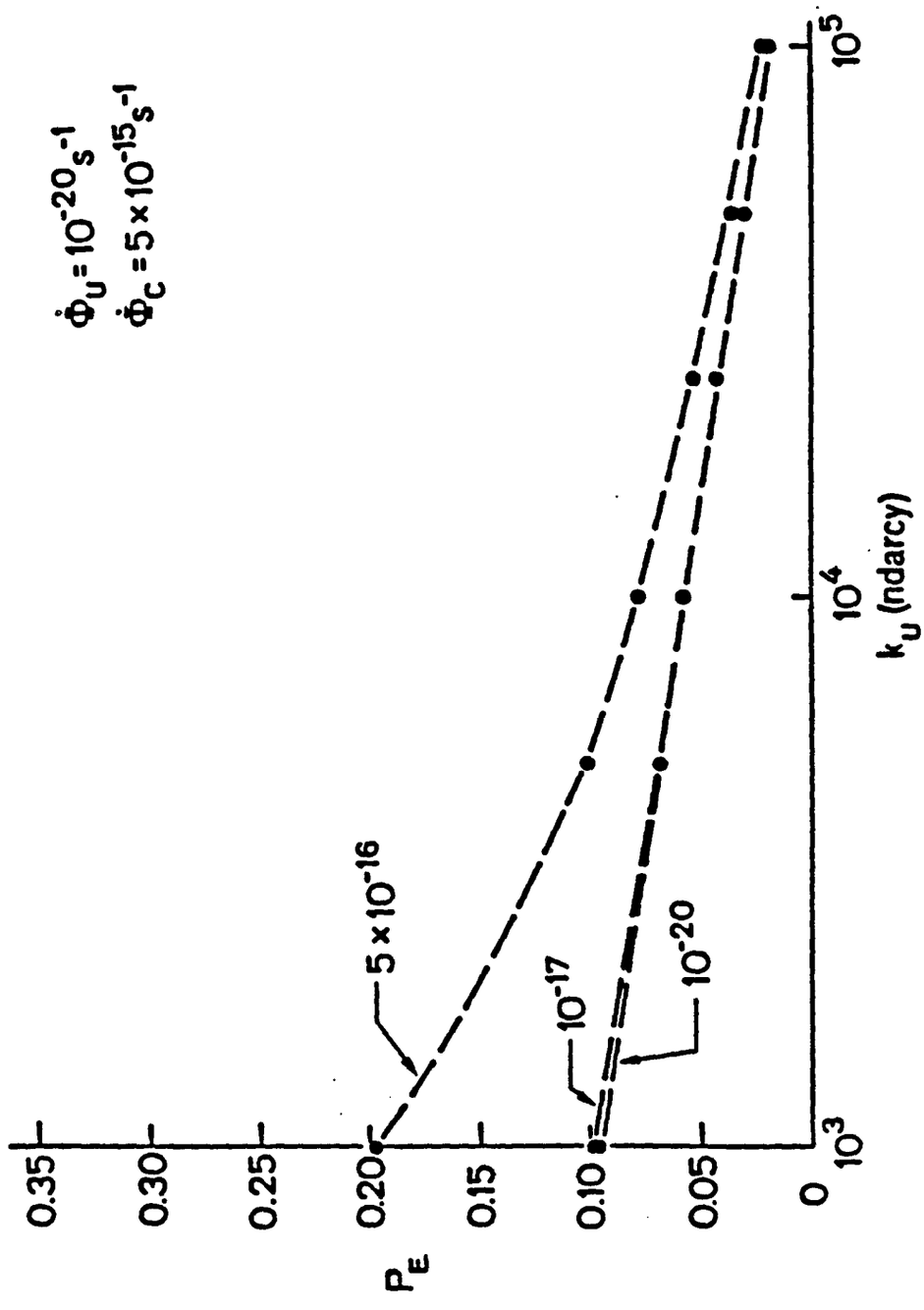

Figure 1-4c: Parameter is $\dot{\Phi}_L$ in s^{-1}.

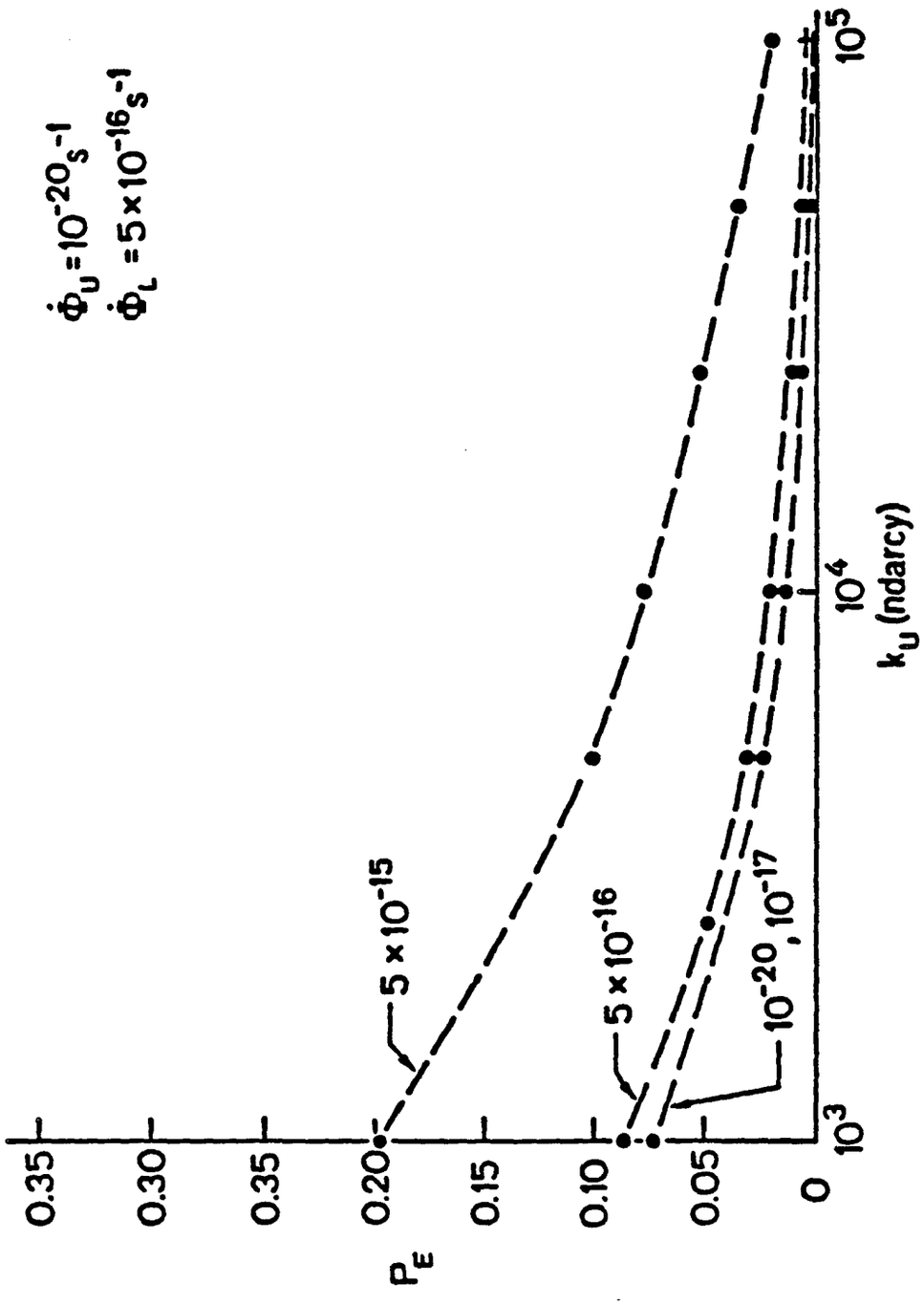

Figure 1-4b: Parameter is $\dot{\Phi}_C$ in s^{-1}.

would probably lead to brittle failure (natural hydraulic fracture) within the high P_f zone, thereby increasing φ and k and allowing the excess fluid pressure to dissipate partially. Our profiles of P_f as a function of depth are thus hypothetical 'snapshots' of P_f distribution.

If fractures were, in fact, to develop across high-P_f zones, thereby locally relieving high P_f, one might suppose that further development of elevated P_f in crustal blocks bounded by such fractures would be strongly inhibited. In order to investigate this hypothesis, we have extended our finite-difference calculations to a two-dimensional crustal model, i.e., we have solved the equation

$$\frac{1}{c}\frac{\partial P_f}{\partial t} = \frac{\partial^2 P_f}{\partial y^2} + \frac{\partial^2 P_f}{\partial z^2} + \frac{\mu \dot{\Phi}}{k} \tag{14}$$

where y is a horizontal coordinate. The boundary and initial conditions are

i) $P_f\,(z = 0) = 0$

ii) $\frac{\partial \hat{P}}{\partial z}(z = L) = 0$

iii) $\hat{P}\,(y = \pm \frac{W}{2}) = 0$

iv) $\hat{P}\,(t = 0) = 0$

where, as before, $\hat{P} = P_f - \rho_f g z$ is the 'excess' fluid pressure. Pressure and flux continuity are also imposed at layer interfaces (cf. Eqns. 13a-b). The important new boundary condition (iii) indicates that we are assuming that fluid pressure at the 'vertical' boundaries of the crustal block is hydrostatic. This might correspond physically to the case of very permeable fault zones. Some results of calculations for P_f development are illustrated in Fig. 1-5, in which we show $\tilde{P}_f$ as a function of z and t along the 'centerline' $y = 0$, for several values of W. It appears that although the existence of very permeable

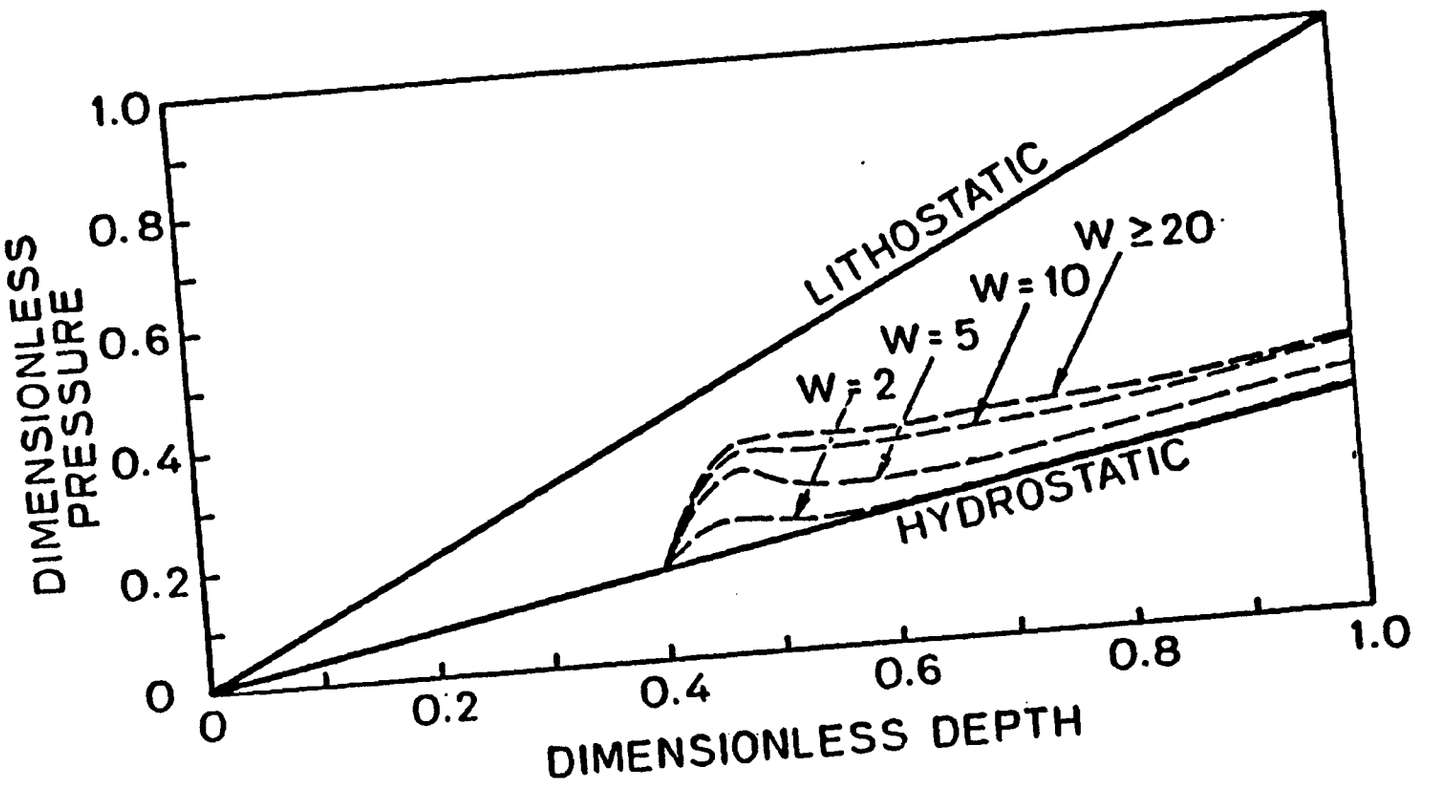

Figure 1-5: Fluid pressure as a function of depth for three-layer, two-dimensional model, for several values of layer width *W*. Parameter values are the same as for Figure 1-3c. Fluid pressure along the 'centerline' of the layers is plotted. Elapsed time is 5000 a.

zones bounding crustal blocks would decrease the rate of P_f increase due to porosity reduction, such pressurization would not be eliminated. Only very dense networks of fault zones would be able to eliminate P_f buildup associated with porosity reduction. As an added complication, it is by no means obvious that natural fault zones are, in fact, particularly permeable [Seeburger, 1981].

3. SOME CONSIDERATIONS OF POROSITY-REDUCTION MECHANISMS

The simple mathematical model presented above indicates that porosity-reduction processes could have a major effect on P_f development in low-porosity crustal rocks. The precise mechanisms by which such porosity reduction might occur are uncertain, although two broad classes might reasonably be considered, viz.:

i) Precipitation of material transported in solution by circulating fluids;

ii) Local redistribution of solid material.

To model porosity reduction by precipitation, we consider deposition in pores of silica transported by rising pore fluids. Solubility of silica (as quartz) generally decreases as fluid pressure and temperature decrease; hence, if fluids are saturated at depth, they should tend to deposit silica as they rise, assuming that significant supersaturation does not occur.

We begin with continuity considerations, this time writing two mass conservation relationships, one for the solvent, the other for the solute. Let S be the solubility of silica (as quartz), expressed as a mass fraction (mass of solute per unit mass of solution), and ρ_S be the solution density. Conservation of solvent mass is then expressed as

$$\frac{\partial}{\partial t}\left[\rho_S (1-S)\varphi\right] = -\nabla\cdot\left[\rho_S (1-S)\vec{u}\right] \qquad (15)$$

Solute mass transport must take account of precipitation of silica from

solution. Assuming that any precipitated material has the same density ρ_r as the host rock, we can express the solute mass balance as

$$\frac{\partial}{\partial t}(\rho_S S\varphi) = -\nabla\cdot(\rho_S S\vec{u}) - \rho_r\dot{\Phi} \tag{16}$$

For cases of interest, with temperatures $<500°C$, S will be less than ca. 0.02 [cf. Kennedy, 1950]. Using tabulated specific volume data (Walther and Helgeson [1977] for silica; Schmidt [1969] for water), it can be shown that the density of the solution will differ from the density of the solvent by much less than 1% for pressures and temperatures of interest. Hence, taking $\rho_S \approx \rho_f$, the continuity relationships may be expressed to a good approximation as

$$\frac{\partial}{\partial t}(\rho_f\varphi) = -\nabla\cdot(\rho_f\vec{u}) \tag{17}$$

$$\frac{\partial}{\partial t}(S\rho_f\varphi) = -\nabla\cdot(S\rho_f\vec{u}) - \rho_r\dot{\Phi} \tag{18}$$

Combining Darcy's law (Eqn. (2)) with Eqn. (17), we find that the modified diffusion equation for P_f development is, as before:

$$\frac{1}{c}\frac{\partial P_f}{\partial t} = \nabla^2 P_f + \frac{1}{k}(\nabla k)_{\text{irrev}}\cdot\nabla P_f + \frac{\mu\dot{\Phi}}{k} \tag{19}$$

The porosity-reduction rate $\dot{\Phi}$ can be found by using Eqn. (18) for solute mass conservation. Expanding Eqn. (18), and assuming that flow is only in the vertical z direction, we find

$$-\rho_r\dot{\Phi} = S\frac{\partial}{\partial z}(\rho_f u) + \rho_f u\frac{\partial S}{\partial z} + S\frac{\partial}{\partial t}(\varphi\rho_f) + \varphi\rho_f\frac{\partial S}{\partial t} \tag{20}$$

where u is the magnitude of $\vec{u}$. S will be, in general, a function of temperature T and fluid pressure P_f. Assuming a steady temperature profile, we can write:

$$\frac{\partial S}{\partial z} = \frac{\partial S}{\partial T}\frac{\partial T}{\partial z} + \frac{\partial S}{\partial P_f}\frac{\partial P_f}{\partial z} \tag{21}$$

and

$$\frac{\partial S}{\partial t} = \frac{\partial S}{\partial P_f}\frac{\partial P_f}{\partial t} \tag{22}$$

Expanding the derivatives in Eqn. (20), using Eqns. (21), (22), and Darcy's law, and neglecting terms of $O[(\partial P_f / \partial z)^2]$, we can write, after some rearrangement:

$$(\rho_r + S\rho_f)\dot{\Phi} = \frac{S k \rho_f}{\mu}\left(\frac{\partial^2 P_f}{\partial z^2} - \frac{1}{\hat{c}}\frac{\partial P_f}{\partial t}\right) + \frac{k\rho_f}{\mu}\frac{\partial S}{\partial T}\frac{\partial T}{\partial z}\frac{\partial P_f}{\partial z} + \frac{S\rho_f}{\mu}\left(\frac{\partial k}{\partial z}\right)_{irrev}\frac{\partial P_f}{\partial z} \tag{23}$$

where

$$\frac{1}{\hat{c}} = \frac{1}{c} + \frac{\mu\varphi}{k}\left(\frac{1}{S}\frac{\partial S}{\partial P_f}\right)$$

In the temperature/pressure range of interest ($T <$ ca. 300° C, $P_f <$ ca. 1 kbar), experimental data on quartz solubility [Kennedy, 1950] indicate that temperature effects on solubility dominate over pressure effects. For example, using Kennedy's Fig. 2, we can estimate that at $T = 260°$ C and $P_f =$ ca. 1 kbar, $(\partial S/\partial T)_{P_f} \approx 6\times10^{-6}$ °C^{-1} and $(\partial S/\partial P_f)_T \approx 10^{-7}$ bar^{-1}. If we imagine fluid at these conditions rising 1 km, cooling by 20–30° C and depressurizing by 100-250 bars, then $(\Delta S)_{cooling} \approx 1.2\text{–}1.8\times10^{-4}$, whereas $(\Delta S)_{depressurization} \approx 1\text{–}2.5\times10^{-5}$. The rate of porosity reduction by precipitation from rising fluid should therefore be given roughly by the second term on the right hand side of Eqn. (23), because this term describes the effect of decreasing temperature on solubility. Recognizing that $S\rho_f \ll \rho_r$, we can write

$$\dot{\Phi} \approx \left(\frac{k\rho_f}{\mu\rho_r}\right)\frac{\partial S}{\partial T}\frac{\partial T}{\partial z}\frac{\partial P_f}{\partial z} \tag{24}$$

To get some idea of the magnitude of $\dot{\Phi}$ in this process, we can approximate the various quantities on the right-hand side of Eqn. (24) as $(\rho_f / \rho_r) \approx 0.35$, $\mu \approx 2\times10^{-3}$Pa s, $\partial S / \partial T \approx 6\times10^{-6}\,°C^{-1}$, $\partial T / \partial z \approx 25°C/km$, and $\partial P_f / \partial z \approx 250$ bar/km $= 2.5\times10^{4}$Pa/m. (The fluid-pressure gradient indicated is nearly lithostatic and could not be maintained if the permeability were very high.) Using these estimated values, we obtain

$$\dot{\Phi} \approx 6.6k \quad [s^{-1}]$$

for k in mks units. Taking $k = 50 ndarcy = 5\times10^{-20}\,m^2$, we find $\dot{\Phi} \approx 3.3\times10^{-19}\,s^{-1}$. Recalling earlier results, we see that this value of $\dot{\Phi}$ is considerably less than what would be required to produce or maintain elevated P_f at the specified permeability. We also recall from Eqn. (11) that the porosity-reduction rate necessary for excess-pressure development increases in proportion to k. Therefore, a calculation similar to that just presented would show the same qualitative result--$\dot{\Phi}$ much less than the 'critical' value--for any value of k. Hence, it appears that porosity reduction due to silica deposition from rising fluids, although it almost certainly occurs, is much too slow to produce or maintain elevated fluid pressures in most geological environments. This mechanism of porosity reduction probably has a significant effect on hydrologic conditions, however, in geologic systems characterized by very high temperature gradients and flow rates, such as found in geothermal systems [e.g., Facca and Tonani, 1967; Elders and Bird, 1976] or laboratory studies of flow down temperature gradients [e.g., Morrow et al., 1981].

Although the discussion above certainly does not eliminate the 'precipitation' mechanism as operative, it does suggest that if porosity reduction is an important process in producing elevated P_f in crystalline crustal rocks, then a 'local' rather than large scale mechanism of porosity

reduction may be responsible. This is in conceptual accord with recent thermodynamic considerations of pressure solution. Robin [1978], in a very lucid discussion of the driving force for pressure solution at grain-to-grain contacts, showed (p. 1386) that whenever two solid grains are in contact, there is a chemical-potential gradient tending to drive the solid component to the periphery of the contact. This chemical potential is essentially *proportional* to the effective pressure $P_e = P_c - P_f$, i.e., the difference between overburden pressure and fluid pressure. Raj [1982] has argued that except at very small effective stresses, such a thermodynamic force will tend to produce "densification", i.e., volumetric strain, even in the absence of deviatoric stresses. This densification results from transfer of solid mass locally (i.e., on the grain scale) via a fluid phase. Raj's preliminary experimental results tended to support his theoretical arguments. Dibble et al. (unpublished) have also argued that a finite value of P_e always produces a thermodynamic tendency for pressure solution and porosity reduction. They suggest, on the basis of experimental work by Sprunt and Nur [1977], that the rate-controlling process in porosity reduction is the growth of 'unstressed' mineral grains, i.e., grains not subjected to deviatoric stresses.

4. DISCUSSION

Relationship between porosity reduction and brittle fracture

We have suggested above that porosity-reduction processes in crustal rocks are likely to involve localized solid mass transfer via a fluid phase. Such mass transfer will probably cause strain within the solid. Possible relationships between porosity reduction and strain, or between porosity reduction and deformation in general, may be indirectly examined by studying rocks that

were once at considerable depths in the crust. The occurrence of porosity-reduction processes in such rocks is indicated by detailed studies by optical- and scanning electron microscopy [e.g., Richter and Simmons, 1977a; Sprunt and Nur, 1979; Padovani et al., 1982]. These studies have clearly demonstrated that crack healing and sealing are ubiquitous in a wide variety of crustal rock types, particularly crystalline rocks, where 'healing' refers to former cracks in which the mineral filling is the same as the host grain, 'sealing' to cases in which the crack filling is mineralogically different from the host grain. The material source for healing is likely to be quite local, whereas sealing requires an 'external' or 'remote' source of crack-filling material. Abundant evidence based on relative dating of microcracks demonstrates that these porosity-reducing healing and sealing processes occur *episodically* during the history of a rock mass, with porosity reduction alternating with microcracking that *increases* porosity. This point has been particularly well documented in studies by Batzle and Simmons [1976] and Padovani et al. [1982]. (For terminological clarity, we note that the pore space of crystalline rocks is composed dominantly of 'cracks', i.e., very tabular pores.)

The notion of episodic porosity reduction and microcracking is consistent with our model of P_f development in crustal rocks. If porosity reduction occurred rapidly enough, P_f could build up to the point where it would reach the least compressive principal stress. This would tend to cause brittle fracturing and a drop in P_f. However, as the results of our two-dimensional model calculations suggest, such fracturing may not be sufficient to inhibit further porosity reduction and buildup of P_f to values approaching lithostatic. Thus, repeated fracturing events followed by crack healing might occur, as suggested by Yardley [1983] and by Smith and Evans [in press]. This notion is

also supported by detailed studies of 'crack-seal' deformation [e.g., Ramsay, 1980; Cox and Etheridge, 1983]. These studies have shown that mineralized extensions veins in deformed rocks, including those subjected to low-grade metamorphic conditions, are often the product of numerous, distinct episodes of fracturing and mineralization. The cyclic fracturing-healing concept has also been advanced in connection with the mechanism of earthquakes [Angevine et al., 1982]. A somewhat similar phenomenon, that of episodic fluid-pressure buildup, followed by abrupt fluid release, has also been suggested to be of significance during development of some sedimentary basins [Cathles and Smith, 1983; chapter 4, this dissertation].

Porosity-reduction rates: guidelines from experimental work

A central issue in discussing porosity reduction and P_f development is the rate of porosity reduction. We have suggested that, for low-permeability crystalline rocks in the crust, porosity-reduction rates greater than about $4 \times 10^{-16} s^{-1}$ could lead to elevated fluid pressure, which might then cause brittle fracturing. Although there has been little laboratory work focused on porosity reduction in crystalline rocks, recent experimental studies give us some indication that porosity reduction could occur relatively rapidly. For example, Sprunt and Nur [1977] measured appreciable porosity loss, presumably due to pressure solution, in sandstone cores subjected to elevated temperatures and pressures for two weeks. However, the macroscopic shear stress in the cores makes it difficult to use this result as an indicator of porosity-reduction rates in rocks not subjected to overall (e.g., tectonic) deviatoric stresses. In fact, in the samples not subjected to deviatoric stresses, porosity reduction during the two-week duration of experiments was too little, if any, to be measured.

In an important recent study, Smith and Evans [in press] examined healing of cracks in synthetic quartz under conditions of elevated pressure ($P_f = P_c = 2$ kbar) and temperature (200–600°C). Morphologically, healed cracks were strikingly similar tc fluid inclusions and 'microtubes' commonly seen in thin sections [e.g., Richter and Simmons, 1977b]. Smith and Evans found that cracks healed extremely rapidly (in less than 1 h) at 400°C, but saw no measurable healing in 48 h at 200°C. They suggested on the basis of kinetic considerations that healing rates would have been less by a factor of roughly 1000 at 200°C than at 400°C, concluding that "microcracks in quartz will have geologically short lifetimes at temperatures of 200°C or greater." If these results are applicable to rock *in situ*, then it seems clear that crack healing could be extremely rapid on a geologic time scale, even under upper crustal conditions. Within the context of the present model, such rapid crack healing could lead to a quasi-equilibrium state in which, averaged over time and space, the porosity of a rock mass would remain relatively constant, the permeability would remain rather low, and fluid pressure would be maintained in excess of hydrostatic.

Additional laboratory studies of pressure solution and crack healing at crustal conditions have the potential of yielding very valuable data on rates and mechanisms of porosity reduction in the crust.

Excess fluid pressure and low velocity zones in the crust

As mentioned previously, remote detection of elevated P_f at depth is difficult, if not impossible, at present. One potential method of indirect detection of zones of elevated P_f might be seismic. Such zones at depth should lead to a decrease in the effective stress $P_c - P_f$, a drop in seismic wave velocities, and possibly to seismic low velocity zones [cf. Berry and Mair, 1977].

To test the sensitivity of seismic parameters to the state of crustal fluid pressure, we have calculated the compressional wave velocity, V_P, as a function of depth for several cases of P_f development in crustal layers. Several examples were calculated by using the empirical relationship developed by Jones [1983]:

$$V_P = A + B P_e - C e^{-D P_e} \tag{25}$$

where A, B, C, and D are constants. The effective pressure P_e in Eqn. (25) is defined by

$$P_e = P_c - \alpha P_f \tag{26}$$

where $\alpha \leq 1$ [Nur and Byerlee, 1971]. Jones [1983] has also given an empirical relationship for $\alpha = \alpha(P_f)$:

$$\alpha = 1 - F e^{-P_f / G} \tag{27}$$

Values for A, B, C, D, F, and G for several rock types have been calculated by Jones [1983]. For our purposes, we have used his values for Westerly Granite, viz., A = 5.98 km s^{-1}, B = 0.068 km s^{-1} kbar^{-1}, C = 0.5 km s^{-1}, D = 5 kbar, F = 0.5, and G = 0.4 kbar.

Within the context of the present model, in which P_f is generally not constant, the calculated magnitude of velocity decrease ΔV_P will obviously be a function of time. Fig. 1-6 shows V_P *vs.* depth for the corresponding P_f profiles in Figs. 1-3a, 1-3c, and 1-3f, at times for which a substantial excess pressure has developed within some depth interval. Clearly, in these model low velocity zones, ΔV_P is very small, certainly less than 0.05 km/s. This is considerably less than values of ΔV_P inferred from crustal seismology studies [e.g., Berry and Mair, 1977; Mueller, 1977], which indicate ΔV_P in the range of 0.5-1 km/s. Such large changes occur only in the pressure range range $P_e \approx$ 0-1 kbar; for

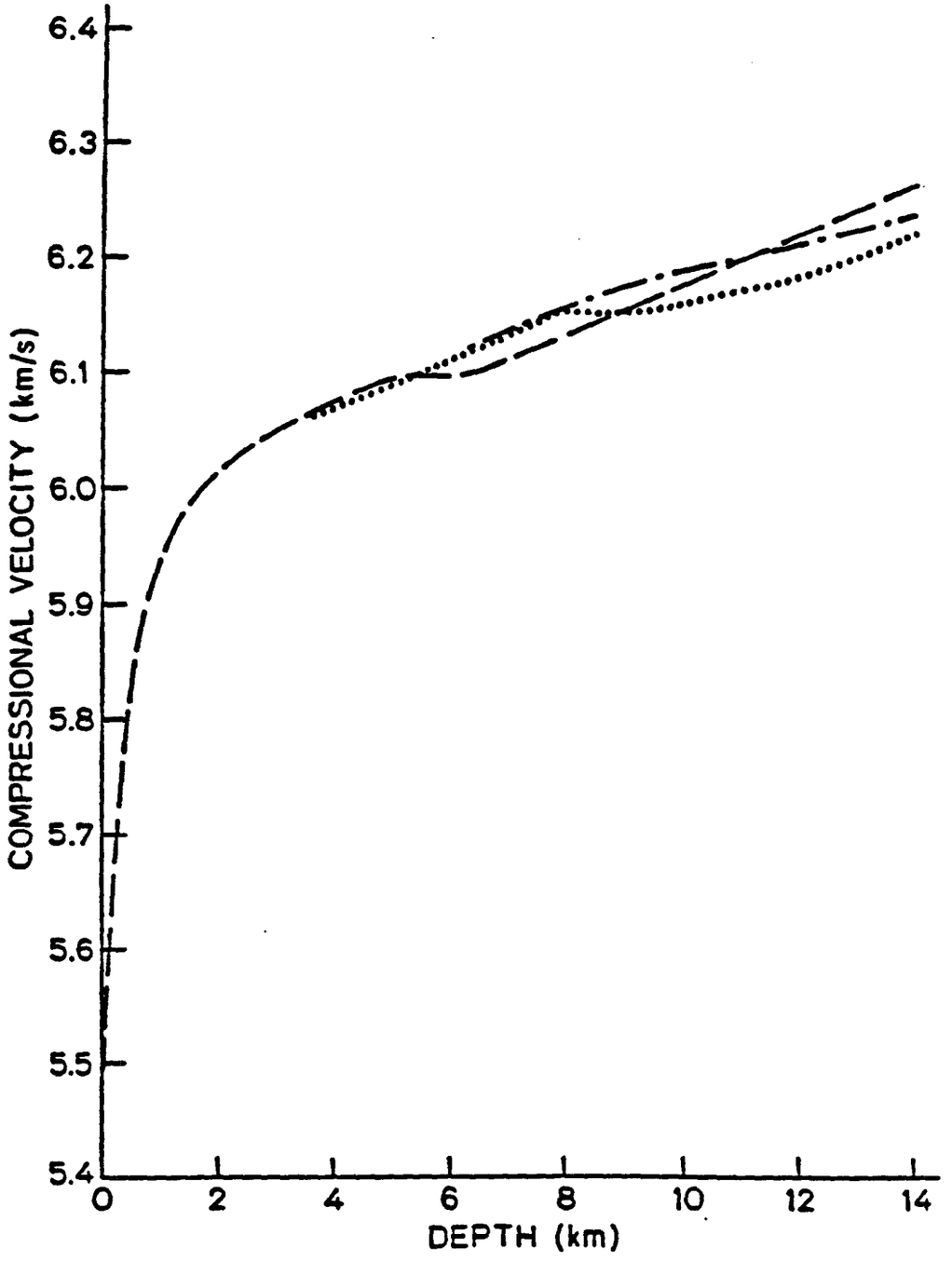

Figure 1-6: Compressional velocity as a function of depth for granitic rock undergoing porosity reduction. Curve with long dashes corresponds to fluid-pressure profile (at 5000 a) in Figure 1-3f; curve with long and short dashes corresponds to Figure 1-3a; dotted curve corresponds to Figure 1-3c. It appears that localized, moderately elevated fluid pressure at depths greater than 5 km has very little effect on compressional velocity.

larger P_e, V_P increases very slowly [cf. Nur and Simmons, 1969, Fig. 3]. Hence, for depths greater than about 5-6 km, for which $P_e >$ ca. 1 kbar (for hydrostatic P_f), elevated P_f will have little effect on V_P unless pore pressure is close to lithostatic. Interestingly, seismologists who have proposed the existence of crustal low velocity zones typically place such zones at > 6-8 km depth [e.g., Berry and Mair, 1977; Mueller, 1977]. An elevated-P_f origin for such zones would therefore require pore-fluid pressures to be close to lithostatic pressure.

5. SUMMARY

We have examined the potential role of porosity-reduction processes in the Earth's crust. Simple mathematical models show that porosity reduction could often lead to the development of elevated fluid pressure in the crust. Porosity-reduction rates greater than a few times 10^{-18} s^{-1} should lead to significant excess pressures for rocks with permeabilities of ca. 50 ndarcy, a value appropriate for unfractured crystalline rocks at upper- to mid-crustal depths. In general, we expect that crustal hydrologic properties--porosity and permeability--as well as fluid pressure, should be time-dependent, even in regions not undergoing significant tectonic activity.

Mathematical modeling, along with considerations of the thermodynamics of 'pressure solution', suggests that porosity-reduction processes in crustal rocks should often involve mass transfer on a local scale. Elevated fluid pressures generated as a result of local porosity reduction may lead to brittle failure, with partial relief of high fluid pressure. Such fracturing may slow, but probably not eliminate, further fluid-pressure buildup. Hence, episodic fracturing and crack healing are likely to be common processes

throughout much of the crust. This concept is supported by detailed studies of the morphology of cracks in exhumed crustal rocks and of crack healing in synthetic laboratory materials.

Calculations based upon laboratory velocity data demonstrate that elevated fluid pressures generated by porosity-reduction processes in crustal rocks will affect the velocity of compressional waves. To cause observed crustal low velocity zones, fluid pressure must be quite close to lithostatic.

APPENDIX: DERIVATION OF THE MODIFIED DIFFUSION EQUATION FOR PORE PRESSURE

To derive the modified diffusion equation for P_f used in our finite-difference calculations, we begin with Eqn. (3) of the main text, reproduced here:

$$\rho_f \frac{\partial \varphi}{\partial t} + \varphi \frac{\partial \rho_f}{\partial t} = \frac{\rho_f k}{\mu} \nabla^2 P_f + \frac{\rho_f}{\mu} \nabla k \cdot \nabla P_f + \frac{k}{\mu} \nabla \rho_f \cdot \nabla P_f - \frac{\rho_f k}{\mu^2} \nabla \mu \cdot \nabla P_f \tag{A-1}$$

All symbols are as defined in the main text. This expression combines the mass-conservation condition with Darcy's law. We also use the assumption, discussed in the main text, that the time rate of change of porosity has both reversible and irreversible parts, viz.:

$$\frac{\partial \varphi}{\partial t} = \left(\frac{\partial \varphi}{\partial t}\right)_{rev} + \left(\frac{\partial \varphi}{\partial t}\right)_{irrev} \tag{A-2}$$

The reversible part of $\partial \varphi / \partial t$ is given by

$$\left(\frac{\partial \varphi}{\partial t}\right)_{rev} = \varphi \beta_\varphi \frac{\partial P_f}{\partial t} \tag{A-3}$$

where $\beta_\varphi = (1/\varphi)(\partial \varphi / \partial P_f)$ is a 'pore compressibility' that characterizes the elastic change in porosity as P_f changes. The gradient in permeability, which is dependent on porosity, also has reversible and irreversible parts:

$$\nabla k = (\nabla k)_{rev} + (\nabla k)_{irrev} \tag{A-4}$$

The reversible part of ∇k is given by

$$(\nabla k)_{rev} = k \beta_k \nabla P_f \tag{A-5}$$

where $\beta_k = (1/k)(\partial k / \partial P_f)$ is a coefficient characterizing the elastic change in permeability as P_f changes. Finally, we need the equation of state of the fluid (considering only the effect of pressure in our approximation):

$$\frac{1}{\rho_f}\frac{\partial \rho_f}{\partial P_f} = \beta_f \qquad \text{(A-6)}$$

where β_f is the fluid compressibility. To a reasonable approximation (cf. Chemical Rubber Co., 1970, p.72), we can take β_f as a constant for the pressure and temperature range of interest. Using Eqns. (A-2)-(A-6) in (A-1), and assuming that μ is constant, we find after expanding and rearranging:

$$\frac{1}{c}\frac{\partial P_f}{\partial t} = \nabla^2 P_f + \frac{1}{k}(\nabla k)_{stress}\cdot\nabla P_f + \frac{\mu\dot{\Phi}}{k} + (\beta_f + \beta_k)\nabla P_f\cdot\nabla P_f \qquad \text{(A-7)}$$

where c, the hydraulic diffusivity, is defined by

$$c = \frac{k}{\mu\varphi(\beta_f + \beta_\varphi)}$$

If pressure gradients are not extremely large, the last term on the right-hand side of Eqn. (A-7) will be negligible. We have made this assumption in the modified diffusion equation given as Eqn. (6) of the main text.

REFERENCES

Angevine, C.L., D.L. Turcotte, and M.D. Furnish, Pressure solution lithification as a mechanism for the stick-slip behavior of faults. *Tectonics*, *1*, 151-60, 1982.

Angevine, C.L., and D.L. Turcotte, Porosity reduction by pressure solution: a theoretical model for quartz arenites. *Geological Society of America Bulletin*, *94*, 1129-34, 1983.

Batzle, M.L., and G. Simmons, Microfractures in rocks from two geothermal areas. *Earth and Planetary Science Letters*, *30*, 71-93, 1976.

Bernabe, Y., B. Evans, and W.F. Brace, Permeability, porosity and pore geometry of hot-pressed calcite. *Mechanics of Materials*, *1*, 173-83, 1982.

Berry, M.J., and J.A. Mair, The nature of the Earth's crust in Canada, in *The Earth's crust (Geophysical Monograph 20)*, edited by J.G. Heacock, pp. 319-48, American Geophysical Union, Washington, D.C., 1977.

Bolz, R.E., and G.L. Tuve (eds.), *Handbook of tables for applied engineering science*, Chemical Rubber Company, Cleveland, p. 26, p. 72, 1970.

Brace, W.F., Permeability from resistivity and pore shape. *Journal of Geophysical Research*, *82*, 3343-49, 1977.

Brace, W.F., Permeability of crystalline and argillaceous rocks. *International Journal of Rock Mechanics and Mining Sciences & Geomechanics Abstracts*, *17*, 241-51, 1980.

Brace, W.F., and D.L. Kohlstedt, Limits on lithospheric stress imposed by laboratory experiments. *Journal of Geophysical Research, 85*, 6248-52, 1980.

Brace, W.F., J.B. Walsh, and W.T. Frangos, Permeability of granite under high pressure. *Journal of Geophysical Research, 73*, 2225-36, 1968.

Bredehoeft, J.D., and B.B. Hanshaw, On the maintenance of anomalous fluid pressures: I. Thick sedimentary sequences. *Geological Society of America Bulletin, 79*, 1097-1106, 1968.

Carter, N.J., Steady state flow of rocks. *Reviews of Geophysics and Space Physics, 14*, 301-60, 1976.

Cathles, L.M., and A.T. Smith, Thermal constraints on the formation of Mississippi Valley-type lead-zinc deposits and their implications for episodic dewatering and deposit genesis. *Economic Geology, 78*, 983-1002, 1983.

Cox, S.F., and M.A. Etheridge, Crack-seal fibre growth mechanisms and their significance in the development of oriented layer silicate microstructures. *Tectonophysics, 92*, 147-70, 1983.

Dibble, W.E., Jr., A. Nur, and J. Potter, Porosity reduction in sandstone, paper presented at 58th Annual Technical Conference and Exhibition, Society of Petroleum Engineers, San Francisco, California, October 5-8, 1983.

Elders, W.A., and D.K. Bird, Active formation of silicified cap rocks in arenaceous sands in a low-temperature, near-surface geothermal environment, in the Salton Trough of California, U.S.A., in *International symposium on water-rock interaction, Prague, 1974, Proceedings*, edited by J. Cadek and T. Paces, pp. 150-57, Czechoslovak Geological Survey, Prague, 1976.

Etheridge, M.A., S.F. Cox, V.J. Wall, and R.H.,Vernon, High fluid pressures during regional metamorphism and deformation: implications for mass transport, deformation mechanisms and crustal strength. *Journal of Geophysical Research*, in press.

Facca, G., and F. Tonani, The self-sealing geothermal field. *Bulletin Volcanologique, 30*, 271-73, 1967.

Fyfe, W.S., N.J. Price, and A.B. Thompson, *Fluids in the Earth's crust*, pp. Elsevier, Amsterdam, 1978.

Hanshaw, B.B., and J.D. Bredehoeft, On the maintenance of anomalous fluid pressure: II. Source layer at depth. *Geological Society of America Bulletin, 79*, 1107-22, 1968.

Jones, T.D., Wave propagation in porous rock and models for crustal structure. Ph. D. thesis, Stanford University, Stanford, California, 1983.

Jones, T.D., and A. Nur, Seismic velocity and anisotropy in mylonite and the reflectivity of deep crustal fault zones. *Geology, 10*, 260-63, 1982.

Kennedy, G.C., A portion of the system silica-water. *Economic Geology, 45*, 629-53, 1950.

Lachenbruch, A.H., and J.H. Sass, Heat flow and energetics of the San Andreas fault zone. *Journal of Geophysical Research, 85*, 6185-6222, 1980.

Morrow, C.W., D. Lockner, D. Moore, and J. Byerlee, Permeability of granite in a temperature gradient. *Journal of Geophysical Research, 86*, 3002-08, 1981.

Mueller, S., A new model of the continental crust, in *The Earth's crust (Geophysical Monograph 20)*, edited by J.G. Heacock, pp. 289-317, American Geophysical Union, Washington, D.C., 1977.

Nekut, A., J.E.P. Connerney, and A.F. Kuckes, Deep crustal electrical conductivity: evidence for water in the lower crust. *Geophysical Research Letters, 4*, 239-42, 1977.

Norton, D., and J. Knight, Transport phenomena in hydrothermal systems: cooling plutons. *American Journal of Science, 277*, 937-81, 1977.

Norton, D., and H.P. Taylor, Jr., Quantitative simulation of the hydrothermal systems of crystallizing magmas on the basis of transport theory and oxygen isotope data: an analysis of the Skaergaard intrusion. *Journal of Petrology, 20*, 421-86, 1979.

Nur, A., and G. Simmons, The effect of saturation on velocity in low porosity rocks. *Earth and Planetary Science Letters, 7*, 183-93, 1969.

Nur, A., and J.D. Byerlee, An exact effective stress law for elastic deformation of rock with fluids. *Journal of Geophysical Research, 76*, 6444-49, 1971.

Olhoeft, G.R., Electrical properties of granite with implications for the lower crust. *Journal of Geophysical Research, 86*, 931-36, 1981.

O'Neil, J.R., and T.C. Hanks, Geochemical evidence for water-rock interaction along the San Andreas and Garlock fault zones of California. *Journal of Geophysical Research, 85*, 6286-92, 1980.

Padovani, E.R., S.B. Shirey, and G. Simmons, Characteristics of microcracks in amphibolite and granulite facies grade rocks from southeastern Pennsylvania. *Journal of Geophysical Research, 87*, 8605-30, 1982.

Raj, R., Creep in polycrystalline aggregates by matter transport through a liquid phase. *Journal of Geophysical Research, 87*, 4731-39, 1982.

Raleigh, C.B., and J. Evernden, Case for low deviatoric stress in the lithosphere, in *Mechanical behavior of crustal rocks (Geophysical Monograph 24)*, edited by N.L. Carter, pp. 173-86, American Geophysical Union, Washington, D.C., 1982.

Richter, D., and G. Simmons, Microcracks in crustal igneous rocks: microscopy, in *The Earth's crust (Geophysical Monograph 20)*, edited by J.G. Heacock, pp. 149-80, American Geophysical Union, Washington, D.C., 1977a.

Richter, D., and G. Simmons, Microscopic tubes in igneous rocks, *Earth and Planetary Science Letters, 34*, 1-12, 1977b.

Robin, P.-Y. F., Pressure solution at grain-to-grain contacts. *Geochimica et Cosmochimica Acta, 42*, 1383-89, 1978.

Schmidt, E. (ed.), *Properties of water and steam in SI-units*. Springer-Verlag, Berlin, pp. 34-145, 1969.

Seeburger, D., Studies of natural fractures, fault-zone permeability, and a pore space-permeability model. Ph.D. thesis, Stanford University, Stanford, California, 1981.

Shankland, T.J., and M.E. Ander, Electrical conductivity, temeperature, and fluids in the lower crust. *Journal of Geophysical Research*, *88*, 9475-84, 1983.

Sleep, N.H., and T.J. Wolery, Egress of water from midocean ridge hydrothermal systems: some thermal constraints. *Journal of Geophysical Research*, *83*, 5913-22, 1978.

Smith, D.L., and B. Evans, Diffusional crack healing in quartz, *Journal of Geophysical Research*, in press.

Smith, L., and D.S. Chapman, On the thermal effects of groundwater flow. 1. Regional scale systems. *Journal of Geophysical Research*, *88*, 593-608, 1983.

Sprunt, E.S., and A. Nur, Destruction of porosity through pressure solution. *Geophysics*, *42*, 726-41, 1977.

Sprunt, E.S., and A. Nur, Microcracking and healing in granites: new evidence from cathodoluminescence. *Science*, *205*, 495-97, 1979.

Taylor, H.P., Jr., Water/rock interaction and the origin of H_2O in granitic batholiths. *Geological Society of London Journal*, *133*, 509-58, 1977.

Thompson, A.B., Fluid-absent metamorphism. *Geological Society of London Journal, 140*, 533-47.

Thompson, B.G., A. Nekut, and A.F. Kuckes, A deep crustal electromagnetic sounding in the Georgia Piedmont. *Journal of Geophysical Research, 88*, 9461-73, 1983.

Trimmer, D., B. Bonner, H.C. Heard, and A. Duba, Effect of pressure and stress on water transport in intact and fractured gabbro and granite. *Journal of Geophysical Research, 85*, 7059-71, 1980.

Walther, J.V., and H.C. Helgeson, Calculation of the thermodynamic properties of aqueous silica and solubility of quartz and its polymorphs at high temperatures and pressures, *American Journal of Science, 277*, 315-51, 1977.

Yardley, B.W.D., Quartz veins and devolatilization during metamorphism. *Geological Society of London Journal, 140*, 657-63, 1983.

NOTATION

A,B,C,D	constants in empirical relation for seismic velocity
c	hydraulic diffusivity
$\hat{c}$	hydraulic diffusivity modified for solubility effects
F,G	constants
$\dot{F}$	dimensionless parameter related to porosity-reduction rate
g	magnitude of acceleration due to gravity
$\vec{g}$	acceleration due to gravity (vector)
H	characteristic length scale
i	subscript denoting "interface"
k	permeability
k_0	initial value of permeability
L	crustal thickness in single-layer models
n	exponent
P_c	confining pressure
P_e	effective pressure
P_E	excess fluid pressure (cf. Figs. 1-4a-c)
P_f	fluid pressure
$\tilde{P}_f$	dimensionless fluid pressure as used in figures
P_s	characteristic pressure
$\hat{P}$	fluid pressure in excess of hydrostatic
$\bar{P}$	dimensionless fluid pressure as used in scaling arguments
S	solubility of quartz in water as mass fraction
t	time
t_s	characteristic time
$\tilde{t}$	dimensionless time
T	temperature
u	magnitude of volumetric flow rate per unit area
$\vec{u}$	volumetric flow rate per unit area (vector)
V_P	compressional velocity
y,z	spatial coordinates
$\tilde{z}$	dimensionless coordinate
α	dimensionless parameter related to effective pressure

β_f fluid compressibility

β_k fluid-pressure sensitivity of permeability

β_φ 'compressibility' of pore space

ΔV_P change in compressional velocity due to elevated fluid pressure

$\Delta\rho$ difference between solid and fluid densities

μ viscosity

ρ_f density of fluid

ρ_r density of solid

ρ_S density of solution

φ porosity

φ_c 'critical' porosity for finite permeability

φ_0 initial permeability

$\dot{\Phi}$ porosity-reduction rate

CHAPTER 2
PHYSICAL PROCESSES IN ACCUMULATING SEDIMENTS I: RHEOLOGY OF COMPACTING CLAY-RICH SEDIMENTS

ABSTRACT

We review experimental results on the time-dependent deformation of clays and shales in order to develop a rheological law for compaction of clay-rich sediments. A good fit to the experimental data is provided by a three-parameter model known as a standard linear solid. We show that, in general, the variables controlling the compaction state--typically characterized by porosity--are overburden pressure, pore-fluid pressure, and the rates of change of these quantities; the rheological parameters are functions of porosity. For time scales and loading rates characteristic of sedimentary basins, the rheological law simplifies to one in which porosity is a unique function of effective stress, i.e., the difference between overburden pressure and fluid pressure. This verifies an assumption commonly made in models of fluid-pressure development in sedimentary basins.

1. INTRODUCTION

Sedimentary rocks comprise a large fraction of the rocks exposed at the Earth's surface, and the study of their origin is a major discipline within the geological sciences. Much attention has been focussed on the mechanics of sediment transport (e.g., Allen, 1970), on chemical processes during sedimentation and burial (e.g., Berner, 1980), and on the mechanics of sediment compaction (e.g., Rieke and Chilingarian, 1974; Chilingarian and Wolf,

1975), the latter work being largely directed at characterizing the porosity of hydrocarbon reservoir rocks. The mechanical behavior of sedimentary rocks has also been of importance to mining engineers, out of concern for the stability of some underground mine openings (e.g., Jaeger and Cook, 1976). Thus, the nature of time-dependent sediment deformation, at both 'long' and 'short' time scales, is of significant practical interest.

In this chapter, we consider in detail the rheological behavior of compacting clay-rich sediments. We first discuss experimental work on time-dependent deformation of clays and shales, as well as rheological models for such materials. Building upon this earlier work, we then propose a simple phenomenological model in which the degree of compaction is generally a function of overburden stress, fluid pressure, and the rate of change of these variables.

In applying our model of clay/shale rheology to the geologically interesting case of sediment accumulation in a basin, certain simplifications will be shown to be valid. In particular, for typical sedimentation rates, and over the time scales of interest in basin formation, we will show that the rheological model essentially reduces to one in which the degree of compaction (or porosity) is simply a function of effective stress, i.e., the difference between overburden pressure and fluid pressure.

2. TIME-DEPENDENT DEFORMATION OF CLAYS AND SHALES

Sediment compaction must properly be viewed as an essentially transient phenomenon. As sediments are buried, the pore volume is usually reduced by a substantial fraction; this loss of pore volume is largely irreversible (e.g., Hamilton, 1976). It is commonly assumed--and we will

carefully examine this assumption below--that when applied stresses are constant, an 'equilibrium' state will be reached, i.e., that after a long enough period of time, fluid pressure will tend toward hydrostatic and porosity will tend toward a well-defined value $\varphi = \varphi(\Sigma)$, where Σ is effective stress, defined as the difference between overburden pressure and pore-fluid pressure (e.g., Smith, 1971, 1973). Similarly, if the loading conditions applied to sediment at 'equilibrium' are abruptly altered, there will be a time-dependent change in pore volume as the sediment 'relaxes' towards a new equilibrium state. This is the phenomenon of creep.

Deformation of clay-rich sediments has been extensively studied by workers in soil mechanics, where an understanding of the mechanical behavior of clay soils subjected to loads is of great practical importance. Numerous studies, both theoretical and experimental, have focussed on time-dependent deformation of clays (e.g., Kravtchenko and Sirieys, 1966; Mitchell, 1976). For triaxial tests in which the axial stress σ_a differs little from the 'confining' stress σ_c (e.g., Christensen and Wu, 1964), clays usually show creep behavior of the type illustrated in Fig. 2-1. Upon sudden increase in the axial load, a small 'instantaneous' strain is observed, followed by a large increase in strain with time, tending towards an asymptotic value.

Experimental studies of the creep behavior of sedimentary rocks, and especially of clay-rich rocks, are regrettably few in number, so there is little data to guide us in developing a rheological model for such rocks. One of the earliest studies of time-dependent deformation of clay-rich rocks appears to be that of Griggs (1939), who subjected a mudstone to a small (ca. 1 MPa) uniaxial load for several months. The creep curve obtained by Griggs was qualitatively similar to that shown for clay in Fig. 2-1, although the magnitude

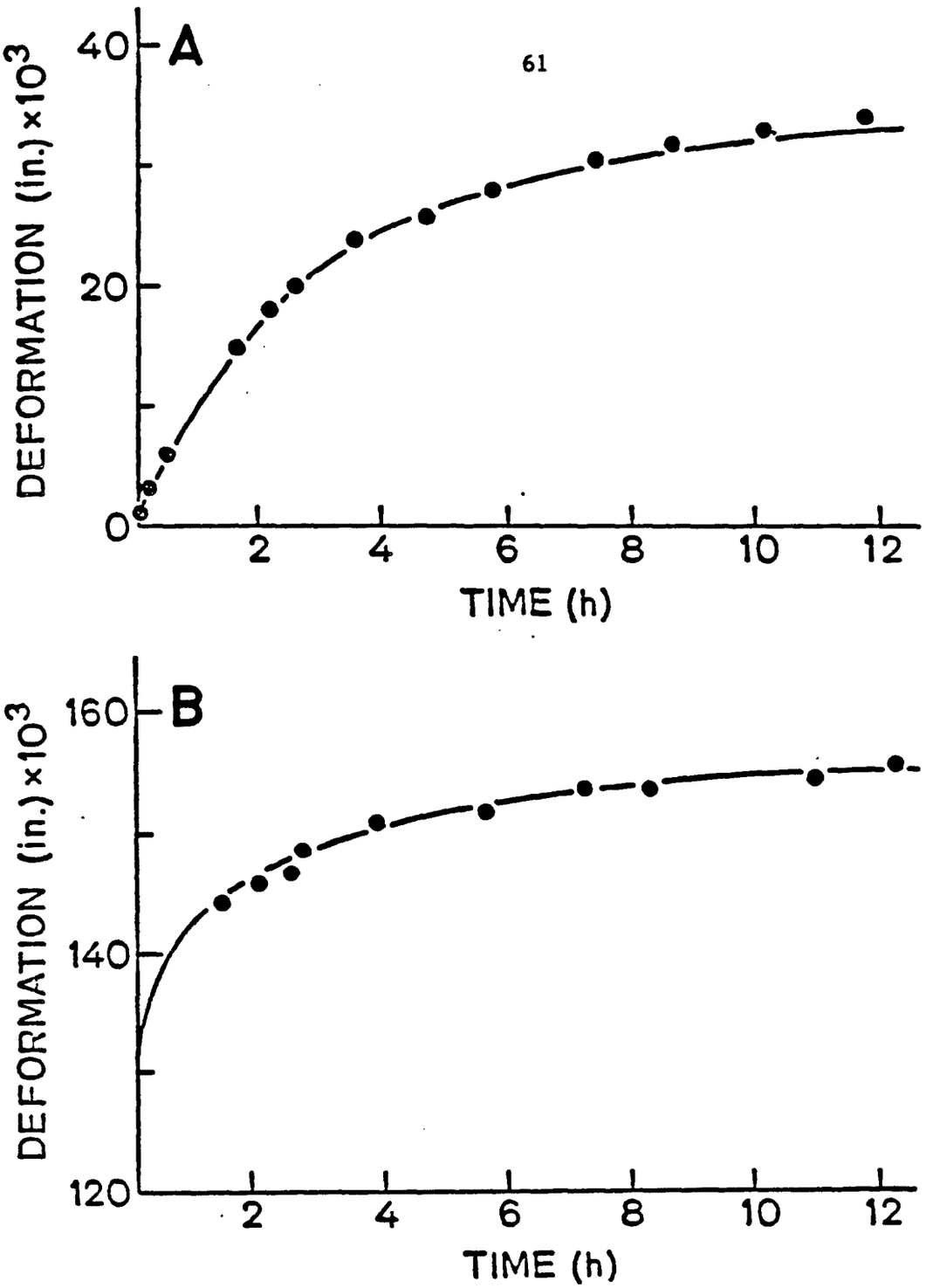

Figure 2-1: Experimental creep curves for clays at very low confining pressure and differential stress (after Christensen and Wu (1964), by permission of the American Society of Civil Engineers). Deformation (axial compression) is measured relative to an initial length of 3 inches.

Figure 2-1a: Initial load of 1.49 bars increased at t = 0 to 1.71 bars.

Figure 2-1b: Initial load of 1.71 bars increased at t = 0 to 1.89 bars.

of strain and time involved were quite different. Later studies of creep of clay-rich rocks (Nishihara, 1952, 1957; Hobbs, 1970; Renzhiglov and Pavlishcheva, 1970) have generally involved uniaxial tests with loads greater than ca. 20% of the uniaxial compressive strength. For the smallest loads, the creep curves are usually of the same form as found by Griggs. With fairly large differential stresses, creep generally leads to rupture. Such load conditions, however, are unlikely to occur commonly in compacting sedimentary rocks.

Any number of empirical creep laws could be constructed that would fit the data on clay and shale creep. Among the simple rheological models commonly considered, the creep behavior of compacting clays and shales subjected to increasing loads appears to have a reasonably close resemblance to that of the standard linear solid (e.g., Ramsay, 1967, pp. 277-79), a phenomenological model that describes time-dependent deformation of some materials. The standard linear solid may be described mathematically by the equation

$$\frac{E}{\tau} + \frac{dE}{dt} = \frac{\sigma}{\tau M_R} + \frac{1}{M_U}\frac{d\sigma}{dt} \qquad (1)$$

where

E = strain

σ = load stress

t = time

M_U = unrelaxed modulus

M_R = relaxed modulus

τ = relaxation time

In light of our focus on compaction, we will use E here to denote *volumetric* strain, and identify σ with overburden stress. The rheological

parameters M_U, M_R, and τ are best understood with reference to a special loading configuration. We imagine the stress σ to be abruptly increased from some datum value (which we can, without loss of generality, set to zero) to $\bar{\sigma}$ at time $t = 0$, i.e.,

$$\sigma(t) = \bar{\sigma} H(t) \tag{2}$$

where $H(t)$ is the unit step function, defined by

$$\begin{aligned} H(t) &= 0, \qquad t<0 \\ H(t) &= 1, \qquad t>0 \end{aligned} \tag{3}$$

The time-dependent strain for the standard linear solid under this loading can be shown to be (e.g., Ramsay, 1967, p. 279)

$$E(t \geq 0) = \frac{\bar{\sigma}}{M_U} e^{-t/\tau} + \frac{\bar{\sigma}}{M_R}(1 - e^{-t/\tau}) \tag{4}$$

for M_U, M_R, and τ all constant. This is illustrated in Fig. 2-2. We see that the instantaneous or 'unrelaxed' strain at $t = 0$ is $\bar{\sigma}/M_U$, while the asymptotic or 'relaxed' strain as $t \to \infty$ is $\bar{\sigma}/M_R$. The parameter τ characterizes the time scale over which the bulk of the creep strain occurs. Note the qualitative similarity between the standard linear solid response (Fig. 2-2) and the experimental results (Fig. 2-1).

It is quite probable that the standard linear solid as a rheological model of sediment compaction may only be applicable for monotonically increasing loads, i.e., for monotonically decreasing porosity, due to the fundamentally nonelastic nature of the compaction process. Unloading will also produce creep (cf. Hamilton, 1976; Lo et al., 1978), but the moduli characterizing this process are likely to be significantly different from the moduli appropriate to the loading process. Therefore, M_U and M_R should not be thought of as *elastic* moduli. For this reason, we denote the 'bulk' moduli with 'M' rather than the

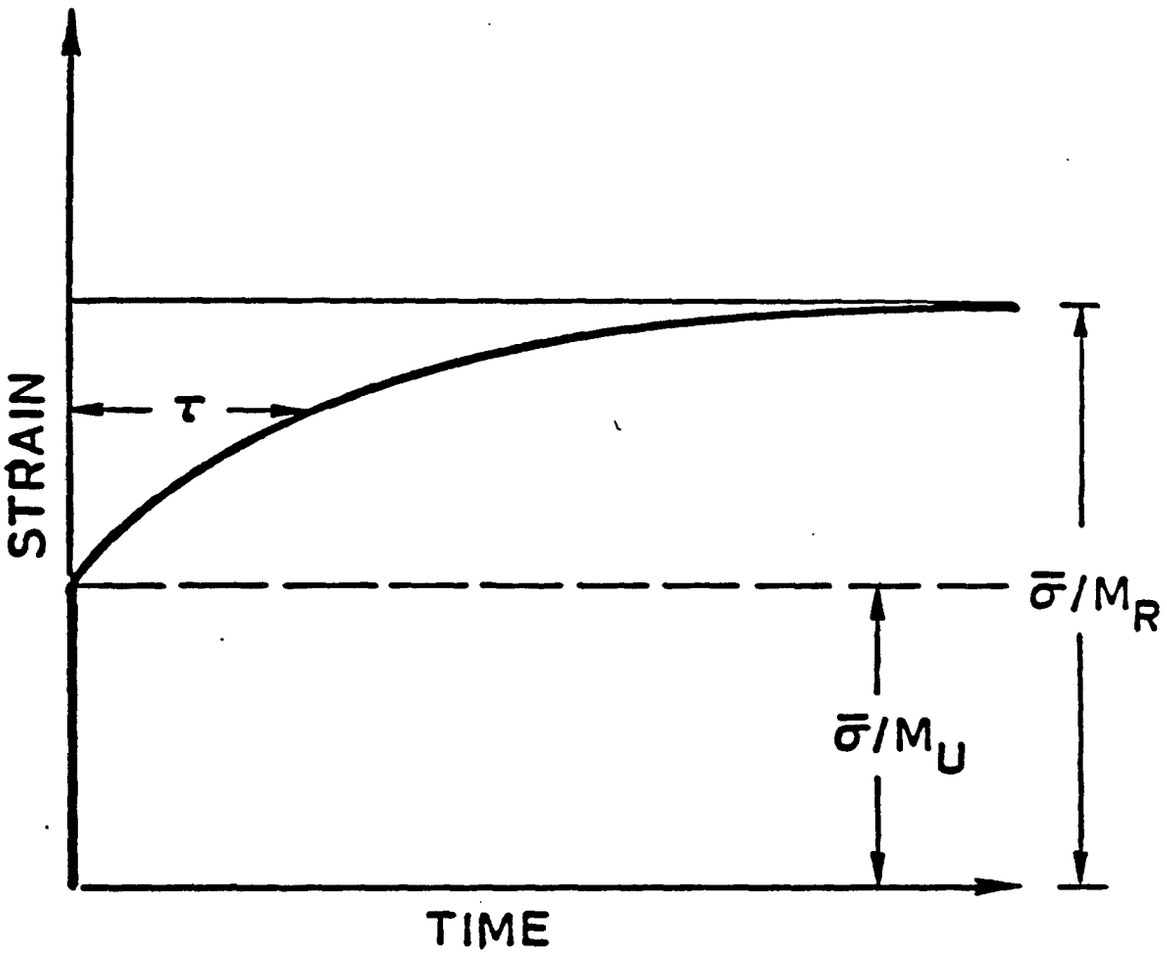

Figure 2-2: Strain-time relationship for a standard linear solid. Instantaneous, 'unrelaxed' strain is $\bar{\sigma}/M_U$; asymptotic, 'relaxed' strain is $\bar{\sigma}/M_R$; τ is the relaxation time, during which most of the creep strain occurs.

standard symbol 'K' used to denote elastic bulk moduli.

In order to study changes in the physical properties of sediments during compaction and lithification--whether we be interested in fluid pressure, strain, pore-fluid chemistry, or any other property--we must necessarily consider the sediments to be motion relative to a fixed reference frame. The rheological model that we suggest is appropriate for compacting sediments--the standard linear solid model as formulated in Eqn. (1)--is not directly applicable to moving media. In order to extend the model to the case of a moving medium, we assume that the time derivatives in Eqn. (1) may be replaced by the material, or substantial, time derivatives (cf. Malvern, 1969, p. 141-43), i.e., the time derivatives *following motion of the solid grains*. We also need to consider the effect of pore-fluid pressure p on compaction. It seems clear that fluid pressure will tend to counteract compaction, just as overburden pressure will enhance compaction. Many elastic processes are characterized by an 'effective stress' $\Sigma = \sigma - \alpha p$, where $\alpha \leq 1$ (Nur and Byerlee, 1971). The exact expression for effective stress for nonelastic processes, such as compaction of clay-rich materials, is generally not known; as a first approximation, we will simply take $\Sigma = \sigma - p$. We thus replace σ in Eqn. (1) by Σ. (We also emphasize that E is generally a *finite* strain.) With these various considerations, we propose as a rheological law for compacting clay-rich sediment:

$$\frac{DE}{Dt} + \frac{E}{\tau} = \frac{\Sigma}{\tau M_R} + \frac{1}{M_U}\frac{D\Sigma}{Dt} \tag{5}$$

D/Dt denotes the material derivative, defined by

$$\frac{D}{Dt} = \frac{\partial}{\partial t} + u_s \frac{\partial}{\partial s} \tag{6}$$

where u_s is the speed at which the solid grains move and s is a spatial coordinate in the direction of movement, which should be very nearly vertical.

Any model of sedimentation and compaction of clay-rich rocks should, in principle, utilize the creep data discussed above. Strictly speaking, as we discuss in the next section, this has not been done. After estimating values of the rheological parameters, however, we will demonstrate that some of the simplified approaches to compaction are nonetheless adequate, at least for the sedimentation rates and the time scales relevant to sedimentary-basin development.

3. SEDIMENT RHEOLOGY IN MODELS OF ACCUMULATING SEDIMENT: A REVIEW

Various mathematical models have been presented that attempt to describe fluid-pressure development in accumulating sediments. Because mechanical compaction is typically considered to be the major influence upon fluid pressure (see, e.g., Smith, 1971, 1973), earlier workers have sought to relate the compaction state of the sediment, as characterized by porosity, to mechanical variables such as overburden pressure and fluid pressure. Perhaps the earliest such work was that of Ortenblad (1929-30), who applied the then-recently developed theory of soil consolidation (e.g., Terzaghi, 1943). The fundamental relationship proposed by Terzaghi, verified repeatedly over the years by laboratory studies, is simply

$$e = e_0 - C_c \ln\left(\frac{\sigma}{\sigma_0}\right) \tag{7}$$

where

$e = \varphi/(1-\varphi)$ = void ratio

e_0 = void ratio at datum load

C_c = compression index

σ = load stress

σ_0 = datum load stress

C_c is strongly dependent upon the relative proportions of clay and sand (cf. Benson, 1981).

More recently, Sharp and Domenico (1976) and Bishop (1979) have also treated sediment compaction and fluid-pressure development in basins by using soil-consolidation theory. Eqn. (7) appears to be valid for clays subjected to pressures of up to several hundred bars in the laboratory (e.g., Parasnis, 1960). However, such compacted materials are not truly *rocks*, such as shales or mudstones, the origin of which involves many complex chemical and physical changes in addition to compaction under pressure (e.g., Meade, 1966; Weaver and Beck, 1971). Hence, it is questionable whether consolidation theory is properly applied when dealing with sedimentary rocks formed over a time span of millions of years.

Smith (1971, 1973) carefully considered the mechanics of sediment compaction in his model of fluid-pressure development in accumulating, clay-rich sediments. He assumed that an effective stress law would hold for sediment compaction, i.e., that fluid pressure would be as effective in *inhibiting* compaction as overburden pressure would be in *enhancing* compaction, and that porosity in compacting shale would be a unique function of the effective stress. Smith used this assumption, along with the commonly observed exponential relationship between porosity and depth (e.g., Athy,

1930) to derive an expression relating porosity to effective stress. Keith (1982) has also taken such an approach to the mechanics of sediment compaction.

Other attempts to incorporate simple rheological considerations into compaction models have also been made. Nagumo (1965) and Marsal and Philipp (1970) proposed that in normally pressured sediments, porosity can be described by an equation of the form

$$\frac{d\varphi}{d\Sigma} + \chi\varphi = 0 \tag{8}$$

where χ is generally a slowly varying function of φ. Eqn. (8) can be rewritten as

$$\frac{d\varphi}{dt} + \chi\varphi\frac{d\Sigma}{dt} = 0 \tag{9}$$

For a constant loading rate, Eqn. (9) predicts an approximately exponential decrease in porosity with time. Another rheological model has been proposed by Palciauskas and Domenico (1980), who suggested that porosity in compacting sediments is related to effective stress by an expression of the form

$$\frac{d\varphi}{d\Sigma} + (1-\varphi)\hat{\alpha} = 0 \tag{10}$$

where $\hat{\alpha}$ is the sediment compressibility. This can be rewritten as

$$\frac{d\varphi}{dt} + (1-\varphi)\hat{\alpha}\frac{d\Sigma}{dt} = 0 \tag{11}$$

Palciauskas and Domenico also considered the possible effects of deviatoric stress on porosity.

When we reconsider the experimental work on creep of clay and clay-rich rocks (Fig. 2-1), it becomes clear that neither the rheological model of Nagumo (1965) and Marsal and Philipp (1970), nor that of Palciauskas and Domenico (1980), can adequately describe the experimental data. This can best be seen

by solving Eqns. (9) and (11) for the case of a step-function change in applied stress, then comparing the predicted strain with experimental results. As before, the step-function change in applied stress is given by

$$\sigma(t) = \bar{\sigma} H(t)$$

where $H(t)$ is the unit step function, defined by

$$H(t) = 0, \qquad t<0$$
$$H(t) = 1, \qquad t>0$$

We find for the Nagumo/Marsal and Philipp rheology (with χ constant)

$$\varphi(t \geq 0) = \varphi_0 e^{-\chi \bar{\sigma}} \tag{12a}$$

and for the Palciauskas and Domenico rheology

$$\varphi(t \geq 0) = \varphi_0 - (1-\varphi_0)(e^{\beta \bar{\sigma}} - 1) \tag{12b}$$

where φ_0 is the porosity for $t<0$. These two rheological laws thus predict an instantaneous porosity (or strain) change in response to a step-function change in applied stress, with no additional time-dependent strain. This is definitely in disagreement with experimental observation. It therefore seems clear that a rheological model that considers both Σ and $D\Sigma/Dt$, such as the standard linear solid (Eqn. 6), is in general a preferable description of clay/shale rheology.

4. ESTIMATION OF PARAMETER VALUES FOR THE STANDARD-LINEAR-SOLID MODEL OF SEDIMENT COMPACTION

Estimating values of the parameters M_U, M_R, and τ for clays and shales is a difficult task. Creep data for clay-rich rocks have been fit to various empirical laws (Nishihara, 1957; Hobbs, 1970; Renzhiglov and Pavlishcheva, 1970), but not including laws appropriate to a standard linear solid. It seems intuitively clear that M_U, M_R, and τ will all be strong functions of porosity,

increasing as φ decreases and the clay or shale 'stiffens'. The studies cited above also indicate little dependence of creep-law coefficients (analogous to our M_U, M_R, and τ) on the absolute stress level, at least for fairly small deviatoric stresses. Hence, to a first approximation, we will take the three parameters in our creep model to be functions only of porosity.

The unrelaxed modulus M_U, which describes the material's instantaneous volumetric strain, should be given, to a reasonable approximation, by bulk moduli measured by acoustic wave propagation. Hamilton (1971) compiled such data for several sediment types; for clays and shales, he suggested that the relationship between bulk modulus and porosity may be written (in our notation) as

$$M_U = U_0 e^{-m\varphi} \tag{13}$$

where $U_0 = 54.5$ GPa and $m = 9.8$. This relationship, which fits the data reasonably well over a wide range of porosities, is shown in Fig. 2-3.

The relaxed modulus M_R describes the material's volumetric strain at 'long' times, such that an equilibrium compaction state has been reached. In analogy with the usual definition of bulk modulus as the ratio between mean stress and the corresponding elastic volumetric strain, we define M_R as

$$M_R = \frac{\Sigma}{E(t \to \infty)} \tag{14}$$

where $E(t \to \infty)$ is the finite strain at 'long' times.

In the most general case, $E(t \to \infty)$ will be related, in a complicated fashion, to porosity change and change in grain density due to, say, dehydration. The rheological law would then be coupled to mass-conservation relationships. However, in the special case of constant volume of solids, we can write a fairly simple expression for M_R, using results in the appendix to replace

E by φ. Smith (1971, p. 246, Eqn. 23) has shown that for the common exponential decrease of porosity with depth, Σ will be related to φ by the expression

$$\Sigma = \frac{g\Delta\rho}{b}\left[\ln\left(\frac{\varphi_0}{\varphi}\right) - (\varphi_0 - \varphi)\right] \tag{15}$$

where φ_0 is a datum porosity, say, the porosity at the sediment-water sediment-water interface, g is the acceleration due to gravity, $\Delta\rho$ is the difference between grain and fluid densities, and b is a constant, with dimensions of reciprocal length, characteristic of the basin in question (cf. Magara, 1976). (It should be emphasized that we do not imply by Eqn. (15) that Σ is a function of φ; rather, the functional relationship is $\varphi = \varphi(\Sigma)$. Eqn. (15) simply is the clearest way of mathematically expressing this functional relationship.) Using Eqns. (14), (15), and (A-6)--the last to replace E by φ--we can write

$$M_R = \frac{\frac{g\Delta\rho}{b}\left[\ln\left(\frac{\varphi_0}{\varphi}\right) - (\varphi_0 - \varphi)\right]}{\ln\left(\frac{1-\varphi}{1-\varphi_0}\right)} \tag{16}$$

M_R as a function of φ is also shown graphically in Fig. 2-3 for several values of b and for φ_0=0.5. $M_R(\varphi = 0.5)$ is obtained by taking the limit of Eqn. (16) as $\varphi \to 0.5$, and is identical to the 'frame compressibility' of Smith (1971, p. 247, Eqn. 27). Our expression for $M_R(\varphi)$ cannot, of course, be strictly valid for $\varphi \to 0$; in that limit, M_R and M_U should both approach the bulk modulus of a pore-free grain aggregate.

We finally need to estimate the value of τ. For porosities near 0.50, we can estimate τ from the experimental data collected by Christensen and Wu (1964) for several clays. Inspection of their Figs. 6-10, along with their

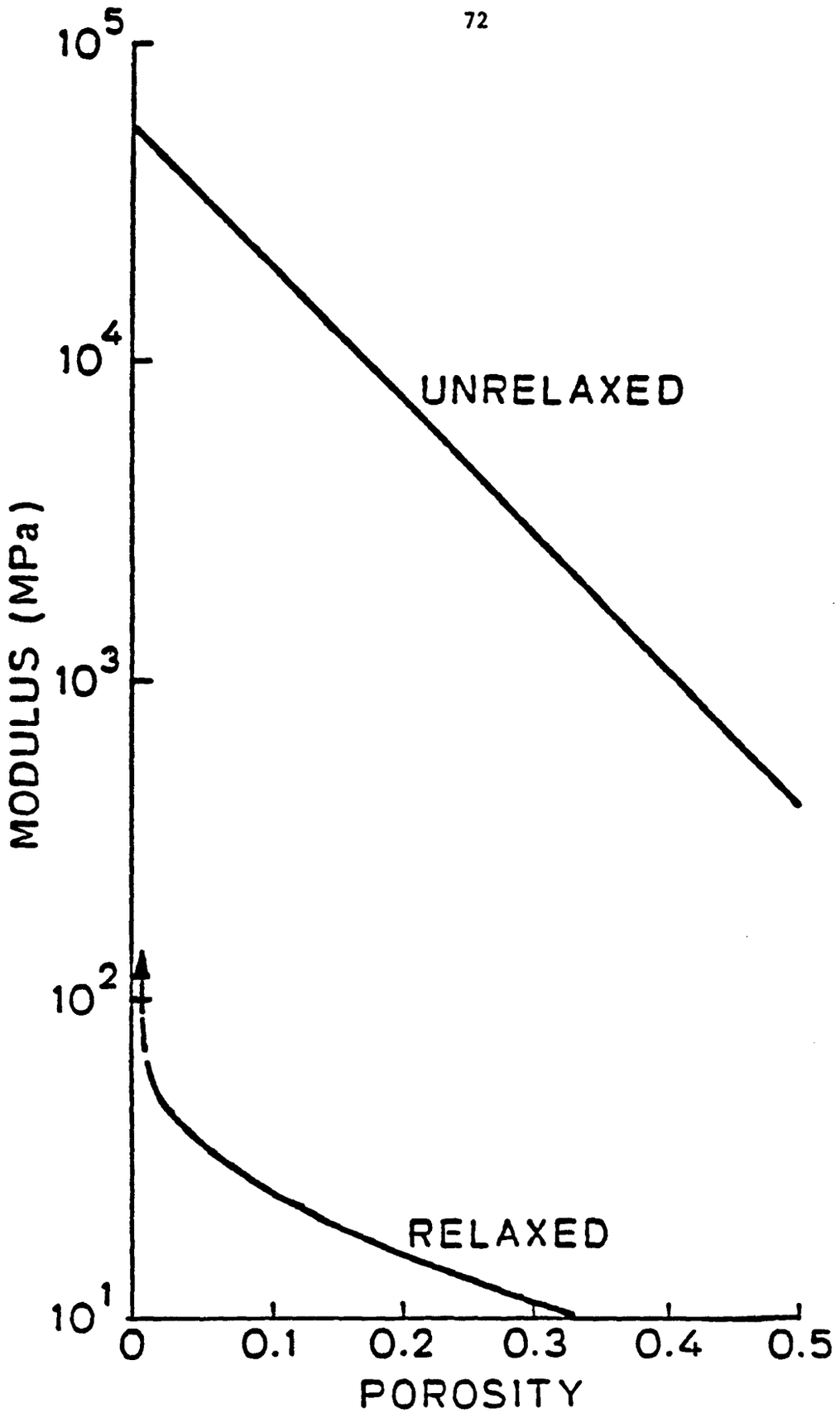

Figure 2-3: Relaxed and unrelaxed moduli of clay-rich sediment as a function of porosity.

tabulated void ratio data, suggests, for example, that $\tau \approx 5 \times 10^3$ s for $\varphi = 0.55$, $\tau \approx 10^5$ s for $\varphi = 0.43$. Estimation of τ for lower porosities cannot, unfortunately, be directly made. Nishihara (1957), Hobbs (1970), and Renzhiglov and Pavlishcheva (1970) give rheological coefficients (for various creep laws), but give no porosity data.

The standard-linear-solid rheological model may not be valid for very low porosities, say, $\varphi <$ ca. 0.05, because in attaining such low porosities, the shale is likely to have become at least partially cemented by 'stiff' materials such as quartz, which will not flow plastically under upper-crustal conditions. For such low porosities, the shale should behave nearly as an elastic solid. An indirect estimate of τ for 'low' porosities greater than this 'elastic limit' may be made, however, by using inferred crustal viscosities. This is because (cf. Ramsay, 1967) the standard linear solid can be as equally well characterized by M_U, M_R, and a viscosity η as by the parameter set M_U, M_R, and τ. It can be shown that

$$\tau = \frac{\eta M_U}{M_R (M_U - M_R)} \tag{17}$$

Suppose we consider shales with porosity φ = ca. 0.05 as the limit of validity of our model. We see from Fig. 2-3 that for such rocks, M_U will be much greater then M_R. We can therefore approximate Eqn. (17) as

$$\tau \approx \frac{\eta}{M_R} \tag{18}$$

Estimates for the apparent viscosity of the upper crust are typically in the range $10^{19} - 10^{20}$ Pa s (cf. Biot and Ode, 1965; Fletcher, 1966), so with M_R = ca. 10^2 MPa, we can estimate τ = ca. $10^{11} - 10^{12}$ s ($3 \times 10^4 - 3 \times 10^5$ a) at low porosities.

We see that τ may vary over a tremendous range (about 7 orders of

magnitude) as sediments compact. Lacking estimates of τ at any intermediate porosities, we suggest tentatively that τ be given by a simple exponential form that roughly matches the high- and low-porosity estimates:

$$\tau = \tau_0 e^{-\lambda\varphi} \tag{19}$$

where $\tau_0 = 10^{11}$ s, $\lambda = 32$.

5. APPLICATION OF RHEOLOGICAL MODEL TO SEDIMENT COMPACTION

We have argued above that in order to properly characterize time-dependent strain (or porosity) of clay-rich sediments, a rheological model for the compaction of such materials must generally take into account overburden pressure, pore fluid pressure, and the rates of change of these quantities. For convenience, we reproduce here our proposed rheological law for clay-rich sediments:

$$\frac{DE}{Dt} + \frac{E}{\tau} = \frac{\Sigma}{\tau M_R} + \frac{1}{M_U}\frac{D\Sigma}{Dt} \tag{5}$$

where $E = \ln[(1-\varphi)/(1-\varphi_0)]$, with φ_0 a datum value. The relative importance of the various terms in Eqn. (5) may be easily estimated if we consider the special case of $D\Sigma/Dt = \dot{\Sigma}_e = \text{const}$. We can then rewrite Eqn. (5) as

$$\frac{DE}{Dt} + \frac{E}{\tau} = \frac{\dot{\Sigma}_e t}{\tau M_R} + \frac{\dot{\Sigma}_e}{M_U} \tag{20}$$

At this point, it is useful to recast Eqn. (20) into dimensionless form. Suppose that the constant rate of loading has been applied for a time T, and that the total strain is E_T. We can then use the dimensionless† variables

$$\tilde{E} = \frac{E}{E_T} \tag{21}$$

$$\tilde{t} = \frac{t}{T}$$

†The strain E is, of course, inherently dimensionless.

where dimensionless variables are denoted by tildes. Substituting Eqns. (21) into Eqn. (20), we can write, after some rearrangement:

$$\frac{D\tilde{E}}{D\tilde{t}} + \left(\frac{T}{\tau}\right)\tilde{E} = \frac{\dot{\Sigma}_a T}{M_R E_T}\left(\frac{M_R}{M_U} + \frac{T}{\tau}\tilde{t}\right) \tag{22}$$

The dimensionless terms $\tilde{E}$, $\tilde{t}$, and $D\tilde{E}/Dt$ will all be $O(1)$ because of the way in which we have scaled strain and time.

Referring to Fig. 2-3, in which we show the relaxed and unrelaxed moduli as functions of porosity, we see that M_R/M_U will be much less than unity unless $\varphi \to 0$. Furthermore, T, the characteristic time scale over which sedimentation takes place, will likely be several orders of magnitude greater than τ, which we estimated to be less than *ca.* 10^4–10^5 a at even the lowest porosities for which our model is valid. Therefore, in nearly all cases of interest, we can ignore the first terms on both the left-hand and right-hand sides of Eqn. (22). Reverting to dimensional form, the rheological law may generally be expressed to an excellent approximation as

$$E = \frac{\Sigma}{M_R} \tag{23}$$

In other words, a clay-rich material will 'relax' sufficiently rapidly that E (or φ) will be essentially a unique function of Σ (at least, during loading; as stated earlier, this rheological model may not be appropriate for unloading). This has been commonly assumed (e.g., Smith, 1971; Plumley, 1980; Keith, 1982), but without reference to data on the mechanical behavior of such materials. Our review and synthesis of the relevant experimental results shows that this assumption may legitimately be made in models of sediment compaction and fluid-pressure development in sedimentary basins.

6. SUGGESTED FUTURE STUDIES

We have reviewed experimental studies of time-dependent deformation of clays and shales in an attempt to synthesize a rheological law that reasonably describes compaction of such materials. These studies have focussed on the average mechanical deformation associated with particular applied stresses. In actuality, the microphysical nature of compaction and lithification must be very complex, involving phenomena such as reorientation and deformation of individual mineral grains, mineralogical changes, and ion exchange between grains and pore fluid (e.g., Meade, 1966; Burst, 1969; Weaver and Beck, 1971; Eberl and Hower, 1976). A variety of experiments will be necessary to further refine our knowledge of the processes by which clay becomes shale. The questions to be addressed should probably include the following:

i) How do elevated temperatures, in the range of probable upper-crustal values ($\leq 300°C$) affect creep behavior of clay-rich sediments?

ii) How do clay chemistry and pore-fluid chemistry affect clay- and shale creep? This work should probably focus on the effects of Na, K, Ca, and Mg, the relative proportions of which appear to have a strong influence on diagenetic reactions during burial (e.g., Eberl and Hower, 1976).

iii) What sort of effective stress law, if any, is appropriate to describe creep of clays and shales?

iv) How do clay-rich sediments respond mechanically to *decreasing* as well as *increasing* loads; i.e., how much deformation is 'elastic' and reversible, as opposed to 'plastic' and irreversible?

7. CONCLUSIONS

In developing models to describe physical processes in accumulating

sediments, careful consideration should be given to experimental studies. We have taken this approach in regards to compaction of clay-rich sediments, reviewing and synthesizing data on time-dependent deformation of clays and shales in order to arrive at a rheological law for sediment compaction. Available data indicate that the compaction state of clay-rich sediments--usually characterized by porosity--will generally depend upon overburden pressure, pore-fluid pressure, and the rates of change of these variables. For time scales and rates of loading typical of sedimentary basins, the model predicts that porosity will be essentially dependent upon simply the effective stress, thereby verifying a commonly held assumption used in models of sedimentary-basin development.

APPENDIX: RELATIONSHIP BETWEEN POROSITY CHANGE AND FINITE STRAIN

The total volume V_T of a sediment packet is made up of solid grains of volume V_r and fluid-filled pores of volume V_p. If, during compaction, grain density remains constant, then any change δV_T in the volume of the sediment packet will be equal to the change δV_p in pore volume. Considering an 'initial' state and a 'final' compacted state, we can express the porosities as

$$\varphi^i = \frac{V_p^i}{V_T^i} \tag{A-1a}$$

and

$$\varphi^f = \frac{V_p^f}{V_T^f} \tag{A-1b}$$

where the superscripts i and f refer to 'initial' and 'final' states. Eqn. (A-1b) may be rewritten as

$$\varphi^f = \frac{V_p^i + \delta V_T}{V_T^i + \delta V_T} \tag{A-2}$$

or

$$\varphi^f = \frac{V_p^i + \delta V_T}{V_T^i (1 + \delta\varepsilon)}$$

where $\delta\varepsilon = \delta V_T / V_T^i$. Expanding in powers of $\delta\varepsilon$, we find

$$\varphi^f = \varphi^i (1 - \delta\varepsilon) + \delta\varepsilon + O\left[(\delta\varepsilon)^2\right] \tag{A-3}$$

Hence, the porosity change in going from the initial to the final state is

$$\delta\varphi = \varphi^f - \varphi^i = \delta\varepsilon (1 - \varphi^i) + O\left[(\delta\varepsilon)^2\right] \tag{A-4}$$

In the limit of infinitesimal deformations, therefore, we have $d\varphi = d\varepsilon (1 - \varphi)$, where $d\varepsilon$ can be identified with the infinitesimal volumetric strain. For *finite* strains, we integrate over all infinitesimal strains to find

$$E = \int d\varepsilon = \int_{\varphi_0}^{\varphi} \frac{d\varphi}{1-\varphi} \qquad \text{(A-5)}$$

or

$$E = \ln\left(\frac{1-\varphi}{1-\varphi_0}\right) \qquad \text{(A-6)}$$

This is the expression used in the main text.

REFERENCES

Allen, J.R.L., 1970, *Physical processes of sedimentation* (4th impression with revised readings), London, George Allen and Unwin Ltd., 248 pp.

Athy, L.F., 1930, Density, porosity, and compaction of sedimentary rocks. *American Association of Petroleum Geologists Bulletin*, *14*, 1-24.

Benson, D.J., 1981, Porosity reduction through ductile grain deformation: an experimental assessment. *Gulf Coast Association of Geological Societies Transactions*, *31*, 235-37.

Berner, R.A., 1980, *Early diagenesis: a theoretical approach*. Princeton, New Jersey, Princeton University Press, 241 pp.

Biot, M.A., and H. Odé, 1965, Theory of gravity instability with variable overburden and compaction. *Geophysics*, *30*, 213-27.

Bishop, R.S., 1979, Calculated compaction states of thick abnormally pressured shales. *American Association of Petroleum Geologists Bulletin*, *63*, 918-33.

Burst, J.F., 1969, Diagenesis of Gulf Coast clayey sediments and its possible relation to petroleum migration. *American Association of Petroleum Geologists Bulletin*, *53*, 73-93

Chilingarian, G.V., and K.H. Wolf (eds.), 1975, *Compaction of coarse-grained sediments, I (Developments in sedimentology, vol. 18A)*. Amsterdam, Elsevier Scientific Publishing Co., 552 pp.

Christensen, R.W., and T.H. Wu, 1964, Analysis of clay deformation as a rate process. *American Society of Civil Engineers Proceedings, Journal of the Soil Mechanics and Foundations Division, 90*, No. SM6, 125-153.

Eberl, D., and J. Hower, 1976, Kinetics of illite formation. *Geological Society of America Bulletin, 87*, 1326-30.

Fletcher, R.C., 1966, A theoretical finite-amplitude model for the emplacement of gneiss domes and salt domes. *Eos (Transactions, American Geophysical Union), 47*, 189.

Griggs, D., 1939, Creep of rocks. *Journal of Geology, 47*, 225-51.

Hamilton, E.L., 1971, Elastic properties of marine sediments. *Journal of Geophysical Research, 76*, 579-604.

Hamilton, E.L., 1976, Variations of density and porosity with depth in deep-sea sediments. *Journal of Sedimentary Petrology, 46*, 280-300.

Hobbs, D.W., 1970, Stress-strain-time behaviour of a number of Coal Measure rocks. *International Journal of Rock Mechanics and Mining Sciences, 7*, 149-70.

Jaeger, J.C., and N.G.W. Cook, 1976, *Fundamentals of rock mechanics* (2nd edition). London, Chapman and Hall, 585 pp.

Keith, L.A., 1982, A numerical compaction model of overpressuring in shales. M.S. thesis, Virginia Polytechnic Institute and State University, Blacksburg, Virginia, 80 pp.

Kravtchenko, J., and P.M. Sirieys (eds.), 1966, *Rheology and soil mechanics*. Springer-Verlag, Berlin, 502 pp.

Lo, K.Y., R.S.C. Wai, J.H.L. Palmer, and R.M. Quigley, 1978, Time-dependent deformation of shaly rocks in southern Ontario. *Canadian Geotechnical Journal, 15*, 537-47.

Magara, K., 1976, Water expulsion from clastic sediments during compaction—directions and volumes. *American Association of Petroleum Geologists Bulletin, 60*, 543-53.

Malvern, L.E., 1969, *Introduction to the mechanics of a continuous medium*. Prentice-Hall Inc., Englewood Cliffs, New Jersey, 713 pp.

Marsal, D., and W. Philipp, 1970, Compaction of sediments. *Geological Institutions of the University of Uppsala Bulletin, New Series, 2*, 59-66.

Meade, R.H., 1966, Factors influencing the early stages of the compaction of clays and sands--review. *Journal of Sedimentary Petrology, 36*, 1085-1101.

Mitchell, J.K., 1976, *Fundamentals of soil behavior*. John Wiley and Sons, New York, 422 pp.

Nagumo, S., 1965, Compaction of sedimentary rock--a consideration by the theory of porous media. *University of Tokyo, Earthquake Research Institute Bulletin, 43*, 339-48.

Nishihara, M., 1952, Creep of shale and sandy-shale. *Geological Society of Japan Journal, 59*, 373-77.

Nishihara, M., 1957, Stress-strain-time relations of rocks. *Doshisha Engineering Review, 8*, 85-115.

Nur, A., and J.D. Byerlee, 1971, An exact effective stress law for elastic deformation of rock with fluids. *Journal of Geophysical Research, 76*, 6444-49.

Ortenblad, A., 1929-30, Mathematical theory of the process of consolidation of mud deposits. *Journal of Mathematics and Physics, 9*, 73-149.

Palciauskas, V.V., and P.A. Domenico, 1980, Microfracture development in compacting sediments: relation to hydrocarbon-maturation kinetics. *American Association of Petroleum Geologists Bulletin, 64*, 927-37

Parasnis, D.S., 1960, The compaction of sediments and its bearing on some geophysical problems. *Geophysical Journal of the Royal Astronomical Society, 3*, 1-28.

Plumley, W.J., 1980, Abnormally high fluid pressure: survey of some basic principles. *American Association of Petroleum Geologists Bulletin, 64*, 414-30.

Ramsay, J.G., 1967, *Folding and fracturing of rocks*. New York, McGraw-Hill Book Company, 568 pp.

Renzhiglov, N.F., and T.V. Pavlishcheva, 1970, On the viscosity of rocks. *Soviet Mining Science*, No.5 (Sept. -Oct. 1970), 582-85.

Rieke, H.H., III, and G.V. Chilingarian, 1974, *Compaction of argillaceous sediments (Developments in sedimentology, vol. 15)*. Amsterdam, Elsevier Scientific Publishing Co., 424 pp.

Sharp, J.M., Jr., and P.A. Domenico, 1976, Energy transport in thick sequences of compacting sediment. *Geological Society of America Bulletin*, *87*, 390-400.

Smith, J.E., 1971, The dynamics of shale compaction and evolution of pore-fluid pressures. *International Association for Mathematical Geology Journal*, *3*, 239-63.

Smith, J.E., 1973, Shale compaction. *Society of Petroleum Engineers Journal*, *13*, 12-22.

Terzaghi, K., 1943, *Theoretical soil mechanics*. New York, John Wiley and Sons, 510 pp.

Weaver, C.E., and K.C. Beck, 1971, Clay-water diagenesis during burial: how mud becomes gneiss. *Geological Society of America Special Paper*, *134*, 96 pp.

NOTATION

b	reciprocal length scale characteristic of sedimentary basin
C_c	compression index
e	void ratio
e_0	datum void ratio
E	finite strain
$\tilde{E}$	'dimensionless' finite strain
g	acceleration due to gravity
m	constant related to unrelaxed modulus
M_U	unrelaxed modulus
M_R	relaxed modulus
p	pore-fluid pressure
s	spatial coordinate in direction of sediment motion
t	time
$\tilde{t}$	dimensionless time
T	characteristic time scale for sedimentation
u_s	speed at which sediment grains move during compaction
U_0	constant related to unrelaxed modulus
V_f	volume of fluid in packet of sediment
V_r	volume of solid grains in packet of sediment
V_t	total volume of packet of sediment
$\hat{\alpha}$	compressibility of sediment
ε	infinitesimal strain
η	viscosity
λ	constant related to relaxation time

$\Delta\rho$	density difference between solid grains and pore fluid
σ	overburden stress
$\bar{\sigma}$	magnitude of step-function change in stress
σ_a	axial stress in triaxial test
σ_c	confining pressure in triaxial test
σ_0	datum value of overburden stress
Σ	effective stress
$\dot{\Sigma}_a$	rate of change of effective stress (constant)
τ	relaxation time
τ_0	constant related to relaxation time
φ	porosity
φ_0	datum value of porosity
χ	parameter in relationship between porosity and effective stress

CHAPTER 3
PHYSICAL PROCESSES IN ACCUMULATING SEDIMENTS II: FLUID FLOW AND FLUID-PRESSURE DEVELOPMENT IN COMPACTING SHALES

ABSTRACT

We derive fundamental equations necessary to describe the development of overpressures in compacting shales, considering the potential effects of mechanical compaction, thermal expansion of pore fluid, and montmorillonite dehydration on the pore-pressure history. Montmorillonite dehydration can be considered as constituting a fluid source, the strength of which we show depends upon several parameters, including the density of adsorbed water and the rate at which the expandable clays dehydrate. We then estimate the relative importances of the three overpressuring mechanisms. Mechanical compaction can potentially lead to pore pressure increasing as rapidly as overburden pressure; thermal effects need not be invoked unless overpressuring rates exceed the rate of increase of overburden pressure, and even then may not be required, because montmorillonite dehydration has the potential to cause very rapid rates of pore pressure increase, exceeding even rates due to mechanical effects. Such rapid overpressuring could lead to lithostatic pore pressures, hence to mechanical failure and abrupt fluid release, perhaps episodically. This could be related to the genesis of 'Mississippi Valley-type' Pb-Zn deposits. We also show that porosity changes associated with montmorillonite dehydration are likely to be quite substantial, explaining at least in part the porosity increase with depth often encountered in the transition zone from normally pressured to overpressured shales.

1. INTRODUCTION

Sedimentary basins are among the major structural features of the Earth's crust, their origin and overall development probably indicative of processes at depth in the mantle (e.g., Sleep, 1971; McKenzie, 1978). The common association between such basins and hydrocarbons makes physical processes within sedimentary basins of great practical interest. Because the development and migration of hydrocarbons are considered to be closely related to phenomena connected with lithification--in particular, compaction, heating, and expulsion of pore water (e.g., Hunt, 1979)--a better understanding of processes occurring within sedimentary basins during lithification should help constrain models of hydrocarbon generation.

A phenomenon of particular importance for hydrocarbon exploration, because of the difficulties it can cause for drilling programs (e.g., Dickinson, 1953; Fertl and Timko, 1970) is the occurrence of fluid overpressure, that is, fluid pressure in excess of hydrostatic (also called geopressure, excess pressure, and abnormal pressure). Fluid pressure in excess of hydrostatic is pressure is therefore commonly considered to be the state of 'regional' equilibrium for pore fluids in the Earth's crust. In fact, thermodynamic arguments (Dibble et al., unpublished) suggest that local chemical-mechanical equilibrium will *not* be satisfied, in general, if pore-fluid pressure is hydrostatic. Nonetheless, the observation that fluid pressure at depth in old sedimentary rocks is usually quite near hydrostatic indicates that such a condition can reasonably be taken as the 'normal' or 'equilibrium' reference state. The occurrence of overpressures in a basin therefore indicates that this 'equilibrium' state has not been reached; fluid expulsion, with concomitant porosity reduction, must take place before the overpressure can be dissipated.

In the previous chapter, we discussed the rheology of compacting clay-rich sediments. In the present chapter, we incorporate that discussion with considerations of mass and energy conservation in order to develop the mathematics to describe fluid pressure during compaction of clay-rich sediments undergoing burial and lithification. In the next section, we briefly mention the major mechanisms proposed to account for overpressure generation in sedimentary basins. All such mechanisms necessarily involve transient changes in the physical state of the sediments, a point also stressed by Keith (1982). We also review previous mathematical models of fluid pressure development in sedimentary basins. In section 3, we present a detailed derivation of the equations describing fluid-pressure development and compaction in accumulating, homogeneous, clay-rich sediments. In the most general case considered, compaction, thermal effects, and fluid sources (e.g., dehydrating clays) all influence fluid pressure. Although the complexity of the problem prevents us from finding analytical solutions to the governing equations, we show in section 4 that we can extract some important generalizations about the relative importance of the various overpressuring mechanisms by considering certain special cases. We show that, in general, montmorillonite dehydration should have a very important influence on pore-pressure development. Thermal effects may be important in achieving very high overpressures, but are not necessary to explain moderate overpressures.

2. MECHANISMS AND MODELS OF OVERPRESSURE GENERATION: A REVIEW

At least ten mechanisms have been proposed as causes of overpressuring in sedimentary basins (see reviews by Bredehoeft and Hanshaw (1968) and

Smith (1971)). Those commonly considered of major importance are:

i) Mechanical compaction as sediment is loaded by accumulating overburden (e.g., Smith, 1971);

ii) Thermal expansion of pore fluid as burial proceeds (e.g., Barker, 1972; Magara, 1975b);

iii) Fluid release by dehydration, especially in regards to the montmorillonite-to-illite transformation (Powers, 1967; Burst, 1969).

Clearly, these proposed mechanisms suggest that sustained overpressuring requires transient changes in the physical state of the sediment. Should continued burial and loading cease, compaction and fluid release due to dehydration will gradually cease, and an equilibrium geotherm will become established.

Most mathematical models of fluid-pressure development in sedimentary basins have focused attention on mechanical compaction of clay-rich sediments. Perhaps the earliest such work was that of Ortenblad (1929-30), who applied the then-recently developed theory of soil consolidation (e.g. Terzaghi, 1943). Ortenblad's numerical results, presented in terms of an unusual set of coordinates, dealt with sediment thicknesses of only a few tens of meters. Bredehoeft and Hanshaw (1968) considered fluid-pressure development in thick (several km) sections of accumulating sediment; their estimate of the maximum permeability permitting maintained overpressures is often quoted. However, their work did not take into account compaction. Bishop (1979) solved essentially the same equations as Bredehoeft and Hanshaw (1968); he attempted to deal with compaction by applying consolidation theory in an *a posteriori* fashion in order to determine the variations with depth of both density and fluid pressure. Bishop's results are

questionable for two reasons. First, it is unclear that soil consolidation theory may properly be extended to cover the complex processes occurring over millions of years as clay becomes shale. Second, density (or porosity) and fluid pressure are intimately coupled throughout the history of sedimentation and compaction; it is invalid to solve for fluid pressure developed over millions of years, then 'correct' the porosity distribution based upon those calculated pressure values.

Smith (1971, 1973) explicitly considered the coupling between compaction and fluid pressure development in accumulating clayey sediments. Following Athy (1930), Smith assumed that porosity in compacting shale is a unique function of the effective stress Σ (=overburden pressure - fluid pressure).‡ However, rather than actually solving a diffusion-type equation for fluid pressure, Smith neglected fluid compressibility and instead solved for porosity throughout the sedimentary column. Fluid pressure was then "backed out" by means of the assumed relationship between effective stress and porosity. Keith (1982) took an essentially identical approach to compaction, but also attempted to correct, in an approximate fashion, for the effects of thermal expansion and clay dehydration. She argued that the latter two mechanisms are generally of minor importance in pore-pressure development in comparison with the effect of sediment loading.

Sharp and Domenico (1976) investigated the thermal, as well as fluid pressure, history of accumulating sediments. Their formulation explicitly accounts for heat transported by fluid flow; the effect of temperature on the fluid-pressure field is treated in an approximate fashion by applying corrections to the fluid density, rather than by coupling the temperature field

‡Rheological laws for compacting sediments proposed by Nagumo (1965) and Marsal and Philipp (1970) reduce essentially to the same form.

directly to fluid pressure (cf. their Equations 1, 3, and 10). Their numerical results also suggest that thermal effects on fluid-pressure development are of secondary importance in comparison with sediment-loading effects.

Another factor possibly influencing fluid pressure in compacting sediments--deviatoric stress--was examined by Palciauskas and Domenico (1980), with emphasis on the possible relationship between deviatoric stress, microfracturing, and hydrocarbon migration.

The various mathematical models described above have clearly aided in understanding pore-pressure development in compacting sediments. The present study is intended to extend earlier work in several regards. In particular, a formal mathematical development shows explicitly the way in which the effects of heating and fluid sources couple to the equation describing fluid-pressure development.

3. ANALYSIS

Following earlier model studies, we consider sediment to accumulate in horizontal layers. We assume that both fluid and solid motion are in the vertical direction only. This should be a good approximation except near basin margins or other discontinuities, such as permeable fault zones (cf. Seeburger, 1981), and as long as abrupt changes in permeability do not occur perpendicular to bedding, in which case fluid flow could have a significant horizontal component (Magara, 1976). Such horizontal flow, which is almost certainly important for hydrocarbon concentration (e.g., Hunt, 1979), and is probably related to the origin of Mississippi Valley-type Pb-Zn deposits (Sharp, 1978; Cathles and Smith, 1983), will be examined in greater depth in chapter 4, but will be neglected here for simplicity of presentation.

Mass conservation and fluid pressure

The coordinate system used is shown in Fig. 3-1. The vertical coordinate z increases downward from the sediment surface, which is considered fixed. The base of the sediment pile lies at $h(t)$, where t is time measured from the start of sedimentation.

We now consider the effect on fluid pressure of changes in porosity and temperature, as well as the effect of fluid released by dehydration of solid grains (e.g., montmorillonite transforming to illite). We first need to consider mass conservation. In an Eulerian (fixed) reference frame, conservation of mass of fluid and solid may be expressed, respectively, as

$$\frac{\partial}{\partial t}(\rho_f \varphi) = -\frac{\partial}{\partial z}(\rho_f u_f \varphi) + S \tag{1}$$

$$\frac{\partial}{\partial t}\left[\rho_s (1-\varphi)\right] = -\frac{\partial}{\partial z}\left[\rho_s u_s (1-\varphi)\right] - S \tag{2}$$

where

ρ_f = pore-fluid density

ρ_s = solid grain density

u_f = average fluid velocity

u_s = average solid velocity

φ = porosity

S = fluid source strength (mass of fluid released per unit volume of sediment per unit time)

These conservation relationships are independent of details of the dehydration process; in particular, they are independent of whether or not bound water in montmorillonite has a different density than free water in the pores.

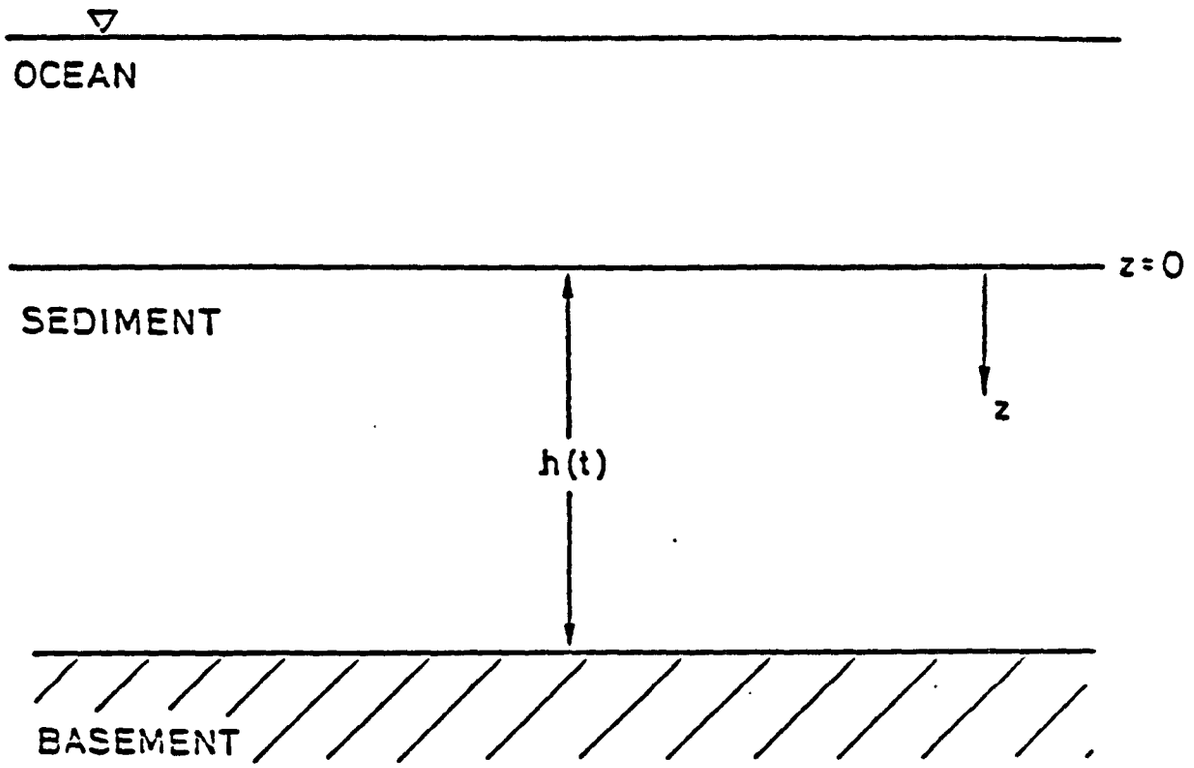

Figure 3-1: Coordinate system for the analysis.

Our assumption that dehydration of clays serves as a fluid source necessitates the presence of the term involving S in the expression for conservation of mass of the solid. Due to this dehydration, ρ_s cannot be treated as a constant, such has been done in earlier models (e.g., Smith, 1971; Sharp and Domenico, 1976; Keith, 1982); In general, S and ρ_s will be related in a complicated fashion, depending upon the exact nature of the fluid-release mechanism. In Appendix A, we discuss the relationship between S and ρ_s for the interesting case of montmorillonite-to-illite transformation. We show there that

$$S = \left(\frac{\rho_B}{\rho_s - \rho_B}\right)(1-\varphi)\frac{D\rho_s}{Dt} \tag{3}$$

where ρ_B is the density of the bound (adsorbed) water on montmorillonite surfaces—the water released during the clay-transformation process. This result will be used later when we discuss the role of clay dehydration in overpressure generation.

We will assume that changes in the chemical composition of the pore fluid will have a negligible effect on fluid density, in comparison with the effects of fluid pressure p and temperature T. These effects are expressed as:

$$\frac{\partial \rho_f}{\partial p} = \beta_f \rho_f \tag{4a}$$

and

$$\frac{\partial \rho_f}{\partial T} = -\alpha_f \rho_f \tag{4b}$$

where β_f and α_f are the compressibility and thermal expansivity, respectively, of the fluid. To a first approximation, we can take β_f and α_f as constants.

In order to arrive at a differential equation for fluid pressure, we need to express fluid flux in terms of p. We assume that pore-fluid flow will be

described by Darcy's law, viz.:

$$\varphi(u_f - u_s) = -\frac{k}{\mu}\left(\frac{\partial p}{\partial z} - \rho_f g\right) \tag{5}$$

where

k = permeability

μ = viscosity

g = acceleration due to gravity

The quantity $\varphi(u_f - u_s)$ is thus the volumetric flow rate, i.e., the volume of fluid that passes through a unit cross-sectional area in unit time. The form of Eqn. (5) indicates that no flow will occur when fluid pressure is hydrostatic ($p = \rho_f g z$). We also expand and rearrange Eqn. (2) to get an expression for the local rate of change of porosity:

$$\frac{\partial \varphi}{\partial t} = \left(\frac{1-\varphi}{\rho_s}\right)\left(\frac{\partial \rho_s}{\partial t} + u_s \frac{\partial \rho_s}{\partial z}\right) + \frac{\partial}{\partial z}\left[u_s (1-\varphi)\right] + \frac{S}{\rho_s} \tag{6}$$

We have implicitly neglected here reversible, 'elastic' porosity change (cf. chapter 1 of this dissertation); such changes should be of minor importance in comparison with irreversible porosity decrease, except possibly for very low porosities, especially when cementation by 'stiff' materials such as quartz has occurred. We will not consider such cases here. Hence, expanding Eqn. (1), using Eqns. (5) and (6), and assuming that second order terms involving $\left(\frac{\partial p}{\partial z}\right)^2$ and $\left(\frac{\partial p}{\partial z}\right)\left(\frac{\partial T}{\partial z}\right)$ are negligible, we find a linearized diffusion-type equation for fluid pressure:

$$\varphi \beta_f \left(\frac{\partial p}{\partial t} + u_s \frac{\partial p}{\partial z}\right) = \frac{\partial}{\partial z}\left[\frac{k}{\mu}\left(\frac{\partial p}{\partial z} - \rho_f g\right)\right] + \varphi \alpha_f \left(\frac{\partial T}{\partial t} + u_s \frac{\partial T}{\partial z}\right) - \frac{\partial u_s}{\partial z} - \quad (7)$$

$$- \left(\frac{1-\varphi}{\rho_s}\right)\left(\frac{\partial \rho_s}{\partial t} + u_s \frac{\partial \rho_s}{\partial z}\right) + \frac{S \Delta \rho}{\rho_f \rho_s}$$

where $\Delta \rho = \rho_s - \rho_f$.

Eqn. (7) can be readily interpreted. The left-hand side is proportional to the rate of change of fluid pressure, modified for the effect of particle motion (due, for example, to subsidence). On the right-hand side, the first term describes diffusive relaxation due to fluid flow; the second term is related to the effect of thermal expansion of the pore fluid; the third, fourth and fifth terms describe the effects of compaction, dehydration and fluid release.

Rheology of compacting sediments

In the previous chapter, we discussed at length the rheological behavior of clay-rich sediments. In general, experimental results on time-dependent deformation of clays and shales require a rheological model in which strain--which, in the absence of fluid sources, can be easily related to porosity change--is a function of both the load stress and the rate at which this load is applied. It was shown that for the rates of loading typically associated with sediment accumulation in basins, the rheological law reduces essentially to the relationship between porosity and effective stress proposed by Smith (1971), viz.:

$$\Sigma = \frac{g \Delta \rho}{b}\left[\ln\left(\frac{\varphi_0}{\varphi}\right) - (\varphi_0 - \varphi)\right] \quad (8)$$

where φ_0 is a datum porosity, often taken as the porosity at the sediment-water interface, and b^{-1} is a scale length for porosity reduction, given by the common exponential relationship between porosity and depth:

$$\varphi = \varphi_0 e^{-bz} \tag{9}$$

The rheological law, Eqn. (8), implies that the porosity of a 'packet' of sediment may be considered to be essentially independent of the history of both overburden pressure and fluid pressure during burial. (This may not be strictly valid if dissolution and precipitation are important porosity-altering processes during burial (e.g., Carstens and Dypvik, 1981)).

Due to the largely irreversible nature of compaction and lithification processes, it seems reasonable to assume that the strain rate in compacting sediments may be negative, but not positive, during burial, where negative strain rate corresponds to an increasing degree of compaction. In other words, we assume that the vertical distance between nearby sediment grains may decrease, but not increase, during burial. This may be expressed mathematically as (cf. Malvern 1969, pp. 145-50):

$$\frac{\partial u_s}{\partial z} \leq 0 \tag{10}$$

Note that we have *not* stated here that porosity must decrease during burial (cf. discussions by Plumley, 1980; Bonham, 1980, p. 554). This would be true only if there were no processes such as dehydration that could add fluid mass to the sediment. This is an important point that we will return to later in our discussion of the porosity profile commonly associated with overpressured zones.

Overburden stress

As stated above, porosity may be taken as essentially a unique function of the effective stress $\Sigma = \bar{\sigma} - p$, the difference between mean stress in the rock matrix and pore-fluid pressure. The stress state in accumulating sediments may be quite complex, with deviatoric stresses generally developed (cf. McGarr

and Gay, 1978, pp. 423-25; Palciauskas and Domenico, 1980). The large strains involved in compaction, the fundamentally nonelastic deformation undergone by the sediment, and the difficulty in specifying stress- or strain boundary conditions makes theoretical estimation of the stress state an imposing task, beyond the scope of this chapter. We will assume, as a first approximation, that the confining pressure is simply equal to the load applied by overburden. This stress is readily determined by integrating the sediment density over depth:

$$\bar{\sigma}(z) = \int_0^z \rho_m g \, d\zeta \tag{11}$$

where $\rho_m = \rho_f \varphi + \rho_s (1-\varphi)$ is the sediment density. Physically, this means we are assuming that any deviatoric stresses will relax on a time scale much less than the time over which sediment accumulates. This is apparently not strictly true (cf. McGarr and Gay, 1978), an observation that may have important consequences for our understanding of the rheology of sediments. Nonetheless, this approximation for $\bar{\sigma}$ should not lead to serious errors in estimating the effect of loading on pore pressure.

4. OVERPRESSURING MECHANISMS: ESTIMATE OF RELATIVE IMPORTANCES

In general, solution of the 'complete' sediment compaction problem requires that we consider the behavior of the seven variables φ, p, $\bar{\sigma}$, T, u_s, ρ_s, and ρ_B. Even more variables would enter if we considered transport through the fluid phase of various chemical species--which is probably necessary for a rigorous treatment of the clay-transformation process (e.g., Perry and Hower, 1970)--or considered other possible mechanisms for overpressuring, such as osmotic pressure associated with salinity gradients (Hanshaw and Zen, 1965).

Solution to the 'complete' problem is therefore quite imposing, if not intractable.

Fortunately, we can gain some important insights into the relative importance of the several potential sources of fluid overpressure by considering special cases in which some of the overpressuring mechanisms are absent. We consider again Eqn. (7) for fluid pressure, which, for convenience, we reproduce here:

$$\varphi \beta_f \left(\frac{\partial p}{\partial t} + u_s \frac{\partial p}{\partial z}\right) = -\frac{\partial u_s}{\partial z} + \frac{\partial}{\partial z}\left[\frac{k}{\mu}\left(\frac{\partial p}{\partial z} - \rho_f g\right)\right] + \varphi \alpha_f \left(\frac{\partial T}{\partial t} + u_s \frac{\partial T}{\partial z}\right) - \quad (7)$$
$$- \left(\frac{1-\varphi}{\rho_s}\right)\left(\frac{\partial \rho_s}{\partial t} + u_s \frac{\partial \rho_s}{\partial z}\right) + \frac{S \Delta \rho}{\rho_f \rho_s}$$

The relative importance of the effects of porosity reduction and fluid heating on pore-pressure development may be estimated in a relatively straightforward manner if no fluid sources are present. In that case, expanding and rearranging Eqn. (8) leads to the expression:

$$\frac{\partial u_s}{\partial z} = \frac{1}{1-\varphi}\frac{D\varphi}{Dt} \quad (12)$$

Thus, *in the absence of fluid sources*, the porosity of an element of the shale will decrease with time for physically plausible strain rates (cf. Eqn. (10)).

Substituting Eqn. (12) into Eqn. (7), we can write, after some rearrangement:

$$\varphi \beta_f \frac{Dp}{Dt} = \frac{\partial}{\partial z}\left[\frac{k}{\mu}\left(\frac{\partial p}{\partial z} - \rho_f g\right)\right] - \frac{1}{1-\varphi}\frac{D\varphi}{Dt} + \varphi \alpha_f \frac{DT}{Dt} \quad (13)$$

where $D/Dt = \partial/\partial t + u_s \partial/\partial z$ is the material time derivative, i.e., the time derivative following the motion of the solid grains (Malvern, 1969, p. 143).

We now use Eqn. (8) to express $D\varphi/Dt$ in terms of $D\Sigma/Dt$, viz.:

$$\frac{D\varphi}{Dt} = -\alpha(1-\varphi)\frac{D\Sigma}{Dt} \tag{14}$$

where $\alpha = b\varphi/g\Delta\rho(1-\varphi)^2$ is the 'compressibility' of the shale (cf. Sharp, 1976, Eqn. 5; 1983, Eqn. A-4), equivalent to the expression given by Smith (1971, p. 247, Eqn. 27). This 'compressibility' should not be thought of as an *elastic* compressibility, but rather as characterizing the irreversible porosity change due to an increase in effective stress. This corresponds with hydrologic usage in describing compaction of an aquifer (e.g., Domenico and Mifflin, 1965, p. 565).

Eqn. (14) is valid, of course, only as long as $D\Sigma/Dt$ is positive. Substituting Eqn. (14) into Eqn. (13), and recalling that $\Sigma = \bar{\sigma} - p$, we find, after rearrangement:

$$(\alpha + \varphi\beta_f)\frac{Dp}{Dt} = \frac{\partial}{\partial z}\left[\frac{k}{\mu}\left(\frac{\partial p}{\partial z} - \rho_f g\right)\right] + \alpha\frac{D\bar{\sigma}}{Dt} + \varphi\alpha_f\frac{DT}{Dt} \tag{15}$$

The last two terms on the right-hand side of Eqn. (15) represent pore-pressure increase due to porosity reduction and thermal expansion of pore fluid, respectively. The effect of porosity reduction by loading is given by the term involving $D\bar{\sigma}/Dt$. If $\bar{\sigma}$ corresponds to overburden pressure, in accord with our earlier approximation, then $D\bar{\sigma}/Dt \approx \rho_u g V$, where ρ_u is the density of sediment added at the sediment surface and V is the thickness of sediment deposited per unit time. The effect of loading-induced compaction on pore pressure is therefore given approximately by

$$\alpha\frac{D\bar{\sigma}}{Dt} \approx \alpha\rho_u g V$$

The sediment compressibility, α, is given by hydrologists (e.g., Domenico and Mifflin, 1965) for a variety of materials. We will instead use b values from the petroleum-geology literature to estimate the effect of sediment

compressibility. From Athy (1930) and Magara (1976), we estimate $b \approx 2\text{–}10 \times 10^{-4}\ \mathrm{m}^{-1}$. Taking $\rho_w / \Delta\rho \approx 1$ and $\varphi \approx 0.2\text{–}0.3$, we find:

$$\alpha \frac{D\bar{\sigma}}{Dt} \approx 0.6\text{–}6 \times 10^{-4}\, V \quad [\mathrm{s}^{-1}]$$

for V in MKS units. For likely sedimentation rates ($V \approx$ 100-500 m/Ma), we find:

$$\alpha \frac{D\bar{\sigma}}{Dt} \approx 2\text{–}100 \times 10^{-16}\ \mathrm{s}^{-1}$$

The effect of thermal expansion of pore fluid is given by the term involving DT/Dt. We can rewrite this term as

$$\varphi \alpha_f \frac{DT}{Dt} \approx \varphi \alpha_f \Gamma V$$

where Γ is the magnitude of the geothermal gradient. With $\alpha_f \approx 5 \times 10^{-4}\ \mathrm{C}^{-1}$ at temperatures and pressures of interest (as estimated from tables in Schmidt (1969)), φ = 0.2-0.3, and Γ = 20–40° C/km, we find

$$\varphi \alpha_f \frac{DT}{Dt} \approx 0.06\text{–}1 \times 10^{-16}\ \mathrm{s}^{-1}$$

for V = 100–500 m/Ma. Considering that heat advection associated with sedimentation tends to reduce the geothermal gradient within a section of accumulating sediments (Sharp and Domenico, 1976, Fig. 4), this may, in fact, be an overestimate. It therefore appears that, averaged over burial times of millions of years, the effect of heating on fluid pressure will probably be negligible in comparison with the effect of porosity reduction by loading. We must emphasize, however, that the latter mechanism by itself can lead to Dp/Dt only as large as $D\bar{\sigma}/Dt$, regardless of the rapidity of sedimentation; larger values of Dp/Dt require an *additional* overpressuring mechanism. (This point is also emphasized by Magara (1975b).) Our analysis does not rule out the possibility that thermal expansion of fluid may be important in

achieving $Dp/Dt > D\bar{\sigma}/Dt$.

The effects of clay transformation and fluid release on pore pressure are less easily described by considering the differential equation for pore-pressure development. This is partially due to the fact that when dehydration of clay occurs, porosity may change independently of any change in loading; hence, $D\varphi/Dt$ can no longer be readily related to changes in p and $\bar{\sigma}$. The exact magnitude of the porosity- and pore-pressure changes induced by the dehydration process will depend on several factors, including the ease with which fluid can escape (i.e., on the permeability distribution), as well as on the mechanical constraint imposed by surrounding sediments.

We can nonetheless get reasonable numerical estimates for the effect of clay dehydration on pore pressure (as well as on porosity) by considering an illustrative special case, that of constant sediment volume during the dehydration process. This is a physically plausible configuration, because the mechanical constraint imposed by hundreds of meters of overlying strata should strongly inhibit any actual expansion of the material undergoing dehydration. There is no mechanical requirement that montmorillonite dehydration at depth cause an overall expansion or 'rebound' of the sedimentary column (cf. Magara, 1975a, p. 296).

Referring to Fig. 3A-1, we consider a small mass δM_B of adsorbed water transforming to free water with density ρ_f. We may write the total volume V_t in the 'initial' and 'final' states as

$$V_t^i = V_s + V_f^i + \delta V_B \tag{16a}$$

$$V_t^f = V_s + V_f^f \tag{16b}$$

where V_s is the volume of clay that remains after bound-water release and V_f is

the volume of free (pore) water. The superscripts i and f refer to 'initial state' and 'final state', respectively. These expressions may be rewritten as

$$V_t^i = V_s + \frac{M_f^i}{\rho_f^i} + \frac{\delta M_B}{\rho_B} \tag{17a}$$

$$V_t^f = V_s + \frac{M_f^i + \delta M_B}{\rho_f^f} \tag{17b}$$

where M_f^i is the initial mass of free water, which has density ρ_f^i. For small changes in density, corresponding to small δM_B, we can approximate

$$\rho_f^f = \rho_f^i (1 + \beta_f \delta p) \tag{18}$$

where δp is the change in pore pressure. Equating Eqns. (17a) and (17b) and using Eqn. (18), and neglecting terms involving the product $\delta M_B \delta p$, we find, after some rearrangement:

$$\delta p = \frac{1}{\beta_f M_f^i}\left(1 - \frac{\rho_f^i}{\rho_B}\right) \delta M_B \tag{19}$$

Noting that $M_f^i = \rho_f^i V_f^i$, and taking the limit of infinitesimal changes in all variables, we find

$$\left.\frac{Dp}{Dt}\right|_{\text{constant sed. vol.}} = \left(\frac{1}{\rho_f} - \frac{1}{\rho_B}\right) \frac{S}{\varphi \beta_f} \tag{20}$$

or using Eqn. (3):

$$\left.\frac{Dp}{Dt}\right|_{\text{constant sed. vol.}} = \left(\frac{1-\varphi}{\varphi \beta_f}\right)\left(\frac{\rho_B}{\rho_f} - 1\right)\left(\frac{1}{\rho_s - \rho_B}\right) \frac{D\rho_s}{Dt} \tag{21}$$

Note that an increase in pore pressure requires that $\rho_B > \rho_f$. A similar algebraic exercise leads to an expression for the rate of change of porosity of a sediment packet. We simply state here the result:

$$\left.\frac{D\varphi}{Dt}\right|_{\text{constant sed. vol.}} = \left(\frac{1-\varphi}{\rho_s - \rho_B}\right) \frac{D\rho_s}{Dt} \tag{22}$$

In the event that the surroundings provide a less-than-ideal mechanical constraint, we would expect Dp/Dt to be smaller, and $D\varphi/Dt$ to be larger, than given by Eqns. (21) and (22), respectively.

Estimates of the magnitudes of Dp/Dt and $D\varphi/Dt$ due to clay dehydration (at constant sediment volume) can be gotten once we have assigned values to ρ_B, the adsorbed-water density, ρ_s, the clay-grain density, and $D\rho_s/Dt$, the rate of change of clay-grain density. As noted in Appendix B, where we discuss the issue of the density of bound (adsorbed) water in montmorillonite, experimental data indicate that $\rho_B > \rho_f$ for adsorbed-water thicknesses less than *ca.* 4 monolayers; as the adsorbed-water content decreases below this value, ρ_B appears to increase monotonically (Martin, 1962, p. 32, Fig. 1). Hence, a constant value cannot be assigned to ρ_B. Rather, we would expect ρ_B to increase during the dehydration process, from a value of $10^3\ kg/m^3$ to perhaps $1.5\times10^3\ kg/m^3$ for the last adsorbed water layer (cf. Martin, 1962, p. 32, Fig. 1). For a clay initially composed solely of montmorillonite, grain density ρ_s will probably increase from *ca.* $2\times10^3\ kg/m^3$ to $2.5\times10^3\ kg/m^3$ during burial and dehydration (cf. Deer et al., 1966). If ρ_s changes through a fairly restricted depth interval of *ca.* 1-2 km (cf. Hower et al., 1976), then for reasonable sedimentation/subsidence rates of 100-500 m/Ma, we find $D\rho_s/Dt \approx 10^{-12}-10^{-11}\ kg\ m^{-3}s^{-1}$. Hence, using Eqns. (21) and (22) with $\varphi = 0.20$, we can estimate:

$$\left.\frac{Dp}{Dt}\right|_{\text{constant sed. vol.}} \approx 1-5\times(10^{-6}-10^{-5})\ Pa/s$$

where the lower limit has been calculated for $\rho_B = 1.1\times10^3\ kg/m^3$, $\rho_s = 2.1\times10^3\ kg/m^3$, and the upper limit for $\rho_B = 1.4\times10^3\ kg/m^3$, $\rho_s = 2.4\times10^3\ kg/m^3$. By way of comparison, we have

$$\left.\frac{Dp}{Dt}\right|_{\text{lithostatic gradient}} \approx \rho_m g V \approx 6\text{–}40 \times 10^{-8}\ \text{Pa/s}$$

We see that the potential rate of overpressure buildup due to montmorillonite dehydration is remarkably high. Rapid buildup of pore pressure to lithostatic values could occur. For example, making the conservative assumption that p is initially hydrostatic, the time t_b for p to reach lithostatic (if no excess-pressure diffusion occurs) will be approximately $\Delta\rho\, gD/(Dp/Dt)_{\text{constant sed. vol.}}$, where D is the depth to the zone of montmorillonite dehydration. Taking D = 3 km (cf. Hower et al., 1976) and the other parameters as above, we find $t_b < ca.$ 1 Ma. Pore pressure could therefore climb to lithostatic on a time scale short in comparison with the time scale for basin development. Mechanical failure and escape of overpressured fluids would then occur. Hence, montmorillonite dehydration could thus lead to repeated, *episodic* buildup and release of overpressure. This could be very important in the genesis of 'Mississippi Valley-type' Pb-Zn deposits (Dozy, 1970; Cathles and Smith, 1983), as elaborated below.

We can also estimate the rate of porosity change due to dehydration:

$$\left.\frac{D\varphi}{Dt}\right|_{\text{constant sed. vol.}} \approx 0.8 \times (10^{-15} - 10^{-14})\ \text{s}^{-1}$$

If excess-pressure diffusion were completely inhibited, this would lead to an increase in φ by about 0.1 in ca. 0.3-3 Ma. Porosity increases with depth in overpressured zones are often of this magnitude, or larger (e.g, Magara, 1975a, pp. 295-99). In comparison, the average rate of porosity change during burial is given by

$$\left|\frac{D\varphi}{Dt}\right| \approx \left|\frac{d\varphi}{dz}\right| V < ca.\ 10^{-14}\ \text{s}^{-1}$$

for compaction along a 'normal' trend, where we have estimated $d\varphi/dz$ by

using Eqn. (9), $b = 2\text{–}10 \times 10^{-4}\ m^{-1}$ and $V = 100\text{-}500$ m/Ma. $D\varphi / Dt$ is, of course, negative for normal compaction.

These estimates are likely to be a bit high, because we have implicitly assumed that the initial clay comprises solely montmorillonite. Nonetheless, it should be apparent from these simple calculations that montmorillonite dehydration has the potential for creating very large overpressures and arresting normal compaction.

5. DISCUSSION

In earlier discussions of the relative efficacy of various overpressuring mechanisms (e.g., Magara, 1975a, 1975b; Chapman, 1980; Keith, 1982), frequent reference has been made to a state of 'compaction disequilibrium.' A shale is considered to be in 'compaction disequilibrium' when its porosity falls off the 'normal' porosity *vs.* depth trend (Fig. 3-2). Magara (1975a) has argued that the likeliest cause of compaction disequilibrium is low permeability, which would inhibit the release of overpressures and permit maintenance of porosities greater than the 'equilibrium' value. Magara has argued that montmorillonite dehydration is not capable of causing porosities to deviate significantly from the 'normal' trend. This conclusion contrasts with our estimate of the effect of clay dehydration on porosity. If mechanical constraints prevent overall expansion of the sediment undergoing dehydration--a plausible situation--then porosity and pore pressure would increase rapidly. This tendency will be opposed, of course, by upward fluid diffusion due to the finite permeability of the overlying shale. Nonetheless, the extreme rapidity of porosity- and pore-pressure increase possible with clay dehydration--compared to values for even fairly rapid sedimentation--strongly

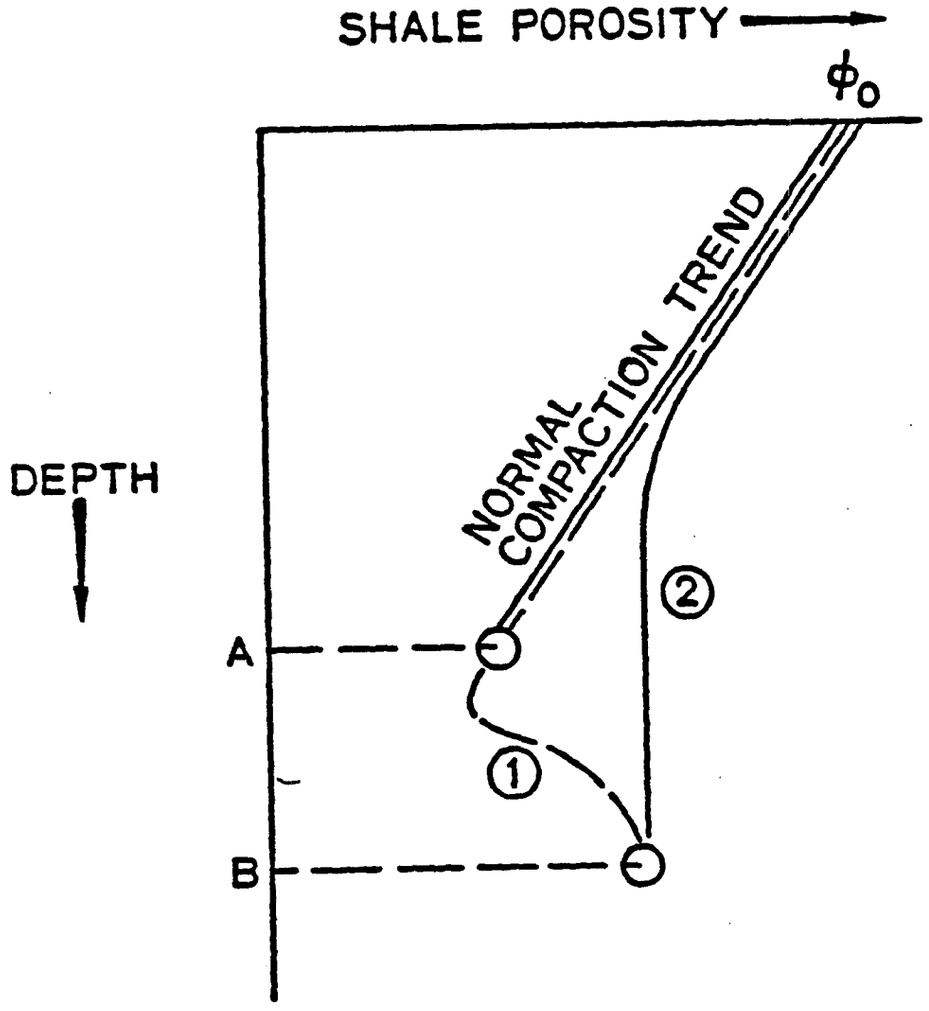

Figure 3-2: Porosity *vs.* depth trends, comparing 'normal' compaction with 'undercompaction' (after Magara (1975a), by permission of the American Association of Petroleum Geologists). Dashed line labeled with numeral 1 is the hypothetical porosity profile, as well as 'path' taken by shale element if porosity is altered by montmorillonite dehydration below depth A. Note that porosity *increases* between depths A and B. Path 2 correspond to the hypothetical situation in which the shale element becomes 'isolated' at some depth, i.e., to Magara's state of 'compaction disequilibrium'.

suggest that montmorillonite dehydration should be seriously considered as an agent of overpressuring and 'compaction disequilibrium'.

We emphasize that *there is no mechanical requirement* for montmorillonite dehydration at depth to cause overall expansion or 'rebound' of strata; in fact, such expansion seems mechanically very unlikely. We agree with Magara (1975a) that "the rebounding of a large sediment mass" would present "a difficult problem in geologic understanding." The redistribution of mass--with concomitant porosity change and probable overpressure development--that occurs when montmorillonite-bearing shales undergo dehydration is likely to cause localized deformation (probably brittle fracturing), but, in all likelihood, no large-scale strain.

The potential rapidity of pore-pressure buildup due to montmorillonite dehydration may have important implications for our understanding of the origin of 'Mississippi Valley-type' Pb-Zn deposits. These deposits, which are associated with sedimentary basins, are commonly considered to have formed as a result of basin dewatering (e.g., Dozy, 1980). Recent theoretical considerations by Cathles and Smith (1983) make it quite clear that the basin-dewatering mechanism can be valid only if dewatering occurs in an unstable, 'pulsatory' fashion, with fluid-flow rates much greater than could occur during 'steady' basin dewatering. Thermal constraints indicate that the source region for the dewatering pulses must be at a depth of 3-5 km (Cathles and Smith, 1983, p. 991). Interestingly, this depth interval coincides with the depths at which most montmorillonite dehydration occurs (e.g., Hower et al., 1976). Montmorillonite dehydration, with the concomitant pore-pressure buildup and release, could therefore supply 'pulses' of hot fluids. We suggest that this may well be the underlying mechanism responsible for genesis of Mississippi Valley-

type Pb-Zn deposits.

6. SUMMARY

We have derived fundamental equations necessary to describe overpressure development in shales, considering mechanical compaction, thermal expansion of pore fluid, and montmorillonite dehydration as potential causes of overpressuring. We then estimate the relative importances of these mechanisms. Rapid loading, together with low permeability, may be effective in causing pore pressure to increase at rates up to the rate of increase of overburden pressure. Thermal effects need not be invoked to explain overpressuring rates of such magnitudes, but could be important in achieving even faster overpressuring.

We estimate the effect of montmorillonite dehydration on porosity and pore pressure in a shale mass by detailed consideration of the dehydration process, in which adsorbed water is released into the pore space, undergoing a change in density. This process has the potential to cause very rapid overpressuring and increase in porosity, possibly leading to episodic buildup and release of overpressures This could play a critical role in the origin of Mississippi Valley-type Pb-Zn deposits.

APPENDIX A: CLAY DEHYDRATION AS A FLUID SOURCE

We can relate the fluid source strength S--the mass of water released per unit sediment volume per unit time--to the rate of change of grain density ρ_s by considering the idealized configuration in Fig. 3A-1. In the initial state, the system comprises montmorillonite (with adsorbed water) and pore water. We imagine that a small mass δM_B of adsorbed water, with volume δV_B, is released, becoming free pore water. The clay densities in the initial and final states, denoted by ρ_s^i and ρ_s^f, respectively, are given by

$$\rho_s^i = \frac{M_s^i + \delta M_B}{V_s^i + \delta V_B} \tag{A-1a}$$

$$\rho_s^f = \frac{M_s^f}{V_s^f} \tag{A-1b}$$

where M_s and V_s are the mass and volume of the clay and the superscripts i and f again denote 'initial' and 'final' states. If the dehydration process does not involve processes other than release of the bound water, then $M_s^i = M_s^f$ and $V_s^i = V_s^f$; hence, we can drop the superscripts. Denoting the change in clay density $\rho_s^f - \rho_s^i$ by $\delta\rho_s$, we find after some algebraic manipulations:

$$\delta\rho_s = \frac{M_s \delta V_B - V_s \delta M_B}{V_s (V_s + \delta V_B)} \tag{A-2}$$

However, $\delta V_B = \delta M_B / \rho_B$, where ρ_B is the density of the bound water. Thus, after some further rearrangement, we find:

$$\delta M_B = \frac{V_s^2 \delta\rho_s}{\frac{M_s}{\rho_B} - V_s \left(1 + \frac{\delta\rho_s}{\rho_B}\right)} \tag{A-3}$$

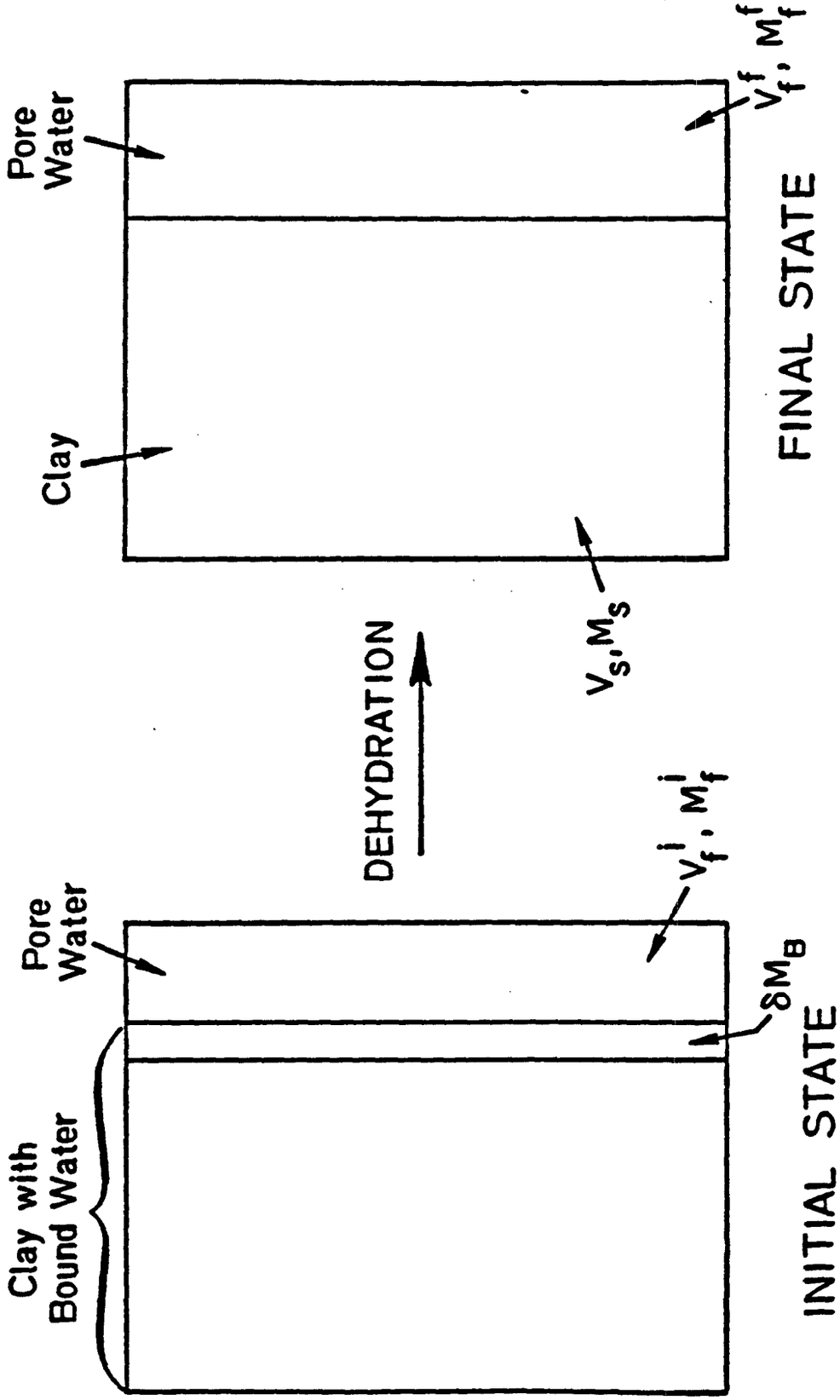

Figure 3A-1: Idealized clay-water system, depicting release of a small amount of water from the bound state into the pore space.

Noting that $M_s = V_s \rho_s^f$, this becomes, after dividing by V_t^f, the total volume in the final state:

$$\frac{\delta M_B}{V_t^f} = \frac{\frac{V_s}{V_t^f}\delta\rho_s}{\frac{\rho_s^f}{\rho_B} - \left(1 + \frac{\delta\rho^s}{\rho_B}\right)} \tag{A-4}$$

or

$$\frac{\delta M_B}{V_t^f} = \frac{(1-\varphi^f)\,\delta\rho_s}{\frac{\rho_s^f}{\rho_B} - (1-\varphi^f)\,\delta\rho_s} \tag{A-5}$$

where φ^f is porosity in the final state. Dividing by δt, the time increment for the bound-water mass δM_B to be released, and taking the limit of infinitesimal mass transfers, we find

$$S = \frac{1}{V_t}\frac{DM_B}{Dt} = \left(\frac{\rho_B}{\rho_s - \rho_B}\right)(1-\varphi)\,\frac{D\rho_s}{Dt} \tag{A-6}$$

This result is independent of the details of how the released fluid is distributed. Eqn. (A-6) should be generally valid for any dehydration reaction involving release of adsorbed water. (Note that we have not considered here other phenomena, such as potassium fixation by the clay (cf. Perry and Hower, 1970) that are probably an integral part of the montmorillonite-illite transformation process.)

APPENDIX B: DENSITY OF BOUND WATER IN MONTMORILLONITE

The issue of whether ρ_B, the density of bound, or adsorbed, water in montmorillonite, is greater than the density ρ_f of free water, has been the focus of considerable disagreement among petroleum geologists. For example, Burst (1969, p. 82) argued that when only two adsorbed monolayers of water were left on montmorillonite surfaces, ρ_B would exceed ρ_f. In contrast, Hunt (1979, p. 203) has stated flatly that "the water between the smectite layers [i.e., the adsorbed water] has a lower density than the water in the larger pores" and that "statements in the literature that clay mineral dehydration causes abnormal pressures are erroneous."

The divergence of opinion as to whether or not ρ_B is greater than ρ_f seems to stem from confusion about experimental data on the subject. Hunt (1979) states that the data of Anderson and Low (1958) prove that $\rho_B < \rho_f$. In fact, a careful examination of their data shows that Anderson and Low determined ρ_B only for water/clay ratios greater than *ca.* 1 g H_2O / g clay. This corresponds (cf. Martin, 1962) to adsorbed water thicknesses of more than *ca.* 10 monolayers. Martin's (p. 32, Fig. 1) review of adsorbed water-density determinations for a sodium montmorillonite indicate that for water contents less than *ca.* 0.4 g H_2O / g clay--that is, for adsorbed-water thicknesses of *ca.* 4 monolayers or less--the adsorbed water density is *greater* than that of free water. These last few monolayers are presumably released during the montmorillonite-illite transformation; any additional bound water will probably have been gradually lost during burial (Burst, 1969). Hence, we are justified in taking $\rho_B > \rho_f$ during the dehydration process.

REFERENCES

Anderson, D.M., and P.F. Low, 1958, The density of water adsorbed by lithium-, sodium-, and potassium-bentonite. *Soil Science Society of America Proceedings, 22*, 99-103.

Athy, L.F., 1930, Density, porosity, and compaction of sedimentary rocks. *American Association of Petroleum Geologists Bulletin, 14*, 1-24.

Barker, C., 1972, Aquathermal pressuring--role of temperature in development of abnormal-pressure zones. *American Association of Petroleum Geologists Bulletin, 56*, 2068-71.

Bishop, R.S., 1979, Calculated compaction states of thick abnormally pressured shales. *American Association of Petroleum Geologists Bulletin, 63*, 918-33.

Bonham, L.C., 1980, Migration of hydrocarbons in compacting basins. *American Association of Petroleum Geologists Bulletin, 64*, 549-67.

Bredehoeft, J.D., and B.B. Hanshaw, 1968, On the maintenance of anomalous fluid pressures: I. Thick sedimentary sequences. *Geological Society of America Bulletin, 79*, 1097-1106.

Burst, J.F., 1969, Diagenesis of Gulf Coast clayey sediments and its possible relation to petroleum migration. *American Association of Petroleum Geologists Bulletin, 53*, 73-93.

Carstens, H., and H. Dypvik, 1981, Abnormal formation pressure and shale porosity. *American Association of Petroleum Geologists Bulletin, 65*, 344-50.

Cathles, L.M., and A.T. Smith, 1983, Thermal constraints on the formation of Mississippi Valley-type lead-zinc deposits and their implications for episodic basin dewatering and deposit genesis. *Economic Geology, 78*, 983-1002.

Chapman, R.E., 1980, Mechanical versus thermal cause of abnormally high pore pressures. *American Association of Petroleum Geologists Bulletin, 64*, 279-83.

Deer, W.A., R.A. Howie, and J. Zussman, 1966, *An introduction to the rock-forming minerals*. London, Longman Group Ltd., 528 pp.

Dibble, W.E., Jr., A. Nur, and J. Potter, Unpublished, Porosity reduction in sandstone. Paper presented at 58th Annual Technical Conference and Exhibition, Society of Petroleum Engineers, San Francisco, California, October 5-8, 1983.

Dickinson, G., 1953, Geological aspects of abnormal reservoir pressures in Gulf Coast Louisiana. *American Association of Petroleum Geologists Bulletin, 37*, 410-32.

Domenico, P.A., and M.D. Mifflin, 1965, Water from low-permeability sediments and land subsidence. *Water Resources Research, 1*, 563-76.

Dozy, J.J., 1970, A geologic model for the genesis of the lead-zinc ores of the Mississippi VAlley, U.S.A. *Institution of Mining and Metallurgy Transactions, 79B*, 163-70.

Fertl, W.H., and D.J. Timko, 1970, Occurrence and significance of abnormal-pressure formations. *Oil and Gas Journal, 68*, No. 1, 97-108.

Hanshaw, B.B., and E. Zen, 1965, Osmotic equilibrium and overthrust faulting. *Geological Society of America Bulletin, 76*, 1379-86.

Hower, J., E.V. Eslinger, M.E. Hower, and J.A. Perry, 1976, Mechanism of burial metamorphism of argillaceous sediments: 1. Mineralogical and chemical evidence. *Geological Society of America Bulletin, 87*, 725-37.

Hunt, J.M., 1979, *Petroleum geology and geochemistry*. San Francisco, W.H. Freeman and Company, 617 pp.

Keith, L.A., 1982, A numerical compaction model of overpressuring in shales. M.S. thesis, Virginia Polytechnic Institute and State University, Blacksburg, Virginia, 80 pp.

McGarr, A., and N.C. Gay, 1978, State of stress in the Earth's crust. *Annual Reviews of Earth and Planetary Science, 6*, 405-36.

McKenzie, D.P., 1978, Some remarks on the development of sedimentary basins. *Earth and Planetary Science Letters, 40*, 25-32.

Magara, K., 1975a, Reevaluation of montmorillonite dehydration as cause of abnormal pressure and hydrocarbon migration. *American Association of Petroleum Geologists Bulletin, 59*, 292-302.

Magara, K., 1975b, Importance of aquathermal pressuring effect in Gulf Coast. *American Association of Petroleum Geologists Bulletin, 59*, 2037-45.

Magara, K., 1976, Water expulsion from clastic sediments during compaction--directions and volumes. *American Association of Petroleum Geologists Bulletin, 60*, 543-53.

Malvern, L.E., 1969, *Introduction to the mechanics of a continuous medium*. Prentice-Hall Inc., Englewood Cliffs, New Jersey, 713 pp.

Marsal, D., and W. Philipp, 1970, Compaction of shale. *Geological Institutions of the University of Uppsala Bulletin, New Series, 2*, 59-66.

Martin, R.T., 1962, Adsorbed water on clay: a review. *Clays and Clay Minerals, 9*, 28-70.

Nagumo, S., 1965, Compaction of sedimentary rock--a consideration by the theory of porous media. *University of Tokyo, Earthquake Research Institute Bulletin, 43*, 339-48.

Ortenblad, A., 1929-30, Mathematical theory of the process of consolidation of mud deposits. *Journal of Mathematics and Physics, 9*, 73-149.

Palciauskas, V.V., and P.A. Domenico, 1980, Microfracture development in compacting sediments: relation to hydrocarbon-maturation kinetics. *American Association of Petroleum Geologists Bulletin, 64*, 927-37.

Perry, E., and J. Hower, 1970, Burial diagenesis in Gulf Coast pelitic sediments. *Clays and Clay Minerals, 18*, 165-77.

Plumley, W.J., 1980, Abnormally high fluid pressure: survey of some basic principles. *American Association of Petroleum Geologists, Bulletin, 64*, 414-30.

Powers, M.C., 1967, Fluid-release mechanisms in compacting marine mudrocks and their importance in oil exploration. *American Association of Petroleum Geologists Bulletin, 51*, 1240-54.

Schmidt, E., preparer, 1969, *Properties of water and steam in SI-units*. Springer-Verlag, Berlin, 205 pp.

Seeburger, D., 1981, Studies of natural fractures, fault zone permeability, and a pore space-permeability model. Ph. D. thesis, Stanford University, Stanford, California, 234 pp.

Sharp, J.M., Jr., 1976, Momentum and energy balance equations for compacting sediments. *International Association for Mathematical Geology Journal, 8*, 305-22.

Sharp, J.M., Jr., 1978, Energy and momentum transport model of the Ouachita basin and its possible impact on formation of economic mineral deposits. *Economic Geology, 73*, 1057-68.

Sharp, J.M., Jr., and P.A. Domenico, 1976, Energy transport in thick sequences of compacting sediment. *Geological Society of America Bulletin, 87*, 390-400.

Sleep, N.H., 1971, Thermal effects of the formation of Atlantic continental margins by continental break up. *Geophysical Journal of the Royal Astronomical Society, 24*, 325-50.

Smith, J.E., 1971, The dynamics of shale compaction and evolution of pore-fluid pressures. *International Association for Mathematical Geology Journal, 3*, 239-63.

Smith, J.E., 1973, Shale compaction. *Society of Petroleum Engineers Journal, 13*, 12-22.

Terzaghi, K., 1943, *Theoretical soil mechanics*. New York, John Wiley and Sons, 510 pp.

NOTATION

b reciprocal of scale length in porosity *vs.* depth relationship

f superscript denoting 'final state'

g acceleration due to gravity

h sediment thickness

i superscript denoting 'initial state'

k permeability

M_B mass of adsorbed water in montmorillonite

M_f mass of free pore water

M_s mass of clay grains

M_T total mass of clay-water system during dehydration

p pore-fluid pressure

S fluid source strength (mass of water released per unit sediment volume per unit time)

t time

t_b time for initially hydrostatic pressure to reach lithostatic due to clay dehydration

T temperature

u_f velocity (i.e., volumetric flux) of pore fluid

u_s velocity of sediment grains

V sedimentation rate

V_B volume of adsorbed water in montmorillonite

V_f volume of free pore water

V_s volume of clay grains

V_T total volume of clay-water system during dehydration

z vertical coordinate

α sediment 'compressibility'

α_f thermal expansivity of fluid

β_f fluid compressibility

Γ magnitude of geothermal gradient

δ denotes small change in parameter, e.g., δM_B

μ viscosity of pore fluid

ρ_B density of adsorbed water in montmorillonite

ρ_f density of pore fluid

$\rho_m = \rho_f \varphi + \rho_s (1-\varphi)$ sediment density

ρ_s clay-grain density

ρ_w density of sediment at the sediment surface

$\Delta\rho$ $\rho_s - \rho_f$

$\overline{\sigma}$ confining pressure, approximated as equal to overburden pressure

$\Sigma = \overline{\sigma} - p$ effective pressure

φ porosity

φ_0 porosity at sediment surface

CHAPTER 4
PHYSICAL PROCESSES IN ACCUMULATING SEDIMENTS III: FLUID FLOW AND PORE PRESSURE IN COMPACTING SAND-SHALE SEQUENCES

ABSTRACT

We present simple mathematical models to examine the nature of fluid flow and pore-pressure development in compacting sand-shale sequences. This study differs from most previous work in that we explicitly consider flow along bedding as well as flow normal to bedding. We show that when relatively permeable sand units have easy hydraulic connection to the sediment surface, water expelled during shale compaction should often become funneled along these sands. Such flow—the magnitude of which is controlled by a number of geometrical and physical parameters, particularly strata thicknesses and permeabilities—could have a major effect on hydrocarbon migration and overpressure development within sedimentary basins.

1. INTRODUCTION

Fluid flow in compacting sediments is widely considered to be of critical importance in hydrocarbon migration and concentration (e.g., Hunt, 1979) and in the genesis of certain types of Pb-Zn deposits (e.g., Dozy, 1970; Cathles and Smith, 1983). Much attention has been focussed on shale dewatering, especially in connection with the development of overpressures, with mathematical models of varying complexity presented by a number of workers, including Bredehoeft and Hanshaw (1968), Smith (1971, 1973), Sharp and Domenico (1976), Bishop (1979), and Keith (1982). These models have all

focussed on the highly idealized case of pore-pressure development within homogeneous, laterally extensive shale units. In all of these models, as an inevitable by-product of the assumed geometry, fluid flow must be assumed to be only vertical, i.e., normal to bedding. Although such models have certainly aided our understanding of pore-pressure development in sedimentary basins, they are limited by their inherent geometrical simplifications. Features such as alternating sand and shale units, as well as the nonuniform thickness of these units, may strongly affect the direction of fluid flow. Magara (1976) has considered the effect of nonuniform strata thicknesses on fluid flow in sand-shale sequences, presenting estimates for the permeability contrast between interlayered sands and shales that would result in volumetrically important lateral flow within sand units. In this chapter, we have significantly extended Magara's work. We consider a range of idealized geometrical configurations of interbedded sands and shales in order to better define the way in which fluid flow and pore pressure in accumulating sediments will be affected by material inhomogeneities. We also discuss the implications of our model for hydrocarbon concentration.

2. ANALYSIS

Excess-pressure development in the presence of lateral flow in sands

As mentioned above, earlier models of pore-pressure development in accumulating sediments have begun with an idealized geometry, one in which fluid flow is only in the vertical direction, i.e., normal to bedding. This should be a very good approximation for homogeneous sediments far from basin margins or other structural discontinuities; it will probably be inadequate, however, for sequences of interlayered sands and shales (Magara, 1976) or in

the vicinity of steeply dipping, permeable fault zones (cf. Bell and Nur, 1976).

The limitations of the one-dimensional compaction model may be quantified, in an approximate fashion, by considerations of flow in a simple 'two-dimensional' sedimentary sequence, as shown diagrammatically in Fig. 4-1. A shale of thickness d_u overlies a sand† layer of thickness l; the sand in turn overlies a shale layer of thickness d_l. The layers are assumed to be horizontal. Vertical structural boundaries of some specified width w and permeability exist at $x=L$ and $x=-L$. It may be convenient to think of these as permeable fault zones (cf. Seeburger, 1981); however, their exact nature is not critical for our analysis.

Localization of flow along 'sandy' units could serve to 'focus' and concentrate hydrocarbons. In order to better understand such phenomena, we must address two important, related questions in regards to lateral flow through relatively permeable strata:

i) Can excess fluid pressure develop in such 'sandy' units during lateral flow, and if so, of what magnitude?

ii) What is the relative proportion of water expelled during shale dewatering that flows laterally through such 'sandy' units?

We begin by determining approximately the conditions under which excess pressure development is possible within relatively permeable units. A simple model for fluid pressure development associated with lateral flow in 'sandy' units may be readily developed. Referring to Fig. 4-1, we consider the case in which all water expelled during dewatering of the lower shale must migrate laterally through the overlying sand, then upward along the

†For convenience, we will refer to all relatively permeable units in the sedimentary section, regardless of actual lithology, as 'sands'.

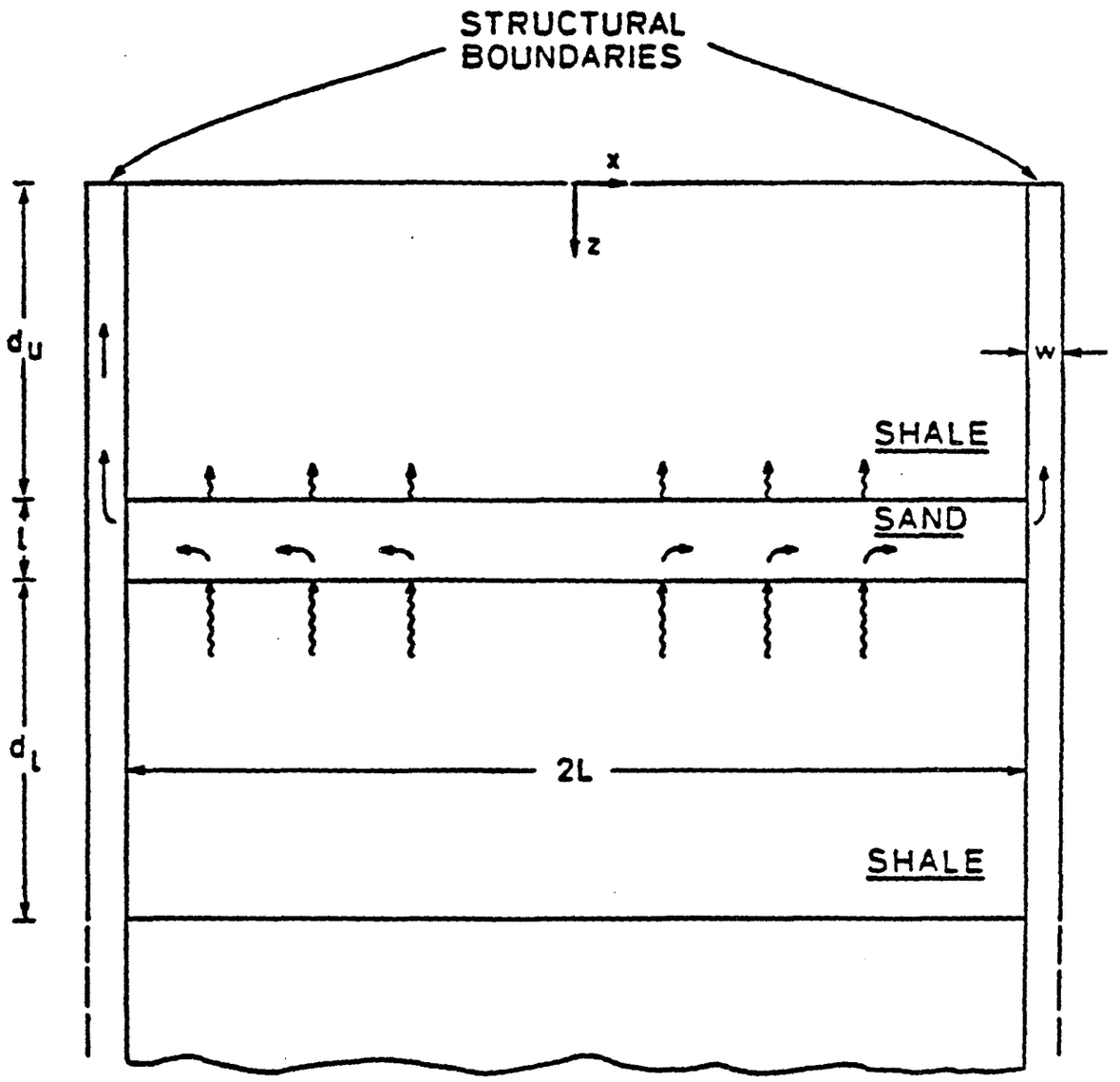

Figure 4-1: Coordinate system and generalized geometry of interbedded shales and sands with vertically dipping 'boundary zones'.

boundaries at L and $-L$. (In some sense, therefore, we are treating the sand layer as a confined aquifer.) The upper shale is considered to be impermeable. Clearly, this will overestimate the tendency for excess-pressure development in the sand; nonetheless, it permits us to reach some important generalizations by dimensional arguments.

A further simplification will be to assume that the sand layer has constant properties during dewatering of the underlying shale; in other words, we assume that l, as well as the sand porosity and permeability, do not change. This may at first appear to be a physically unjustifiable assumption, given the nature of the study; after all, we are investigating *compaction*. However, the constant-properties assumption should not lead us far astray as long as we restrict our attention to fluid-pressure development on time scales short enough that the sand properties would not change significantly. (In fact, the constant-properties assumption should generally lead to *underestimates* of fluid pressure in the sand, because decreasing porosity and permeability, for a specific shale-dewatering flux, would tend to inhibit fluid escape, thereby enhancing any overpressure.)

An equation describing fluid pressure in the sand layer may be written once we realize that the water expelled from the underlying shale may be characterized, in the mathematical sense, as a continuous fluid source $R(t)$, the mass of fluid expelled upward per unit time and unit area of sand-shale interface. The mass conservation relationship for the sand is therefore

$$\frac{\partial}{\partial t}(\rho_f \varphi) = -\frac{\partial}{\partial x}(\rho_f u_f \varphi) + \frac{R(t)}{l} \qquad (1)$$

where

ρ_f = fluid density

φ = sand porosity

u_f = volumetric flow rate of fluid

t = time

We now assume that pore-fluid flow along the sand layer can be described by Darcy's law, viz.:

$$\varphi u_f = -\frac{k_{sand}}{\mu}\frac{\partial p}{\partial x} \tag{2}$$

where

p = pore pressure

k_{sand} = permeability of sand

μ = viscosity

We have implicitly assumed in Eqn. (2) that the sand is not deforming, in accord with the constant-properties assumption as elaborated above. We also assume that the fluid density will be a function only of pore pressure, i.e., we neglect thermal effects and salinity gradients. Hence, the equation of state of the pore fluid can be written as

$$\frac{\partial \rho_f}{\partial p} = \beta_f \rho_f \tag{3}$$

where β_f is the fluid compressibility. Using Eqns. (2) and (3) in (1), holding sand properties constant, and neglecting terms of $O[(\partial p / \partial x)^2]$, we find a diffusion-type equation for p_{sand}, the fluid pressure within the sand layer:

$$\frac{\partial p_{sand}}{\partial t} = c_{sand}\frac{\partial^2 p_{sand}}{\partial x^2} + \frac{R(t)}{l\rho_f \varphi \beta_f} \tag{4}$$

where $c_{sand} = k_{sand} / \mu\varphi\beta_f$ is the hydraulic diffusivity; other symbols are as defined above.

A simple physical model permits us to express $R(t)$ in terms of more readily identifiable parameters. First, we note that the total fluid mass that potentially can be expelled from the lower shale is limited by the 'initial' values of the shale's thickness and average porosity, viz.:

$$\int_0^{\infty} R(t)\,dt = d_i \Phi \rho_f \tag{5}$$

where d_i and Φ may be considered the 'initial' thickness and average porosity, respectively, for the lower shale. (The choice of 'initial' values is arbitrary as long as we do not choose an 'initial' time for which the lower shale is completely dewatered. We have implicitly assumed, of course, that the shale *will* become compacted and dewatered due to continued sediment loading.)

It seems physically reasonable that $R(t)$ should be a decreasing function of time; after all, fluid expulsion must cease as porosity is reduced to zero. Assuming, for simplicity, that $R(t) \propto e^{-t/\tau}$, where τ is a characteristic time scale--say, the duration of sedimentation--and using Eqn. (5), Eqn. (4) can be rewritten as

$$\frac{\partial p_{sand}}{\partial t} = c_{sand} \frac{\partial^2 p_{sand}}{\partial x^2} + \left(\frac{d_i}{l}\right)\left(\frac{\Phi}{\varphi}\right)\left(\frac{1}{\beta_f \tau}\right) e^{-t/\tau} \tag{6}$$

The form of the source term on the right-hand side of Eqn. (6) clearly shows that the effect of the dewatering source on fluid pressure in the sand depends strongly on the relative thicknesses and porosities of the 'source' and 'sink' strata, as well as on the time scale τ over which dewatering occurs.

Recasting Eqn. (6) into dimensionless form leads us to an estimate of a 'critical' permeability for significant overpressures to develop within the sand.

We adopt the scalings

$$p = \rho_f g d_u \tilde{p}$$

$$t = T\tilde{t}$$

$$x = L\tilde{x}$$

where g is the acceleration due to gravity and dimensionless variables are denoted by tildes. The characteristic pressure chosen is the hydrostatic pressure at the depth of the sand layer. Using these scalings in Eqn. (6), and recognizing that $L^2/c = \tau_d$, the characteristic time scale for excess-pressure diffusion, we find, after some rearrangement:

$$\left(\frac{\tau_d}{T}\right)\frac{\partial \tilde{p}}{\partial \tilde{t}} = \frac{\partial^2 \tilde{p}}{\partial \tilde{x}^2} + \left(\frac{L^2}{k_{sand}}\right)\left(\frac{d_l}{l}\right)\left(\frac{\mu\Phi}{\rho_f g d_u \tau}\right) e^{-\left(\frac{T}{\tau}\right)\tilde{t}} \qquad (7)$$

There are clearly two characteristic time scales in the physical system, viz., τ and τ_d. For times $T \gg \tau_d$, pore pressure in the sand layer will be in a quasi-steady state, changing very slowly only because the source term varies slowly with time. Because the value of the exponential term cannot exceed unity, we see that the fluid source will have a major influence on pore pressure in the sand when

$$\left(\frac{L^2}{k_{sand}}\right)\left(\frac{d_l}{l}\right)\left(\frac{\mu\Phi}{\rho_f g d_u \tau}\right) > 1$$

Therefore, when water expelled from a shale unit is concentrated within, and flows laterally along a relatively permeable sand unit, significant overpressures are likely to build up within that sand if k_{sand} satisfies the condition

$$k_{sand} < k_1 = \left(\frac{d_l}{l}\right)\left(\frac{\mu\Phi}{\rho_f g d_u \tau}\right) L^2 \qquad (8)$$

For sand permeabilities in the range *ca.* $k_1 < k_{sand} < 10\,k_1$, some overpressuring

will occur, but not of large magnitude. Overpressuring will be essentially negligible for $k_{sand} > 10k_1$.

Importance of lateral fluid flow during sedimetn compaction

The dimensional arguments presented above indicate that if a sand layer acts as a 'confined' aquifer--funneling along itself all water expelled from underlying compacting shales--then, under appropriate conditions, significant overpressures may develop within that sand layer. In making those arguments, we assumed that all of the water expelled by compaction of the underlying shale would flow laterally along the sand layer. We now must address the issue of the actual quantitative importance of flow through such a layer, relative to the flow normal to stratification. We proceed by assuming that some fraction f of the water expelled from the lower shale (see Fig. 4-1) will travel laterally through the overlying sand layer, then upward along the vertical 'fault' boundaries. The remaining fraction $(1-f)$ of the water expelled during compaction of the lower shale will 'leak' upward through the upper shale. The fraction f may be expected to be a complex function of parameters such as thicknesses and permeabilities of the various rock units. Our goal here is to determine that function in an approximate fashion.

We will assume, for simplicity, that flow is in a quasi-steady state. This should be valid as long as we consider only time scales small compared with τ, so that $R(t)$ is nearly constant. The fluid pressure in the sand will therefore satisfy the equation (cf. Eqn. (4)):

$$c_{sand}\,\frac{\partial^2 p_{sand}}{\partial x^2} = -f\,\left(\frac{d_i}{l}\right)\left(\frac{\Phi}{\varphi}\right)\left(\frac{1}{\beta_f \tau}\right) \qquad (9)$$

We have implicitly assumed here that $l \ll d_u$ and $l \ll L$, so that variation of p_{sand} in the z-direction is negligible in comparison with the variation along x.

Because the sand layer and vertical boundaries are hydraulically connected, we cannot solve for p_{sand} independently of p_B, the fluid pressure in the boundary zones (although the solution for p_B itself will not be needed later). Assuming that the vertical boundaries may be treated as zones of finite width w and permeability k_B, p_B will satisfy the equation (for the assumed quasi-steady state):

$$\frac{\partial^2 p_B}{\partial z^2} = 0 \tag{10}$$

The dependence of p_B on x may be safely neglected as long as $w \ll d_u$.

The boundary conditions needed to complete the specification of the lateral flow problem are

i) $\frac{\partial p_{sand}}{\partial x}(x=0) = 0$

ii) $p_B\ (z=0) = 0$

iii) $-k_{sand}\, l\, \frac{\partial p_{sand}}{\partial x}(x=L) = k_B w\, \frac{\partial p_B}{\partial z}(z=d_u)$

The first boundary condition expresses the assumed symmetry (equal flow towards both vertical boundaries); the second is the usual free-surface condition on pressure; the third expresses flux continuity between sand layer and boundary zone. We find that the fluid pressure in the sand layer is given by

$$p_{sand}(x) = \left[\rho_f g + f\left(\frac{d_l}{l}\right)\left(\frac{\Phi}{\varphi}\right)\left(\frac{k_{sand}}{k_B}\right)\left(\frac{l}{w}\right)\left(\frac{1}{\beta_f \tau}\right)\left(\frac{L}{c_{sand}}\right)\right] d_u + \tag{11.}$$

$$+ f\left(\frac{d_l}{l}\right)\left(\frac{\Phi}{\varphi}\right)\left(\frac{1}{\beta_f \tau}\right)\left(\frac{1}{2c_{sand}}\right)(L^2 - x^2)$$

This solution allows us now to compute the lateral and vertical fluid fluxes. The net lateral fluid flux through the sand per unit 'width', Q_x, is given by

$$Q_z = -\frac{2k_{sand}l}{\mu}\frac{\partial p_{sand}}{\partial x}(x=L)$$

or

$$Q_z = \frac{2fd_l\Phi L}{\tau} \tag{12}$$

In order to examine the magnitude of the 'leakage' from sand to overlying shale, we must also consider the fluid pressure in the upper shale. Although a 'complete' solution for this pressure, in the form of a Fourier series, could be found by solving the appropriate boundary-value problem, such a solution could not easily be used to calculate the quantity of most interest to us, namely, the vertical fluid flux through the shale. This flux may be determined approximately, however, by an averaging technique. Let $\langle p_e \rangle = (1/2L)\int_{-L}^{L} p_e(x)\,dx$ be the average excess pressure in the shale; $\langle p_e \rangle$ will be a function of z, but not of x. Using Eqn. (11), we find that the average excess pressure along the sand-upper shale interface, denoted by $\overline{\langle p_e \rangle}$, is given by

$$\overline{\langle p_e \rangle} = \frac{fd_l\Phi\mu L}{\tau}\left[\frac{d_u}{k_B w} + \frac{L}{3l\,k_{sand}}\right] \tag{13}$$

This must equal the drop in excess pressure as fluid goes from $z = d_u$ to $z = 0$. This pressure drop causes an upward volumetric fluid flux $\langle q_z \rangle$ given by Darcy's law as

$$\langle q_z \rangle = \frac{k}{\mu}\frac{d\langle p_e \rangle}{dz}$$

This expression can be integrated to give another expression for $\overline{\langle p_e \rangle}$:

$$\overline{\langle p_e \rangle} = \mu\int_0^{d_u} \frac{\langle q_z \rangle}{k_{shale}(\zeta)}\,d\zeta \tag{14}$$

However, if pressure in the shale is at a steady state, as we have assumed, then, ignoring the very minor effect of fluid compressibility, $\langle q_z \rangle$ will not vary with z. We may therefore write

$$\overline{\langle p_e \rangle} = \mu \langle q_z \rangle \int_0^{d_u} \frac{d\zeta}{k_{shale}(\zeta)} \tag{15}$$

The net upward fluid flux through the shale per unit 'width', Q_z, is therefore given by

$$Q_z = 2L\langle q_z \rangle = \frac{2L\overline{\langle p_e \rangle}}{\mu \int_0^{d_u} \frac{d\zeta}{k_{shale}(\zeta)}} \tag{16}$$

As the final step in determining Q_z, we now assume that $k_{shale}(z) = k_0 e^{-z/z_0}$ (see the Appendix for a discussion of this assumption). Using this assumed functional form for $k_{shale}(z)$ in Eqn. (16), along with Eqn. (13), we finally find

$$Q_z = \frac{2fk_0\Phi d_l L^2}{\tau z_0} e^{-d_u/z_0} \left[\frac{d_u}{k_B w} + \frac{L}{3l\,k_{sand}} \right] \tag{17}$$

This must be equal to the fraction of the total dewatering flux that does *not* flow through the sandy layer, viz.:

$$Q_z = \frac{2(1-f)d_l \Phi L}{\tau} \tag{18}$$

Equating Eqns. (17) and (18), we finally solve for f:

$$f = \left\{ 1 + \left(\frac{L}{z_0}\right) e^{-d_u/z_0} \left[\left(\frac{d_u}{w}\right)\left(\frac{k_0}{k_B}\right) + \left(\frac{L}{3l}\right)\left(\frac{k_0}{k_{sand}}\right) \right] \right\}^{-1} \tag{19}$$

As expected, f is a complex function of geometrical parameters, as well as of the permeabilities of the various units. For $f > 0.5$, lateral flow through the sandy unit will predominate over vertical flow through the upper shale. This

condition is met when

$$\left(\frac{L}{z_0}\right) e^{-d_u/z_0} \left[\left(\frac{d_u}{w}\right)\left(\frac{k_0}{k_B}\right) + \left(\frac{L}{3l}\right)\left(\frac{k_0}{k_{sand}}\right)\right] \leq 1 \qquad (20)$$

Consideration of two limiting cases casts light on the meaning of the criterion expressed by Eqn. (20). First, consider the case of 'very permeable' boundary zones. By 'very permeable', we mean (cf. Eqn. (19))

$$\left(\frac{d_u}{w}\right)\left(\frac{k_0}{k_B}\right) \ll \left(\frac{L}{3l}\right)\left(\frac{k_0}{k_{sand}}\right)$$

or

$$\frac{k_B}{k_{sand}} \gg \left(\frac{3l}{w}\right)\left(\frac{d_u}{L}\right)$$

In this case, we have

$$f \approx \left[1 + \left(\frac{L}{z_0}\right)\left(\frac{L}{3l}\right)\left(\frac{k_0}{k_{sand}}\right) e^{-d_u/z_0}\right]^{-1} \qquad (21)$$

and the condition for horizontal flow to predominate is $k_{sand} > \alpha k_0$, where $\alpha = (L/3l)(L/z_0)e^{-d_u/z_0}$, independent of the boundary-zone width and permeability. We see that the tendency for lateral flow to predominate will increase as (L/l) and (L/z_0) decrease.

The other limiting case is that of 'low permeability' boundary zones, i.e., those for which k_B is small enough that

$$\frac{k_B}{k_{sand}} \ll \left(\frac{3l}{w}\right)\left(\frac{d_u}{L}\right)$$

In this case, we find

$$f \approx \left[1 + \left(\frac{L}{z_0}\right)\left(\frac{d_u}{w}\right)\left(\frac{k_0}{k_B}\right) e^{-d_u/z_0}\right]^{-1} \qquad (22)$$

and the condition for predominance of lateral flow becomes $k_B < \gamma k_0$, where

$\gamma = (d_u / w)(L / z_0) e^{d_u / z_0}$, independent of sand thickness and permeability.

These two limiting cases are illustrated by Figs. 4-2a and 4-2b, for the 'very permeable' and 'low permeability' cases, respectively. The values of f were calculated using L = 10 km, d_u = 1 km, l = 100 m, and w = 10 m, and two plausible values of k_0 (see the Appendix). For these parameter values, the 'very permeable' and 'low permeability' conditions become $k_B / k_{sand} \gg 3$ and $k_B / k_{sand} \ll 3$, respectively. Other geometrical parameters would clearly lead to different numerical results, but the cases illustrated should allow us to reach some general conclusions:

i) In the 'very permeable' boundary case, for typical reservoir sand permeabilities, a very large fraction of the water expelled during clay compaction should flow laterally through sand layers.

ii) Even for 'low permeability' boundaries, lateral flow is likely to be volumetrically significant for boundary-zone permeabilities in excess of *ca.* 100 μdarcy. Boundary zones must have permeabilities substantially less than those of typical reservoir sands for lateral flow to be essentially eliminated.

We also recall (cf. Eqn. (8)) that for certain limited conditions, not only will lateral flow within the sand predominate over vertical 'leakage', but this lateral aquifer-like flow will be accompanied by significant overpressures. The conditions for such to occur may be expressed as

$$\alpha k_0 < k_{sand} < k_1 \qquad \text{('very permeable' boundary)} \qquad (23a)$$

$$k_{sand} < k_1; k_0 < \gamma k_B \qquad \text{('low permeability' boundary)} \qquad (23b)$$

These limiting cases are shown schematically in Figs. 4-3a and 4-3b, respectively. In general, there should be at least three different flow/pore-

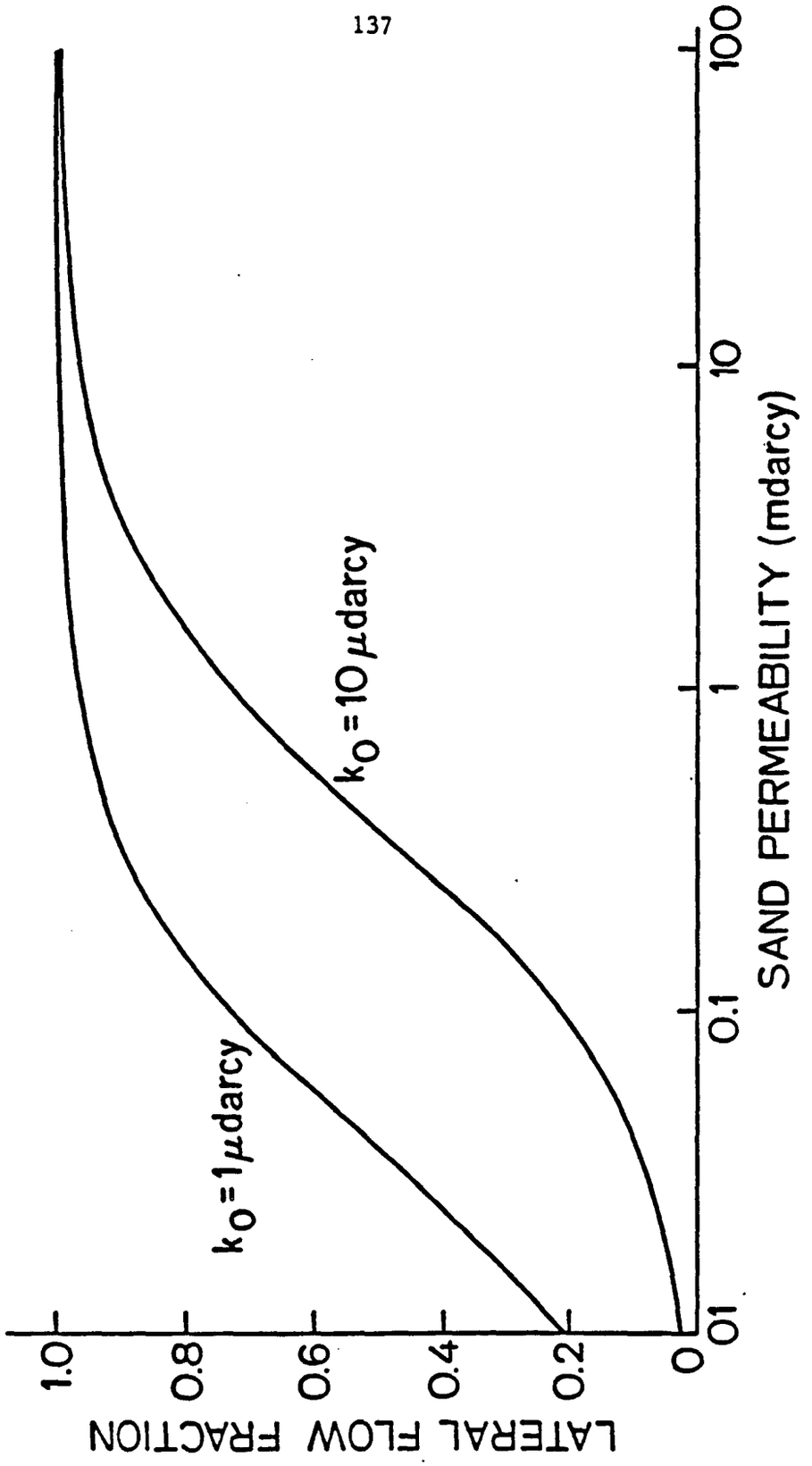

Figure 4-2a: Limiting case of very permeable boundary zones.

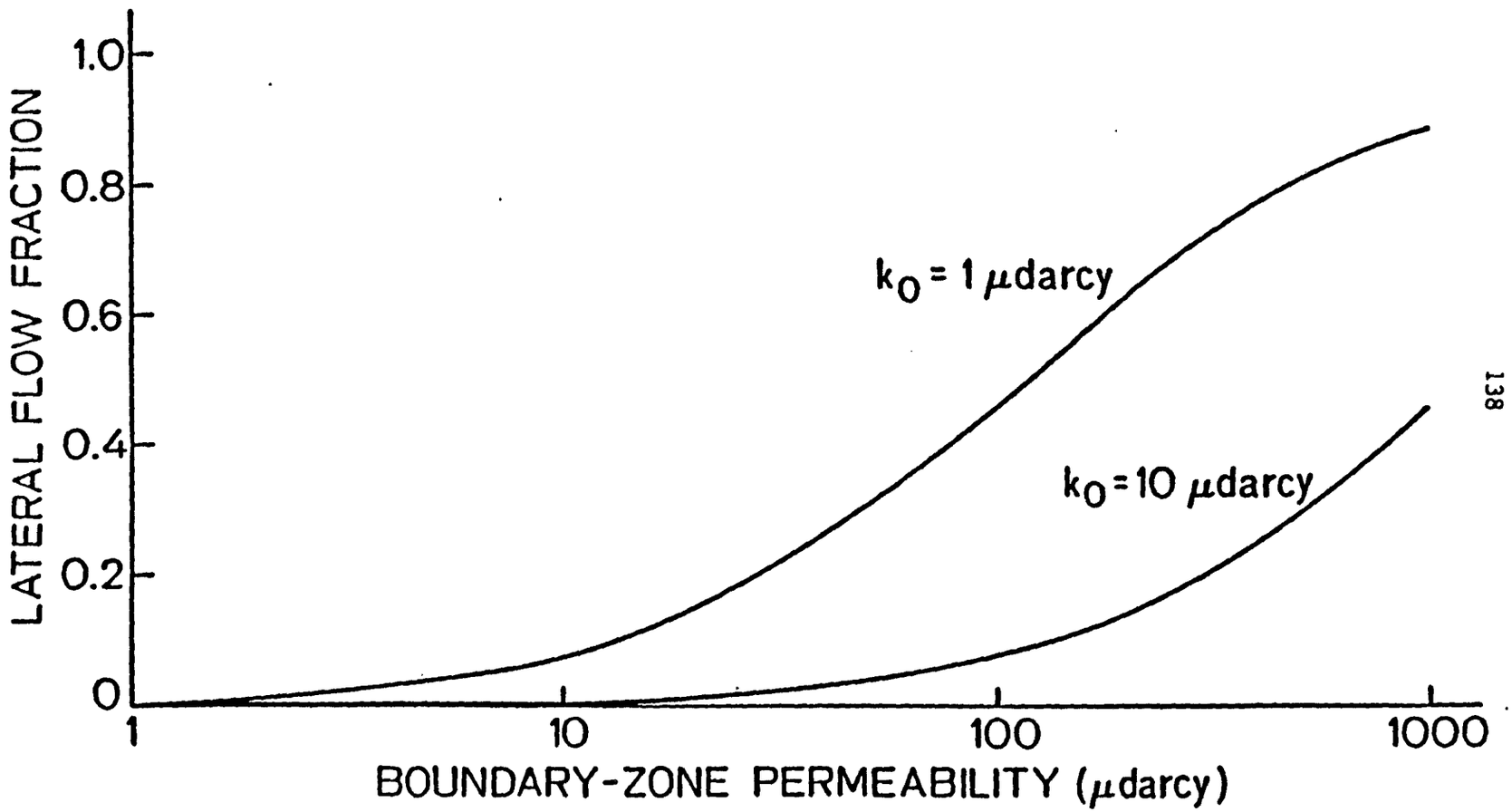

Figure 4-2b: Limiting case of low permeability boundary zones.

Figure 4-3: Generalized diagram showing the three flow-pressure regimes likely to be found in interbedded sands and shales. See text for explanation.

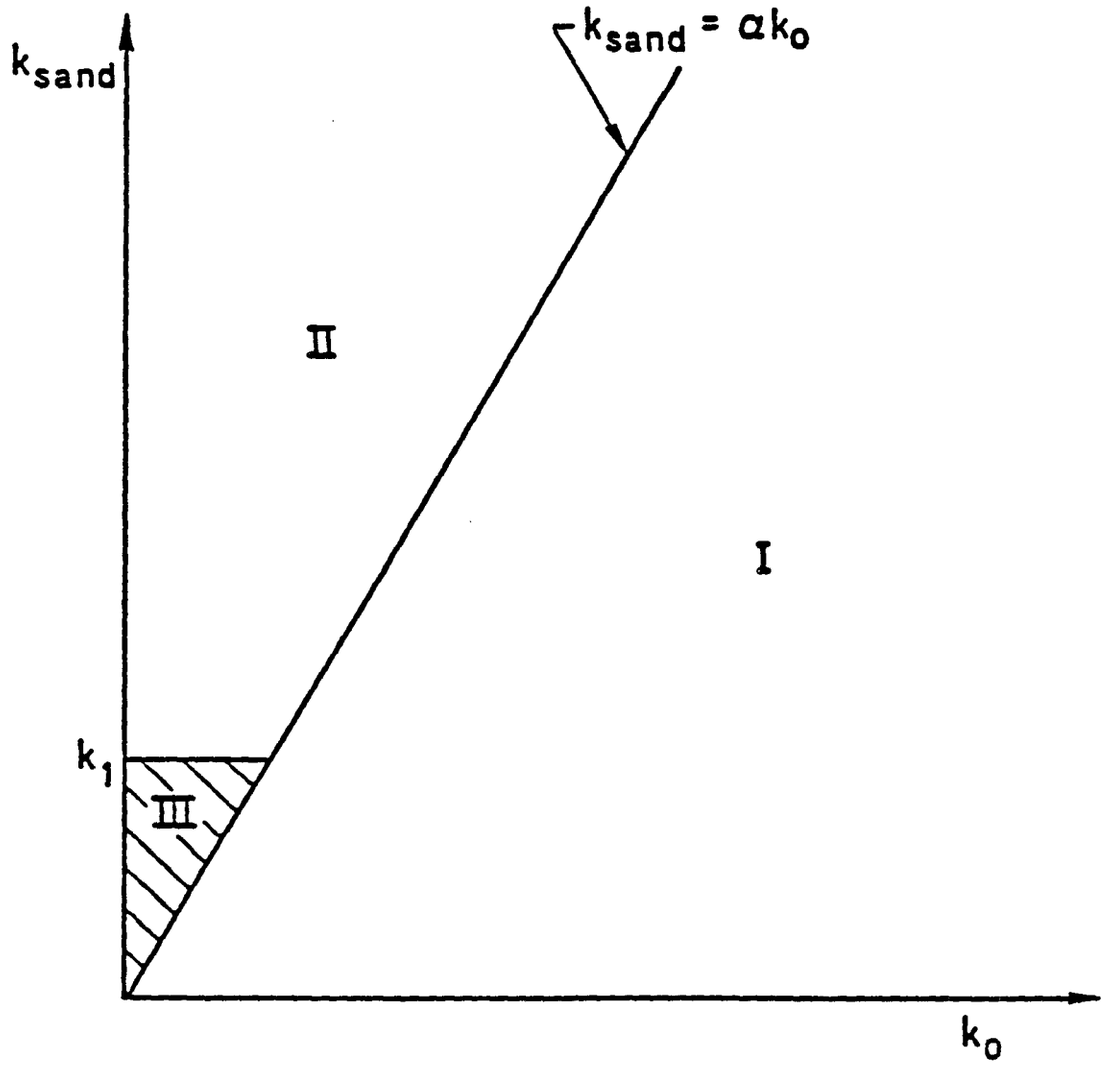

Figure 4-3a: Very permeable boundary case.

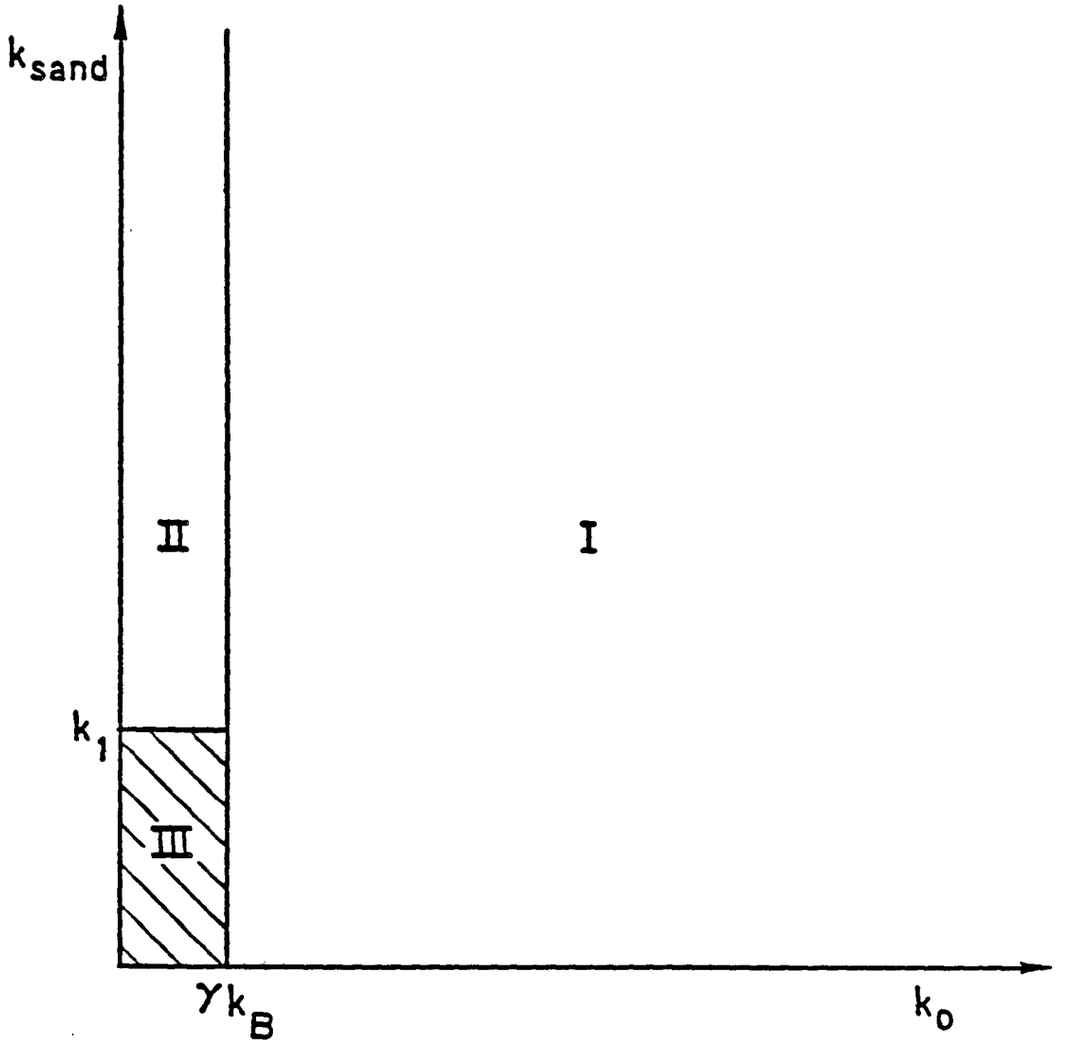

Figure 4-3b: Low permeability boundary case.

pressure configurations possible when sandy layers occur within dominantly shale sections:

Region I--Fluid flow is predominantly upward, even in sandy layers; overpressure development within the entire sedimentary section may be treated approximately by a one-dimensional compaction model that accounts for the different hydraulic properties of sand and shale.

Region II--Flow within sands tends to be focussed laterally, but little or no overpressuring occurs within those units; overpressuring in the underlying shales should be inhibited by the availability of the high-permeability flow path through sands and permeable conduits.

Region III--Flow in sands is focussed laterally; significant overpressuring occurs within these layers. Overpressuring in the underlying shales is therefore also probable.

For permeabilities in regions II and III, a one-dimensional compaction model of pore-pressure development in the underlying shale will be a poor approximation to physical reality unless the boundary conditions at the sand-shale interfaces are carefully and explicitly considered.

To calculate a value for k_1, the maximum sand permeability for there to be large overpressures within the sand, we assume that the lower shale is characterized by $d_l = 1$ km and $\Phi = 0.25$. The characteristic time τ should be on the order of the time for most of the shale porosity to be eliminated; we will use $\tau = 10$ Ma, perhaps an underestimate. Taking $\rho_f = 10^3\ \mathrm{kg/m^3}$, $g = 9.8\ \mathrm{m/s^2}$, $\mu = 5\times10^{-4}$ Pa s, and L, l, d_u as above, we find $k_1 = 4\times10^{-17}\ \mathrm{m^2} = 40\ \mu\mathrm{darcy}$. Thus, overpressuring in the sand would be very large only for $k_{sand} < \mathrm{ca.}\ 40\ \mu$darcy, and practically negligible for $k_{sand} > \mathrm{ca.}\ 400\ \mu$darcy, a value less than the permeability of many reservoir

rocks (e.g., Magara, 1971). We therefore conclude that for the particular geometry considered in our calculations, lateral flow through sands will often be volumetrically very important, but rarely accompanied by significant overpressures. Considering again Figs. 4-3a and 4-3b, this means that region III should generally be very small in comparison with region II.

Estimates of the bounds on regions II and III could be made for other combinations of geometrical parameters, but the essential qualitative conclusions of our approximate analysis of the two-dimensional flow problem would not be changed. To summarize:

i) As long as 'sandy' units are in hydraulic communication with relatively permeable, cross-cutting zones, lateral flow within these units of the fluids expelled during shale compaction is likely to be of major importance throughout sedimentary-basin development. Some faults could serve the role of permeable conduits.

ii) The importance of lateral flow will increase as the distance between permeable, cross-cutting zones decreases. Furthermore, lateral flow will be of greatest importance for relatively thick, deep sand units.

iii) Development of overpressures within sand layers carrying a large lateral fluid flux will probably occur only for sands with permeabilities less than those of most reservoir rocks.

Effect of sand-shale interlayering on fluid-flow direction in compacting shale

In the preceding part of our analysis, we have considered the way in which a sandy layer at depth may 'focus' water expelled by compaction of underlying shales. It seems intuitively clear that such a sandy layer could affect hydraulic conditions in the *overlying* shale as well. If the sand is sufficiently permeable,

and if cross-cutting permeable conduits are sufficiently nearby--or if the dip of the strata results in the sand cropping out at the surface--water expelled by compaction of the overlying shale might migrate downward into the sand, along the sand layer, and finally upward along the permeable conduits. We can quantify this tendency in an approximate fashion, as developed next.

Referring to Fig. 4-4, we assume that an excess pressure $p_e(x,z)$ exists within the upper shale; this excess pressure may be imagined to have developed as a result of compaction and, perhaps, other processes, such as clay dehydration. Imagine now a volumetric flux q_v moving vertically upward through the shale as a result of this excess pressure. For steady flow, the pressure drop Δp_v in going from (x,z) to $(x,0)$ will be (assuming, for simplicity, that μ is constant)

$$\Delta p_v = q_v \mu \int_0^z \frac{d\zeta}{k_{shale}(\zeta)} + \rho_f g z \tag{24}$$

where the first term on the right-hand side of Eqn. (24) is equivalent to $p_e(x,z)$. We can think of the quantity $\int_0^z k_{shale}^{-1}(\zeta)\, d\zeta$ as a 'hydraulic resistance'; the greater the hydraulic resistance, the smaller the fluid flux that can be moved through a specified pressure drop.

We now imagine a fluid flux q_h taking a different path to the surface (see Fig. 4-4), namely, downward to the sand, along the sand to the cross-cutting conduit, and finally upward through that conduit. Proceeding as above, we find that the pressure drop will be given by

$$\Delta p_h = \rho_f g z + q_h \mu \left[\int_z^{d_w} \frac{d\zeta}{k_{shale}(\zeta)} + \int_x^L \frac{d\xi}{k_{sand}(\xi)} + \int_0^{d_w} \frac{d\zeta}{k_B(\zeta)} \right] \tag{25}$$

However, the pressure drop must be independent of the path taken by the

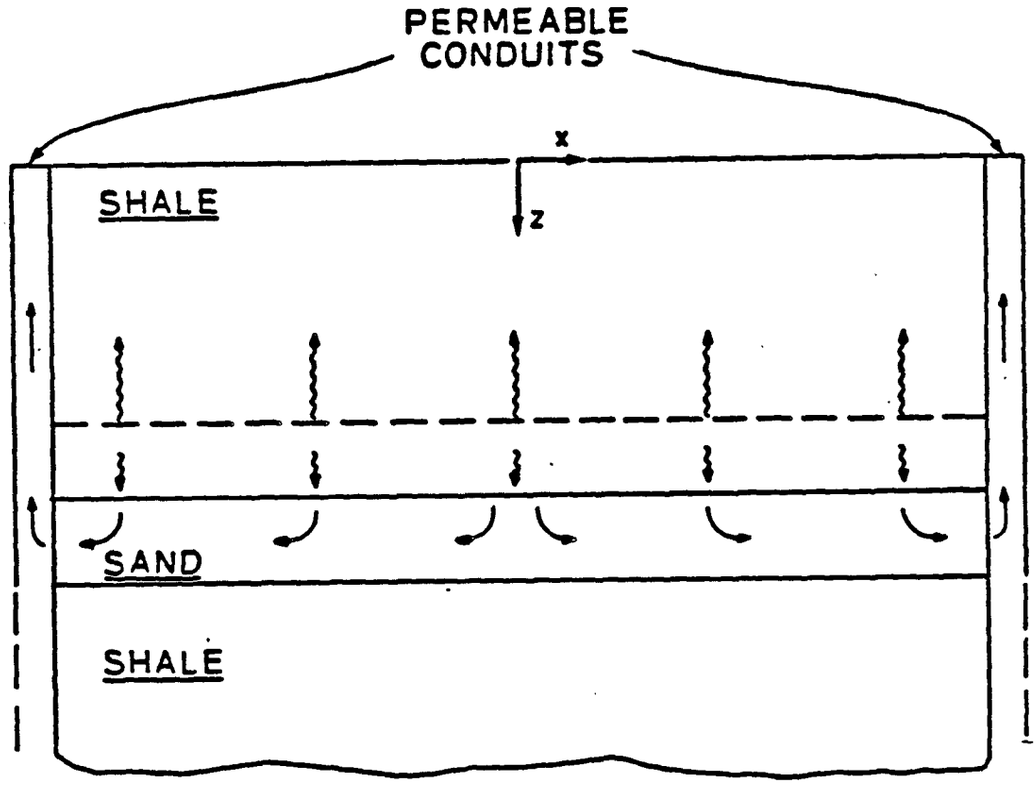

Figure 4-4: Effect of sandy layers on flow direction in overlying shales. In the part of the shale between the dashed line and the sand-shale interface, water expelled during compaction tends to flow downward into the sand layer, then laterally, and finally up along the permeable boundaries.

fluid; i.e., $\Delta p_h = \Delta p_v$. We therefore find that

$$q_v \int_0^z \frac{d\zeta}{k_{shale}(\zeta)} = q_h \left[\int_z^{d_u} \frac{d\zeta}{k_{shale}(\zeta)} + \int_z^L \frac{d\xi}{k_{sand}(\xi)} + \int_0^{d_u} \frac{d\zeta}{k_B(\zeta)} \right] \tag{26}$$

If the total hydraulic resistance for the flow path involving the sand is less than the hydraulic resistance for the simple upward flow path, then q_h will be grater than q_v; the 'lateral' migration path will then be favored. In other words, water expelled by compaction of the upper shale should tend to migrate 'downward' and 'laterally' if

$$\int_0^z \frac{d\zeta}{k_{shale}(\zeta)} > \int_z^{d_u} \frac{d\zeta}{k_{shale}(\zeta)} + \int_z^L \frac{d\xi}{k_{sand}(\xi)} + \int_0^{d_u} \frac{d\zeta}{k_B(\zeta)} \tag{27}$$

Some feeling for the meaning of this criterion may be gotten by appropriate simplifications. We assume that k_{sand} and k_B are constants. We again assume that $k_{shale}(z) = k_0 e^{-z/z_0}$. We can therefore rewrite the criterion Eqn. (27) as

$$\frac{z_0}{k_0}(e^{z_c/z_0} - 1) = \frac{z_0}{k_0}(e^{d_u/z_0} - e^{z_c/z_0}) + \frac{(L-x)}{k_{sand}} + \frac{d_u}{k_B} \tag{28}$$

where z_c is the 'critical' depth within the shale below which expelled water tends to flow into the underlying sand.

We now assume that $k_0 \ll k_B$, i.e., that the vertical 'conduits' are relatively permeable, and that k_0 is less than k_{sand}. If L/z_0 is small compared to k_{sand}/k_0--a likely condition for plausible geometries and permeabilities--then, after taking logarithms and rearranging, we may approximate Eqn. (28) as

$$\frac{z_c}{z_0} = \left[\ln(1 + e^{d_u/z_0}) - \ln 2 \right] \tag{29}$$

We suggest in the Appendix that z_0 is probably no more than a few hundreds of meters. Thus, if d_u = *ca.* 1 km, then $e^{d_u/z_0} \gg 1$, and we can further approximate Eqn. (29) as

$$z_c = d_u - z_0 \ln 2 \tag{30}$$

In other words, for the 'slice' of the upper shale unit lying roughly between $z = d_u$ and $z = d_u - z_0 \ln 2$, water expelled during compaction will tend to move *downward*, then *laterally* through the relatively permeable sand. Within that slice, the availability of the 'alternate' flow path involving the sand will tend to inhibit overpressuring. (We likewise expect overpressures within the sand to be small.) This is in qualitative agreement with numerical results of Smith (1971, Tables 5-7), which indicate downward flow in the lowermost part of a shale unit underlain by "normally pressured" sand, and agrees with conceptual models reviewed by Hunt (1979, pp. 221-25). In the part of the shale unit above the depth z_c, and at a distance greater than *ca.* d_u from the permeable boundaries, fluid flow and pore pressure may be adequately described by a one-dimensional compaction model, with the boundary condition at $z = z_c$ being, to a first approximation, that excess pressure vanishes. Furthermore, shales in the vicinity of relatively permeable sand layers will tend to compact more rapidly than shales at the same depth but *not* hydraulically connected to sands. This may cause porosity *vs.* depth relationships to vary spatially within a single sedimentary basin (Teslenko and Korotkov, 1967).

The major results of our analysis of fluid flow and pore-pressure development in laterally extensive, sand-shale sequences are conveniently illustrated with the aid of Fig. 4-5. Our analysis indicates that when permeable sand layers exist, and are hydraulically connected to permeable, cross-cutting

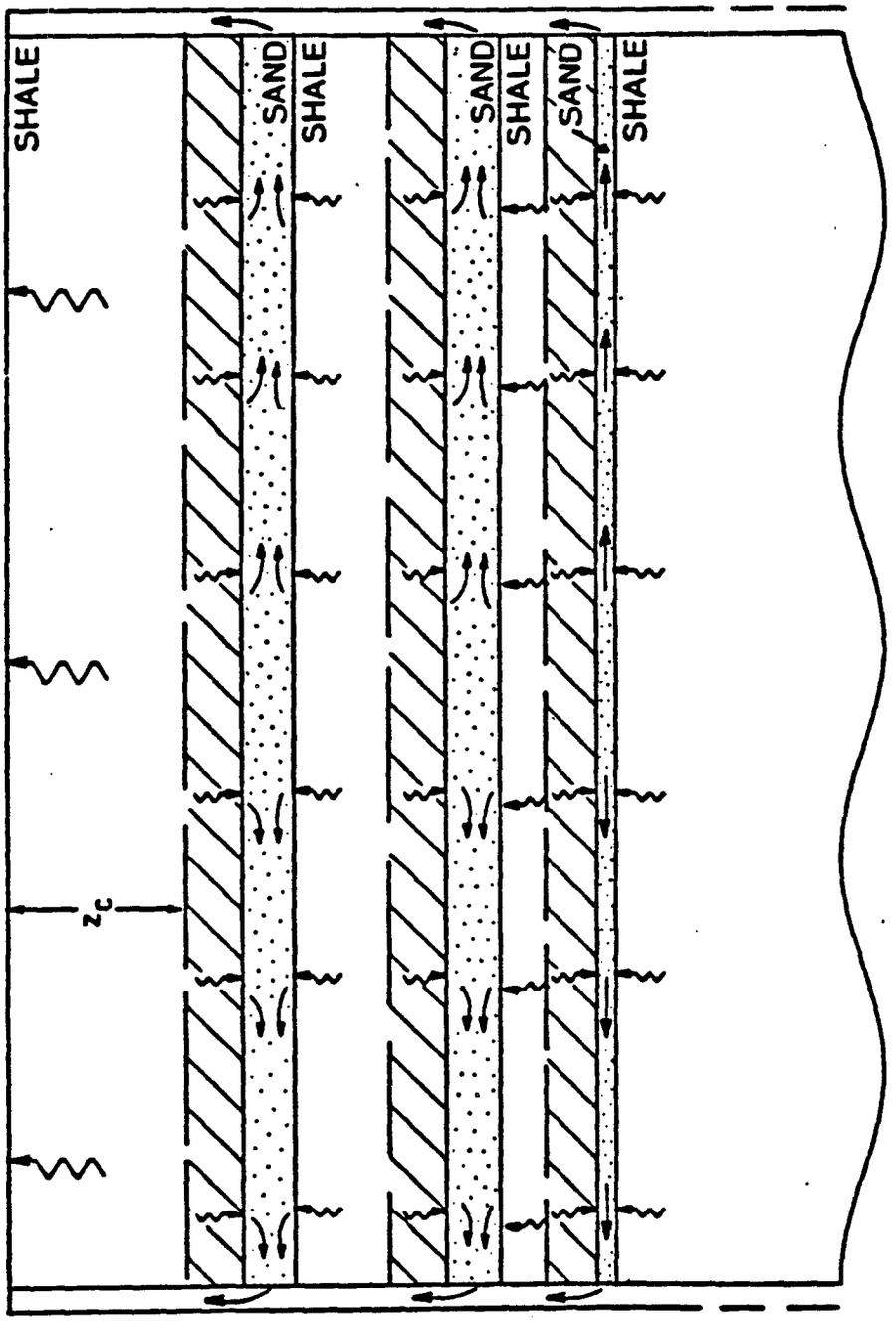

Figure 4-5: Generalized sketch of flow directions within interbedded sands and shales when permeable boundary zones allow egress of fluid expelled during sediment compaction.

conduits, *much of the water expelled during compaction of the sedimentary section* should tend to become funneled along these sand layers and conduits. Vertically directed flow during compaction might be restricted to the uppermost shale section.

3. DISCUSSION

Many of our conclusions about directions of fluid flow in sand-shale sequences will not be surprising to petroleum geologists, who have reached many of the same qualitative conclusions without mathematical models (see e.g., the review by Hunt (1979, pp. 221-32)). Our analysis has provided semi-quantitative guidelines to help estimate the fraction of the water expelled from compacting shales that becomes concentrated in lateral flow along sand units. This analysis has shown how the magnitude of this flow depend upon various geometrical and physical parameters.

Our analysis indicates that for many plausible geometries and permeabilities, a large fraction (often greater than one-half) of all water expelled during shale compaction is likely to become funneled laterally along sand layers. This could result in conditions very favorable for hydrocarbon concentration within such sand layers. One somewhat paradoxical point, however, is that lateral funneling and concentration of expelled fluids will tend to be unimportant unless these fluids have relatively easy access to the sediment surface (cf. Figs. 4-2a and 4-2b). In this case, it is difficult to understand how hydrocarbons could accumulate within deep sand layers; they should tend to continue migrating upward to sand outcrops or along 'fault' zones. Although this certainly does occur in some places, trapping at depth is probably more common. There may be explanations that avert the apparent paradox, however:

i) The permeability of boundary zones--possibly physically represented by fault zones--may be large during periods of rapid sedimentation and compaction, then fall with time due to a variety of 'sealing' mechanisms (e.g., Angevine et al., 1983; chapter 1, this dissertation). Hydrocarbons expelled into sand layers from neighboring shales could then migrate to the boundary zones, but become essentially trapped when 'fault' permeability falls.

ii) 'Fault-zone' materials may have microstructural characteristics that tend to prevent hydrocarbon penetration. For example, if the 'fault zones' are extremely fine-grained, as are many fault gouges, then strong capillary forces must be overcome to permit hydrocarbon penetration (cf. Hunt, 1979, pp. 254-56).

Either of these explanations, if valid, would have important implications for our understanding of the physical constitution and mechanics of fault zones. ore genesis.

4. SUMMARY

We have presented simple mathematical models to describe fluid flow and pore-pressure development in compacting sand-shale sequences. When permeable sand units have easy hydraulic connection to the sediment surface--either through relatively permeable fault zones or along other structural discontinuities, or by direct outcrop--water expelled during shale compaction should often become funneled along these sands. Such flow will have a major effect on hydrocarbon migration and overpressure development within sedimentary basins.

APPENDIX: PERMEABILITY VS. DEPTH IN COMPACTING SHALES

The relationship between permeability and porosity--or between permeability and depth--for compacting shales is not easily defined. Keith (1982) has reviewed measured values of shale permeability and porosity and shown that considerable scatter exist in the data, with no obvious, unique correlation between the two properties. Some of the uncertainty may well be related to different sediment compositions, as well as the measurement techniques.

Correlations between shale porosity and permeability are usually expressed in the form $k_{shale} \propto \varphi_{shale}^{n}$, where n may be as large as 8 (cf. Smith, 1971), or as $k_{shale} \propto \exp(m \varphi_{shale})$, with $m \approx 8\text{-}14$ (Keith, 1982; Bryant et al., 1975). It is also well known that the porosity φ_{shale} of 'normally compacted' shale usually shows an exponential decrease with depth (e.g., Athy, 1930; Dickinson, 1953; Magara, 1976):

$$\varphi_{shale}(z) = \varphi_0 e^{-bz} \qquad \text{(A-1)}$$

where φ_0 is a datum value and b^{-1} is a length scale characteristic of the sedimentary basin of interest. The relationship between shale permeability and depth should then have a functional form such as $k_{shale} = k_0 \exp(-z/z_0)$, where $z_0 = 1/mb$. The scale length z_0 for permeability decrease should therefore be substantially less than the scale length b^{-1} for porosity decrease. Considering that values of b^{-1} for some basins (Athy, 1930; Magara; 1976) are in the range of *ca.* 700-2500 m, it seems reasonable to suppose that z_0 will be no more than a few hundreds of meters.

We also need to estimate the value of k_0, the permeability value at $z = 0$. Here we will follow the lead of other investigators interested in overpressure

development (Smith, 1971; Sharp and Domenico, 1976; Keith, 1982, Sharp, 1983), who have suggested permeability-porosity and permeability-depth relationships that correspond to $k_0 \approx 0.2$-50 μdarcy.

REFERENCES

Angevine, C.L., D.L. Turcotte, and M.D. Furnish, 1982, Pressure solution lithification as a mechanism for the stick-slip behavior of faults. *Tectonics, 1*, 151-60.

Athy, L.F., 1930, Density, porosity, and compaction of sedimentary rocks. *American Association of Petroleum Geologists Bulletin, 14*, 1-24.

Bell, M.L., and A. Nur, 1976, Strength changes due to reservoir-induced pore pressure and stresses and application to Lake Oroville. *Journal of Geophysical Research, 83*, 4469-83.

Bishop, R.S., 1979, Calculated compaction states of thick abnormally pressured shales. *American Association of Petroleum Geologists, Bulletin, 63*, 918-33.

Bredehoeft, J.D., and B.B. Hanshaw, 1968, On the maintenance of anomalous fluid pressures: I. Thick sedimentary sequences. *Geological Society of America Bulletin, 79*, 1097-1106.

Bryant, W.R., W. Hottman, and P. Trabant, 1975, Permeability of unconsolidated and consolidated marine sediments, Gulf of Mexico. *Marine Geotechnology, 1*, 1-23.

Burst, J.F., 1969, Diagenesis of Gulf Coast clayey sediments and its possible relation to petroleum migration. *American Association of Petroleum Geologists Bulletin, 53*, 73-93.

Cathles, L.M., and A.T. Smith, 1983, Thermal constraints on the formation of Mississippi Valley-type lead-zinc deposits and their implications for episodic basin dewatering and deposit genesis. *Economic Geology, 78*, 983-1002.

Dickinson, G., 1953, Geological aspects of abnormal reservoir pressures in Gulf Coast Louisiana. *American Association of Petroleum Geologists Bulletin, 37*, 410-32.

Dozy, J.J., 1970, A geologic model for the genesis of the lead-zinc ores of the Mississippi Valley, U.S.A. *Institution of Mining and Metallurgy Transactions, 79B*, 163-70.

Hubbert, M.K., and W.W. Rubey, 1959, Role of fluid pressure in mechanics of overthrust faulting. I: Mechanics of fluid-filled porous solids and its application to overthrust faulting. *Geological Society of America Bulletin, 70*, 115-166.

Hunt, J.M., 1979, *Petroleum geochemistry and geology*. San Francisco, W.H. Freeman and Co., 617 pp.

Keith, L.A., 1982, A numerical compaction model of overpressuring in shales. M.S. thesis, Virginia Polytechnic Institute and State University, Blacksburg, Virginia, 80 pp.

Magara, K., 1971, Permeability considerations in generation of abnormal pressures. *Society of Petroleum Engineers Journal, 11*, 236-42.

Magara, K., 1976, Water expulsion from clastic sediments during compaction--directions and volumes. *American Association of Petroleum Geologists Bulletin, 60*, 543-53.

Seeburger, D., 1981, Studies of natural fractures, fault zone permeability, and a pore space-permeability model. Ph. D. thesis, Stanford University, Stanford, California, 234 pp.

Sharp, J.M., Jr., 1983, Permeability controls on aquathermal pressuring. *American Association of Petroleum Geologists Bulletin, 67*, 2057-61.

Sharp, J.M., Jr., and P.A. Domenico, 1976, Energy transport in thick sequences of compacting sediment. *Geological Society of America, Bulletin, 87*, 390-400.

Smith, J.E., 1971, The dynamics of shale compaction and evolution of pore-fluid pressures. *International Association for Mathematical Geology, Journal, 3*, 239-63.

Smith, J.E., 1973, Shale compaction. *Society of Petroleum Engineers, Journal, 13*, 12-22.

Teslenko, P.F., and B.S. Korotkov, 1967, Effect of arenaceous intercalations in clays on their compaction. *International Geology Review, 9, 699-701.*

NOTATION

b	reciprocal of scale length in porosity *vs.* depth relationship
c_{sand}	hydraulic diffusivity of sand layer
d_l	thickness of lower shale
d_u	thickness of upper shale
f	fraction of expelled water that flows laterally through sand layer
g	acceleration due to gravity
k_B	permeability of boundary zones
k_{sand}	permeability of sand layer
k_{shale}	permeability of shale
k_0	permeability of shale at sediment surface
k_1	'critical' sand permeability for significant overpressuring
l	thickness of sand layer
L	half-spacing of vertical boundary zones
m	coefficient in permeability *vs.* porosity relationship
n	exponent in permeability *vs.* porosity relationship
p	pore pressure
p_B	pore pressure in boundary zones
p_e	excess pressure in upper shale
p_{sand}	pore pressure in sand layer
$\tilde{p}$	dimensionless pore pressure in sand layer
Δp_v	pressure drop for 'upward' flow (cf. Fig. 4)
Δp_h	pressure drop for 'lateral' flow (cf. Fig. 4)
$\langle p_e \rangle$	laterally averaged excess pressure in upper shale
$\overline{\langle p_e \rangle}$	value of $\langle p_e \rangle$ at sand-shale interface
q_h	volumetric fluid flux for 'lateral' flow path (Fig. 4)
q_v	volumetric fluid flux for 'vertical' flow path (Fig. 4)
$\langle q_z \rangle$	laterally averaged upward volumetric fluid flux
Q_x	lateral volumetric flow rate per unit 'width'
Q_z	vertical volumetric flow rate per unit 'width'
R	volumetric fluid flux into sand layer due to compaction of underlying shale
t	time
$\tilde{t}$	dimensionless time

T characteristic time scale

u_f velocity (i.e., volumetric flux) of pore fluid

w width of boundary zones

x horizontal coordinate

$\tilde{x}$ dimensionless horizontal coordinate

z vertical coordinate

z_c 'critical' depth in shale below which expelled water moves downward into sand

z_0 scale length in permeability *vs.* depth relationship

α $(L/3l)(L/z_0)e^{-d_u/z_0}$

β_f fluid compressibility

γ $(d_u/w)(L/z_0)e^{d_u/z_0}$

μ pore-fluid viscosity

ρ_f pore-fluid density

τ characteristic time scale for shale dewatering

τ_d characteristic time for pore-pressure diffusion

φ porosity of sand

φ_{shale} porosity of shale

Φ porosity of 'source' shale underlying sand

CHAPTER 5
PORE PRESSURE IN THE EARTH'S CRUST: EFFECTS OF UPLIFT AND TECTONIC STRAIN

ABSTRACT

We develop a formalism that describes the way in which pore pressure in the Earth's crust is coupled to the state of stress, the temperature field, and the strains applied to a rock mass. This formalism is valid as long as the rock behaves in an essentially elastic manner. We apply this model to an examination of pore-pressure history in a rock mass in two geologic situations: during uplift, and when subjected to lateral compressive strains, such as in rocks caught between converging plates. During uplift and erosion, development of abnormal pore pressure in low porosity rocks is possible, especially if such rocks also have low permeability or are surrounded by rocks that have this property. Pore pressures either below or above hydrostatic may develop, depending upon whether or not grain-scale stress inhomogeneities developed during uplift lead to microcracking.

Rocks in accretionary wedges at convergent plate margins are subjected to high compressive strain rates. We show that this strain can lead to rapid buildup of substantial fluid overpressures. Such overpressures could be very important in facilitating deformation of rocks in accretionary wedges.

1. INTRODUCTION

Pore pressure is an important variable that must be carefully considered if we are to understand the mechanical behavior of the Earth's crust. The mechanisms by which rocks deform are strongly influenced by the presence of water, as well as by the pore pressure, with brittle behavior favored under

some conditions, ductile behavior under others [e.g., Carter, 1976; Brace and Kohlstedt, 1980]. A number of studies have examined the possible role of elevated pore pressure, i.e., pore pressure in excess of hydrostatic, in the origin of some common geological structures. Perhaps the best-known is the work by Hubbert and Rubey [1959] and Rubey and Hubbert [1959] on the mechanics of thrust-faulting. These authors proposed that the motion of large thrust sheets would be greatly facilitated by the presence of excess pore pressure, approaching overburden pressure, within some stratum at depth. The potential role of elevated pore pressure in joint formation has also been examined [e.g., Secor, 1965; Narr and Currie, 1982].

Previous studies of the mechanical role of crustal pore pressure, such as those mentioned above, have tended to treat pore pressure as a parameter that is essentially independent of the overall stress- and deformation state of the rock body of interest. This is not strictly true. Various aspects of the coupling between the stress state and fluid pressure have been considered by a number of workers, beginning with Biot [1941] and later by Rice and Cleary [1976], Ruina [1978], and others. A fundamental result of these studies of 'poroelastic' materials is that, in general, stress and pore pressure are intimately coupled, whether we consider quasi-static phenomena such as fluid diffusion [Biot, 1941; Rice and Cleary, 1976], dynamic processes such as elastic wave propagation [Biot, 1956; Plona, 1980], or phenomena on time scales that overlap these categories, such as fracture propagation [Ruina, 1978].

In this chapter, we examine in detail the way in which crustal pore pressure is influenced by its coupling to the overall stress state of a rock mass. A formalism is developed showing that we must generally consider not only the coupling between stress and pore pressure, but also the coupling of both of

these to temperature and tectonic strain. In certain cases, we can find approximate analytical solutions to the governing differential equations. We apply these solutions to an examination of the history of pore pressure in a rock mass during uplift, using our results to examine the potential role of pore pressure in joint formation. We also apply our model to examine the pore-pressure history of rocks in an accretionary wedge at convergent plate margins, showing that strain-induced pore pressure could be very important in facilitating deformation of such rocks.

2. OUTLINE OF THE ANALYSIS

We assume that deformation due to changes in stress, pore pressure, or temperature are essentially elastic. Obviously, this approach does not permit us to examine *directly* such phenomena as faulting, but does let us evaluate changes in the physical state of a rock mass that may lead to such irreversible phenomena. This is a common approach in the earth sciences.

Based on well-known models for thermoelastic materials [e.g., Boley and Weiner, 1960] and poroelastic materials [e.g., Rice and Cleary, 1976], we propose a simple constitutive law that includes the effects of *both* pore pressure and temperature on strain and pore volume. We then examine the way in which the stress field in a rock mass changes during uplift or as a result of tectonic strains. This development follows Price [1966], Voight and St. Pierre [1974], and Haxby and Turcotte [1976]. We also consider the effect of time-dependent changes in the various elastic moduli during such processes. This mimics, to some extent, the recent work by Bruner [in press] on crack growth and stress development during unloading. Finally, after considering the thermal state of the rock, we arrive at a set of three coupled, partial

differential equations for pore pressure p, mean stress $\bar{\sigma}$, and temperature T, as well as an equation for the 'horizontal' principal stress σ_h.

We show by scaling arguments that for a number of cases of interest, the temperature field may be essentially decoupled from the pore-pressure and stress fields. With suitable approximations, and assuming that the elastic moduli are either constants or slowly varying functions of time, we can then find analytic expressions for p and $\bar{\sigma}$ during the history of a rock mass. The factors that principally affect development of pore pressure and stress are the elastic moduli, as well as their rates of change; the rate of uplift or subsidence; the geothermal gradient; the rate of applied tectonic strain; and, finally, the hydrologic characteristics of the rock mass.

3. ANALYSIS

Constitutive law and field equation for pore pressure

We begin by briefly reviewing constitutive laws for thermoelastic and poroelastic materials. We assume that the materials are homogeneous and isotropic. In standard models of linear thermoelasticity [e.g., Boley and Weiner, 1960], the strains ε_{ij} are taken as linear functions of the stresses σ_{ij} and temperature T, viz.:

$$d\varepsilon_{ij} = \frac{d\sigma_{ij}}{2G} - \left(\frac{\nu}{1+\nu}\right)\left(\frac{1}{2G}\right) d\sigma_{kk}\,\delta_{ij} + \alpha\, dT\,\delta_{ij} \qquad (1)$$

where

G = shear modulus

ν = Poisson's ratio

α = coefficient of linear thermal expansion

We are using here the summation convention for repeated subscripts; σ_{kk} is thus the sum of the principal stresses. The Kronecker delta, δ_{ij}, has the usual definition:

$$\delta_{ij} = 1, \qquad i = j$$
$$\delta_{ij} = 0, \qquad i \neq j$$

The stresses σ_{ij} and temperature T are measured relative to some datum, or reference, state that may be defined as convenient. (The sign convention used here is that tensile stresses and strains are taken as positive.) The analogous linearized constitutive law for poroelastic materials is given by the two equations [cf. Biot, 1941; Rice and Cleary, 1976]:

$$d\varepsilon_{ij} = \frac{d\sigma_{ij}}{2G} - \left(\frac{\nu}{1+\nu}\right)\left(\frac{1}{2G}\right) d\sigma_{kk}\,\delta_{ij} + \frac{dp}{3H}\delta_{ij} \tag{2a}$$

$$dv = v - v_0 = \frac{d\sigma_{kk}}{3H} + \frac{dp}{R} \tag{2b}$$

where we may specify the reference state for p as convenient. The moduli H and R were introduced by Biot [1941]. We have used Rice and Cleary's [1976] notation for v, the fluid volume per unit reference volume, where v_0 is the value of v in the reference state.

Proceeding by analogy with the thermoelastic and poroelastic constitutive laws, we propose a linearized constitutive law that includes the effects of both temperature and pore pressure on strain and pore volume:

$$d\varepsilon_{ij} = \frac{d\sigma_{ij}}{2G} - \left(\frac{\nu}{1+\nu}\right)\left(\frac{1}{2G}\right) d\sigma_{kk}\,\delta_{ij} + \frac{dp}{3H}\delta_{ij} + \alpha\, dT\,\delta_{ij} \tag{3a}$$

$$dv = \frac{d\sigma_{kk}}{3H} + \frac{dp}{R} + \gamma\, dT \tag{3b}$$

These are similar (in a formal sense) to expressions given by Bruner [1979,

p. 5582, Eqns. 20a and 20b]. The essential new ingredient here, as compared to the Biot [1941] formalism, is the inclusion of a term describing the thermoelastic effect on the fluid volume fraction.

We now follow an argument by Nur and Byerlee [1971] to arrive at a relationship between the thermoelastic moduli α and γ. Assuming that the pore space is continuous (that is, that there are no isolated pores), that the fluid is chemically inert, and that the solid grains have uniform elastic properties, we now imagine a stress state with $p = -\sigma_{kk}/3$, i.e., a state in which the pore pressure is equal to the mean stress. We then find from Eqns. (3a) and (3b), after some rearrangement:

$$\varepsilon_{kk} = -\frac{p}{K} + \frac{p}{H} + 3\alpha T \tag{4a}$$

$$v - v_0 = -\frac{p}{H} + \frac{p}{R} + \gamma T \tag{4b}$$

where $K = 2(1+\nu)G/3(1-2\nu)$ is the rock's bulk modulus. Nur and Byerlee [1971, p.6416] argued, on the basis of the uniqueness theorem for stress boundary-value problems, that for this specified stress- and pore-pressure configuration, the unique deformational pattern in the porous solid would be one in which all linear dimensions were strained by a magnitude of p/K_s, where K_s is the bulk modulus of the mineral grains. This leads to expressions for H and R in terms of K, K_s, and v_0 [cf. Nur and Byerlee, 1971, p.6416; Cornet and Fairhurst, 1974, p. 639; Rice and Cleary, 1976, p.228]:

$$\frac{1}{H} = \frac{1}{K} - \frac{1}{K_s} \tag{5a}$$

$$\frac{1}{R} = \frac{1}{K} - \frac{1+v_0}{K_s} \tag{5b}$$

If we now *assume* that these relationships still hold for the case in which

thermoelastic effects are added to the poroelastic effects--that is, if we assume that the thermoelastic and poroelastic phenomena are independent--then we find that α and γ are related as

$$\gamma = 3\nu_0\alpha \tag{6}$$

Recognizing that, for an isotropic solid, 3α is simply the volumetric thermal expansion coefficient, $\hat{\alpha}$, we can rewrite Eqn. (6) as

$$\gamma = \nu_0\hat{\alpha} \tag{7}$$

In other words, the thermoelastic change in fluid volume fraction would be simply the thermoelastic volume strain multiplied by the initial fluid volume fraction.

We now follow Rice and Cleary [1976, pp.228-29] to find a differential equation describing the coupling between p, σ_{kk}, and T. Details of the derivation are given in Appendix A. For the special case of one-dimensional (vertical) motion, and assuming that the moduli may be functions of time and space, we find, to a good approximation, the following equation for small deformations:

$$\frac{D}{Dt}(\hat{\beta}p) - \frac{D}{Dt}\left[(\beta-\beta_s)p_c\right] + \varphi_0 \frac{D}{Dt}\left[(\hat{\alpha}-\alpha_f)T\right] = \frac{\partial}{\partial z}\left[\frac{k}{\mu}\left(\frac{\partial p}{\partial z}-\rho_f g\right)\right] \quad (8)$$

where

$\hat{\beta} = (\beta-\beta_s) + \varphi_0(\beta_f-\beta_s)$

$\beta = 1/K$ = rock compressibility

$\beta_s = 1/K_s$ = grain compressibility

β_f = fluid compressibility

α_f = thermal expansivity of fluid

ρ_f = fluid density

$\varphi_0 = v_0$ = initial porosity

k = permeability

μ = viscosity

g = accelerration due to gravity

$p_c = -\sigma_{kk}/3$ = mean compressive stress ('confining pressure')

and z is a vertical coordinate, increasing downwards (Fig. 5-1). We have assumed in the derivation of Eqn. (8) that the solid moves as a rigid body at a speed u_s. (This differs from the situation considered in chapter 3, in which u_s was generally variable in space.) The material time derivative D/Dt, the time derivative following motion of the solid, is defined as (e.g., Malvern, 1969, p. 143) $D/Dt = \partial/\partial t + u_s \partial/\partial z$.

Stresses developed as a result of vertical movement and strain

We now seek another expression, in addition to Eqn. (11), that describes the coupling between pore pressure and confining pressure. The way in which the stress state of a rock mass changes during uplift has been considered by several previous workers [Price, 1966; Voight and St. Pierre, 1974; Haxby and

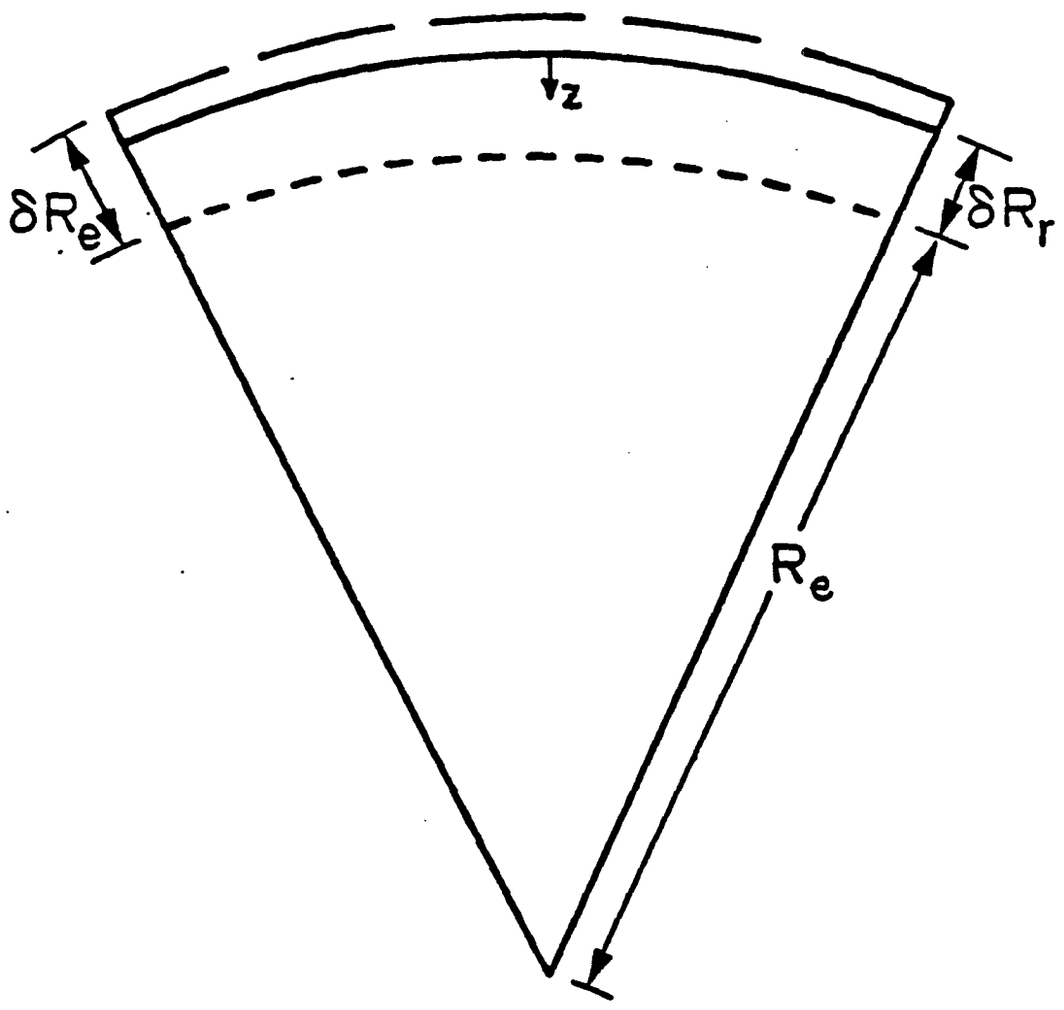

Figure 5-1: Uplift on a sphere of radius R_e, after Haxby and Turcotte [1976]. The original surface (short dashes) is imagined uplifted by a distance δR_e to the surface indicated by the long dashes. After erosion and isostatic compensation, the surface lies at the position indicated by the solid arc, with a net change in radius of δR_r. The 'downward' coordinate z is measured from the instantaneous surface.

Turcotte, 1976; Bruner, in press]; these earlier studies have considered the effects of changes in overburden load and temperature, as well as isostatic effects. We present here an essentially parallel development, including in addition the effects of changes in pore pressure and tectonic strain.

We again assume that the rock mass of interest is homogeneous and isotropic. We further assume that the rock is initially free of deviatoric stresses. Considering uplift on a spherical Earth (Fig. 5-1), we can express the elastic strains parallel to the sphere's surface as

$$d\varepsilon_h = \left(\frac{1-\nu}{E}\right) d\sigma_h - \frac{\nu}{E} d\sigma_v + \frac{dp}{3H} + \alpha\, dT \qquad (9)$$

where

ε_h = 'lateral' (i.e., circumferential) strain

σ_v = vertical stress

σ_h = lateral stress

$E = 2(1+\nu)G$ = Young's modulus

We have implicitly assumed that stresses and strains are uniform in the azimuthal sense; hence, we need consider only a single 'lateral' stress or strain.

Eqn. (9) can be inverted to yield an expression for $d\sigma_h$, the change in lateral stress, as a function of $d\varepsilon_h$, $d\sigma_v$, dp and dT:

$$d\sigma_h = \left(\frac{E}{1-\nu}\right) d\varepsilon_h + \left(\frac{\nu}{1-\nu}\right) d\sigma_v - \left(\frac{E}{1-\nu}\right)\left(\frac{dp}{3H} + \alpha dT\right) \qquad (10)$$

We can also write an expression for $d\bar{\sigma} = d\sigma_{kk}/3$:

$$d\bar{\sigma} = \frac{2}{3}\left(\frac{E}{1-\nu}\right) d\varepsilon_h + \frac{1}{3}\left(\frac{1+\nu}{1-\nu}\right) d\sigma_v - \frac{2}{3}\left(\frac{E}{1-\nu}\right)\left(\frac{dp}{3H} + \alpha dT\right) \qquad (11)$$

Eqn. (11) indicates that lateral strain, e.g., regional compression, will generally

be coupled to pore pressure, in that both will affect the stress state. In some cases, as we will show later, this coupling may be substantial, leading to pore pressures significantly in excess of hydrostatic.

When the moduli are constant, Eqns. (10) and (11) lead to a relatively straightforward approximation for the stress state during unloading (or burial), if sufficiently simple functional forms are assumed for ε_h, σ_v, p, and T [cf. Price, 1966; Voight and St. Pierre, 1974; Haxby and Turcotte, 1976; Bruner, in press]. In the general case, with the moduli *not* constant, it is more illustrative to express Eqns. (10) and (11) as differential equations. Recalling that we have focussed on the change in stress state of a rock mass *following the motion of that mass*, we can write

$$\frac{Dp_c}{Dt} = -2\left(\frac{1-2\nu}{1-\nu}\right)\left(\frac{1}{\beta}\right)\frac{D\varepsilon_h}{Dt} - \frac{1}{3}\left(\frac{1+\nu}{1-\nu}\right)\bar{\rho}gV + \frac{2}{3}\left(\frac{1-2\nu}{1-\nu}\right)\left(\frac{\beta-\beta_s}{\beta}\right)\frac{Dp}{Dt} + \frac{2}{3}\left(\frac{\hat{\alpha}}{\beta}\right)\left(\frac{1-2\nu}{1-\nu}\right)\frac{DT}{Dt} \tag{12}$$

$$\frac{Ds_h}{Dt} = -3\left(\frac{1-2\nu}{1-\nu}\right)\left(\frac{1}{\beta}\right)\frac{D\varepsilon_h}{Dt} - \left(\frac{\nu}{1-\nu}\right)\bar{\rho}gV + \left(\frac{1-2\nu}{1-\nu}\right)\left(\frac{\beta-\beta_s}{\beta}\right)\frac{Dp}{Dt} + \left(\frac{\hat{\alpha}}{\beta}\right)\left(\frac{1-2\nu}{1-\nu}\right)\frac{DT}{Dt} \tag{13}$$

where $p_c = -\bar{\sigma}$ is the 'confining pressure' and $s_h = -\sigma_h$ is the lateral compression. We have assumed that the radial, or vertical, position of the rock mass changes at a rate V, taken as positive in the case of uplift, that erosion keeps pace with uplift, and that [cf. McGarr and Gay, 1978, p. 419] σ_v is simply given by the overburden load, viz.:

$$\sigma_v(z) = -\bar{\rho}gz \qquad \text{and} \qquad \frac{D\sigma_v}{Dt} = \bar{\rho}gV$$

where $\bar{\rho}$ is the average density of the overburden. We have also re-expressed the moduli E and H in terms of ν, β, and β_s.

Thermal state of fluid-filled porous rock

In order to to complete our description of the physical state of the rock mass, we need to determine the way that temperature changes during uplift. The thermal energy equation, derived in Appendix B, may be expressed to a good approximation as

$$\rho_m \hat{C}_m \frac{\partial T}{\partial t} = k_m \frac{\partial^2 T}{\partial z^2} + \tilde{\rho}\tilde{C} V \frac{\partial T}{\partial z} + \frac{\rho_f \hat{C}_f T k}{\mu} \frac{\partial}{\partial z}\left(\frac{\partial p}{\partial z} - \rho_f g\right) \qquad (14)$$

where

$\rho_m = \rho_s (1-\varphi) + \rho_f \varphi$ = density of fluid-saturated rock

ρ_s = grain density

$\hat{C}_m$ = specific heat of fluid-saturated rock

$\hat{C}_s$ = specific heat of grains

$\hat{C}_f$ = specific heat of fluid

$\tilde{\rho}\tilde{C} = \rho_s (1-\varphi) \hat{C}_s + \rho_f \varphi \hat{C}_f$

k_m = thermal conductivity of fluid-saturated rock

The left-hand side of Eqn. (14) describes the net accumulation of thermal energy. On the right-hand side, the first term describes heat conduction, the second term gives the heat advected by the saturated rock, and the last term describes heat advection due to fluid flow relative to the solid framework. Eqn. (14) implicitly neglects thermoelastic heating, which can be shown to be negligible [Boley and Weiner, 1960], as well as the energy involved in irreversible processes such as crack growth [cf. Bruner, 1979, pp. 5580-81]. Crack growth is likely to have a very important effect on stress history during unloading [Bruner, in press]; in the present analysis, this effect is included in an approximate manner through the variability of the elastic moduli.

By combining Eqns. (8), (12), and (14), and choosing simple functional forms for $\varepsilon_h(t)$ and the time-dependent moduli, we can solve for the stress, pore pressure, and temperature in a rock mass during uplift or as a result of tectonic strain. This is greatly simplified by the fact that for reasonable rates of uplift, the last two terms on the right-hand side of Eqn. (14), related to advected heat, are negligible, as we show in Appendix B. The thermal energy equation then becomes effectively decoupled from the equations for p and p_c. Furthermore, as also shown by the scaling arguments in Appendix B, for depths of $< ca.$ 10 km and typical uplift rates of a few hundreds of meters per million years, the rock will cool or heat sufficiently rapidly that an essentially steady-state temperature is maintained; i.e., we will have

$$\frac{DT}{Dt} = -\Gamma V \tag{15}$$

where Γ is the magnitude of the geothermal gradient. In other words, the temperature of the rock mass will change at a constant rate.

4. APPLICATIONS OF THE MODEL

Pore pressure and stress during uplift

Constant moduli case

Various aspects of the stress history of an uplifted rock mass have been examined by Price [1966], Voight and St. Pierre [1974], Haxby and Turcotte [1976], and Bruner [1979, in press]. The fundamental result of all of these analyses, as emphasized by Bruner [in press], is that as long as the various elastic moduli are constant during unloading, then the thermoelastic effect will dominate for nearly all rock types and geophysically reasonable values of Γ; a tensile lateral stress is predicted for rocks uplifted to near the Earth's surface.

This prediction conflicts markedly with observation [McGarr and Gay, 1978]. There appear to have been no previous models directed at examining pore-pressure development during uplift; the common assumption [e.g., Bruner, in press] is that p will stay hydrostatic. The present model is well suited to examine the validity of this assumption.

Although the constant-moduli approximation is probably not strictly correct, it leads to a mathematically simple form of coupling between stress and pore pressure; hence, it is a useful starting point for examining pore-pressure development during uplift.

For constant moduli, the relevant expression for p is [cf. Eqn. (8)]

$$\hat{\beta}\frac{Dp}{Dt} = (\beta - \beta_s)\frac{Dp_c}{Dt} - \varphi_0(\alpha_f - \hat{\alpha})\Gamma V + \frac{\partial}{\partial z}\left[\frac{k}{\mu}\left(\frac{\partial p}{\partial z} - \rho_f g\right)\right] \tag{16}$$

where we have used Eqn. (15) to replace DT/Dt. Again, V is the rate of uplift, assumed constant throughout the rock body of interest. We can now write a differential equation in terms of p only by substituting Eqn. (12) into Eqn. (16), using Eqn. (15), and expanding, viz.:

$$\tilde{\beta}\frac{Dp}{Dt} = \frac{k}{\mu}\frac{\partial^2 p}{\partial z^2} - \left(\frac{k\rho_f\beta_f g}{\mu}\right)\frac{\partial p}{\partial z} - S \tag{17}$$

where

$$\tilde{\beta} = \hat{\beta} - \frac{2}{3}\left(\frac{1-2\nu}{1-\nu}\right)\frac{(\beta-\beta_s)^2}{\beta}$$

$$S = \frac{1}{3}\left(\frac{1+\nu}{1-\nu}\right)(\beta-\beta_s)\bar{\rho}gV + \left[\varphi_0(\alpha_f - \hat{\alpha}) + \frac{2}{3}\left(\frac{\hat{\alpha}}{\beta}\right)\left(\frac{1-2\nu}{1-\nu}\right)(\beta-\beta_s)\right]\Gamma V +$$
$$+ 2\left(\frac{1-2\nu}{1-\nu}\right)\left(\frac{\beta-\beta_s}{\beta}\right)\frac{D\varepsilon_h}{Dt}$$

The first and second terms on the right-hand side of Eqn. (17) describe

the effect of pore-pressure diffusion; the last relates to the thermoelastic- and poroelastic coupling effects.

We now make the important assumption—one which will be relaxed in a later section—that lateral strains due to tectonic causes are absent, and that ε_h will be due solely to isostatic adjustments at depth. Following Haxby and Turcotte [1976, p. 182], we consider uplift of a sector of a spherical shell of radius R_e (Fig. 5-1), confined such that during uplift and erosion, the solid angle subtended by the sector remains unchanged (i.e., we assume that there is no lateral 'spreading' of elevated regions). In this case, isostatic compensation leads to a lateral strain rate in the uplifted sector equal to $\bar{p}V/\rho_m R_e$, where ρ_m is the density of upper mantle material and R is the Earth's radius. We can then rewrite the term S as

$$S = \frac{1}{3}\left(\frac{1+\nu}{1-\nu}\right)(\beta-\beta_s)\bar{p}gV + \left[\varphi_0(\alpha_f-\hat{\alpha}) + \frac{2}{3}\left(\frac{\hat{\alpha}}{\beta}\right)\left(\frac{1-2\nu}{1-\nu}\right)(\beta-\beta_s)\right]\Gamma V + \\ + 2\left(\frac{1-2\nu}{1-\nu}\right)\left(\frac{\beta-\beta_s}{\beta}\right)\frac{\bar{p}V}{\rho_m R_e}$$

We can examine the relative magnitudes of the various terms by recasting Eqn. (17) into dimensionless form. We adopt the scalings

$$p = \bar{p}\,p'$$

$$t = \tau t'$$

$$z = L z'$$

where $\bar{p}$ may be conveniently chosen as $\bar{p} = \rho_f g L$, the hydrostatic pressure at depth L. Dimensionless variable are denoted by primes. Using these scalings in Eqn. (17), we find, after some rearrangement:

$$\frac{\partial p'}{\partial t'} = \left(\frac{\tau}{\tau_d}\right)\left[\frac{\partial^2 p'}{\partial z'^2} - \rho_f \beta_f g L \frac{\partial p'}{\partial z'} + \left(\frac{\tau_d}{\tau_u}\right)\frac{\partial p'}{\partial z'} - \left(\frac{\tau_d}{\tau_e}\right)\right] \qquad (18)$$

where we have expanded the total time derivative in terms of partial derivatives. The various time scales are defined as $\tau_d = \mu\tilde{\beta}L^2/k$, $\tau_u = L/V$, and $\tau_e = \tilde{\beta}\bar{p}/S$. The first two terms on the right-hand side of Eqn. (18) are both related to pore-pressure diffusion. The coefficient $\rho_f\beta_f gL$ of the second term is much less than unity for crustal depths; hence, that term can be safely ignored in comparison with the first term. We now need to estimate the importance of the last two terms in Eqn. (18).

The time scale for excess-pressure diffusion, τ_d, may be estimated once we specify L and the quantity $k/\mu\tilde{\beta}$, which is approximately equal to the 'hydraulic diffusivity' c [cf. Rice and Cleary, 1976, p.230], defined as $k/\mu\hat{\beta}$ in our notation. Rice and Cleary [1976, p. 238, Table 1] have estimated that at "low to moderate effective stresses", $c > c\alpha$. $10^{-5}\,m^2\,s^{-1}$ for granitic rocks and $c\alpha$. $10^{-2}\,m^2\,s^{-1}$ for sandstones. Skempton [1970, p. 382] suggests that c may be as low as $c\alpha$. $3\times10^{-8}\,m^2\,s^{-1}$ for clays. This is probably an extreme value; we will use a value of $10^{-7}-10^{-6}\,m^2\,s^{-1}$ for argillaceous rocks. Hence, taking L = 1-10 km, we estimate $\tau_d = 10^6-10^{10}$ s for sandstones, $\tau_d = 10^{11}-10^{13}$ s for granitic rocks, and $\tau_d = 3\times10^{13}-3\times10^{15}$ s for argillaceous rocks. These values apply to rocks without macroscopic fractures.

The time scale τ_u is the time for rocks at depth L to be uplifted to the surface at a rate V. Again taking L = 1-10 km, we can estimate

$$\tau_u \approx 6\times10^{14}-6\times10^{15}\,s \qquad \text{for } V = 50\ m/Ma$$
$$\approx 0.6\times10^{14}-0.6\times10^{15}\,s \qquad \text{for } V = 500\ m/Ma$$

Finally, τ_e is the time scale over which the thermoelastic and poroelastic effects have a significant influence on pore pressure. Recalling the definition of S above, we see that $\tau_e \propto 1/V$. In Appendix C, we present estimates of $\tilde{\beta}$ and S; to a first approximation, we take $\tilde{\beta}/S \approx 0.6-1\times10^7$ s/Pa for V = 100 m/Ma, the

lower bound appropriate for moderate-porosity rocks ($\varphi \approx 0.10$), the upper bound for very low porosities ($\varphi \approx 0.01$). With L = 1-10 km, we have $\bar{p} = 10^7 - 10^8$ Pa; hence,

$$\tau_e \approx (1.2-2)\times(10^{14}-10^{15})\ \text{s} \qquad \text{for } V = 50\ \text{m/Ma}$$
$$\approx (0.1-0.2)\times(10^{14}-10^{15})\ \text{s} \qquad \text{for } V = 500\ \text{m/Ma}$$

For sandstones and granitic rocks, we see that τ_d/τ_u and τ_d/τ_e will typically be much less than unity. In this case, the last two terms on the right-hand side of Eqn. (18) may be safely neglected. Pore pressure will then be governed essentially by a simple diffusion equation, given in dimensional form as

$$\frac{\partial p}{\partial t} = \frac{k}{\mu\hat{\beta}}\frac{\partial^2 p}{\partial t^2} \tag{19}$$

For times large in comparison with τ_d, departures of pore pressure from hydrostatic should be small.

For very 'tight' argillaceous rocks, τ_d/τ_e and τ_d/τ_e may not necessarily be small in comparison with one. For these rocks, pore pressure may be significantly influenced by uplift, as well as by thermoelastic and poroelastic coupling. These effects will tend to offset each other, as is most readily seen by considering again Eqn. (17) for the limiting case of a 'sealed' rock mass (mathematically mimicked by letting $k \to 0$). We then find

$$\left.\frac{Dp}{Dt}\right|_{\text{sealed}} = -\frac{S}{\hat{\beta}} \tag{20}$$

If the thermoelastic and poroelastic effects vanished ($S \to 0$), pore pressure in the sealed zone would remain constant during uplift. Pore pressure would then exceed hydrostatic by an increasing amount as uplift proceeded. For the physically reasonable case of finite S, however, pore pressure in a sealed zone

(following the motion) would be

$$p(t)\,\big|_{\text{sealed}} = p_0 - \frac{St}{\tilde{\beta}} \tag{21}$$

where p_0 is the 'initial' value of pore pressure. We show in Appendix C that $S/\tilde{\beta}$ is probably greater than $c\alpha$. 2.5 times the rate of change of pore pressure following a hydrostatic gradient. Hence, pore pressure in a sealed zone might fall below hydrostatic during uplift. In the general case with finite permeability, the pore pressure of a rock mass during uplift will be bounded above by hydrostatic and below by the value in Eqn. (21), viz.:

$$p_0 - \frac{St}{\tilde{\beta}} \le p(t)\,\big|_{\substack{\text{sealed} \\ \text{constant moduli}}} \le p_0 - \rho_f g V t \tag{22}$$

Development of underpressuring in a rock mass should be most favored when the surrounding rocks have very low permeability, thus inhibiting diffusive relaxation of the underpressure. It is interesting to note that measured pore pressures in lenticular sands in some U.S. basins--basins that have most recently been subjected to periods of uplift and erosion--are frequently below hydrostatic [Russell, 1972].

The lateral stress s_h during uplift will be given by Eqn. (13), which becomes, using Eqn. (15):

$$\frac{Ds_h}{Dt} = -3\left(\frac{1-2\nu}{1-\nu}\right)\left(\frac{1}{\beta}\right)\frac{D\varepsilon_h}{Dt} - \left(\frac{\nu}{1-\nu}\right)\bar{\rho} g V + \left(\frac{1-2\nu}{1-\nu}\right)\left(\frac{\beta-\beta_s}{\beta}\right)\frac{Dp}{Dt} - \\ - \left(\frac{\hat{\alpha}}{\beta}\right)\left(\frac{1-2\nu}{1-\nu}\right)\Gamma V$$

Because Dp/Dt would be negative, the effect of poroelastic coupling would be to cause the compressive lateral stress s_h to decrease even more rapidly during uplift than in the absence of poroelastic coupling. This would tend to enhance the tensile stress expected upon uplift to near-surface depths--in

contradiction to observation, as has been pointed out earlier. This reinforces the contention [McGarr and Gay, 1978] that some inelastic process--perhaps crack growth, as argued by Bruner [in press]--must prevent compressive stresses from falling too greatly.

Time-dependent moduli

We now turn to the issue of pore-pressure development during uplift when inelastic processes affect the various elastic moduli of the rock. A likely cause of such time-dependence of the elastic moduli is microcrack growth that may occur during unloading as a result of grain-scale stress inhomogeneities [e.g., Nur and Simmons, 1970; Bruner, in press]. Thermodynamic considerations [Bruner, 1979, pp. 5581-84] suggest that crack growth should generally lead to increases in β, ν, and (in many cases) $\hat{\alpha}$. The fluid properties α_f and β_f should also change during uplift [cf. data in Schmidt, 1969].

Detailed evaluation of the history of pore pressure and stress during uplift, when crack growth alters the elastic moduli, would require an analysis--perhaps of the type presented by Bruner [in press]--that explicitly considers the thermodynamic- and fracture-mechanical aspects of the crack-growth process and its interaction with the macroscopic stress field. Nonetheless, we can reach some important conclusions about the development of pore pressure and stress by a simpler, heuristic approach--that is, by simply letting the various moduli be slowly varying functions of time. The results of this analysis are in qualitative agreement with Bruner's [in press] conclusions about crack-growth effects on the stress field; more importantly, this approach also permits us to reach some qualitative conclusions about pore-pressure history. We will see that variations in elasstic moduli may strongly affect pore-pressure

history during uplift.

The relevant equations for pore pressure and mean stress are [cf. Eqns (8) and (12)]:

$$\hat{\beta}\frac{Dp}{Dt} + p\frac{D\hat{\beta}}{Dt} = (\beta-\beta_s)\frac{Dp_c}{Dt} + p_c\frac{D}{Dt}(\beta-\beta_s) + \tag{23}$$
$$-\varphi_0(\alpha_f-\hat{\alpha})\Gamma V + \varphi_0 T\frac{D}{Dt}(\alpha_f-\hat{\alpha}) + \frac{\partial}{\partial z}\left[\frac{k}{\mu}\left(\frac{\partial p}{\partial z}-\rho_f g\right)\right]$$

$$\frac{Dp_c}{Dt} = -2\left(\frac{1-2\nu}{1-\nu}\right)\left(\frac{1}{\beta}\right)\frac{D\varepsilon_h}{Dt} - \frac{1}{3}\left(\frac{1+\nu}{1-\nu}\right)\bar{\rho}gV + \frac{2}{3}\left(\frac{1-2\nu}{1-\nu}\right)\left(\frac{\beta-\beta_s}{\beta}\right)\frac{Dp}{Dt} - \tag{24}$$
$$-\frac{2}{3}\left(\frac{\hat{\alpha}}{\beta}\right)\left(\frac{1-2\nu}{1-\nu}\right)\Gamma V$$

In general, these equations cannot be decoupled. If we assume, however, that the moduli are all slowly varying functions of time, we can write, to a first approximation, $D\hat{\beta}/Dt$ = constant, and analogous expressions for the other moduli. Using such expressions in Eqns. (23) and (24), and considering the limiting case of a sealed zone ($k\to 0$), we then take the Laplace transforms of these equations to find 2 ordinary differential equations for $\tilde{P}(s)$ and $\tilde{P}_c(s)$, the Laplace transforms of p and p_c, respectively. After much algebraic manipulation, we can solve for $\tilde{P}$ and invert the transform. Details of the analysis are given in Appendix D, where we show that the first-order expression for Dp/Dt, the rate of change of pore pressure following motion of the rock mass, is

$$\frac{Dp}{Dt} = \left.\frac{Dp}{Dt}\right|_{\substack{\text{sealed}\\ \text{constant moduli}}} + \frac{1}{\tilde{\beta}}\left[\pi_1\frac{D\beta}{Dt} + \pi_2\frac{D\alpha_f}{Dt} + \pi_3\frac{D\beta_f}{Dt} + \pi_4\frac{D\nu}{Dt}\right] \tag{25}$$

where

$$\pi_1 = \sigma_{0-} p_0 \left[1 - 2(\beta - \beta_s)\left(\frac{1-2\nu}{1-\nu}\right)\left(\frac{\beta_s}{\beta^2}\right) \right]$$

$$\pi_2 = \varphi_0 T_0$$

$$\pi_3 = \varphi_0 p_0$$

$$\pi_4 = 2p_0 \left[\frac{(\beta - \beta_s)^2}{\beta(1-\nu)^2} \right]$$

The subscript '0' denotes initial values, i.e., values at the beginning of uplift. Also, for our 'short time' approximation, all moduli may be assigned their initial values for the purposes of evaluating the expressions above. Estimates of the four bracketed terms (Appendix D) indicate that the terms involving $D\beta/Dt$ and $D\alpha_f/Dt$ should be dominant. These terms have opposite sign--the first positive, the second negative--with the first term of larger magnitude. As a result, Dp/Dt may become positive by a small amount. We estimate in Appendix D that for very low porosities ($\varphi \approx 0.01$):

$$Dp/Dt \Big|_{\substack{\text{sealed} \\ \text{constant moduli}}} \approx 15 \times 10^{-8}\,\text{Pa/s} \qquad \text{for } V = 50\ \text{m/Ma}$$

$$\approx 150 \times 10^{-8}\,\text{Pa/s} \qquad \text{for } V = 500\ \text{m/Ma}$$

whereas for moderate porosities ($\varphi \approx 0.1$),

$$Dp/Dt \Big|_{\substack{\text{sealed} \\ \text{constant moduli}}} \approx (-8 \rightarrow 1) \times 10^{-8}\,\text{Pa/s} \qquad \text{for } V = 50\ \text{m/Ma}$$

$$\approx (-80 \rightarrow 10) \times 10^{-8}\,\text{Pa/s} \qquad \text{for } V = 500\ \text{m/Ma}$$

In comparison, the rate of change of pore pressure along a hydrostatic gradient (Appendix C) varies from ca. $-1.6 \times 10^{-8}\,\text{Pa/s}$ to $-16 \times 10^{-8}\,\text{Pa/s}$ for the same range of uplift rates.

The simple model presented here indicates that when the moduli are time-dependent, pore pressure in a very low-porosity 'sealed' zone would tend to *increase* during uplift. Physically, this would result from the increased

compliance of the rock mass as cracks are introduced; this added compliance would cause the pore fluid to be 'squeezed'. (The energy needed to increase pore pressure would presumably come from release of elastic strain energy, just as does the energy required for crack growth [e.g., Lawn and Wilshaw, 1975]). If porosity were high enough, this effect would be counteracted by the thermal contraction of the pore fluid as it cools.

Two phenomena should tend to oppose the development of overpressures during uplift in very low porosity rocks. The first, which also applied in the constant-moduli case, is the finite permeability of any real rock mass; any local deviation of pore pressure from hydrostatic will tend to be damped diffusively. Secondly, we intuitively expect that inelastic changes in pore volume will accompany microcracking [cf. Bruner, 1979, p. 5581, Eqn. (11)]. Slight increases in pore volume associated with microcracking would--if the new cracks were in hydraulic communication with the 'old' pore space--tend to decrease p. Such microcracking would probably also lead to increased permeability, thereby enhancing the diffusive dissipation of overpressures.

If overpressures actually develop during uplift, there would be important implications for the mechanical behavior of the overpressured rocks, because elevated pore pressure enhances the likelihood of brittle fracture [e.g., Jaeger and Cook, 1976]. Overpressure development within a laterally extensive rock mass, such as a thick shale unit with interlayered sands, could facilitate the formation of pervasive fracture systems, such as joints. Some detailed studies of the timing of 'fracture-porosity' development in petroleum reservoir rocks [e.g., Currie and Nwachukwu, 1974; Narr and Currie, 1982] indicate that fracturing probably occurred during uplift. Throughgoing fractures would quite possibly form by coalescence of early formed microcracks, which would

tend to be steeply dipping [Bruner, in press].

The rate of change of s_h, the lateral compressive stress, may be readily found by substituting Eqn. (25) into Eqn. (13). We find

$$\frac{Ds_h}{Dt} = \frac{Ds_h}{Dt}\Big|_{\substack{\text{sealed} \\ \text{constant moduli}}} + \left[\left(\frac{1-2\nu}{1-\nu}\right)\left(\frac{\beta-\beta_s}{\beta\tilde{\beta}}\right)\right]_0 M(t) \qquad (26)$$

where

$$M(t) = \left[\pi_1 \frac{D\beta}{Dt} + \pi_2 \frac{D\alpha_f}{Dt} + \pi_3 \frac{D\beta_f}{Dt} + \pi_4 \frac{D\nu}{Dt}\right]$$

The effect of $M(t)$ is generally to increase s_h, the lateral compression, because of the dominance of the term involving $D\beta/Dt$, which is positive. Not surprisingly, this result is in qualitative agreement with the results of Bruner [in press] and lends support to the notion that the observed state of stress in rocks near the Earth's surface would be strongly affected by inelastic processes during uplift.

To summarize, our analysis of the coupling between pore pressure and stress during uplift (in the absence of tectonic strains) indicates that:

i) As long as there are no inelastic processes at work--specifically, as long as there is neither microcracking nor crack healing--pore pressure in most rocks will stay essentially hydrostatic during uplift. For very low permeability rocks, such as some argillaceous rocks, pore pressure may fall more rapidly than if the fluid stayed in a hydrostatic state; the magnitude of this deviation will depend upon details of the thermoelastic- and poroelastic coupling.

ii) When microcracking alters the elastic properties of a rock mass during uplift, pore pressure may deviate significantly from hydrostatic. This effect should be greatest for very low porosity rocks, for which significant

overpressures could develop if the permeability were low enough. Such overpressuring could be important in the development of pervasive fractures.

iii) The tensile lateral stress that would be expected in a rock mass uplifted to the surface from depth would be enhanced by poroelastic coupling effects. In contrast, the moduli reductions associated with microcracking during uplift would tend to prevent the development of tensile lateral stresses in a rock mass. Because lateral stresses in rocks near the surface are almost invariably compressive, these results reinforce the notion that crack growth or other inelastic processes must occur during uplift and significantly affect the stress field.

Effects of tectonic strain on pore pressure in accretionary-wedge sediments

Up to this point, we have assumed that any overall lateral strain in a rock mass is due solely to isostatic adjustment [Haxby and Turcotte, 1976]. If, in fact, there are tectonic strains applied to a rock layer at depth, the pore pressure within that layer may be substantially affected. This can be shown by considering the simple case of lateral compression (Fig. 5-2). We imagine that some crustal section is being shortened at a strain rate $\dot{\varepsilon}_h = -\dot{E}_h$, taken as a constant,and that no buckling occurs. It can be shown that for strain rates greater than ca. $10^{-17}\ s^{-1}$--not an exceptionally large value for tectonically active regions--the strain-rate term in Eqn. (17) for pore pressure should dominate. We then find, to a good approximation:

$$\tilde{\beta}\frac{Dp}{Dt} = 2\left(\frac{\beta-\beta_s}{\beta}\right)\left(\frac{1-2\nu}{1-\nu}\right)\dot{E}_h + \frac{\partial}{\partial z}\left(\frac{k}{\mu}\frac{\partial p_e}{\partial z}\right) \qquad (27)$$

where $p_e = p - \rho_f g z$ is the excess pore pressure, i.e., the pore pressure above hydrostatic. Eqn. (27) indicates that regional compression will tend to enhance

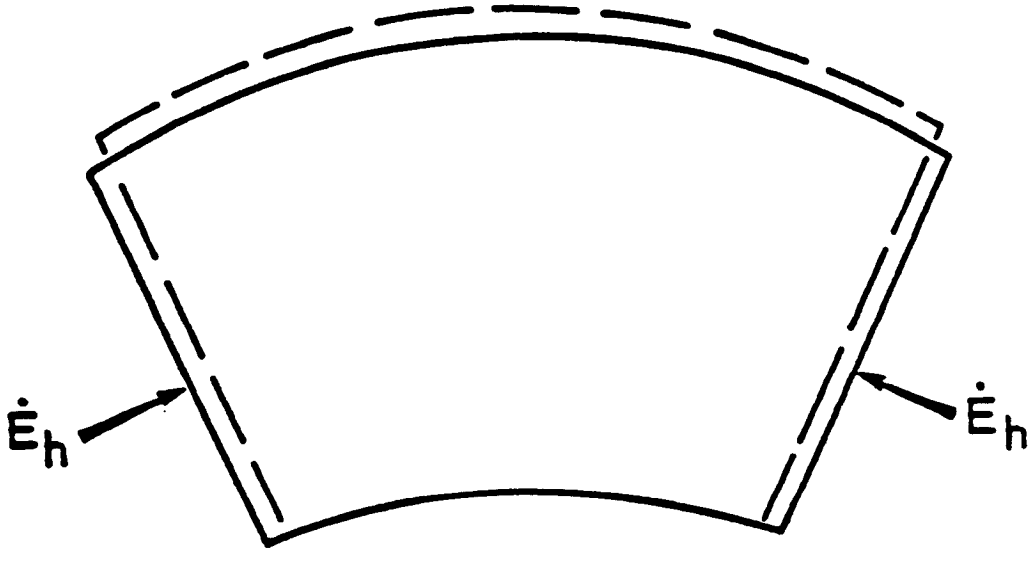

Figure 5-2: Uniform lateral compression of a crustal section at a strain rate $\dot{E}_h$. Initial section will shorten and thicken slightly (dashed lines) as a result of compression.

pore pressure in a layer at depth. If permeability is high enough, this excess pore pressure should dissipate quickly. However, if k is sufficiently low, pore pressure may build up ($Dp/Dt > 0$), probably leading to some sort of brittle failure.

We can get some estimate of the minimum permeability k_c for which excess pore pressure *cannot* build up to large values by considering the special case in which Dp/Dt vanishes. We then find:

$$\frac{k_c}{\mu}\left(\frac{\partial^2 p_e}{\partial z^2}\right) = -2\left(\frac{\beta-\beta_s}{\beta}\right)\left(\frac{1-2\nu}{1-\nu}\right)\dot{E}_h \qquad (28)$$

where we have taken μ and k as constants. Dimensional arguments indicate that $\partial^2 p_e/\partial z^2$ should be roughly of magnitude $\Delta\rho\, g/D$, where $\Delta\rho$ is the difference between solid and fluid densities, and D is the depth to the rock layer of interest. The critical permeability will then be roughly

$$k_c \approx 2\left(\frac{\beta-\beta_s}{\beta}\right)\left(\frac{1-2\nu}{1-\nu}\right)\dot{E}_h\left(\frac{\mu D}{\Delta\rho\, g}\right) \qquad (29)$$

Taking $\Delta\rho = 1.7\times10^3\ \mathrm{kg/m^3}$, $g = 9.8\ \mathrm{m/s^2}$, $\mu = 5\times10^{-4}$ Pa s, and moduli values as suggested in Appendix C, we find

$$k_c \approx 1.9\times10^{-8}\,\dot{E}_h\,D \quad [\mathrm{m^2}]$$

where $\dot{E}_h$ and D are in MKS units.

Fig. 5-3 shows k_c as a function of $\dot{E}_h$ for three values (1, 5, 10 km) of D. (Again, we emphasize that for $k < ca.\ k_m$, Dp/Dt will be positive at the depth D of interest.) To better understand the significance of our estimate of$m k_c$, consider the interesting case of convergent plate margins. Davis et al. [1983], von Huene and Lee [1983], and others have reviewed evidence for the common occurrence of excess pore pressure within sedimentary rocks of 'accretionary wedges'. The strain rates within such rocks should be on the order of a few

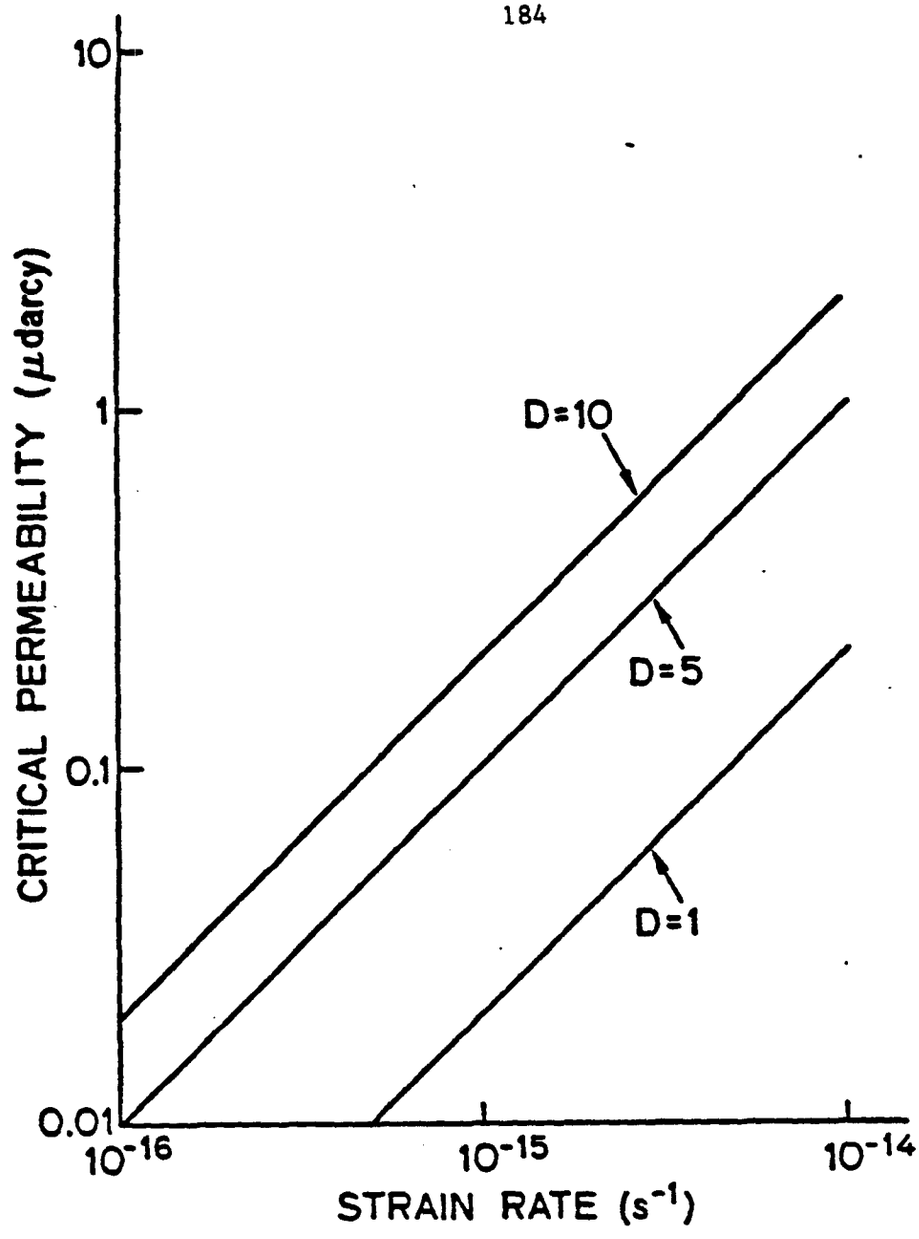

Figure 5-3: 'Critical' permeability for large overpressuring due to compressive strains, as a function of strain rate, for three values of stratum depth D in km.

times $10^{-14}\ s^{-1}$ (obtained by distributing strain due to a typical convergence velocity of 0.1 m/a over a width of ca. 100 km). From Fig. 5-3, we see that for $\dot{E}_h = 10^{-14}\ s^{-1}$, $k_c \approx 10^{-18}\ m^2 = 1\ \mu$darcy. Although this is rather low if the section is predominantly sandstone, it is quite plausible if there are interlayered shales. (The net resistance to upward flow of overpressured fluid will be proportional to $\int k^{-1}\, dz$; hence, a few thin, low permeability units could contribute more 'flow resistance' than a thick section of relatively permeable rock.) Therefore, our simple model indicates that tectonic strain clearly has the potential to cause overpressuring in sedimentary strata between converging plates. Such overpressuring could be very important in facilitating deformation within the sedimentary rocks caught between convergent plates [Davis et al., 1983; von Huene and Lee, 1983].

The time scale for significant strain-induced overpressures to develop could be surprisingly short at moderately high strain rates. We can estimate the time for pore pressure to reach lithostatic for the special case of a 'sealed' zone, for which (cf. Eqn. (27))

$$\tilde{\beta}\,\frac{Dp}{Dt}\Big|_{\text{sealed}} = 2\left(\frac{\beta-\beta_s}{\beta}\right)\left(\frac{1-2\nu}{1-\nu}\right)\dot{E}_h \qquad (30)$$

or, using parameter values suggested in Appendix C, for porosities of 0.10:

$$\frac{Dp}{Dt}\Big|_{\text{sealed}} \approx (1.6\times 10^{10}\ \text{Pa})\,\dot{E}_h$$

Assuming initially hydrostatic conditions, the time t_c for pore pressure in a sealed zone at depth D to reach lithostatic will be

$$t_c \approx \frac{\Delta\rho\, g D}{Dp/Dt\,\big|_{\text{sealed}}}$$

or using $\Delta\rho \approx 1.5\times 10^3\ kg/m^3$, $g = 9.8\ m/s^2$:

$$t_c \approx 3.3 \times 10^{-11} D / \dot{E}_h \quad [a]$$

for D in km and $\dot{E}_h$ in s^{-1}. This relationship is plotted in Fig. 5-4 for several values of D and $\dot{E}_h$. For the strain rate that we have suggested may be typical of convergent plate margins, ($10^{-14}\ s^{-1}$), we see from Fig. 5-4 that pore pressure in a sealed zone could reach lithostatic on a time scale of only several thousands or tens of thousands of years. On such short time scales, the rheological behavior of low porosity sediments should be reasonably close to elastic (cf. chapter 2 of this dissertation). There will be essentially no diffusive relaxation of overpressures on such a time scale if there are significant amounts of low permeability shales in the overlying section.

The calculations above suggest that large overpressures could be common within sedimentary strata of accretionary wedges, in accord with observations (e.g., as reviewed in Davis et al. [1983] and von Huene and Lee [1983]). Large overpressures would very clearly be important in facilitating deformation of the rocks caught between convergent plates. Our calculations lend support to the mechanical model for deformation within accretionary wedges recently advanced by Davis et al. [1983].

We emphasize that other mechanisms of overpressuring may exist, such as rapid sedimentation [e.g., Smith, 1971] and clay dehydration [e.g, Powers, 1967; Burst, 1969; chapter 3, this dissertation]; the first of these has been previously discussed as a possible cause of overpressuring in accretionary-wedge sediments [e.g., Karig et al., 1980]. However, these would be of minor importance compared to strain-induced overpressuring if strain rates are as high as would seem likely at convergent plate margins.

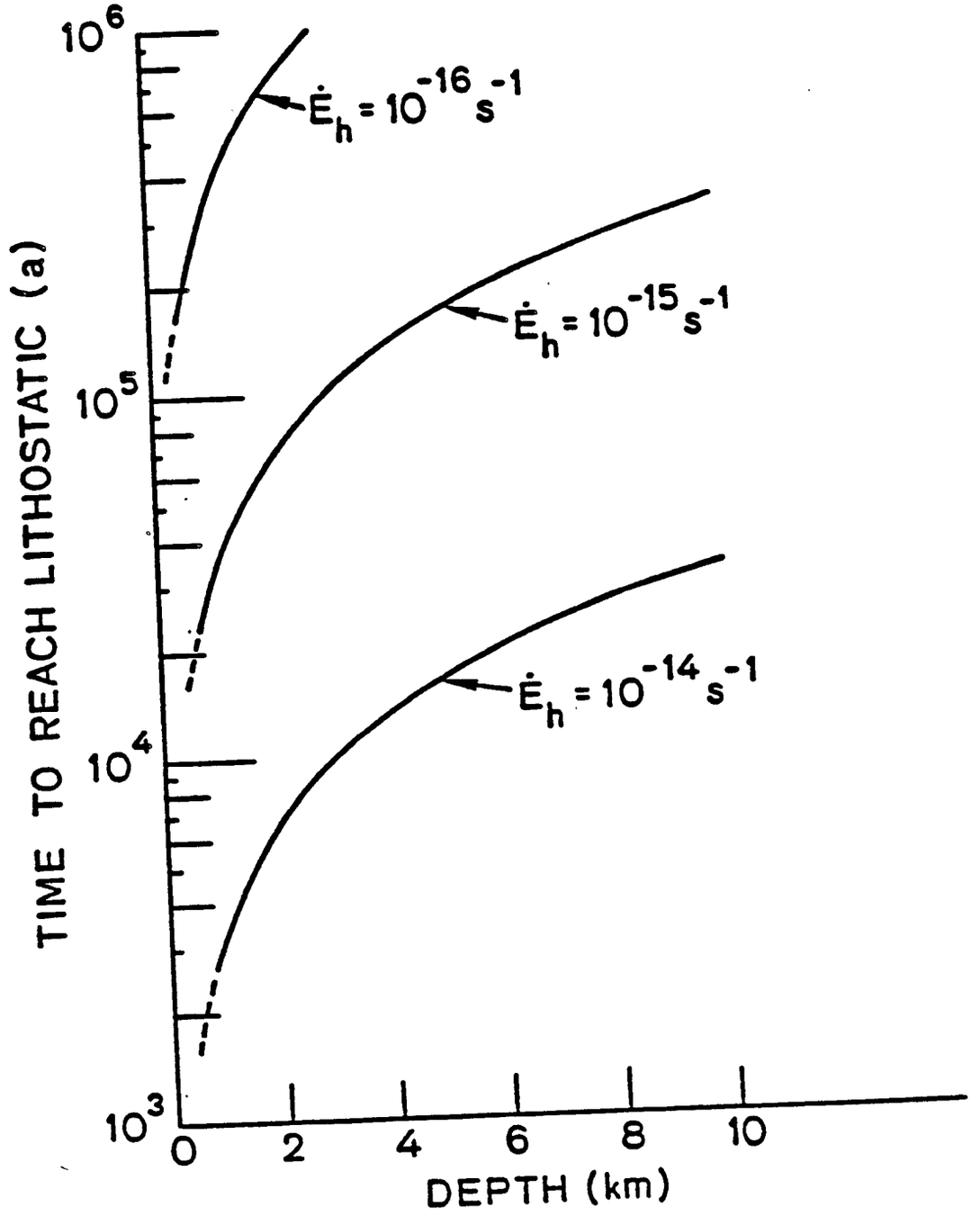

Figure 5-4: Time for initially hydrostatic pore pressure in a 'sealed' rock mass to reach lithostatic as a result of lateral strain-induced overpressuring, as a function of depth to the rock mass, for three values of strain rate. For strain rates typical of convergent plate margins, pore pressure may reach lithostatic within only a few thousand or tens of thousands of years.

5. DISCUSSION: FURTHER APPLICATIONS OF THE ANALYSIS

The formalism that we have developed here should be generally applicable for examining the pore-pressure history of a rock mass in a variety of geologic situations besides the ones we have examined. For example, certain aspects of pore-pressure and stress development in a subsiding rock mass could be examined simply by 'inverting' the analysis we have applied to the case of uplift. In the constant-moduli approximation, an analysis parallel to that in section 4 would indicate that pore pressure in low permeability rocks would tend to increaase above hydrostatic during subsidence. The rate of pore-pressure increase could be quite substantial, perhaps as high as the rate of increase of overburden pressure. This would appear to be a very attractive mechanism for joint development. There are complications, however, that make it necessary to proceed with caution. For one, would the lateral boundary condition used in the analysis of uplift apply to subsidence? That boundary condition was essentially a statement that strain would be due solely to isostatic compensation on a sphere. However, recent considerations of the physical processes involved in subsidence [e.g., McKenzie, 1978] suggest that crustal extension may be very important. This would translate into a 'boundary condition' on applied strain in our formulation. We can also question whether subsidence will be accompanied by flexure of strata [e.g., Price, 1966]. Finally, and importantly, we need to consider under what circumstances our rheological model may break down. During subsidence, the inelastic, permanent strains associated with porosity reduction [cf. chapter 3 of this dissertation] may overwhelm any elastic strains. Clearly, one must carefully consider the characteristic time scale of processes of interest, and determine whether the rock mass will behave elastically on that time scale, before

applying our formalism to an examination of pore-pressure history.

6. SUMMARY

We have developed a formalism to shows the way that pore pressure in the Earth's crust is coupled to the state of stress and the temperature field. We have applied this formalism to examining pore-pressure history in two common geological situations: in rocks undergoing uplift and erosion, and at convergent plate boundaries. In the case of uplift and erosion, the development of abnormal pore pressure in low porosity rocks is quite likely, especially if such rocks either have very low permeability or are surrounded by rocks that do. Subhydrostatic pore pressure may develop if uplift occurs without the development of microcracks. In the event that grain-scale stress heterogeneities do lead to microcracking, the compliance of the rock mass may become substantially increased, tending to 'squeeze' the pore fluid and increase pore pressure above hydrostatic in low porosity rocks. Such microcracks, as well as possible overpressuring, could be related to the development of pervasive macroscopic fractures.

Compressive strains applied to sedimentary rocks caught between converging plates may cause large overpressures if there are sufficient amounts of low permeability rock in the sedimentary column. Such overpressures may develop very rapidly, on a geological time scale, at strain rates typical of converging plate margins, and could be very important in facilitating the deformation of rocks within accretionary wedges.

APPENDIX A: DERIVATION OF PORE-PRESSURE EQUATION

Following Rice and Cleary [1976, pp. 228-29], we arrive at a partial differential equation for pore pressure by combining a constitutive relation for the fluid mass content of the 'poro-thermoelastic' material with mass conservation considerations and Darcy's law. We write the fluid mass per unit reference volume, m, as

$$m = \rho_f v \tag{A-1}$$

where ρ_f is the fluid density. For small changes in m, we can write [cf. Rice and Cleary, 1976, p. 228, Eqn. 3]:

$$dm = m - m_0 = (\rho_f - \rho_0) v_0 + (v - v_0) \rho_0 \tag{A-2}$$

where m_0 and ρ_0 are the reference values of m and ρ_f, respectively. Using a linearized expansion for ρ_f as a function of p and T, this expression becomes

$$dm = m - m_0 = \rho_0 \beta_f v_0 dp - \rho_0 \alpha_f v_0 dT + \rho_0 \left(\frac{d\sigma_{kk}}{H} + \frac{dp}{R} + 3\alpha v_0 dT \right) \tag{A-3}$$

where α_f and β_f are the fluid's thermal expansivity and compressibility, respectively.

As long as deformation is small, the fluid mass fraction m is very nearly equal to the porosity φ. Restricting ourselves to the small-deformation case, we can rewrite Eqn. (A-3) as

$$\rho_f \varphi - \rho_0 \varphi_0 = \rho_0 \beta_f v_0 dp - \rho_0 \alpha_f v_0 dT + \rho_0 \left(\frac{d\sigma_{kk}}{H} + \frac{dp}{R} + 3\alpha v_0 dT \right) \tag{A-4}$$

Conservation of mass of the fluid is expressed by the equation

$$\frac{\partial}{\partial t}(\rho_f \varphi) = - \frac{\partial}{\partial z}(\rho_f u_f \varphi) \tag{A-5}$$

where u_f is the volumetric flow rate. We have assumed flow in only the vertical

direction. Because we are generally interested in moving media, we add to both sides of Eqn. (A-5) the quantity $u_s \partial(\rho_f \varphi)/\partial z$, where u_s is the speed at which the solid moves; u_s is assumed to be constant. We can therefore write

$$\frac{D}{Dt}(\rho_f \varphi) = -\frac{\partial}{\partial z}\left[\rho_f \varphi (u_f - u_s)\right] \tag{A-6}$$

Finally, we need Darcy's law for flow in a porous medium:

$$\varphi(u_f - u_s) = -\frac{k}{\mu}\left(\frac{\partial p}{\partial z} - \rho_f g\right) \tag{A-7}$$

Substituting Eqn. (A-7) into Eqn. (A-6), we find

$$\frac{D}{Dt}(\rho_f \varphi) = \frac{\partial}{\partial z}\left[\frac{k\rho_f}{\mu}\left(\frac{\partial p}{\partial z} - \rho_f g\right)\right] \tag{A-8}$$

Substituting Eqn. (A-4) into Eqn. (A-8), we finally arrive at the expression given as Eqn. (8) of the main text.

APPENDIX B: THERMAL ENERGY EQUATION

We begin by assuming that motion of the fluid and solid is in the vertical direction only. We can then write the various terms in the energy equation as

$$\text{conducted heat} = k_m \frac{\partial^2 T}{\partial z^2}$$

$$\text{heat advected by fluid} = -\frac{\partial}{\partial z}(\varphi \rho_f u_f \hat{C}_f T)$$

$$\text{heat advected by solid} = -\frac{\partial}{\partial z}\left[(1-\varphi)\rho_s u_s \hat{C}_s T\right]$$

$$\text{rate of change of heat content} = \frac{\partial}{\partial t}(\rho_m \hat{C}_m T)$$

where all symbols are as defined previously. We are assuming here that thermoelastic heating and the energy involved in irreversible processes, such as crack growth, are negligible in the overall energy balance. Also, the thermal conductivity k_m implicitly includes the effect of dispersion (cf. Sharp, 1976; Sharp and Domenico, 1976). Energy conservation may therefore be expressed as

$$\frac{\partial}{\partial t}(\rho_m \hat{C}_m T) = k_m \frac{\partial^2 T}{\partial z^2} - \frac{\partial}{\partial z}(\varphi \rho_f u_f \hat{C}_f T) - \frac{\partial}{\partial z}\left[(1-\varphi)\rho_s u_s \hat{C}_s T\right] \quad \text{(B-1)}$$

Using Darcy's law (Eqn. A-5), we can rewrite this expression as

$$\frac{\partial}{\partial t}(\rho_m \hat{C}_m T) = k_m \frac{\partial^2 T}{\partial z^2} - \frac{\partial}{\partial z}\left[(\tilde{\rho}\tilde{C})u_s T\right] + \frac{\partial}{\partial z}\left[\rho_f \hat{C}_f T\left(\frac{k}{\mu}\frac{\partial p}{\partial z}\right)\right] \quad \text{(B-2)}$$

We now assume that ρ_m, $\hat{C}_m$, $\tilde{\rho}\tilde{C}$, ρ_f, $\hat{C}_f$, k, and μ are constant. We have also taken u_s as constant in the general model. Hence, we can rewrite Eqn. (B-2) as

$$\rho_m \hat{C}_m \frac{\partial T}{\partial t} = k_m \frac{\partial^2 T}{\partial z^2} + \tilde{\rho}\tilde{C} V \frac{\partial T}{\partial z} + \frac{\rho_f \hat{C}_f T k}{\mu}\frac{\partial}{\partial z}\left(\frac{\partial p}{\partial z} - \rho_f g\right) \quad \text{(B-3)}$$

This is the energy equation given as Eqn. (22) of the main text.

Recasting Eqn. (B-3) into dimensionless form leads us to estimates of the relative importances of the various terms in that equation. For this purpose, it is convenient to first rewrite the last term in Eqn. (B-3) in terms of fluid flow velocity rather than pore pressure. The modified form of Eqn. (B-3) is

$$\rho_m \hat{C}_m \frac{\partial T}{\partial t} = k_m \frac{\partial^2 T}{\partial z^2} + \tilde{\rho}\tilde{C} V \frac{\partial T}{\partial z} - \rho_f \hat{C}_f T \varphi \frac{\partial u_f}{\partial z} \qquad \text{(B-4)}$$

We now adopt the following scalings:

$$T = T_0 T'$$
$$z = L z'$$
$$t = t_c t'$$

where T_0 may be taken as the initial temperature, L is a characteristic length scale, e.g., initial depth, and t_c is the characteristic time scale for conduction, viz., $t_c = L^2 \rho_m \hat{C}_m / k_m$. We also scale the fluid velocity by $\varphi u_f = U u_f'$. Dimensionless varibles are denoted by primes. The dimensionless thermal energy equation may then be written, after some rearrangement, as

$$\frac{\partial T'}{\partial t'} = \frac{\partial^2 T'}{\partial z'^2} + \left(\frac{\tilde{\rho}\tilde{C} u_s L}{k_m}\right) \frac{\partial T'}{\partial z'} - \left(\frac{\rho_f \hat{C}_f U L}{k_m}\right) T' \frac{\partial u_f'}{\partial z'} \qquad \text{(B-5)}$$

We can estimate the magnitude of the dimensionless terms $\tilde{\rho}\tilde{C} u_s L / k_m$ and $\rho_f \hat{C}_f U L / k_m$ by substituting approximate values for the various parameters. In MKS units, $\rho_f \approx 10^3$, $\hat{C}_f \approx 5 \times 10^3$, $\tilde{\rho}\tilde{C} \approx 2 \times 10^6$ for $\varphi = 0.1$, and $k_m \approx 2$ [Clark, 1966; Sissom and Pitts, 1972].

We will focus our attention on rocks fairly close to the surface, such that they are within the zone of brittle, not ductile, behavior. We therefore take $L <$ ca. 10 km $= 10^4$ m [cf. Brace and Kohlstedt, 1980]. Hence, we find:

$$\frac{\tilde{\rho}\tilde{C} u_s L}{k_m} < \text{ca. } 10^{10} u_s \qquad \text{(B-6a)}$$

$$\frac{\rho_f \hat{C}_f UL}{k_m} < \text{ca. } 2.5 \times 10^{10} U \qquad \text{(B-6b)}$$

The advection terms are therefore negligible for u_s and U less than ca. 10^{-11} m/s (300 m/Ma); this is, in fact, a lower bound, even greater velocities being required for there to be a significant influence at depths less than 10 km. Hence, in general, we are safe in neglecting the advection terms in the energy equation. This equation may therefore be expressed to a close approximation as

$$\frac{\partial T}{\partial t} = \kappa_m \frac{\partial^2 T}{\partial z^2} \qquad \text{(B-7)}$$

where $\kappa_m = k_m / \rho_m \hat{C}_m$ is the thermal diffusivity of the fluid-saturated rock.

When dealing with heat flow during uplift or subsidence, there are two characteristic time scales that arise naturally. The first, $t_c = L^2 / \kappa_m$, is a measure of the time for thermal disturbances at a depth L to be damped out by heat conduction. The second, $t_u = L / V$, is a measure of the time for materials to move a vertical distance L at a rate V. If $t_c \ll t_u$, then the temperature field will be essentially unperturbed by uplift or subsidence. This condition is equivalent to $V \ll \kappa_m / L$. For water-saturated rocks, $\kappa_m \approx 10^{-6}\,\text{m}^2/\text{s}$ [cf. Clark, 1966; Sissom and Pitts, 1972]; taking L = 10 km, we see that the temperature field will be essentially the same as for steady-state conditions as long as

$$V \ll 10^{-10}\,\text{m/s} = 3 \times 10^{3}\,\text{m/Ma}$$

while for L = 1 km, this condition becomes

$$V \ll 10^{-9}\,\text{m/s} = 3 \times 10^{4}\,\text{m/Ma}$$

These conditions will be satisfied for all but the most extreme rates of uplift.

Hence, we can treat the problem as essentially one of a steady state:

$$\frac{\partial T}{\partial t} = 0 \tag{B-8}$$

or

$$\frac{DT}{Dt} = -\Gamma V \tag{B-9}$$

where Γ is the magnitude of the geothermal gradient and V is defined so as to be positive for uplift. This is the result used in the main text.

Appendix C: ESTIMATE OF PARAMETER VALUES

We showed in section 4 of the main text that the rate of change during uplift of pore pressure and stress are related to the ratio of tha parameters S and $\tilde{\beta}$, which are defined as

$$S = \left\{ \frac{1}{3}\left(\frac{1+\nu}{1-\nu}\right)(\beta-\beta_s)\bar{\rho}g + \left[\varphi_0(\alpha_f-\hat{\alpha}) + \frac{2}{3}\left(\frac{\hat{\alpha}}{\beta}\right)\left(\frac{1-2\nu}{1-\nu}\right)(\beta-\beta_s)\right]\Gamma + \right. \tag{C-1}$$
$$\left. + 2\left(\frac{1-2\nu}{1-\nu}\right)\left(\frac{\beta-\beta_s}{\beta}\right)\frac{\bar{p}}{\rho_m R}\right\} V$$

$$\tilde{\beta} = \hat{\beta} - \frac{2}{3}\left(\frac{1-2\nu}{1-\nu}\right)\frac{(\beta-\beta_s)^2}{\beta} \tag{C-2}$$

where we have assumed in Eqn. (C-1) that isostatic compensation is maintained at all times and that tectonic strains vanish. All symbols are defined in the main text.

We now compute plausible values for the various terms that comprise Eqns. (C-1) and (C-2). We begin by considering the various compressibilities that enter into those equations. The average grain compressibility, β_s, should be ca. $2\times10^{-11}\,\mathrm{Pa}^{-1}$ for a variety of rocks [Birch, 1966]. Whole-rock compressibility, β, should be larger than β_s as long as the rock has any pore space. Measurements by Brace [1965, p. 395] indicate that β for cracked rocks is commonly several times larger than the predicted crack-free value. For the purposes of our calculations, we will take $\beta = 4\times10^{-11}\,\mathrm{Pa}^{-1}$. Fluid compressibility, β_f, should be ca. $3\times10^{-10}\,\mathrm{Pa}^{-1}$ at pressures and temperatures of interest [cf. Schmidt, 1969].

The other moduli that we need to estimate are ν, $\hat{\alpha}$, and α_f. Poisson's ratio, ν, is typically about 0.25 for crustal rocks if not too highly fractured [Birch, 1966]. Measured volumetric expansion coefficients, $\hat{\alpha}$, show wide

variability [Richter and Simmons, 1974], presumably due to complex crack geometries and crack histories [Bruner, 1979, p. 5884], but are typically on the order of $10^{-5}\,C^{-1}$. Finally, α_f, the thermal expansivity of the pore fluid--which we assume, for simplicity, to be pure water--is *ca.* $0.5-1\times10^{-3}\,C^{-1}$ at pressures and temperatures of relevance, as computed from tabulated specific volume data in Schmidt [1969].

The magnitude of the geothermal gradient, Γ, varies significantly from place to place. A typical value for stable continental crust is 15°C/km [Blackwell, 1971]; higher values may be appropriate for tectonically active regions. A reasonable range of values to use in our calculations is Γ = 15–30°C/km. Other parameters entering into Eqn. (C-1) may be estimated as $g = 9.8\ m/s^2$, $\bar{\rho} = 2.7\times10^{3}\ kg/m^3$, $\rho_m = 3.4\times10^{3}\ kg/m^3$, $R = 6.4\times10^{3}$ km, and φ_0 = 0.01-0.1.

We can now compute the various terms within braces in the expression for S above:

$$\frac{1}{3}\left(\frac{1+\nu}{1-\nu}\right)(\beta-\beta_s)\bar{\rho}g \approx 3\times10^{-7}\ m^{-1}$$

$$\frac{2}{3}\hat{\alpha}\left(\frac{1-2\nu}{1-\nu}\right)\left(\frac{\beta-\beta_s}{\beta}\right)\Gamma \approx 0.3-0.7\times10^{-7}\ m^{-1}$$

$$\varphi_0(\alpha_f-\hat{\alpha})\Gamma \approx 0.7-3\times10^{-7}\ m^{-1} \qquad \text{for } \varphi_0 = 0.01$$

$$\varphi_0(\alpha_f-\hat{\alpha})\Gamma \approx 7-30\times10^{-7}\ m^{-1} \qquad \text{for } \varphi_0 = 0.10$$

$$2\left(\frac{1-2\nu}{1-\nu}\right)\left(\frac{\beta-\beta_s}{\beta}\right)\left(\frac{\bar{\rho}}{\rho_m R_e}\right) \approx 0.8\times10^{-7}\ m^{-1}$$

Summing up, we find

$$S \approx 4.8-6.5\times10^{-7}\,V \quad [s^{-1}] \qquad \text{for } \varphi_0 = 0.01$$

$$\approx 11-34\times10^{-7}\,V \quad [s^{-1}] \qquad \text{for } \varphi_0 = 0.1$$

where V is in MKS units. The compressibility term $\tilde{\beta}$ may be estimated as well:

$\tilde{\beta} \approx 1.8 \times 10^{-11}\ \mathrm{Pa}^{-1}$ for $\varphi_0 = 0.01$

$\approx 4.3 \times 10^{-11}\ \mathrm{Pa}^{-1}$ for $\varphi_0 = 0.10$

The ratio $S/\tilde{\beta}$ is therefore given approximately by

$S/\tilde{\beta} \approx 2.7\text{–}3.6 \times 10^{4}\ V\ [\mathrm{Pa/s}]$ for $\varphi_0 = 0.01$

$\approx 2.6\text{–}8 \times 10^{4}\ V\ [\mathrm{Pa/s}]$ for $\varphi_0 = 0.10$

with V again in MKS units. Uplift or subsidence rates are typically no more than a few hundreds of meters per million years; therefore, we can estimate that for very low porosity rocks (φ = ca. 0.01):

$S/\tilde{\beta} \approx 4\text{–}6 \times 10^{-6}\ \mathrm{Pa/s}$ for $V = 50\ \mathrm{m/Ma}$

$\approx 40\text{–}60 \times 10^{-6}\ \mathrm{Pa/s}$ for $V = 500\ \mathrm{m/Ma}$

and for moderate porosity rocks ($\varphi = 0.10$):

$S/\tilde{\beta} \approx 4\text{–}13 \times 10^{-6}\ \mathrm{Pa/s}$ for $V = 50\ \mathrm{m/Ma}$

$\approx 40\text{–}130 \times 10^{-6}\ \mathrm{Pa/s}$ for $V = 500\ \mathrm{m/Ma}$

It should be recalled (Eqn. 25) that $S/\tilde{\beta}$ is the rate of change of pore pressure for a 'sealed' zone, i.e., one for which the permeability of the surrounding rock is negligibly small. By way of comparison, if the pore pressure stays hydrostatic during uplift or subsidence, we have $\left| Dp/Dt \right|_{hydrostatic} = \rho_f g V$, where $\rho_f \approx 10^3\ \mathrm{kg\ m^{-3}}$ is the fluid density. Thus, $\left| Dp/Dt \right|_{hydrostatic}$ increases from ca. $1.6 \times 10^{-6}\ \mathrm{Pa/s}$ for $V = 50$ m/Ma to $16 \times 10^{-6}\ \mathrm{Pa/s}$ for $V = 500$ m/Ma. This indicates that, if moduli stay constant, pore pressure initially at hydrostatic within a 'sealed' zone would fall below hydrostatic during uplift and erosion. Interestingly, the magnitude of $S/\tilde{\beta}$ is not only larger than $\left| Dp/Dt \right|_{hydrostatic}$, but also, in many cases, larger than the rate of change of overburden stress, which is roughly $2.5 \times \left| Dp/Dt \right|_{hydrostatic}$. Thus, underpressuring could be quite substantial.

APPENDIX D: PORE PRESSURE-STRESS COUPLING WITH VARIABLE MODULI

We begin here with the two differential equations describing the history of pore pressure and confining pressure during uplift, given in the main text as

$$\hat{\beta}\frac{Dp}{Dt} + p\frac{D\hat{\beta}}{Dt} = (\beta-\beta_s)\frac{Dp_c}{Dt} + p_c\frac{D}{Dt}(\beta-\beta_s) - \varphi_0(\alpha_f - \hat{\alpha})\Gamma V + \tag{D-1}$$
$$+ \varphi_0 T\frac{D}{Dt}(\alpha_f - \hat{\alpha}) + \frac{\partial}{\partial z}\left[\frac{k}{\mu}\left(\frac{\partial p}{\partial z} - \rho_f g\right)\right]$$

$$\frac{Dp_c}{Dt} = -2\left(\frac{1-2\nu}{1-\nu}\right)\left(\frac{1}{\beta}\right)\frac{D\varepsilon_h}{Dt} - \frac{1}{3}\left(\frac{1+\nu}{1-\nu}\right)\bar{\rho}gV + \frac{2}{3}\left(\frac{1-2\nu}{1-\nu}\right)\left(\frac{\beta-\beta_s}{\beta}\right)\frac{Dp}{Dt} - \tag{D-2}$$
$$- \frac{2}{3}\left(\frac{\hat{\alpha}}{\beta}\right)\left(\frac{1-2\nu}{1-\nu}\right)\Gamma V$$

where all symbols are as defined previously. Generally, these equations cannot be decoupled and solved analytically. However, in the limit of a 'sealed' rock mass (mimicked by letting $k \to 0$), we can find an approximate analytical solution for $p(t)$ if the various moduli are slowly varying functions of time. We now assume that the moduli may be expressed by a first-order Taylor series expansion, viz.:

$$\hat{\beta} = b_1 + b_2 t$$
$$\beta - \beta_s = B_1 + B_2 t$$
$$\alpha_f - \hat{\alpha} = a_1 + a_2 t$$
$$\frac{1+\nu}{1-\nu} = n_1 + n_2 t$$
$$\frac{1}{3}\left(\frac{1-2\nu}{1-\nu}\right)\left(\frac{\beta-\beta_s}{\beta}\right) = c_1 + c_2 t$$
$$\frac{2\hat{\alpha}}{3\beta}\left(\frac{1-2\nu}{1-\nu}\right) = d_1 + d_2 t$$
$$\frac{2}{\beta}\left(\frac{1-2\nu}{1-\nu}\right) = e_1 + e_2 t$$

where b_1, B_1, etc., are the 'initial' values of the moduli and b_2, B_2, etc., are the material time derivatives of the moduli, these derivatives being taken as constants in our approximation. Substituting these expressions into Eqn. (D-1)

and taking the Laplace transform, we find, after some rearrangement:

$$-b_2\frac{d\tilde{P}}{ds}+b_1\tilde{P}+B_2\frac{d\tilde{P}_c}{ds}-B_1\tilde{P}_c+f_1(s)=0 \qquad \text{(D-3)}$$

where $\tilde{P}$ and $\tilde{P}_c$ are the Laplace transforms of $p(t)$ and $p_c(t)$, respectively, and $f_1(s)$ is defined as

$$f_1(s)=\frac{-b_1p_0+B_1\sigma_0}{s}+\varphi_0\Gamma V\left(\frac{a_1}{s^2}+\frac{a_2}{s^3}\right)-\frac{\varphi_0(T_s+\Gamma l)a_2}{s^2} \qquad \text{(D-4)}$$

where T_s is the surface temperature and l is the depth to the rock mass of interest. Similarly, using the expressions for the time-varying moduli in Eqn. (D-2), and taking the Laplace transform, we find:

$$\tilde{P}_c+2c_2\frac{d\tilde{P}}{ds}-2\left(c_1-\frac{c_2}{s}\right)\tilde{P}-g_2\frac{d\tilde{E}}{ds}=\left(g_1-\frac{g_2}{s}\right)\tilde{E}+f_2(s)=0 \qquad \text{(D-5)}$$

where $\tilde{E}$ is the Laplace transform of $\varepsilon_h(t)$ and $f_2(s)$ is defined as

$$f_2(s)=-\frac{\sigma_0}{s}+\frac{1}{3}\bar{\rho}gV\left(\frac{n_1}{s^2}+\frac{n_2}{s^3}\right)+\frac{2c_1p_0}{s}+\Gamma V\left(\frac{d_1}{s^2}+\frac{d_2}{s^3}\right) \qquad \text{(D-6)}$$

Using Eqn. (D-5), we can eliminate $\tilde{P}_c$ and $d\tilde{P}_c/ds$ from Eqn. (D-3), arriving at a differential equation in terms of $\tilde{P}$ and $\tilde{E}$:

$$a_1\frac{d^2\tilde{P}}{ds^2}+a_2\frac{d\tilde{P}}{ds}+a_3\tilde{P}+a_4\frac{d^2\tilde{E}}{ds^2}+a_5\frac{d\tilde{E}}{ds}+a_6\tilde{E}+f_3(s)=0 \qquad \text{(D-7)}$$

where

$$a_1=-2B_2c_2$$

$$a_2=-b_2+2B_2\left(c_1-\frac{c_2}{s}\right)+2b_3c_2$$

$$a_3=b_1+\frac{2B_2c_2}{s^2}-2B_1\left(c_1-\frac{c_2}{s}\right)$$

$$a_4=B_2g_2$$

$$a_5=-B_2\left(g_1-\frac{g_2}{s}\right)+B_1g_2$$

$$\alpha_6 = -\frac{B_2 g_2}{s^2} - B_1\left(g_1 - \frac{g_2}{s}\right)$$

$$f_3 = \frac{\xi_1}{s} + \frac{\xi_2}{s^2} + \frac{\xi_3}{s^3} + \frac{\xi_4}{s^4}$$

and the coefficients in the expression for $f_3(s)$ are

$$\xi_1 = (2B_1 c_1 - b_1)p_0$$

$$\xi_2 = -B_2 a_0 + 2c_1 B_2 p_0 + B_1 \bar{\rho} g V n_1 / 3 + B_1 \Gamma V d_1 + \varphi_0 \Gamma V a_1 - \varphi_0 (T_e + \Gamma l) a_2$$

$$\xi_3 = 2\bar{\rho} g V B_2 n_1 / 3 + 2\Gamma V d_1 B_2 + B_1 \bar{\rho} g V n_2 / 3 + B_1 \Gamma V d_2 + \varphi_0 \Gamma V a_2$$

$$\xi_4 = 3B_2 n_2 + 3d_2 \Gamma V B_2$$

When ε_h, hence $\tilde{E}$, is prescribed, we can solve for $\tilde{P}$. We will consider here only the case of constant strain rate, viz., $\varepsilon_h = \dot{\varepsilon}_h t$, where the strain in the reference state is taken as zero. $\tilde{E}$ and its derivatives with respect to s are then easily found. For the case in which this strain is due solely to isostatic adjustment [Haxby and Turcotte, 1976], $\dot{\varepsilon}_h = \bar{\rho} V / \rho_m R_e$, where V is the uplift rate.

We can find an approximate solution for pore pressure for 'short times' fairly readily by keeping only the highest order terms in the coefficients $\alpha_1 - \alpha_6$ and the two highest order terms in $f_3(s)$. (Keeping only the highest order term in f_3 would lead to a solution of the form p = constant.) We then assume that $\tilde{P}$ may be expressed as a power series in $1/s$:

$$\tilde{P} = \sum_{n=1}^{\infty} \frac{\lambda_n}{s^n} \qquad \text{(D-10)}$$

where the λ_n are coefficients to be determined. Using this expression in Eqn. (D-7), equating coefficients of powers of $1/s$ term by term, inverting the transform, and replacing b_2, B_2, etc., by the appropriate material derivatives, we find that the lowest-order approximation of Dp/Dt is:

$$\frac{Dp}{Dt} - \frac{Dp}{Dt}\Big|_{\substack{\text{constant}\\\text{moduli}}} = \frac{\sigma_0 \frac{D}{Dt}(\beta - \beta_s) + \varphi_0 (T_s + \Gamma l) \frac{D}{Dt}(\alpha_f - \hat{\alpha})}{\tilde{\beta}_0} + \tag{D-11}$$

$$+ \frac{p_0}{\tilde{\beta}_0}\left\{ -\frac{D\hat{\beta}}{Dt} + 2(\beta - \beta_s)\frac{D}{Dt}\left[\left(\frac{1-2\nu}{1-\nu}\right)\left(\frac{\beta - \beta_s}{\beta}\right)\right]\right\}$$

The right-hand side of Eqn. (D-11) can be rearranged and simplified somewhat by using the following approximations:

$$\frac{D}{Dt}(\beta - \beta_s) \approx \frac{D\beta}{Dt}$$

$$\frac{D}{Dt}(\alpha_f - \hat{\alpha}) \approx \frac{D\alpha_f}{Dt}$$

$$\frac{D\hat{\beta}}{Dt} \approx \frac{D\beta}{Dt} + \varphi_0 \frac{D\beta_f}{Dt}$$

$$\frac{D}{Dt}\left[\left(\frac{1-2\nu}{1-\nu}\right)\left(\frac{\beta - \beta_s}{\beta}\right)\right] \approx \left(\frac{1-2\nu}{1-\nu}\right)\left(\frac{\beta_s}{\beta^2}\right)\frac{D\beta}{Dt} - \left(\frac{\beta - \beta_s}{\beta}\right)\left(\frac{1}{1-\nu}\right)^2 \frac{D\nu}{Dt}$$

These approximations allow us to rewrite Eqn. (D-11) as

$$\frac{Dp}{Dt} - \frac{Dp}{Dt}\Big|_{\substack{\text{constant}\\\text{moduli}}} = \frac{\hat{S}}{\tilde{\beta}_0} \tag{D-12}$$

where

$$\hat{S} = \left\{ \sigma_0 - p_0 \left[1 - 2(\beta - \beta_s)\left(\frac{1-2\nu}{1-\nu}\right)\left(\frac{\beta_s}{\beta^2}\right)\right]\right\}\frac{D\beta}{Dt} + \varphi_0 (T_s + \Gamma l)\frac{D\alpha_f}{Dt} -$$

$$- \varphi_0 p_0 \frac{D\beta_f}{Dt} - 2p_0(\beta - \beta_s)\left(\frac{\beta - \beta_s}{\beta}\right)\left(\frac{1}{1-\nu}\right)^2 \frac{D\nu}{Dt}$$

We now need to estimate the actual magnitudes of the terms comprising $\hat{S}$ to see how significant are the effects of time-dependent moduli on pore pressure. Using the estimated values of the various moduli given in Appendix C, the first term in the expression for $\hat{S}$ may be estimated as

$$\left\{\sigma_0 - p_0\left[1 - 2(\beta-\beta_s)\left(\frac{1-2\nu}{1-\nu}\right)\left(\frac{\beta_s}{\beta^2}\right)\right]\right\}\frac{D\beta}{Dt} \approx (\sigma_0 - \frac{2}{3}p_0)\frac{D\beta}{Dt}$$

The compressibility β might change by a factor of about two during uplift [cf. Brace, 1965; discussion in Bruner, 1979, p.5584]. The actual change in β, if due to microcracking, will probably occur over a relatively limited range of depths, perhaps *ca.* 1 km, beginning at a depth of less than *ca.* 3 km [Bruner, in press]. We therefore estimate

$$\frac{D\beta}{Dt} \approx 6\times10^{-26}\ \mathrm{Pa^{-1}\,s^{-1}} \qquad \text{for } V = 50\ \mathrm{m/Ma}$$

$$\approx 6\times10^{-25}\ \mathrm{Pa^{-1}\,s^{-1}} \qquad \text{for } V = 500\ \mathrm{m/Ma}$$

If we assume initially hydrostatic pressure, we may estimate $(\sigma_0 - 2p_0/3) < ca.\ 6\times10^7$ Pa for $L < ca.$ 3 km. Hence, we can finally estimate

$$(\sigma_0 - \frac{2}{3}p_0)\frac{D\beta}{Dt} < ca.\ 3.6\times10^{-18}\ \mathrm{s^{-1}} \qquad \text{for } V = 50\ \mathrm{m/Ma.}$$

$$< ca.\ 3.6\times10^{-17}\ \mathrm{s^{-1}} \qquad \text{for } V = 500\ \mathrm{m/Ma}$$

The second term on the right-hand side of Eqn. (D-12) describes the effect of changes in α_f on pore pressure. This term can be rewritten as

$$\varphi_0(T_s + \Gamma l)\frac{D\alpha_f}{Dt} \approx -\varphi_0(T_s + \Gamma l)\frac{\partial\alpha_f}{\partial T}\Gamma V$$

For T_s = 20° C, Γ = 15–30° C/km, $l < ca.$ 3 km, and estimating $\partial\alpha_f/\partial T$ from data in Schmidt [1969], we find for very low porosities ($\varphi \approx 0.01$):

$$\varphi_0(T_s + \Gamma l)\frac{\partial\alpha_f}{\partial T}\Gamma V \approx (1-2)\times10^{-19}\ \mathrm{s^{-1}} \qquad \text{for } V = 50\ \mathrm{m/Ma}$$

$$\approx (1-2)\times10^{-18}\ \mathrm{s^{-1}} \qquad \text{for } V = 500\ \mathrm{m/Ma}$$

and for moderate porosities ($\varphi \approx 0.10$):

$$\varphi_0 (T_s + \Gamma l) \frac{\partial \alpha_f}{\partial T} \Gamma V \approx (1-2) \times 10^{-18}\ \mathrm{s}^{-1} \qquad \text{for } V = 50\ \mathrm{m/Ma}$$

$$\approx (1-2) \times 10^{-17}\ \mathrm{s}^{-1} \qquad \text{for } V = 500\ \mathrm{m/Ma}$$

The third term, involving the rate of change of fluid compressibility, β_f, will depend in a complex way upon both p and T [cf. Schmidt, 1969]. We estimate for p_0 corresponding to a depth of 3 km, for low porosity rocks ($\varphi \approx 0.01$):

$$\varphi_0 p_0 \frac{D\beta_f}{Dt} \approx 2 \times 10^{-20}\ \mathrm{s}^{-1} \qquad \text{for } V = 50\ \mathrm{m/Ma}$$

$$\approx 2 \times 10^{-19}\ \mathrm{s}^{-1} \qquad \text{for } V = 500\ \mathrm{m/Ma}$$

and for moderate porosities ($\varphi \approx 0.10$):

$$\varphi_0 p_0 \frac{D\beta_f}{Dt} \approx 2 \times 10^{-19}\ \mathrm{s}^{-1} \qquad \text{for } V = 50\ \mathrm{m/Ma}$$

$$\approx 2 \times 10^{-18}\ \mathrm{s}^{-1} \qquad \text{for } V = 500\ \mathrm{m/Ma}$$

Finally, the last term can be estimated, using the parameter values in Appendix C, as

$$2 p_0 (\beta - \beta_s) \left(\frac{\beta - \beta_s}{\beta}\right) \left(\frac{1}{1-\nu}\right)^2 \frac{D\nu}{Dt} \approx (3.6 \times 10^{-11}\ \mathrm{Pa}^{-1})\, p_0 \frac{D\nu}{Dt}$$

Again taking p_0 corresponding to a depth of 3 km, and estimating that ν will not change by more than about 0.1 [cf. Birch, 1966; Walsh, 1965], we find

$$2 p_0 (\beta - \beta_s) \left(\frac{\beta - \beta_s}{\beta}\right) \left(\frac{1}{1-\nu}\right)^2 \frac{D\nu}{Dt} \approx 1.8 \times 10^{-19}\ \mathrm{s}^{-1} \qquad \text{for } V = 50\ \mathrm{m/Ma}$$

$$\approx 1.8 \times 10^{-18}\ \mathrm{s}^{-1} \qquad \text{for } V = 500\ \mathrm{m/Ma}$$

The rather lengthy numerical exercise above demonstrates that the major influence of 'crack growth' on pore pressure during uplift would come

about as a result of changes in β and α_f; the other terms are of minor importance in comparison. The term involving $D\beta/Dt$ should dominate for likely porosities and uplift rates.

Summing up the estimates above of the various terms comprising $\hat{S}$, and using the estimates for $\tilde{\beta}_0$ in Appendix C, we find for very low porosities ($\varphi \approx 0.01$):

$$\hat{S}/\tilde{\beta}_0 \approx 20\times10^{-8}\ \text{Pa/s} \qquad \text{for } V = 50\ \text{m/Ma}$$
$$\approx 200\times10^{-8}\ \text{Pa/s} \qquad \text{for } V = 50\text{–}500\ \text{m/Ma}$$

and for moderate porosities ($\varphi \approx 0.10$):

$$\hat{S}/\tilde{\beta}_0 \approx 5\times10^{-8}\ \text{Pa/s} \qquad \text{for } V = 50\ \text{m/Ma}$$
$$\approx 50\times10^{-8}\ \text{Pa/s} \qquad \text{for } V = 500\ \text{m/Ma}$$

Hence, the net effect of time-varying moduli should usually be to *increase* p during uplift. Physically, this is due to the increased compliance of the rock as a result of microcracking.

For the 'sealed' zone that we have been considering in our analysis, the total rate of change of pore pressure, following the motion, would be given by (cf. Eqns. (20) and (D-12)):

$$\frac{Dp}{Dt} = \frac{\hat{S} - S}{\tilde{\beta}_0} \tag{D-13}$$

Combining the estimates above for $\hat{S}/\tilde{\beta}_0$ with the estimates for $S/\tilde{\beta}_0$ (Appendix C), we find for $\varphi \approx 0.01$:

$$(\hat{S} - S)/\tilde{\beta}_0 \approx 15\times10^{-8}\ \text{Pa/s} \qquad \text{for } V = 50\ \text{m/Ma}$$
$$\approx 150\times10^{-8}\ \text{Pa/s} \qquad \text{for } V = 500\ \text{m/Ma}$$

and for $\varphi \approx 0.10$:

$$(\hat{S} - S)/\tilde{\beta}_0 \approx (-8 \rightarrow 1) \times 10^{-8}\ \text{Pa/s} \qquad \text{for } V = 50\ \text{m/Ma}$$
$$\approx (-80 \rightarrow 10) \times 10^{-8}\ \text{Pa/s} \qquad \text{for } V = 500\ \text{m/Ma}$$

These compare with the rate of change of pore pressure along a hydrostatic gradient (cf. Appendix C):

$$\frac{Dp}{Dt}\Big|_{\text{hydrostatic}} \approx -1.6 \times 10^{-8}\ \text{Pa/s} \qquad \text{for } V = 50\ \text{m/Ma}$$
$$\approx -16 \times 10^{-8}\ \text{Pa/s} \qquad \text{for } V = 500\ \text{m/Ma}$$

REFERENCES

Biot, M.A., General theory of three-dimensional consolidation, *Journal of Applied Physics*, *12*, 155-64, 1941.

Biot, M.A., Theory of propagation of elastic waves in a fluid-saturated porous solid. I. Low-frequency range, *Acoustical Society of America Journal*, *28*, 168-78, 1956.

Birch, F., Compressibility; elastic constants, in *Handbook of physical constants (Geological Society of America Memoir 97)*, edited by S.P. Clark, Jr., pp. 97-174, Geological Society of America, New York, 1966.

Blackwell, D.D., The thermal structure of the continental crust, in *The structure and physical properties of the Earth's crust (Geophysical Monograph 23)*, edited by J.G. Heacock, pp. 169-83, American Geophysical Union, Washington, D.C., 1971.

Boley, B.A., and J.H. Weiner, *Theory of thermal stresses*, John Wiley, New York, 1960.

Brace, W.F., Some new measurements of linear compressibility of rocks, *Journal of Geophysical Research*, *70*, 391-98, 1965.

Brace, W.F., and D.L. Kohlstedt, Limits on lithospheric stress imposed by laboratory experiments, *Journal of Geophysical Research*, *85*, 6248-52, 1980.

Bruner, W.M., Crack growth and the thermoelastic behavior of rocks, *Journal of Geophysical Research*, *84*, 5578-90, 1979.

Bruner, W.M., Crack growth during unroofing of crustal rocks: effects on thermoelastic behavior and near-surface stresses, *Journal of Geophysical Research*, in press.

Burst, J.F., Diagenesis of Gulf Coast clayey sediments and its possible relation to petroleum migration, *American Association of Petroleum Geologists Bulletin*, *53*, 73-93, 1969.

Carter, N.J., Steady state flow of rocks, *Reviews of Geophysics and Space Physics*, *14*, 301-60, 1976.

Clark, S.P., Jr., Thermal conductivity, in *Handbook of physical constants (Geological Society of America Memoir 97)*, edited by S.P. Clark, Jr., pp. 159-82, Geological Society of America, New York, 1966.

Cornet, F.H., and C. Fairhurst, Influence of pore pressure on the deformation behavior of saturated rocks, in *Advances in Rock Mechanics: Proceedings of the Third Congress of the International Society for Rock Mechanics*, vol. 1, part B, pp. 638-44, National Academy of Sciences, Washington, D.C., 1974.

Davis, D., J. Suppe, and F.A. Dahlen, Mechanics of fold-and-thrust belts and accretionary wedges, *Journal of Geophysical Research*, *88*, 1153-72, 1983.

Haxby, W.F., and D.L. Turcotte, Stresses induced by the addition or removal of overburden and associated thermal effects, *Geology*, *4*, 181-84, 1976.

Hubbert, M.K., and W.W. Rubey, Role of fluid pressure in mechanics of overthrust faulting. I: Mechanics of fluid-filled porous solids and its application to overthrust faulting, *Geological Society of America Bulletin*, *70*, 115-166, 1959.

Jaeger, J.C., and N.G.W. Cook, *Fundamentals of rock mechanics* (2nd edition), Chapman and Hall, London, pp. 223-25, 1976.

Karig, D.E., G.F. Moore, J.R. Curray, and M.B. Lawrence, Morphology and shallow structure of the lower trench slope off Nias Island, Sunda arc, in *The tectonic and geologic evolution of Southeast Asian seas and islands (Geophysical Monograph 23)*, edited by D.E. Hayes, pp. 179-208, American Geophysical Union, Washington, D.C., 1980.

Lawn, B.R., and T.R. Wilshaw, *Fracture of brittle solids*, Cambridge University Press, Cambridge, pp. 5-9, 46-51, 1975.

McGarr, A., and N.C. Gay, State of stress in the Earth's crust, *Annual Reviews of Earth and Planetary Science*, *6*, 405-36, 1978.

McKenzie, D.P. 1978. Some remarks on the development of sedimentary basins. *Earth and Planetary Science Letters*, *40*, 25-32.

Malvern. L.E., *Introduction to the mechanics of a continuous medium*, Prentice-Hall Inc., Englewood Cliffs, New Jersey, pp. 143-45, 1969.

Narr, W., and J.B. Currie, Origin of fracture porosity: example from Altamont field, Utah, *American Association of Petroleum Geologists Bulletin*, *66*, 1231-47, 1982.

Nur, A., and J.D. Byerlee, An exact effective stress law for elastic deformation of rock with fluids, *Journal of Geophysical Research*, *76*, 8444-49, 1971.

Nur, A., and G. Simmons, The origin of small cracks in igneous rocks, *International Journal of Rock Mechanics and Mining Sciences & Geomechanics Abstracts*, *7*, 307-14, 1970.

Plona, T.J., Observation of a second bulk compressional wave in a porous medium at ultrasonic frequencies, *Applied Physics Letters*, *36*, 259-61, 1980.

Powers, M.C., Fluid-release mechanisms in compacting marine mudrocks and their importance in oil exploration, *American Association of Petroleum Geologists Bulletin*, *51*, 1240-54, 1967.

Price, N.J., *Fault and joint development in brittle and semi-brittle rock*, Pergamon Press, Oxford, pp. 130-41, 1966.

Rice, J.R., and M.P. Cleary, Some basic stress diffusion solutions for fluid-saturated elastic porous media with compressible constituents, *Reviews of Geophysics and Space Physics*, *14*, 227-41, 1976.

Richter, D., and G. Simmons, Thermal expansion behavior of igneous rocks, *International Journal of Rock Mechanics and Mining Sciences & Geomechanics Abstracts*, *11*, 403-11, 1974.

Rubey, W.W., and M.K. Hubbert, Role of fluid pressure in mechanics of overthrust faulting. II: Overthrust belt in geosynclinal area of western Wyoming in light of fluid-pressure hypothesis, *Geological Society of America Bulletin*, *70*, 167-206, 1959.

Ruina, A.L., Influence of coupled deformation-diffusion effects on the retardation of hydraulic fracture, *Porous Media Series Report, No. 15*, Division of Engineering, Brown University, Providence, Rhode Island, 1978.

Russell, W.L., Pressure-depth relations in Appalachian region, *American Association of Petroleum Geologists Bulletin*, *56*, 528-36, 1972.

Schmidt, E. (ed.), *Properties of water and steam in SI-units*, Springer-Verlag, Berlin, pp. 34-145, 1969.

Secor, D.T., Jr., Role of fluid pressure in jointing, *American Journal of Science*, *263*, 633-46, 1965.

Sissom, L.E., and D.R. Pitts, *Elements of transport phenomena*, McGraw-Hill Book Company, New York, pp. 754-55, 1972.

Skempton, A.W., The consolidation of clays by gravitational compaction, *Geological Society of London Journal*, *125*, 371-433, 1970.

Smith, J.E., The dynamics of shale compaction and evolution of pore-fluid pressures, *International Association for Mathematical Geology Journal*, *3*, 239-63, 1971.

Voight, B., and B.H.P. St. Pierre, Stress history and rock stress, in *Advances in Rock Mechanics: Proceedings of the Third Congress of the International Society for Rock Mechanics*, vol. 2, part A, pp. 580-82, National Academy of Sciences, Washington, D.C., 1974.

von Huene, R., and H. Lee, The possible significance of pore fluid pressure in subduction zones, in *Studies in continental margin geology (American Association of Petroleum Geologists Memoir 34)*, edited by J.S. Watkins and C.L. Drake, pp. 781-91, American Association of Petroleum Geologists, Tulsa, Oklahoma, 1983.

Walsh, J.B., The effect of cracks in rock on Poisson's ratio, *Journal of Geophysical Research*, *70*, 5249-58, 1965.

NOTATION

$\hat{C}_f$ specific heat of pore fluid

$\hat{C}_m$ specific heat of sediment

$\hat{C}_s$ specific heat of grains

E Young's modulus

$\dot{E}_h$ compressive lateral strain rate

g acceleration due to gravity

G shear modulus

H poroelastic modulus

k permeability

k_c critical permeability for overpressure buildup

k_m thermal conductivity of sediment

K bulk modulus

K_s bulk modulus of grains

L characteristic length scale

m fluid mass fraction relative to reference state

M function related to effect of time-varying moduli on lateral stress

p pore pressure

p_c confining pressure

p' dimensionless pore pressure

R poroelastic modulus

R_e radius of the Earth

s_h lateral stress, positive when tensile

S parameter related to pore-pressure history during uplift

t time

t_c critical time for pore pressure to reach lithostatic

t' dimensionless time

T temperature

u_f volumetric flux of pore fluid

u_s average grain velocity

v fluid volume fraction relative to reference state

v_0 initial value of v

V uplift rate

z vertical coordinate, increasing downwards

z' dimensionless vertical coordinate

α coefficient of linear thermal expansion of rock

α_f thermal expansivity of pore fluid

$\hat{\alpha}$ coefficient of volumetric thermal expansion of rock

$\beta = 1/K$ compressibility

β_f fluid compressibility

β_s grain compressibility

$\tilde{\beta}, \hat{\beta}$ compressibility terms

γ coefficient relating fluid volume fraction to temperature changes

Γ magnitude of geothermal gradient

δ_{ij} Kronecker delta

ε_h lateral strain rate, posotive for tension

ε_{ij} strain

κ_m thermal diffusivity of sediment

μ viscosity of pore fluid

ν Poisson's ratio

$\pi_1, \pi_2, \pi_3, \pi_4$ coefficients in expression for $M(t)$

ρ_f pore-fluid density

ρ_m sediment density

ρ_s grain density

$\bar{\rho}$ average density of overburden

$\tilde{\rho}\tilde{C}$ parameter related to specific heats

σ_h, σ_v lateral and vertical stresses, respectively

σ_{ij} stresses, positive when tensile

$\bar{\sigma}$ mean stress

τ characteristic time scale

τ_d time scale for diffusive relaxation of overpressures

τ_e time scale for poroelastic effect on pore pressure to become significant

τ_u time scale for uplift

φ_0 initial porosity

CHAPTER 6
PERMEABILITY MEASUREMENT BY THE PULSE-DECAY METHOD: EFFECTS OF POROELASTIC PHENOMENA AND NONLINEAR PORE-PRESSURE DIFFUSION

ABSTRACT

Permeability values inferred from data obtained by the pulse-decay, or transient pulse method, may be affected by two phenomena not previously considered as important: poroelastic coupling between sample cores and pore fluid, and nonlinear pore-pressure diffusion associated with large pore-pressure gradients. We discuss the theoretical reasons for these complications, as well as the results of two simple experiments designed to test the theory. Poroelastic effects introduce an inherent sample-size dependence into the transient-pulse method; experiments show such a dependence, but possibly masked by slight material inhomogeneity. Nonlinear pore-pressure diffusion limits the size of the pore-pressure pulse that may be used in the pulse-decay scheme; this is well-demonstrated by experimental results. Furthermore, direct measurements of poroelastic strains associated with pulse propagation show very good agreement with predictions of linear poroelasticity theory.

1. INTRODUCTION

The pulse-decay, or transient pulse method of permeability measurement has been frequently used to investigate the fluid-transport properties of low permeability rocks. Originated by Brace et al. [1968], the pulse-decay method since has been used by many investigators, including Zoback and Byerlee [1975], Trimmer et al. [1980], and Walls [1982]. In this chapter, we discuss results of two simple experiments that examine factors that could potentially

complicate the interpretation of pulse-decay measurements. In section 2, we discuss transient pulse measurements in the context of poroelasticity [Biot, 1941; Rice and Cleary, 1976], considering the way that mechanical coupling between solid and pore fluid may influence inferred permeability values. In particular, theory suggests that there should be an inherent sample-size dependence in the interpretation of pulse-decay data. Results of a simple experiment designed to examine this prediction are then described.

We then turn in section 3 to considerations of nonlinear pore-pressure diffusion. Theoretical considerations show that the pulse-decay method might become invalid if pulses of a 'large' magnitude are utilized. Experimental results supporting this prediction are then described, along with direct measurements of the poroelastic strain accompanying pressure-pulse propagation. The latter are in very good agreement with predictions of the linearized Biot poroelastic formulation. Finally, in section 4, we apply our results to suggest experimental guidelines that should help avert complications due to poroelastic- and nonlinear pressure-diffusion phenomena.

2. POROELASTIC PHENOMENA IN PULSE-DECAY PERMEABILITY MEASUREMENTS

Theoretical Framework

We briefly review here the poroelastic formalism developed by Biot [1941] and extended by Rice and Cleary [1976]. The fundamental assumption in this formalism is that strains ε_{ij} in the solid frame, as well as changes in the fluid mass fraction m, are linear functions of changes in the stresses σ_{ij} and pore pressure p, viz.:

$$2G\, d\varepsilon_{ij} = d\sigma_{ij} - \left(\frac{\nu}{1+\nu}\right) d\sigma_{kk}\, \delta_{ij} + \frac{3(\nu_u - \nu)}{B(1+\nu)(1+\nu_u)} dp\, \delta_{ij} \qquad (1a)$$

$$dm = \frac{3\rho_f(\nu_u - \nu)}{2GB(1+\nu)(1+\nu_u)}\left(d\sigma_{kk} + \frac{3}{B}dp\right) \tag{1b}$$

where G (shear modulus) and ν (Poisson's ratio) are the usual elastic moduli; B, sometimes known as 'Skempton's coefficient' [cf. Skempton, 1954], and ν_u, the 'undrained Poisson's ratio', are the poroelastic moduli as given by Rice and Cleary [1976] in their reformulation of Biot's [1941] original work. We have used here the summation convention for repeated subscripts. The Kronecker delta, δ_{ij}, has the usual definition:

$$\delta_{ij} = 1, \quad i = j$$
$$\delta_{ij} = 0, \quad i \neq j$$

Rice and Cleary [1976, p.228-29] have shown that, in general, pore pressure cannot be decoupled from the stress state, greatly complicating the mathematical analysis of boundary-value problems involving poroelastic materials. In contrast, in the usual development of the governing diffusion-type equation for pore pressure in porous rocks [e.g., Brace et al., 1968, pp. 2234-35]—that is, in the sort of analysis applied to laboratory permeability measurements--poroelastic coupling is not considered at all. As we show next, poroelastic coupling will generally introduce an inherent sample-size dependence into permeability testing by the pulse-decay method.

In the pulse-decay technique (Fig. 6-1), a small differential pore pressure, Δp, is abruptly applied across the length of a cylindrical core of rock at confining pressure p_c and pore pressure p. (In other words, the pore pressure at one end surface of the core is suddenly changes to $p \pm \Delta p$.) The resultant pore-pressure differential as a function of time, $\Delta p(t)$, is then analyzed to determine permeability [e.g., Brace et al., 1968; Zoback and Byerlee, 1975?; Walls, 1982]. Within the framework of poroelastic theory, we expect that the

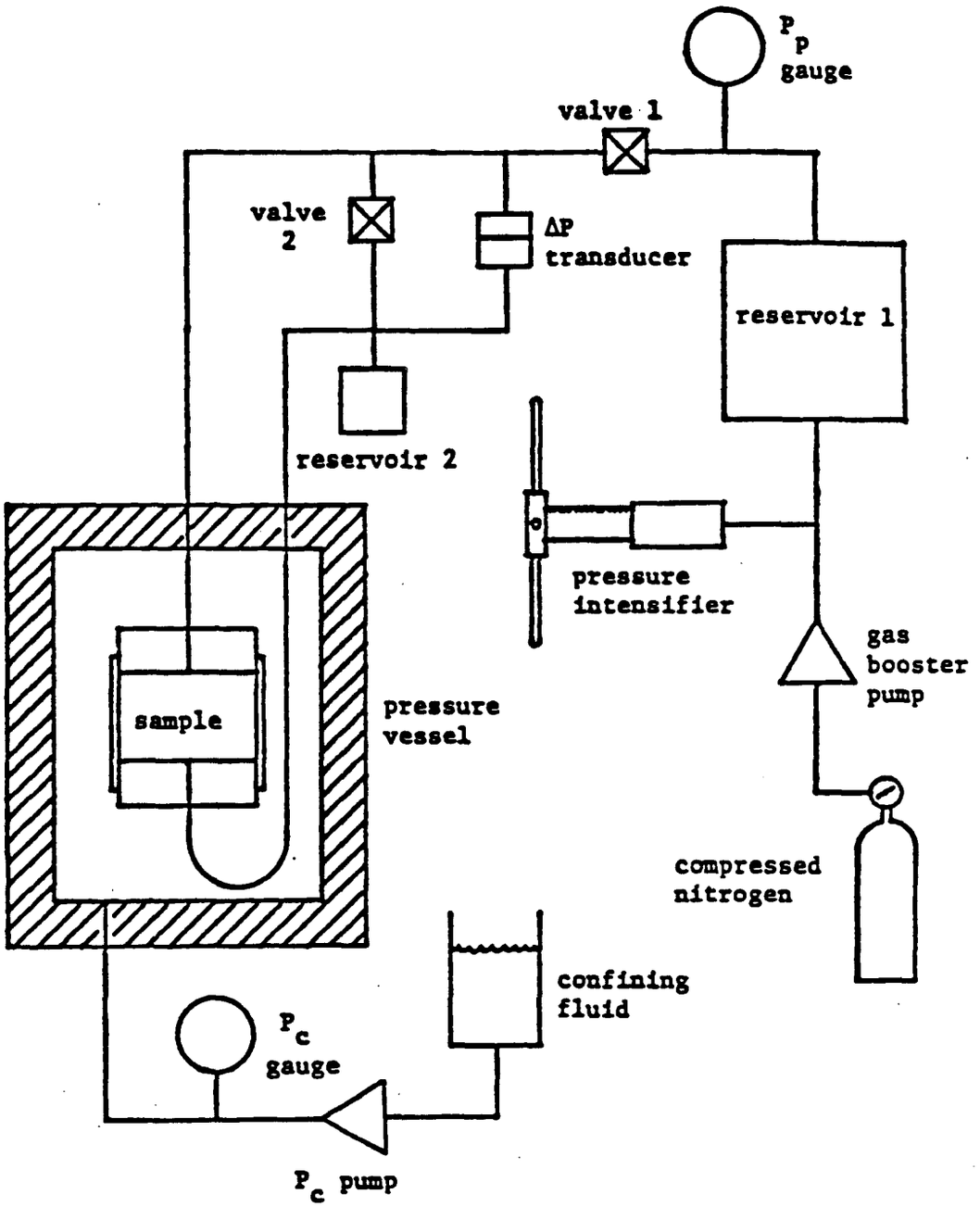

Figure 6-1: Schematic diagram of experimental system for pulse-decay measurements (from Walls [1982], by permission of the author). Initially, both valves are open. After closing valve 1, pore pressure is changed slightly in the (large) reservoir 1. After waiting for thermal equilibrium, valve 2 is closed and valve 1 is opened, applying a small differential pore pressure Δp along the sample. This differential pressure is recorded as a function of time.

pressure-pulse decay will be accompanied by time-dependent elastic strain of the core.

Following a suggestion by J. Rice [written communication, 1981], we consider pore-pressure pulses applied to two samples of different lengths, cored from the same homogeneous block of rock, and held at the same ambient conditions (Fig. 6-2). In the short core (length small in comparison with radius), the approximations of classical consolidation theory apply [Biot, 1941, pp. 160-64]; i.e., the core will be in a state of uniaxial strain ($d\varepsilon_{zz} \neq 0$, $d\varepsilon_{rr} = d\varepsilon_{\theta\theta} = 0$, where r, θ, and z are the usual radial, circumferential, and axial coordinates for a cylindrical coordinate system, respectively). In contrast, for the long sample (length large in comparison with radius), a state approximating uniaxial *stress* will be set up (all $d\sigma_{ij}$ except possibly $d\sigma_{zz}$ must vanish). Proceeding as in Rice and Cleary [1976, pp. 228-29], it can be shown that pore pressure is governed by a diffusion-type equation for both the uniaxial strain and uniaxial stress cases, viz.:

$$\frac{\partial^2 p}{\partial z^2} = \frac{1}{c}\left(\frac{\partial p}{\partial t} + \frac{B}{3}\frac{\partial \sigma_{zz}}{\partial t}\right) \tag{2}$$

where c is the hydraulic diffusivity. For the two cases considered here, we have

$$c_{short} = \frac{k}{\mu}\left[\frac{2GB^2(1-\nu)(1+\nu_u)^2}{9(1-\nu_u)(\nu_u-\nu)}\right] \tag{3a}$$

$$c_{long} = \frac{k}{\mu}\left[\frac{2GB^2(1+\nu)(1+\nu_u)}{9(\nu_u-\nu)}\right] \tag{3b}$$

where k is permeability and μ is viscosity. (The expression for c_{short} is equivalent to the hydraulic diffusivity as usually defined [e.g., Brace et al., 1968; Trimmer et al., 1980].)

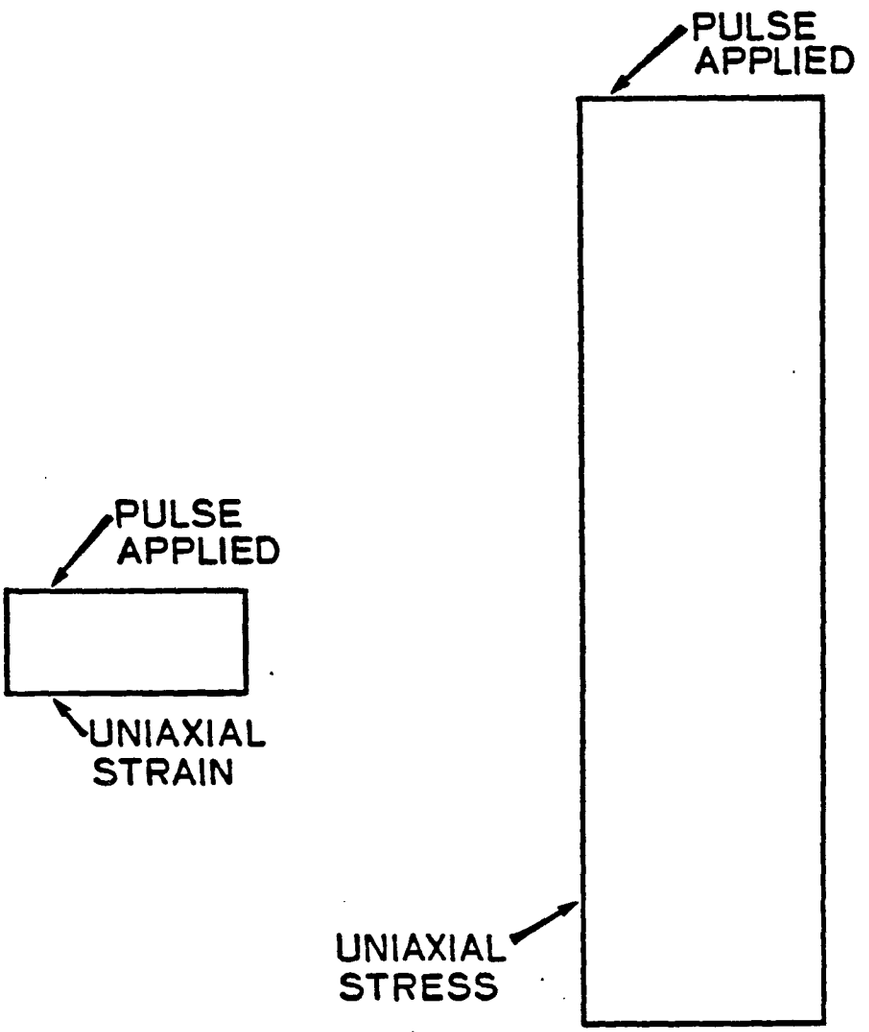

Figure 6-2: Pulse-decay tests on two samples, one short compared to its radius, the other long, will be affected by poroelastic coupling.

The stress σ_{zz} in Eqn. (2) may be interpreted as the total axial force per unit area applied to the core. In a pulse-decay experiment, application of the pore-pressure differential does not change σ_{zz}, which is constrained by considerations of mechanical equilibrium to be equal to p_c (although the detailed stress distribution near the sample holders may be altered); hence, the term in Eqn. (2) involving $\partial\sigma_{zz}/\partial t$ will vanish, leaving a simple diffusion equation for p.

In the general case of arbitrary sample length, stress components other than σ_{zz} may enter the analysis, precluding the decoupling of p from the stress field. For the 'short' and 'long' samples, however, p may be effectively decoupled from the stress field. We see, however, that the effective hydraulic diffusivities are different for these two extreme cases. From Eqns. (3a) and (3b), we find

$$\frac{c_{short}}{c_{long}} = \left(\frac{1+\nu_u}{1+\nu}\right)\left(\frac{1-\nu}{1-\nu_u}\right) \tag{4}$$

Noting that $\nu_u \geq \nu$ [Rice and Cleary, 1976, p.229], it is clear that $c_{short} \geq c_{long}$. Using parameter values estimated by Rice and Cleary [1976, p. 240], it appears that c_{short}/c_{long} may be as much as ca. 1.5 for some rocks.

Another way of interpreting the sample-size dependence of c comes from defining an overall compressibility $\hat{\beta}$ by the relationship

$$c = \frac{k}{\mu\hat{\beta}} \tag{5}$$

The permeability k and viscosity μ are intrinsic material properties, independent of sample size (for a homogeneous rock), whereas the compressibility $\hat{\beta}$ depends upon both intrinsic material properties (G, ν, B, and ν_u) and, in some complicated fashion, upon sample dimensions, with

$\hat{\beta}_{short} < \hat{\beta}_{long}$.

Sample-size dependence of the hydraulic diffusivity could be important in interpreting pulse-decay test results to give permeability values. For example, in the method developed by Walls [1982], a value of c is determined that gives the best fit of an analytical expression for $\Delta p(t)$ to the actual Δp *vs.* t data; the corresponding value of k is then calculated by using an expression such as Eqn. (5). If one assumes $\hat{\beta}$ = constant, independent of sample size (as in Walls [1982]), then the inferred values of k (equal to $\mu\hat{\beta}c$) for various-sized samples of a homogeneous rock would vary.

Experimental test of sample-size dependence

We conducted pulse-decay tests using the apparatus build by Walls [1982]. Several 5.1 cm diameter cores, of various lengths, were taken from a 30 cm long piece of drill core supplied by Canadian Hunter Exploration Ltd. All cores had their end faces ground flat and parallel to within 0.05 mm. The rock is a low-permeability, gas-bearing sandstone from the Spirit River member of the Fahler formation of Alberta, Canada. The samples used in our tests had a porosity of 0.07. Pertinent mineralogical information for similar Spirit River core samples is given by Walls [1982].

Pulse-decay tests were all conducted with an ambient pore pressure (applied by N_2 gas) of 140 bars, approximately equal to the *in situ* pore pressure at the depth from which the core was recovered [Walls, 1982], and at confining pressures of 240 bars or greater. The confining pressure was increased in steps of 50 bars, after first cycling the core to a confining pressure of approximately 700 bars. A minimum of three runs were performed at each confining pressure value, allowing sufficient time between runs (and after changes in p_c) for thermal equilibrium to be attained. The pulse

magnitude used was consistently 1 bar, for which flow should be quite well described by Darcy's law [cf. Walls, 1982]. Permeability values were calculated from the pressure decay data using a slightly modified form (Appendix A) of the analysis presented by Walls [1982], taking $\hat{\beta}$ as a constant. (Specifically, we assumed $\hat{\beta} = \varphi\beta_f$, where φ is porosity and β_f is fluid compressibility. This approximation is commonly used in the oil industry [ref] and elsewhere [e.g., Brace, 1980].) In other words, we effectively calculate k by using the relationship

$$k = \mu\varphi\beta_f c \tag{6}$$

If the cores were identical in their physical properties, then the apparent k values determined by this method should vary from core to core, for a given p_c value, with the apparent k values greater for 'short' cores than for 'long' ones, due to the dependence of c on sample size (cf. Eqns. (3a) and (3b)).

Results of these measurements are shown in Fig. 6-3, in which we have plotted k *vs.* effective pressure p_e ($=p_c - p$). Permeabilities are accurate to about 5%. We see that the apparent permeabilities for a given effective pressure vary from core to core, with the ratio between the greatest values (for the 47.6 mm long core) and the least values (for the 21.7 mm long core) being roughly 1.5. There is not any simple relationship between core length and permeability, however; in fact, the smallest apparent k values were found with the shortest core, a result opposite to the prediction from poroelasticity considerations. This could very likely be due to slight variability in the physical properties (e.g., porosity, pore geometry, grain geometry) between cores. Interestingly, however, the k *vs.* P_e trends are very similar from core to core.

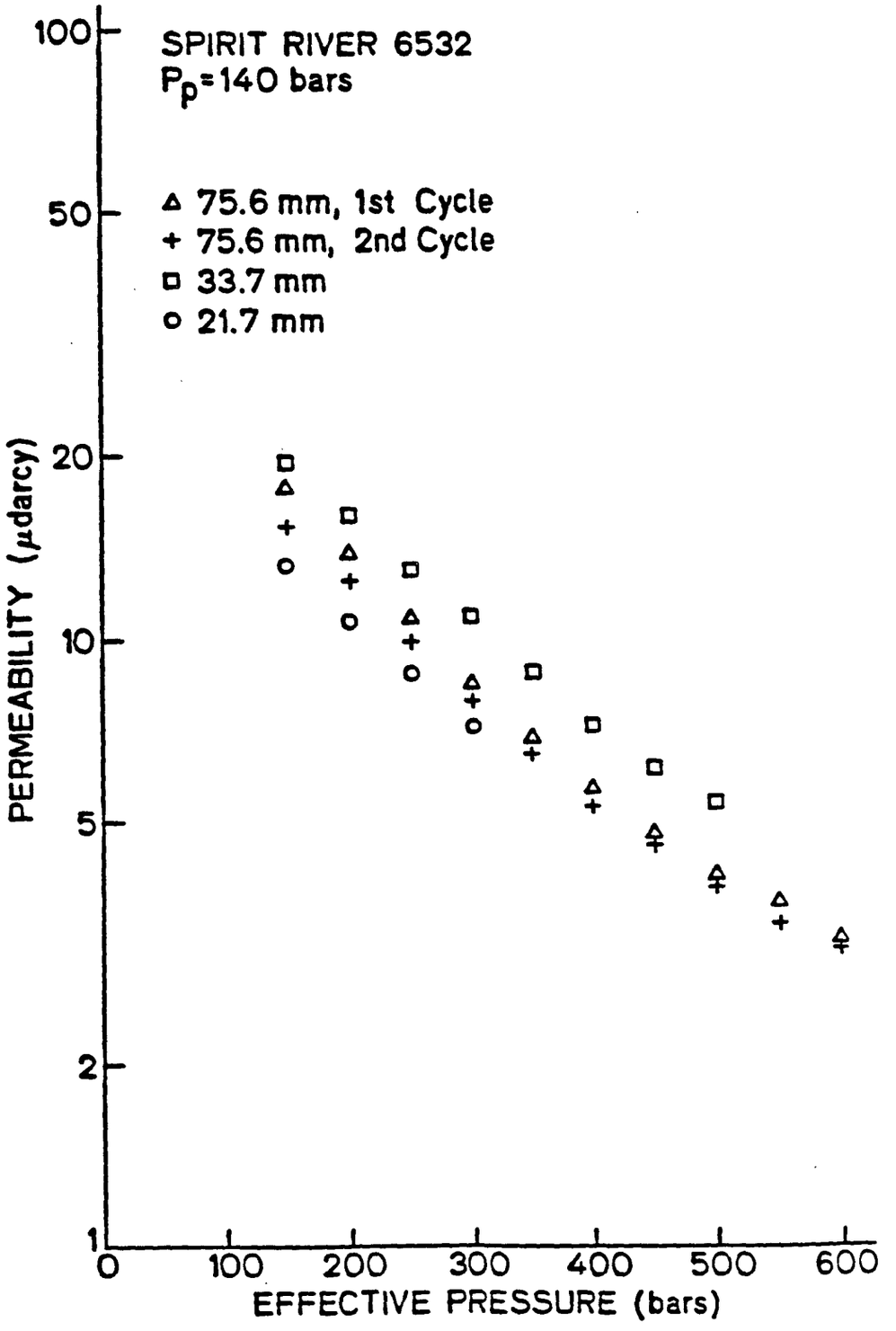

Figure 6-3: Measured permeability values as a function of effective pressure for Spirit River sandstone cores of various lengths.

These measurements clearly suggest that sample size may have an influence on the apparent permeability of a rock core. We cannot state definitely, however, that this sample-size dependence is due to poroelastic effects rather than simply to slight variability in material properties from core to core. The magnitude of the scatter in apparent permeability at a given p_c value, although large on a relative basis (about 50%), is small on an absolute basis (a few μdarcy), and not of major importance in evaluating *in situ* properties of this hydrocarbon-reservoir rock.

The close similarity of k *vs.* p_c trends for the various length cores is quite striking. One possible interpretation of this phenomenon is that the mechanical properties of the sandstone cores--that is, the 'stiffness' of the cores, as reflected in the way that pores close under increasing confining pressure--were very uniform from core to core.

3. NONLINEAR PHENOMENA IN PORE-PRESSURE DIFFUSION

Theoretical Background

In the theoretical development leading to the partial differential equation for pore pressure (Eqn. 2), we assumed that Darcy's law holds, i.e., that the flow rate is everywhere proportional to the local pore-pressure gradient:

$$\vec{q} = -\frac{k}{\mu}\nabla p \tag{7}$$

where $\vec{q}$ is the volumetric flow rate. We have also neglected the dependence of k upon the local pore pressure. When these approximations hold, the results of a pulse-decay test are independent of the magnitude of Δp. This is easily seen by recasting Eqn. (2) into dimensionless form, using the scalings

$$p = \Delta p\, p'$$

$$z = L z'$$
$$t = \tau t'$$

where L is the sample length and dimensionless variables are denoted by tildes. Choosing the characteristic time $\tau = L^2/c$, we therefore can write (neglecting, once again, the term involving $\partial \sigma_{zz}/\partial t$):

$$\frac{\partial^2 p'}{\partial z'^2} = \frac{\partial p'}{\partial t'} \tag{8}$$

The characteristic time $\tau = L^2/c$, a measure of the time for the pressure pulse to decay by some specific fraction (say, to 1/e of the original value) is quite independent of Δp. The pulse-decay test is therefore 'self-similar'. Walls [1982] has verified this experimentally with the Spirit River sandstone, showing that inferred k values are independent of Δp in the range *ca.* 0.25-4 bars.

If Δp were large enough that either Darcy's law became invalid, or that the variability of k with p became important, the linearity and self-similarity properties of Eqns. (2) and (8) would break down. This is most readily illustrated by considering the case in which Darcy's law remains valid, but the variability of k with p becomes important. The governing equation for p then becomes [Nur and Yilmaz, 1978]

$$\frac{\partial^2 p}{\partial z^2} + \beta_k \left(\frac{\partial p}{\partial z}\right)^2 = \frac{\partial p}{\partial t} \tag{9}$$

where $\beta_k = (1/k)\,\partial k/\partial p$ is a coefficient describing the dependence of k upon p. Measurements by Walls [1982] suggest that for the Spirit River sandstone, β_k is of the same order as $\tilde{\beta}_k = (1/k)\,\partial k/\partial p_c$, which in our measurements (Fig. 6-3) is nearly constant as p_c varies.

Recasting Eqn. (9) into dimensionless form, we find

$$\frac{\partial^2 p'}{\partial z'^2} + (\beta_k \Delta p)\left(\frac{\partial p'}{\partial z'}\right)^2 = \left(\frac{L^2}{c\tau}\right)\frac{\partial p'}{\partial t'} \tag{10}$$

The presence of the nonlinear term in Eqn. (10) destroys the self-similarity property of the pulse-decay experiments. Let us make the reasonable assumption that $\tau = L^2 / cf(\Delta p)$, where $f(\Delta p)$ is some dimensionless function of Δp, constrained by the condition that $f(\Delta p) \to 1$ as $\Delta p \to 0$. We can then rewrite Eqn. (10) as

$$\frac{\partial^2 p'}{\partial x'^2} + (\beta_k \Delta p)\left(\frac{\partial p'}{\partial x'}\right)^2 = f(\Delta p)\frac{\partial p'}{\partial t'} \tag{11}$$

Pore pressure diffusion in the pulse-decay test is now clearly seen to be an explicit function of Δp.

Experimental test

In order to examine pulse-test conditions that might give rise to the nonlinearity discussed above, and also to directly measure poroelastic strains during a pulse decay, we conducted a series of pulse-decay tests on a second set of Spirit River sandstone samples, using an apparatus similar to that used in the previous experiment, but with 1.9 cm diameter cores, which were jacketed with 0.25 mm thick copper tubes on which foil strain gages (6.3 mm gage length) were bonded. Confining pressure and pore pressure (the latter applied by N_2 gas) were independently controlled. In this series of tests, we were primarily concerned with measuring $\Delta p(t)$ and the associated poroelastic strains as a function of time at several positions along the core. No permeability calculations were made.

The differential pore pressure transducer and the strain gages were interfaced to a Hewlett-Packard 85 minicomputer via a Hewlett-Packard 3497A data acquisition and control unit. Pressure pulses were applied by manually opening a valve; data collection was then done automatically. Computer programs were written to convert measured voltages to differential pore

pressure and strain; results were then stored on tape, and could later be plotted using the minicomputer's internal printer.

A consistent problem encountered in this experiment was 'noise' in the strain measurements. This appears to have been due to at least two causes in addition to random noise: imperfect bonding of gages to the copper jackets, and electronic switching between gage channels. The magnitude of the noise was sometimes a significant fraction of the poroelastic strain signal, particularly for relatively small values of Δp.

Because p during a pulse test varies along the length of a core, we expected that strain as a function of time would vary along the core. Although we tried mounting gages at several positions along the test cores, the noise level was generally such that we were unable to resolve any systematic difference in the strain signals at different positions.

Typical results of a pulse test are illustrated by Figs. 6-4a, 6-4b, and 6-4c, for a Δp value of 15 bars. The core for this particular test was 14.2 cm long. The indicated strain readings were gotten by averaging the signals from two gages mounted 180° apart, at the same axial position along the core (Fig. 6-5).

The importance of nonlinear phenomena in pressure-pulse propagation was tested by recording $\Delta p(t)$ for a variety of pulse magnitudes, digitizing the plotted records, and finally normalizing the results (i.e., dividing all Δp values by the pulse magnitude). In the absence of nonlinearities, the normalized plots of Δp *vs.* t should superpose. In Fig. 6-6, we show results obtained using the 14.2 cm long core, with p_c = 150 bars. Pore pressure was varied between 50 bars and 50 bars - Δp (e.g., for Δp = 5 bars, we ran tests with p = 50 bars and a 'negative' pulse, and also tests with p = 45 bars and a 'positive' pulse). Four runs were performed for each Δp to assure repeatability.

Figure 6-4: Typical results of a pulse test.

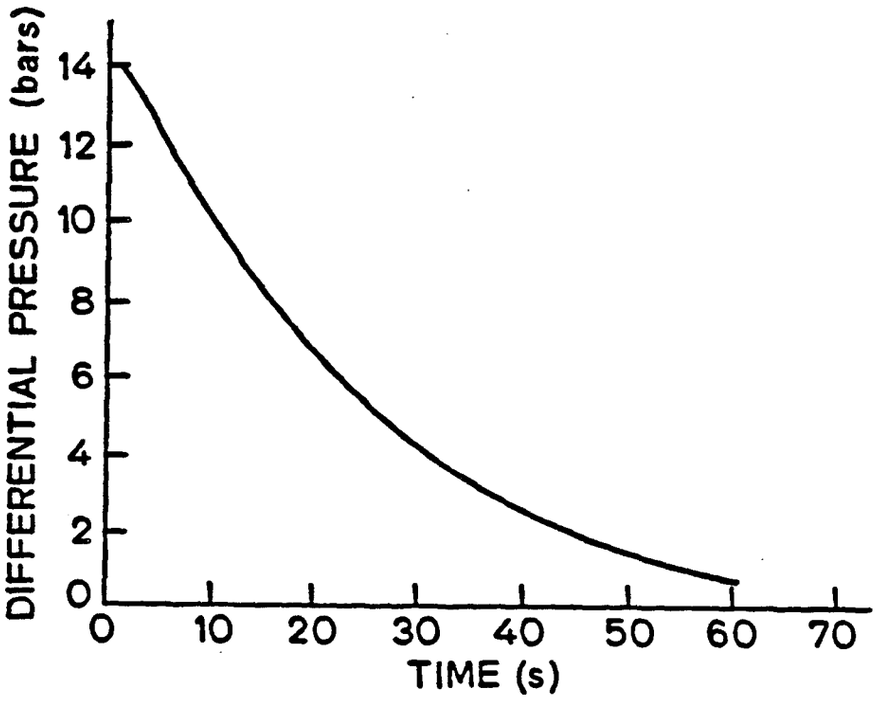

Figure 6-4a: Differential pore pressure *vs.* time.

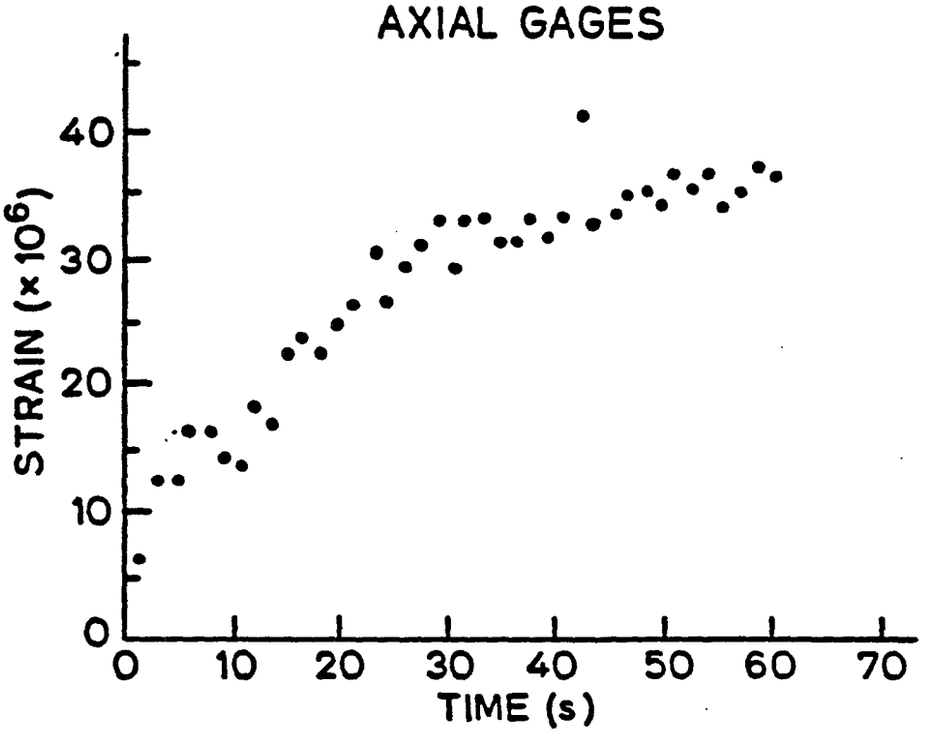

Figure 6-4b: Strain in axial gages.

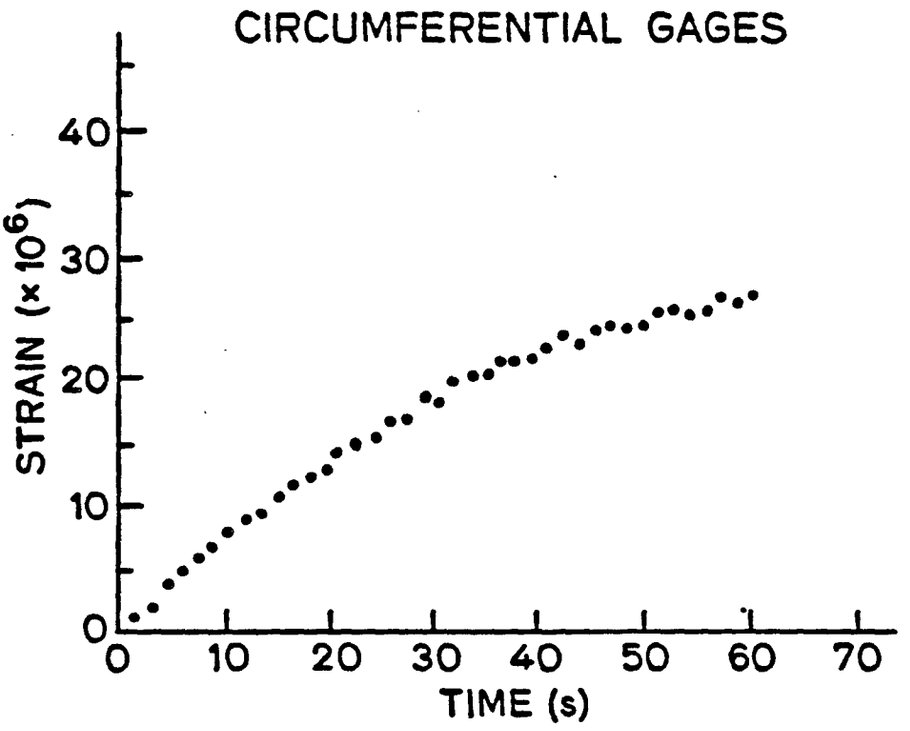

Figure 6-4c: Strain in circumferential gages.

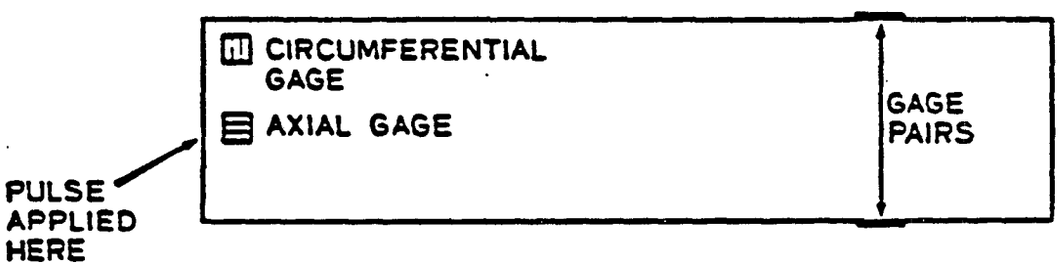

Figure 6-5: Strain-gage configuration during pulse tests.

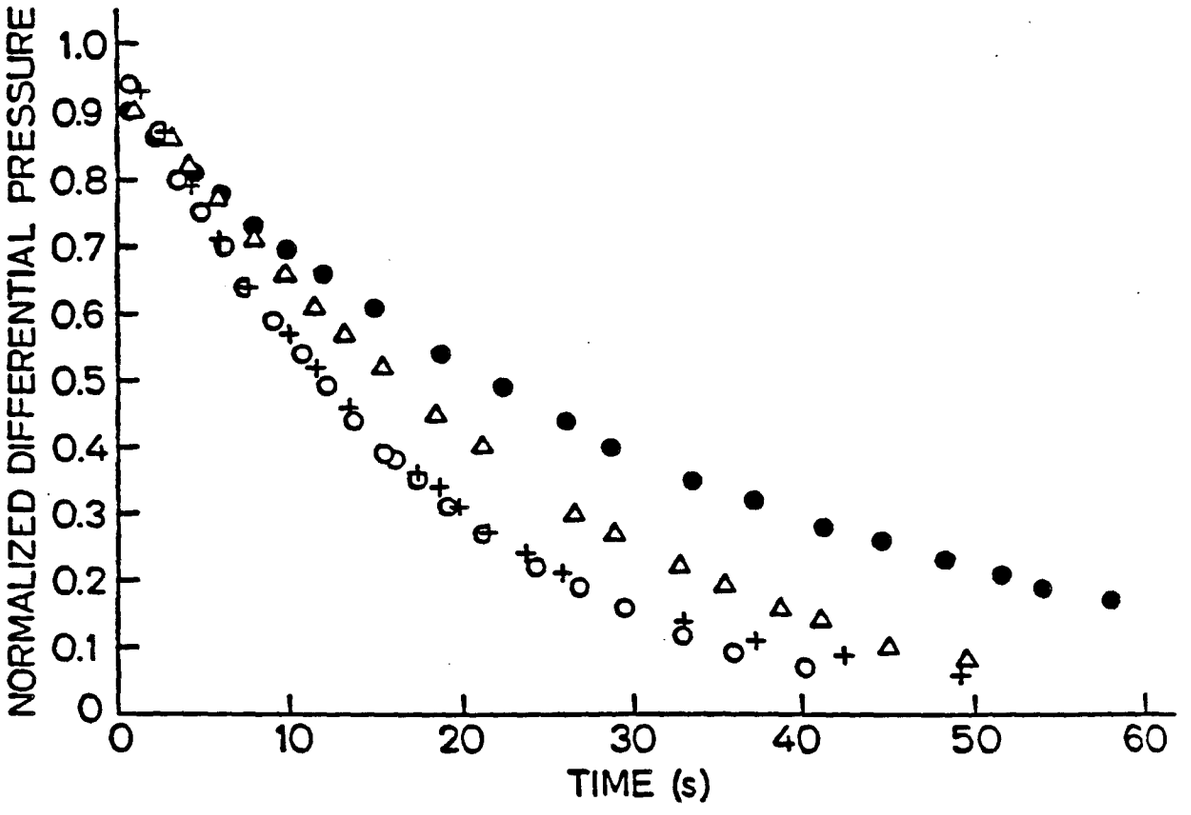

Figure 6-6: Normalized pore-pressure *vs.* time records for pulses of various magnitudes. Nonlinear effects are apparent for Δp larger than about 5 bars.

We see from Fig. 6-6 that the normalized records for $\Delta p = 1.5$ bars and 5 bars match quite well. Normalized results for $\Delta p = 3$ bars, not plotted in Fig. 6-6 to avoid unnecessary clutter, also match these two records. In contrast, the normalized pressure decays for $\Delta p =$ 15 bars and 25 bars diverge strongly from the lower-pressure results.

In Fig. 6-7, we have plotted the 'decay time' for these tests as a function of Δp, where the decay time is defined here as the time at which $\Delta p(t)$ has fallen to 40% of its original value. This figure emphasizes that the nonlinearity has a negligible effect for Δp less than about 5 bars (10% of the 'total' pore pressure), but becomes increasingly important at larger Δp values.

Fig. 6-8 shows strains measured on circumferential gages (the least noisy gages) on the same 14.2 cm long core, as a function of pulse magnitude, with each point the average of four runs. The accuracy of these strain data is about $1-1.5\times10^{-6}$. The strains plotted here correspond to values at times for which the differential pore pressure had essentially vanished. For the 15 bar and 25 bar pulses, the decays were terminated somewhat before the differential pressure had completely dissipated (strains indicated in Fig. 6-8 by circles). We extrapolated these results by assuming that the strain due to the remaining few bars of differential pressure, Δp_r, would simply be the same as for a pulse of magnitude Δp_r.

The data show a quite linear relationship between strain and pulse magnitude. This is in accord with predictions of poroelasticity theory, and indicates that assuming a linear dependence of strain on pore pressure is quite adequate, even for relatively large (50%) fractional changes in pore pressure, at least at the conditions of our experiment.

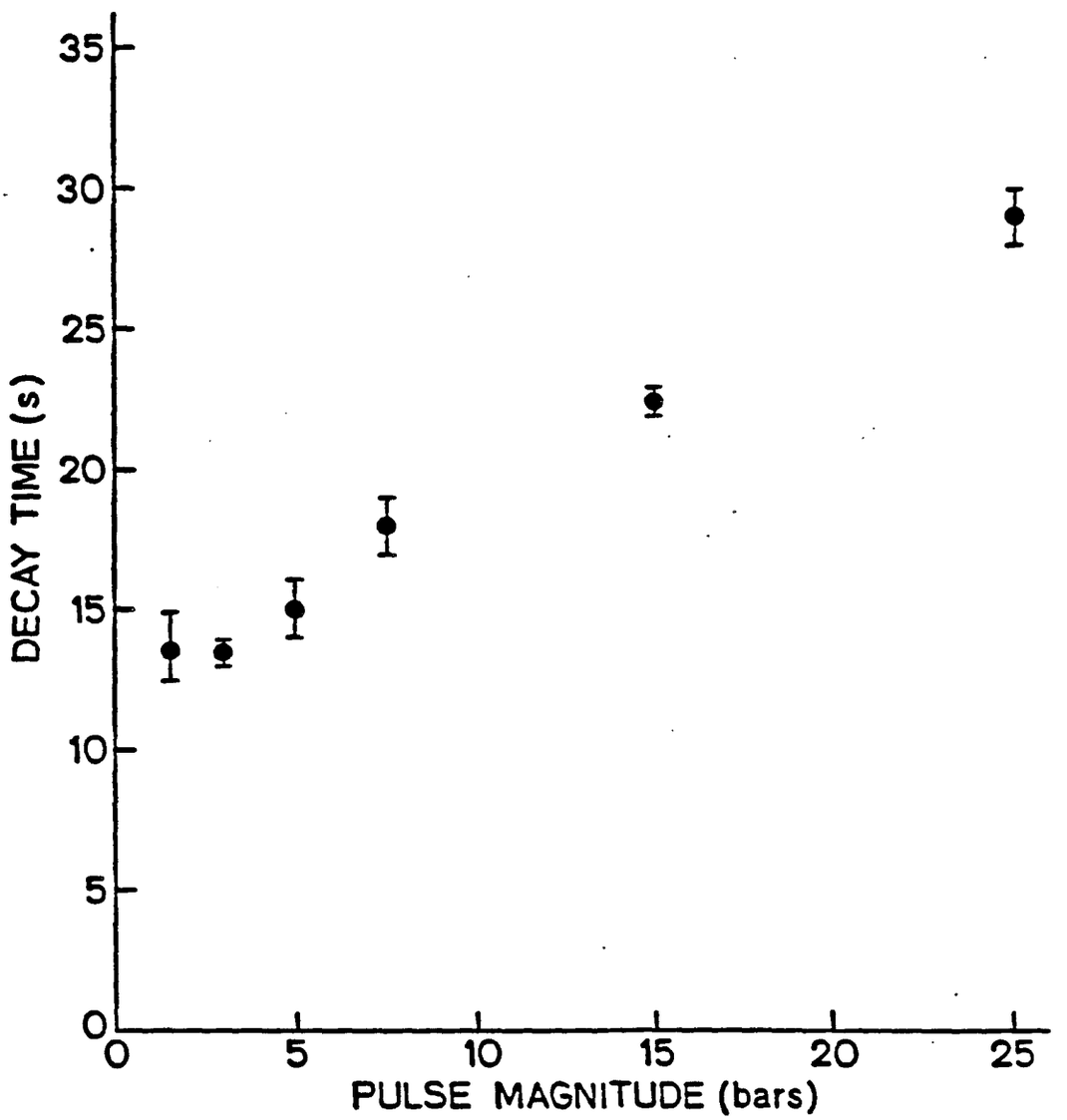

Figure 6-7: Decay time of pulse tests as a function of pulse magnitude. Nonlinear effects are important for Δp greater than about 5 bars.

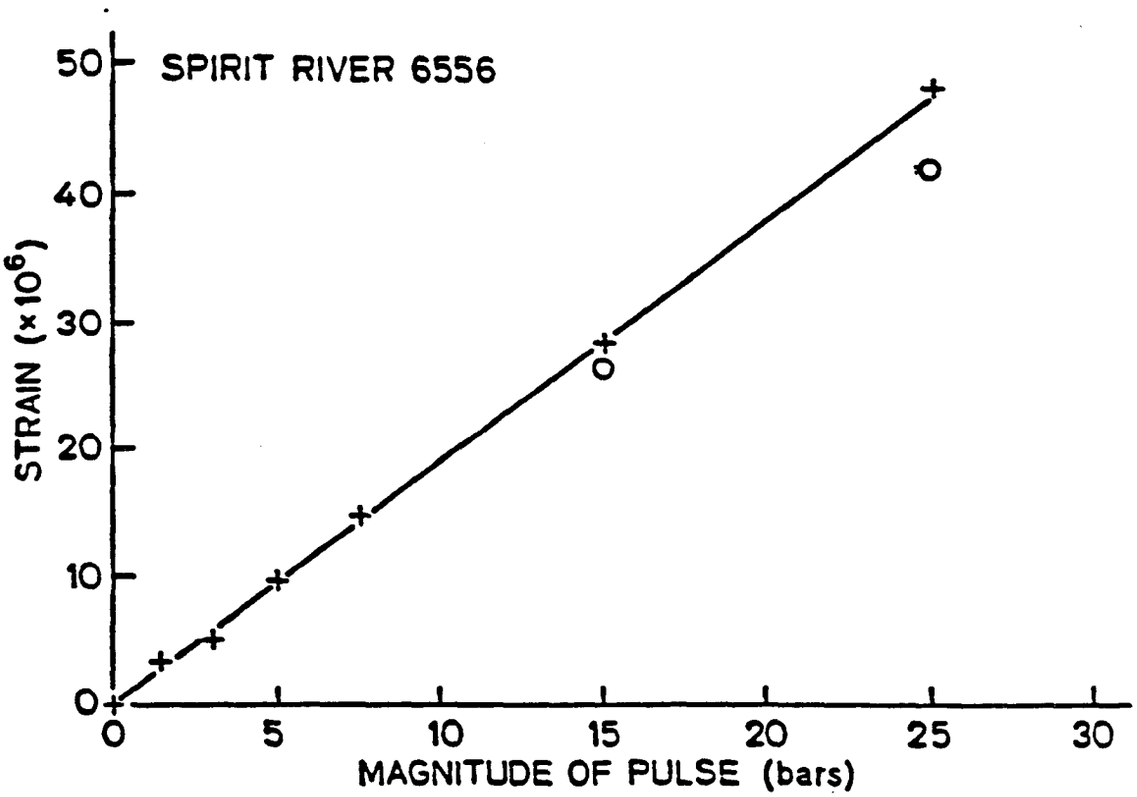

Figure 6-8: 'Final' strain in circumferential gages as a function of pulse magnitude. Results are in accord with predictions of linear poroelasticity theory. Values for Δp = 15 and 25 bars have been 'corrected' from the values given by circles (see discussion in text).

4. DISCUSSION

The theory and experimental results presented above have some practical importance for investigators who intend to use the pulse-decay method to study low-permeability rocks. First, poroelastic theory makes it clear that sample size may have an effect on the apparent permeability inferred from pressure *vs.* time records. Whether or not this will be important in practice--particularly in light of the possibly more important effect of material inhomogeneity--cannot yet be confidently stated. It would seem reasonable, however, to suggest that in any experimental program of permeability measurements, possible complications in comparing data could be avoided by standardizing sample sizes.

Our study of nonlinear phenomena in pore-pressure diffusion suggests some guidelines for the maximum allowable magnitude of pressure pulse. Our results showed significant deviation from linearity for $\Delta p/p$ in excess of *ca.* 0.1. Walls [1982] previously showed consistently linear behavior with a similar rock for $\Delta p/p < ca.$ 0.03. It would seem reasonable to propose that experimenters use $\Delta p/p$ well below 0.1; $\Delta p/p < 0.05$ may be a reasonable guideline. Some experiments described by previous investigators [e.g., Brace et al, 1968; Trimmer et al., 1980] have utilized $\Delta p/p$ as high as 0.2-0.4, raising the possibility that nonlinear pore-pressure diffusion phenomena could have lead to misinterpretation of some results. In any case, it would seem prudent in any program of pulse-decay measurements to follow Walls' [1982] lead and explicitly test for possible dependence of results on pulse magnitude.

5. SUMMARY

Poroelasticity and nonlinear pore-pressure diffusion phenomena may affect the interpretation of permeability measurements by the pulse-decay

method. We have discussed the theoretical bases for expecting such complications, and reported results of two simple experiments designed to test the theory. The theoretical developments and experimental test results suggest guidelines to be used in pulse-decay testing in order to eliminate possible complications of sample-size effects (due to poroelastic coupling between rock and pore fluid) and of nonlinear pore-pressure diffusion (due to excessively large pulse magnitudes).

APPENDIX: MATHEMATICAL ANALYSIS OF PULSE-DECAY TEST

A variety of mathematical approaches for interpretation of pulse-decay measurements have been presented by other investigators. Two basic approaches have been used: regression-type fit of a particular mathematical equation to pressure *vs.* time data [Brace et al., 1968; Zoback and Byerlee, 1975; Walls et al., 1980] and 'matching' of experimental data to numerically generated 'type curves' [Trimmer et al., 1980; Hsieh et al., 1981]. As we began our series of pulse-decay tests with samples of various lengths, we used the particular regression method (and computer code) developed by Walls et al. [1980]. Later in our experimental program, we noticed that with very short cores, this method appeared to produce small systematic errors in curve-fitting. A better fit of the theoretical curve to the data was gotten by slightly modifying the analytical solution of Walls et al. [1980]. Details of our derivation are given next.

Walls et al. [1980] solved the pore-pressure diffusion equation:

$$\frac{\partial^2 p}{\partial z^2} = \frac{1}{c}\frac{\partial p}{\partial t} \tag{A-1}$$

with the initial and boundary conditions

(i) $p(z, t = 0) = p_2$

(ii) $p(z = 0, t) = p_1$

(iii) $\frac{\partial p}{\partial t}(z = L, t) = -\kappa_2 \frac{\partial p}{\partial z}(z = L, t)$

where $\kappa_2 = kA / \mu\beta_f V_2$, with A the cross-sectional area of the core and V_2 the volume of reservoir 2 (cf. Fig. 6-1). The boundary condition (ii) corresponds to the assumption that V_1, the volume of reservoir 1, is infinite. We modified this boundary condition to be analogous to (iii), viz.:

$$\text{(ii')}\ \frac{\partial p}{\partial t}(z=0,t) = -\kappa_1 \frac{\partial p}{\partial z}(z=0,t)$$

where $\kappa_1 = kA/\mu\beta_f V_1$, with V_1 the volume of reservoir 1. The boundary conditions are now equivalent to those in the analysis by Hsieh et al. [1981] if we assume that both of the reservoirs are perfectly rigid.

With the modified boundary conditions, we proceeded as in Walls et al. [1980] to solve Eqn. (A-1) by Laplace transform methods. The transform can be expressed as a complicated infinite series. Inverting term by term, and keeping terms to second order (as opposed to Walls et al. [1980], who kept only first-order terms), we find a very complicated expression for $\Delta p(t)$, the differential pressure as a function of time:

$$\frac{\Delta p}{p_1 - p_2} = 1 + 2\left(\frac{\alpha_1}{\pi}\right)^{1/2}\left[-1 + 2e^{-\xi^2/4} + 2e^{-\xi^2} - 3e^{-9\xi^2/4} + 40e^{-4\xi^2}\right] + \qquad \text{(A-2)}$$

$$+ \left[50\left(\frac{\alpha_1}{\pi}\right)^{1/2} + 8\left(\frac{\alpha_2}{\pi}\right)^{1/2}\right] - 2(1+\beta_1+\gamma)\,\mathrm{erfc}\left(\frac{\xi}{2}\right) - 4(\beta_1+\gamma)\,\mathrm{erfc}(\xi) +$$

$$+ 2(1+9\beta_1+9\gamma)\,\mathrm{erfc}\left(\frac{3\xi}{2}\right) - 32(\beta_1+\gamma)\,\mathrm{erfc}(2\xi) +$$

$$+ 4\gamma\exp(2\beta_2+\alpha_2^2)\,\mathrm{erfc}(\xi+\alpha_2) + 2(1+\gamma)\exp(\beta_2+\alpha_2^2)\,\mathrm{erfc}\left(\frac{\xi}{2}+\alpha_2\right) -$$

$$- 2(1+9\gamma-6\beta_2-4\alpha_2^2-12\alpha_1\alpha_2-18\beta_1)\exp(3\beta_2+\alpha_2^2)\,\mathrm{erfc}\left(\frac{3\xi}{2}+\alpha_2\right) -$$

$$-32(2\alpha_1\alpha_2-\gamma+4\beta_1)\exp(4\beta_2+\alpha_2^2)\,\mathrm{erfc}(2\xi+\alpha_2) -$$

$$-4(10\alpha_1\alpha_2-5\gamma+25\beta_1+5\beta_2+2\alpha_2^2)\exp(5\beta_2+\alpha_2^2)\,\mathrm{erfc}\left(\frac{5\xi}{2}+\alpha_2\right)$$

where $\alpha_1 = \kappa_1\sqrt{t/c}$, $\alpha_2 = \kappa_2\sqrt{t/c}$, $\beta_1 = \kappa_1 L/c$, $\beta_2 = \kappa_2 L/c$, $\gamma = \kappa_1/\kappa_2$, and $\xi = L/\sqrt{ct}$.

In Figs. 6A-1, 6A-2, and 6A-3, we show the curve-fits (and the inferred permeability values) for a pulse decay with 21.7 mm long, 51 mm diameter core (at p_c = 490 bars) for three different analytical approximations: the

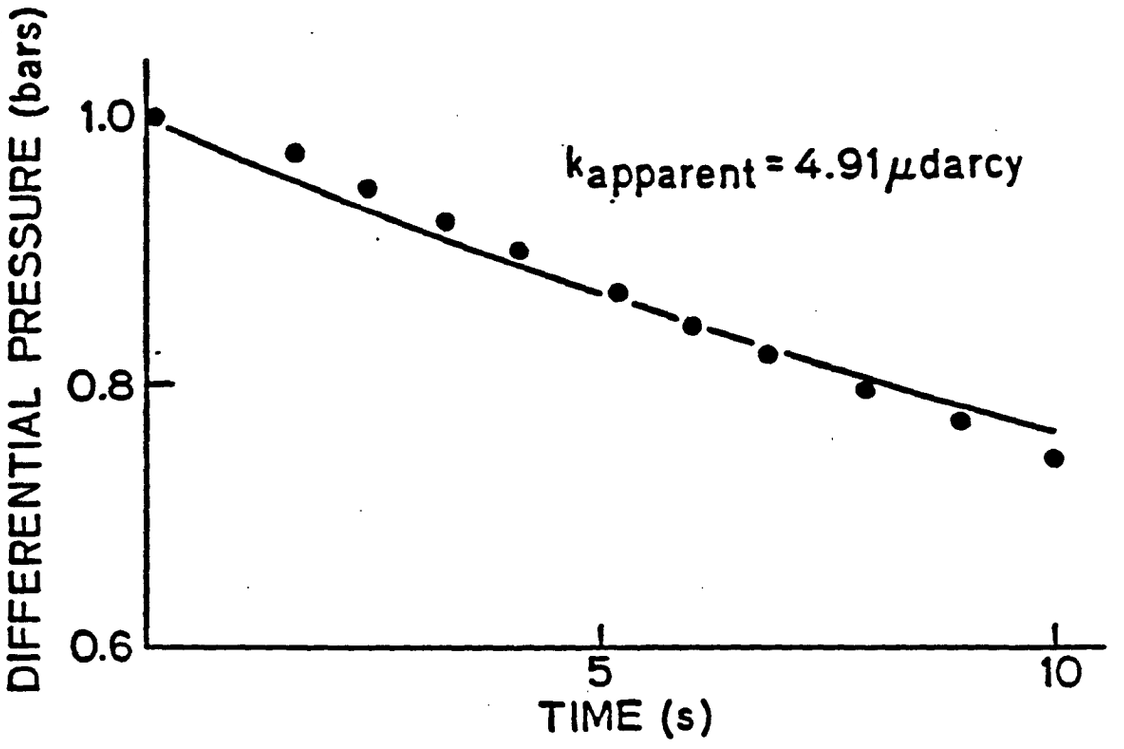

Figure 6A-1: Best fit of analytic expression of Brace et al. [1968] to pressure-transient data for a 21.7 mm length Spirit River sandstone core.

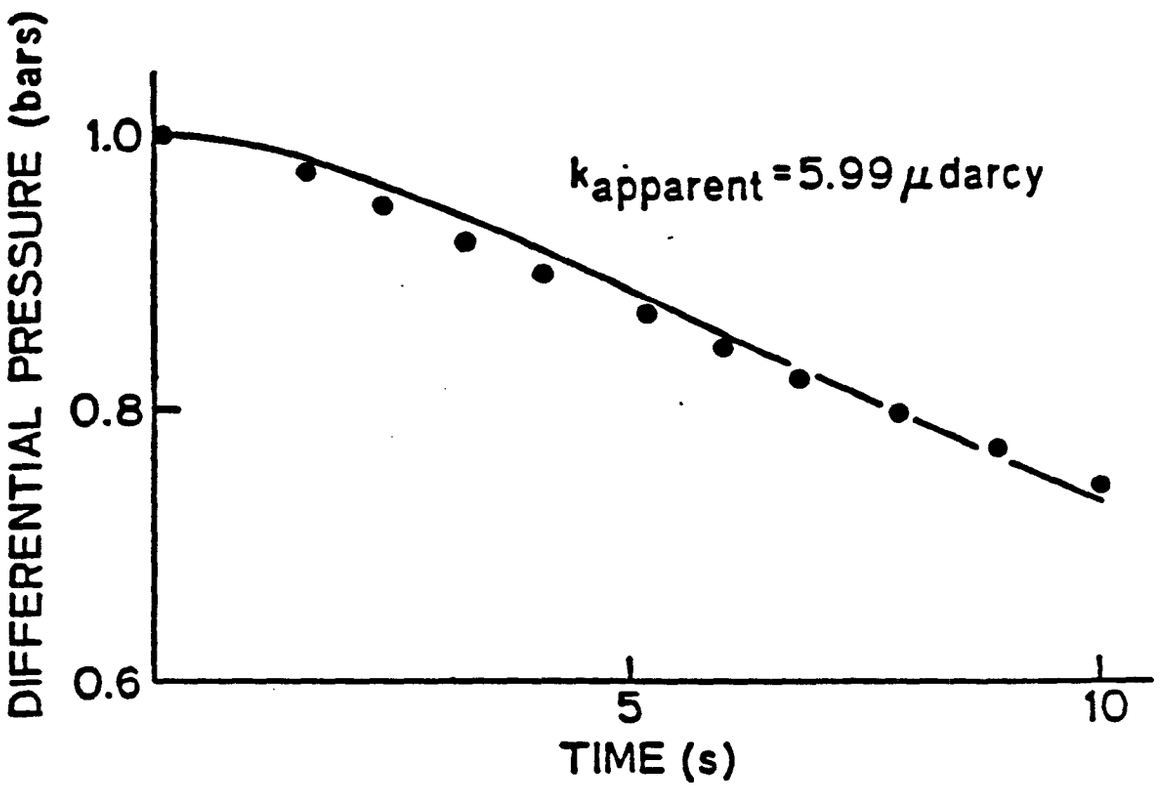

Figure 6A-2: Best fit of 'first order error function' expression of Walls et al. [1980] to same pressure-transient data as in Figure 6A-1.

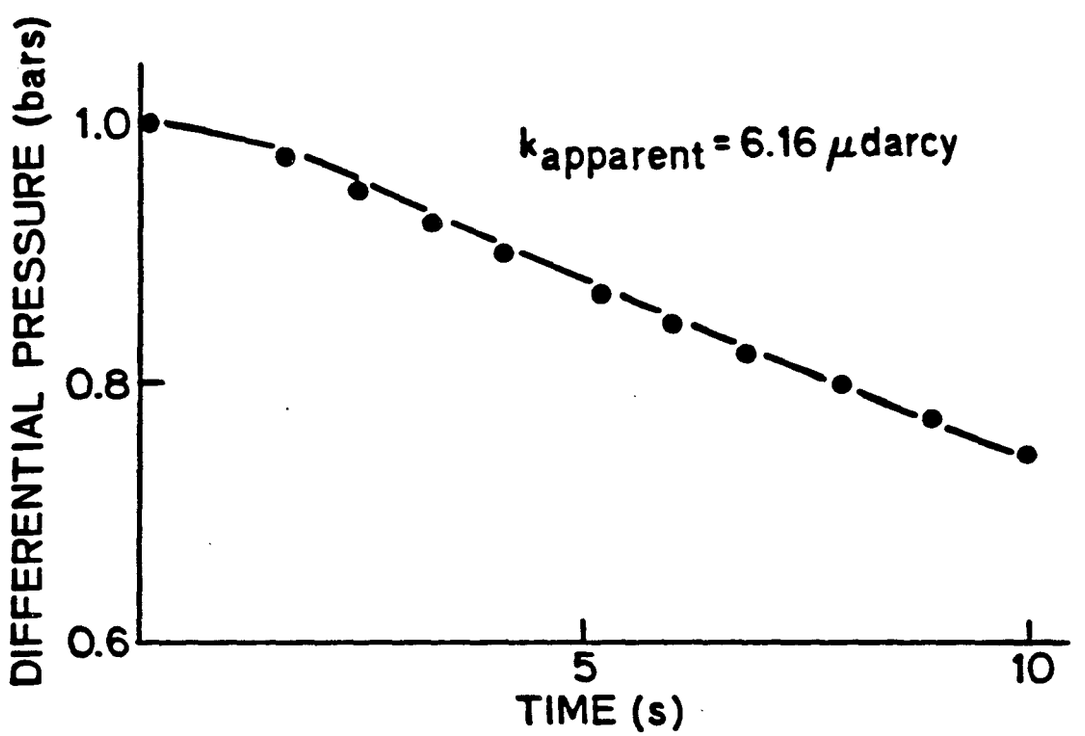

Figure 6A-3: Best fit of 'second order error function' expression, derived in this chapter, to the same pressure-transient data as in Figure 6A-1.

Brace et al. [1968] solution, the '1st order error function' solution of Walls et al. [1980], and the '2nd order error function' solution of the present chapter, respectively. All three solutions show a slight systematic mismatch between data and analytical solution; this mismatch is the least for the 2nd order error function solution. The 'goodness of fit' may be mathematically expressed by the sum of the squares of the residuals, $\sum R_i$, defined as

$$\sum R_i = \sum (p_i - \hat{p}_i)^2 \qquad \text{(A-3)}$$

where the p_i are the measured differential pressures at times t_i and the $\hat{p}_i$ are the corresponding values of the analytical approximation. For the example presented here, $\sum R_i = 1.92 \times 10^{-3}$, 1.17×10^{-3}, and3.84×10^{-4} for the curve-fits in Figs. 6A-1, 6A-2, and 6A-3, respectively. Our 'second order error function' fit therefore gives a substantially smaller residual than either of the other two approximations. This comparison points out yet another complication in permeability determinations, namely, the way in pressure *vs.* time data are manipulated to infer permeability. (It should be noted that for longer cores, the problem with systematic mismatch between analytical solution and data does not appear. This results suggests that either the mathematical analysis should be carried to higher order--a very tedious process--or that experimenters should avoid using very short cores.)

REFERENCES

Biot, M.A., General theory of three-dimensional consolidation, *Journal of Applied Physics*, *12*, 155-64, 1941.

Brace, W.F., Permeability of crystalline and argillaceous rocks, *International Journal of Rock Mechanics and Mining Sciences & Geomechanics Abstracts*, *17*, 241-51, 1980.

Brace, W.F., J.B. Walsh, and W.T. Frangos, Permeability of granite under high pressure, *Journal of Geophysical Research*, *73*, 2225-36, 1968.

Hsieh, P.A., J.V. Tracy, C.E. Neuzil, J.D. Bredehoeft, and S.E. Silliman, A transient laboratory method for determining the hydraulic properties of of "tight" rocks, I: theory, *International Journal of Rock Mechanics and Mining Sciences & Geomechanics Abstracts*, *18*, *245-52*, *1981*.

Nur, A., and O. Yilmaz, Pore pressure fronts in fractured rocks, *Stanford Rock Physics Project Report*, *3*, Stanford University, Stanford, California, p. 78 , 1978.

Rice, J.R., and M.P. Cleary, Some basic stress diffusion solutions for fluid-saturated elastic porous media with compressible constituents, *Reviews of Geophysics and Space Physics*, *14*, 227-41, 1976.

Skempton, A.W., The pore-pressure coefficients A and B, *Geotechnique*, *4*, 143-47, 1954.

Trimmer, D., B. Bonner, H.C. Heard, and A. Duba, Effect of pressure and stress on water transport in intact and fractured gabbro and granite, *Journal of Geophysical Research*, *85*, 7059-71, 1980.

Walls, J.D., Effects of pore pressure, confining pressure and partial saturation on permeability of sandstones, Ph.D. thesis, Stanford University, Stanford, California, 1982.

Walls, J.D., A. Nur, and T. Bourbié, Effects of pressure and partial water saturation on gas permeability in tight sands: experimental results, *Journal of Petroleum Technology*, *34*, 930-36, 1980.

Zoback, M.D., and J.D. Byerlee, The effect of microcrack dilatancy on the permeability of Westerly Granite, *Journal of Geophysical Research*, *80*, 752-55, 1975.

NOTATION

A	cross-sectional area of core
B	poroelastic modulus ('Skempton's parameter')
c	hydraulic diffusivity
f	dimensionless function related to characteristic diffusion time
G	shear modulus
k	permeability
L	sample length
m	fluid mass fraction
p	pore pressure
p_c	confining pressure
p_e	effective pressure
p'	dimensionless pore pressure
$\vec{q}$	volumetric flow rate
r	radial coordinate
t	time
t'	dimensionless time
V_1, V_2	reservoir volumes
z	axial coordinate
z'	dimensionless axial coordinate
β_f	fluid compressibility
β_k	coefficient describing effect of pore pressure on permeability
$\hat{\beta}_k$	coefficient describing effect of confining pressure on permeability
$\hat{\beta}$	compressibility term
δ_{ij}	Kronecker delta
Δp	magnitude of differential pore pressure

Δp_r 'residual' value of Δp

ε_{ij} strains

θ circumferential coordinate

κ_1, κ_2 parameters related to fluid storage in reservoirs

μ viscosity

ν Poisson's ratio

ν_u undrained Poisson's ratio

ξ $L/\sqrt{ct}$

ρ_f fluid density

σ_{ij} stresses

τ characterristic time scale

φ porosity

SUMMARY

The studies described in this dissertation have addressed phenomena on a wide variety of scales, from laboratory to global. It has been shown that for several common geological processes, including sedimentary basin development, plate convergence, and uplift, the coupling between fluid and solid plays a critical role in determining the magnitude of pore pressure and, hence, the susceptibility of the host rock to brittle fracture. Furthermore, even in regions of the Earth's crust not usually thought of as tectonically active, fluid-solid coupling will be very important if localized, essentially chemical processes introduce a time-dependence into crustal hydrologic parameters (porosity and permeability). Again, fluid flow, pore pressure, and rock deformation become inextricably linked phenomena.

By further integrating and expanding the various studies presented here, additional understanding of the role of pore fluids in tectonic processes would certainly result. For example, the work on poroelasticity could be combined with that on overpressuring in sedimentary basins to better understand pore-pressure development during subduction of oceanic crust. This, in turn, could help elucidate the state of stress and the style of deformation in subducted crust. The poroelastic formalism may also be quite useful in better defining the mechanical interaction between igneous intrusions and host rock. Another intriguing problem--one that was touched upon briefly in chapter 3—is that of the origin of Mississippi Valley-type Pb-Zn deposits. By combining concepts presented in that chapter with work done by other investigators, we may not

only be able to model the ore-genesis process, but also learn a great deal about sedimentary basin development.

If there is to be a central 'lesson' to be learned from the work presented here, it is that crustal hydrologic processes must be considered as fundamentally dynamic. Generalizations about the 'ambient' or 'average' hydrologic properties of the Earth's crust may be useful in some contexts, but for the geologist or geophysicist seeking fundamental explanations for tectonic phenomena, such generalizations are almost certainly misleading.